

Syracuse University

SURFACE

Dissertations - ALL

SURFACE

May 2015

Synthesis towards Polyhedral and Rigid Organic Non-Linear Optic Materials

Casey R. Simons
Syracuse University

Follow this and additional works at: <https://surface.syr.edu/etd>



Part of the [Physical Sciences and Mathematics Commons](#)

Recommended Citation

Simons, Casey R., "Synthesis towards Polyhedral and Rigid Organic Non-Linear Optic Materials" (2015).
Dissertations - ALL. 237.
<https://surface.syr.edu/etd/237>

This Dissertation is brought to you for free and open access by the SURFACE at SURFACE. It has been accepted for inclusion in Dissertations - ALL by an authorized administrator of SURFACE. For more information, please contact surface@syr.edu.

Abstract

Currently, there is intense research interest in new molecular compounds that display enhanced second harmonic generation nonlinear optical (NLO) properties. Previous computational research has shown that both polyhedral carborane compounds and sterically constrained hydrindacene show great potential as NLO compounds. Their calculated β values exceed those of compounds currently in use. Initial synthetic obstacles in the formation of polyhedral carborane based compounds led us to investigate targets using multiple polyhedral cage bridges. Initial calculations on these compounds have shown promising results. [2-[2-(3,4-dimethylcyclopentadienyl)-*o*-carborane]-*o*-carborane]-tropylium, **27**, in particular has shown great promise as a target for synthesis. Preliminary synthetic attempts towards homo- and hetero- polyhedral cage compounds are reported.

Current synthesis towards hindered organic NLO molecules have shown promise, with some synthetic difficulties encountered. Multiple pathways for the initial target, 4-tropylium-8-(3,4-diphenylcyclopentadienyl)-1,1,3,3,5,5,7,7-octamethyl-*s*-hydrindacene have been created and tested with varying results. These synthetic strategies include nucleophilic addition into a preformed bridge, formation of a bridge from a substituted quinarene compound, and a multistep partial backbone construction method which will be discussed further in Chapter 3. Computational exploration of extended quinarene/hydrindacene hybrids for their use as NLO materials have yielded mixed results, varying with amount of extension of the pendant groups. Initial synthesis of these materials have shown great promise and shall be discussed in Chapter 4.

Synthesis towards Polyhedral and Rigid Organic Non-Linear Optic Materials

By

Casey R. Simons

B.S., University of Arizona, 2009

M.Phil., Syracuse University, 2011

Dissertation

Submitted in partial fulfilment of the requirements for the
degree of Doctor of Philosophy in Chemistry
in the Graduate School of Syracuse University

May 2015

©Copyright by Casey R. Simons, 2015.
All rights reserved.

Acknowledgements

I would like to express my sincere thanks to my advisor Dr. James T. Spencer. His support over the last five years has led me to be a very versatile chemist. I thank him for his support, valuable guidance and constant encouragement. I would also like to thank my committee members Dr. Jon Zubieta, and Dr. Ari Chakraborty for their helpful discussions, great classes and support of my research.

I would like to acknowledge Dr. Deborah Kerwood for her assistance in acquiring the NMR data and allowing me to assist her in the installation and maintenance of the instruments in her lab.

From Chemistry I would like to thank Dr. Damian Allias and Dr. Bruce Hudson for their patience in explaining computational method to me.

I would also like to acknowledge the graduate students that had helped obtain crystallographic data and form images for this dissertation, Stephanie Jones-Labadie, Ana Torvisco and Alan Goos.

I would like to acknowledge the Department of Chemistry of Syracuse University for allowing me to carry out my research. I also thanks all members of my research group, as well as Faculty and Staff of the Department of Chemistry, for their friendly accommodation. I would also like to express my thanks to my loving fiancé Amanda Imundo who helped me remember there was life outside of lab and has been my best friend and companion over all the rough times. And last, I would like to express my deepest thanks to my parents, without whom I would not be here today. I thank them for the love, support and encouragements.

Table of Contents

Abstract	i
Title Page	ii
Acknowledgements	iv
List of Figures	viii
List of Schemes	x
List of Tables	xi
List of Equations	xiv
List of Compounds	xiv
1 Introduction to Non-Linear Optics	1
1.1 Non-Linear Optic Theory	2
1.1.1 Introduction	2
1.1.2 Push Pull Systems	4
1.1.3 Calculations In NLO materials	6
1.1.4 [5.6.7] Quinarene Derivatives	7
1.2 Polyhedral NLO Compounds	9
1.2.1 Introduction	9
1.2.2 Previous Work in Polyhedral NLO Systems	12
1.3 Rigid Organic NLO Compounds	17
1.3.1 Introduction	17
1.3.2 Previous Synthetic Work in Rigid NLO Compounds	20

2	Synthesis towards Polyhedral Based NLO Materials	21
2.1	Introduction	22
2.2	Experimental	25
2.2.1	Physical Measurements	25
2.2.2	Materials	26
2.2.3	Synthesis	27
2.2.4	Calculations	33
2.2.5	Crystallographic Studies	34
2.3	XRD Crystallographic Data and Tables	35
2.4	Results	46
2.4.1	Calculations	46
2.4.2	Synthesis	49
2.5	Conclusions and Future Work	59
3	Rigid Organic NLO Compounds	62
3.1	Introduction	63
3.2	Experimental	66
3.2.1	Physical Measurements	68
3.2.2	Materials	68
3.2.3	Synthesis	69
3.2.4	Crystallographic Studies	79
3.3	XRD Crystallographic Data and Tables	80

3.4 Results and Discussion	90
3.5 Conclusions and Future Work	110
4 Extended Rigid Organic NLO Compounds	113
4.1 Introduction	114
4.2 Experimental	118
4.2.1 Physical Measurements	118
4.2.2 Materials	118
4.2.3 Synthesis	119
4.2.4 Calculations	125
4.3 Results and Discussion	126
4.3.1 Coupling Agents	126
4.3.2 Extended Quinarene/Hydrindacene Calculations	129
4.3.3 Extended Quinarene/Hydrindacene Synthesis	135
4.4 Conclusions and Future Work	139
Appendix A – Crystallographic Data	143
Appendix B – Calculation Input	178
References	198
CV	205

List of Figures

- Figure 1** A. Block diagram representation of a NLO system. B. Excitation diagram of a NLO compound
- Figure 2** *para*-nitroaniline, 1.
- Figure 3** [5.6.7] quinarene in its electron delocalized, 2, and localized, 3, form.
- Figure 4** Stabilized NLO compounds found in literature.
- Figure 5** 5 – [5.6.7] quinarene target from literature. 8 – *p*-carborane analog of 5. 9 & 10 – Computationally calculated NLO carborane systems.
- Figure 6** A view of the hindered rotation and the target compound 22.
- Figure 7** Orbital diagrams for ideally-substituted hydrindacene bridge NLO compounds.
- Figure 8** Schematic drawing of compounds 8 and 26.
- Figure 9** Hypothesized multi cage systems for use as NLO materials.
- Figure 10** ORTEP drawing of the crystallographically-determined molecular structures of compound 30.
- Figure 11** ORTEP drawing of the crystallographically-determined molecular structures of compound 38.
- Figure 12** ORTEP drawing of the crystallographically-determined molecular structures of 36 (L) and 39 (R).
- Figure 13** HOMO-1 and LUMO+1 molecular orbitals of compounds 27, 28, and 29.
- Figure 14** Convergent Synthesis for a multi-cage NLO compound
- Figure 15** Energy profile diagram for the kinetic vs thermodynamic product reaction
- Figure 16** Cerium intermediate coordination to oxygen promoting 1,2-addition

- Figure 17** Schematic showing several possible new nonlinear optical compounds based on charged aromatic donor-acceptor units bridged by aromatic units.
- Figure 18** Select members of the *s*-hydrindacene family of compounds from literatures.
- Figure 19** The twisted zwitterionic compound explored in literature.
- Figure 20** The two reactions to turn precursor units in to the active charged species.
- Figure 21** ORTEP drawing of the crystallographically-determined molecular structures of compound 63.
- Figure 22** ORTEP drawing of the crystallographically-determined molecular structures of compound 64.
- Figure 23** ORTEP drawing of the crystallographically-determined molecular structures of compound 65.
- Figure 24** ORTEP drawing of the crystallographically-determined molecular structures of compound 70.
- Figure 25** ORTEP drawing of the crystallographically-determined molecular structures of compound 71.
- Figure 26** 4-Bromo-1,1,3,3,5,5,7,7-octamethyl-*s*-hydrindacene.
- Figure 27** Compound 68.
- Figure 28** Compound 70 with ¹H-NMR shifts.
- Figure 27** A NMR comparison between the 72 and 73.
- Figure 28** Mechanism of the Friedel-Craft alkylation ring closure.
- Figure 30** Substituted hydrindacene compounds from literature.
- Figure 31** Literature method for the palladium catalyzed ring structure into an *s*-hydrindacene backbone.

- Figure 32** Extended pendant targets to be examined computationally and synthetically.
- Figure 33** Formation of vinylstannanes from ketones.
- Figure 34** Twist angles calculated in extended pendant group compounds **79** through **83**.
- Figure 35** Calculated HOMO-1 and LUMO+1 diagrams of compounds **79** – **83**.
- Figure 36** Literature metathesis of hindered compounds using RuPhos.
- Figure 37** Formation of the boronic ester, **96**.
- Figure 38** Crystal data and structure refinement of **30**.
- Figure 39** Crystal data and structure refinement of **36**.
- Figure 40** Crystal data and structure refinement of **38**.
- Figure 41** Crystal data and structure refinement of **39**.
- Figure 42** Crystal data and structure refinement of **63**.
- Figure 43** Crystal data and structure refinement of **64**.
- Figure 44** Crystal data and structure refinement of **65**.
- Figure 45** Crystal data and structure refinement of **70**.
- Figure 46** Crystal data and structure refinement of **71**.

List of Schemes

- Scheme 1** Neim's synthetic pathway to **5**.
- Scheme 2** Hypothesis for synthesized **21** proceeded in a similar fashion.
- Scheme 3** The retrosynthetic pathway of the target compounds.
- Scheme 4** Synthesis of 3-(*p*-carborane)-1,3,5-cycloheptatriene (**30**)

- Scheme 5** Initial Synthesis of cyclopentadiene substituted *o*-carborane cages.
- Scheme 6** The observed 1,4-addition of α,β -unsaturated ketones to *o*-carborane.
- Scheme 7** Copper catalyzed addition of **30** onto **38** to form targeted compound **40**.
- Scheme 8** Literature example of copper catalyzed cage coupling
- Scheme 9** Synthesis attempt towards a dual substituted 1,1-bis-*o*-carborane.
- Scheme 10** Synthesis of compound **50** attempted previously in literature.
- Scheme 11** The remaining synthesis from key intermediate **51**.
- Scheme 12** The retrosynthesis of key intermediate **51** *via* a pendant ring first method.
- Scheme 13** The potential oxidation reaction of **58** to **59**.
- Scheme 14** The retrosynthetic approach for the preparation of **21**.
- Scheme 15** The synthetic pathway towards the synthesis of **51**.
- Scheme 16** Partial bridge construction *via* dehydration of **64**.
- Scheme 17** The synthetic strategy for the formation of **51** through coupling methodology.
- Scheme 18** Attempted synthesis of a cyclopentadiene coupling agents.
- Scheme 19** The retrosynthesis of an extended quinarene/hydrindacene compound, **100**.
- Scheme 20** Initial synthesis towards coupling agents.
- Scheme 21** Synthesis of the donor Suzuki reagent, **99**.
- Scheme 22** Formation of **100** and **101** through palladium catalyzed coupling using RuPhos.

List of Tables

- Table 1** A summary of computed hyperpolarizability values.
- Table 2** A comparison of different NLO materials to the hypothesized **23** and **24**.

Table 3	Crystallographic Parameters for Compounds <u>30</u> .
Table 4	Selected bond distances (Å) for <u>30</u> .
Table 5	Selected Bond Angles (°) for Compound <u>30</u> .
Table 6	Crystallographic Parameters for Compounds <u>36</u> , <u>38</u> and <u>39</u>
Table 7	Selected Bond Lengths (Å) for Compound.
Table 8	Selected Bond Angles (°) for Compound <u>38</u> .
Table 9	Selected Bond Lengths (Å) for Compound <u>36</u> .
Table 10	Selected Bond Angles (°) for compound <u>36</u> .
Table 11	Selected Bond Lengths (Å) for Compound <u>39</u> .
Table 12	Selected Bond Angles (°) for Compound <u>39</u> .
Table 13	Calculated Mulicage hyperpolarizability values.
Table 14	XRD data and details of measurements for compounds <u>63</u> and <u>64</u> .
Table 15	Selected Bond Lengths (Å) for Compound <u>63</u> .
Table 16	Selected Bond Angles (°) for Compound <u>63</u> .
Table 17	Selected Bond Lengths (Å) for Compound <u>64</u> .
Table 18	Selected Bond Angles (°) for compound <u>64</u> .
Table 19	Crystallographic data and details of measurements for compounds <u>65</u> , <u>70</u> and <u>71</u> .
Table 20	Selected Bond Lengths (Å) for compound <u>65</u> .
Table 21	Selected Bond Angles (°) for compound <u>65</u> .
Table 22	Selected Bond Lengths (Å) for Compound <u>70</u> .

Table 23	Selected Bond Angles (°) for Compound <u>70</u>
Table 24	Selected Bond Lengths for compound <u>71</u> .
Table 25	Selected Bond Angles for compound <u>71</u> .
Table 26	Calculated β values for extended rigid NLO systems.
Table 27	Atomic coordinates and equivalent isotropic displacement parameters (\AA^2) for <u>30</u> .
Table 28	Atomic displacement parameters (\AA^2) for <u>30</u> .
Table 29	Atomic coordinates and equivalent isotropic displacement parameters (\AA^2) for <u>36</u> .
Table 30	Atomic displacement parameters (\AA^2) for <u>36</u> .
Table 31	Atomic coordinates and equivalent isotropic displacement parameters (\AA^2) for <u>38</u> .
Table 32	Atomic displacement parameters (\AA^2) for <u>38</u> .
Table 33	Atomic coordinates and equivalent isotropic displacement parameters (\AA^2) for <u>39</u> .
Table 34	Atomic displacement parameters (\AA^2) for <u>39</u> .
Table 35	Atomic coordinates and equivalent isotropic displacement parameters (\AA^2) for <u>63</u> .
Table 36	Atomic displacement parameters (\AA^2) for <u>63</u> .
Table 37	Atomic coordinates and equivalent isotropic displacement parameters (\AA^2) for <u>64</u> .
Table 38	Atomic displacement parameters (\AA^2) for <u>64</u> .
Table 39	Atomic coordinates and equivalent isotropic displacement parameters (\AA^2) for <u>65</u> .
Table 40	Atomic displacement parameters (\AA^2) for <u>65</u> .
Table 41	Atomic coordinates and equivalent isotropic displacement parameters (\AA^2) for <u>70</u> .
Table 42	Atomic displacement parameters (\AA^2) for <u>70</u> .

Table 43 Atomic coordinates and equivalent isotropic displacement parameters (\AA^2) for 71.

Table 44 Atomic displacement parameters (\AA^2) for 71.

List of Equations

- Equation 1** The hyperpolarizability equation
- Equation 2** Total energy in an electromagnetic field
- Equation 3** Total energy in a one dimensional electromagnetic field
- Equation 4** Substitution to solve for a one dimensional β value
- Equation 5** Substitution to solve for a multi-dimensional β value
- Equation 6** Calculating β_{total} from b components

List of Compounds

- Compound 1** *para*-nitroaniline
- Compound 2** [5.6.7] Quinarene (*delocalized*)
- Compound 3** [5.6.7] Quinarene (*localized*)
- Compound 4** 7-(4-(2,3-cyano-3,4-dimethyl-cyclopentadienyl)phenyl)-tropylium
- Compound 5** 7-(4-(2,3,4,5-tetraphenyl-cyclopentadienyl)phenyl)- tropylium
- Compound 6** 7-(4-(2,3-cyano-3,4-diphenyl-cyclopentadienyl)phenyl)- tropylium
- Compound 7** 7-(4-(2,3-cyano-3,4-dimethyl-cyclopentadienyl)phenyl)-cyclopentenyl
- Compound 8** $(R_1R_2R_3R_4C_5)$ -*p*-($C_2B_{10}H_{10}$)-(C₇H₆)
- Compound 9** $(R_1R_2R_3R_4C_5)$ -*p*-($C_2B_3H_3$)-(C₇H₆)
- Compound 10** $(R_1R_2R_3R_4C_5)$ -*p*-($B_{10}H_{10}$)-(C₇H₆)
- Compound 11** 1,4-dibromobenzene
- Compound 12** 7-(4-bromophenyl)-cycloheptatriene
- Compound 13** 7-(4-(2,3,4,5-tetraphenylcyclopent-3-en-1-ol)phenyl)-cycloheptatriene
- Compound 14** 7-(4-(2,3,4,5-tetraphenylcyclopenta-1,3-diene)phenyl)-cycloheptatriene
- Compound 15** 1-(4-(2,3,4,5-tetraphenylcyclopent-3-en-1-ol)phenyl)-tropylium
- Compound 16** *para*-carboarane

- Compound 17** 7-(*p*-carborane)-1,3,5-cycloheptatriene
- Compound 18** 7-[12-(2,3,4,5-tetraphenylcyclopent-3-ene-1-ol)-*p*-carborane]-1,3,5-cycloheptatriene
- Compound 19** 7-[12-(3,4-dimethylcyclopenta-1,3-diene)-*p*-carborane]-1,3,5-cycloheptatriene
- Compound 20** 1-[12-(3,4-dimethylcyclopenta-1,3-diene)-*p*-carborane]-tropylium
- Compound 21** 1-[12-(3,4-dimethylcyclopentadienyl)-*p*-carborane]-tropylium
- Compound 22** 4-tropylium-8-cyclopentadienyl-1,1,3,3,5,5,7,7-octamethyl-*s*-hydrindacene
- Compound 23** 4-tropylium-8-(3,4-dimethylcyclopentadienyl)-1,1,3,3,5,5,7,7-octamethyl-*s*-hydrindacene
- Compound 24** 4-tropylium-8-(3,4-diphenylcyclopentadienyl)-1,1,3,3,5,5,7,7-octamethyl-*s*-hydrindacene
- Compound 25** 4,8-dibromo-1,1,3,3,5,5,7,7-octamethyl-*s*-hydrindacene
- Compound 26** (R₁R₂R₃R₄C₅)-*m*-(C₂B₁₀H₁₀)-(C₇H₆)
- Compound 27** [2-[2-(3,4-dimethylcyclopentadienyl)-*o*-carborane]-*o*-carborane]-tropylium
- Compound 28** [7-[2-(3,4-dimethylcyclopentadienyl)-*o*-carborane]-*p*-carborane]-tropylium
- Compound 29** [12-[2-(3,4-dimethylcyclopentadienyl)-*o*-carborane]-*p*-carborane]-tropylium
- Compound 30** 3-(*p*-carborane)-1,3,5-cycloheptatriene
- Compound 31** 1-(*o*-carborane)-3-methyl-cyclopenta-2-en-1-ol
- Compound 32** 1-(*o*-carborane)-3-methyl-cyclopenta-1,3-diene
- Compound 33** 3-(*o*-carborane)-3-methylcyclopenta-1-one
- Compound 34** 1-(*o*-carborane)-2,3,4,5-tetramethylcyclopenta-2-en-1-ol
- Compound 35** 1-(*o*-carborane)-2,3,4,5-tetramethylcyclopenta-1,3-diene
- Compound 36** 3-(*o*-carborane)-2,3,4,5-tetramethylcyclopenta-1-one
- Compound 37** 1-(*o*-carborane)-3,4-dimethylcyclopenta-2-en-1-ol
- Compound 38** 1-(*o*-carborane)-3,4-dimethylcyclopenta-1,3-diene
- Compound 39** 3-(*o*-carborane)-3,4-dimethylcyclopenta-1-one
- Compound 40** 3-[7-[2-(3,4-dimethylcyclopenta-1,3-diene)-*o*-carborane]-*p*-carborane]-1,3,5-cycloheptatriene
- Compound 41** 1,1'-bis(*o*-carborane)

- Compound 42** 7-[2-(*o*-carborane)-*o*-carborane]-1,3,5-cycloheptatriene
- Compound 43** 7-[2-(2-(3,4-dimethyl-2-cyclopenten-1-ol)-*o*-carborane)-*o*-carborane]-1,3,5-cycloheptatriene
- Compound 44** 1,1,3,3,5,5,7,7-octamethyl-*s*-hydrindacene
- Compound 45** 1,1,3,3,5,5,8,8-octamethyl-cyclopenta[*b*]naphthalene
- Compound 46** 1,1,4,4,5,5,8,8-octamethyl-anthracene
- Compound 47** 4-(3,5-(CH₃)-C₄NH₃)-C₆H₄O⁻
- Compound 48** *p*-bis(1-hydroxy-1-methylethyl)benzene
- Compound 49** *p*-dicumyl chloride
- Compound 50** 4-bromo-8-(7-(1,3,5-cycloheptatrien-7-yl)-1,1,3,3,7,7,9,9-octamethyl-*s*-hydrindacene
- Compound 51** 4-(3,4-dimethylcyclopenta-1,3-diene)-8-(1,3,5-cycloheptatrien-3-yl)-1,1,3,3,5,5,7,7-octamethyl-*s*-hydrindacene
- Compound 52** 4-bromo-8-(1,3,5-cycloheptatrien-3-yl)-1,1,3,3,5,5,7,7-octamethyl-*s*-hydrindacene
- Compound 53** 4-bromo-1,1,3,3,5,5,7,7-octamethyl-*s*-hydrindacene
- Compound 54** 2,2'-(2-(cyclohepta-2,4,6-trien-1-yl)-5-(cyclopenta-1,3-dien-1-yl)-1,4-phenylene)bis(propan-2-ol)
- Compound 55** 2-(cyclohepta-2,4,6-trien-1-yl)-5-(cyclopenta-1,3-dien-1-yl)terephthalic acid
- Compound 56** 7-(4-(cyclopenta-1,3-dien-1-yl)-2,5-dimethylphenyl)cyclohepta-1,3,5-triene
- Compound 57** 2,5-dibromo-*p*-xylene
- Compound 58** 7-(4-bromo-benzene)cyclohepta-1,3,5-triene
- Compound 59** 2-bromo-5-(cyclohepta-2,4,6-trien-1-yl)terephthalic acid
- Compound 60** dimethyl-2,5-dibromo-terephthate acid
- Compound 61** 2,5-dibromo-terephthalic acid
- Compound 62** 2,5-dibromo-4-methyl-benzoic acid
- Compound 63** dibutyl-2,5-dibromo-terephthalate
- Compound 64** 2,5-dibromo-1,4-bis-(2-hydroxy-2-propyl)benzene
- Compound 65** 2,5-dibromo-1,4-bis-(2-(dimethyl-*t*-butyl silyl ether)-2-propyl)benzene

- Compound 66** 1,4-bis-(2-(dimethyl-*t*-butylsilyl ether)-2-propyl)-2-bromo-5-cyclohepta-1,3,5-triene-benzene
- Compound 67** 1,4-bis-(2-(dimethyl-*t*-butylsilyl ether)-2-propyl)-2-(3,4-dimethylcyclopenta-1,3-diene)-5-cyclohepta-1,3,5-triene-benzene
- Compound 68** 1,4-bis(2-(dimethyl-*t*-butylsilyl ether)-2-propyl)-2-bromo-benzene
- Compound 69** 1,4-bis-(2-chloro-2-propyl)-2-(3,4-dimethylcyclopenta-1,3-diene)-5-cyclohepta-1,3,5-triene-benzene
- Compound 70** 1,4-dibromo-2,5-diisopropenyl-benzene
- Compound 71** 7-(4-bromo-2,5-diisopropenylphenyl)-1,3,5-cycloheptatriene
- Compound 72** 1-(4-(1,3,5-cycloheptatriene)-2,5-diisopropenylphenyl)-3,4-dimethylcyclopent-2-enol
- Compound 73** 7-(4-(3,4-dimethylcyclopenta-1,3-dien-1-yl)-2,5-di(prop-1-en-2-yl)phenyl)cyclohepta-1,3,5-triene
- Compound 74** 8-mercapto-1,1,3,3,5,5,7,7-octamethyl-*s*-hydrindacene-4-ol
- Compound 75** 8,8'-disulfanediylobis(1,1,3,3,5,5,7,7-octamethyl-*s*-hydrindacene-4-ol)
- Compound 76** 3-(1,1,7,7-tetraethyl-3,3,5,5-tetramethyl-*s*-hydrindacene-4-yl)thiophene
- Compound 77** phenyl(3,3,5,5-tetraethyl-1,1,7,7-tetramethyl-*s*-hydrindacene-4-yl)silane
- Compound 78** 4-bromo-1,1,7,7-tetraethyl-3,3,5,5-tetramethyl-*s*-hydrindacene
- Compound 79** 4-(4-(tropylium)phenyl)-8-(cyclopentadienyl)-1,1,3,3,5,5,7,7-octamethyl-*s*-hydrindacene
- Compound 80** 4-(4-(tropylium)phenyl)-8-(4-(cyclopentadienyl)phenyl)-1,1,3,3,5,5,7,7-octamethyl-*s*-hydrindacene
- Compound 81** 4-(tropylium)-8-(4-(cyclopentadienyl)phenyl)-1,1,3,3,5,5,7,7-octamethyl-*s*-hydrindacene
- Compound 82** 4-(4'-(tropylium)-[1,1'-biphenyl]-4-yl)-8-(4-(cyclopentadienyl)phenyl)-1,1,3,3,5,5,7,7-octamethyl-*s*-hydrindacene
- Compound 83** 4-(4'-(tropylium)-[1,1'-biphenyl]-4-yl)-8-(4'-(cyclopentadienyl)-[1,1'-biphenyl]-4-yl)-1,1,3,3,5,5,7,7-octamethyl-*s*-hydrindacene

- Compound 84** 4-bromo-8-(3,4-dimethylcyclopenta-1,3-diene)-1,1,3,3,5,5,7,7-octamethyl-s-hydrindacence
- Compound 85** lithium 3,4-dimethyl-1-(tributylstannyl)cyclopent-2-enolate
- Compound 86** tributyl(3,4-dimethylcyclopenta-1,4-dien-1-yl)stannane
- Compound 87** lithium 3,4-dimethylcyclopenta-1,4-dienolate
- Compound 88** 3,4-dimethylcyclopenta-1,4-dien-1-yl diethyl phosphate
- Compound 89** potassium 3,4-dimethylcyclopenta-1,4-dienolate
- Compound 90** 3,4-dimethylcyclopenta-1,4-dien-1-yl triflate
- Compound 91** 4-(4'-(tropylium)-[1,1'-biphenyl]-4-yl)-8-(4-(2,3,4,5-tetraphenylcyclopentadienyl)phenyl)-1,1,3,3,5,5,7,7-octamethyl-s-hydrindacene
- Compound 92** 4,8-bis(4-bromophenyl)-1,1,3,3,5,5,7,7-octamethyl-s-hydrindacene
- Compound 93** 4-bromobenzoic acid
- Compound 94** 7-(4-bromophenyl)-1,3,5-cycloheptatriene
- Compound 95** 3-(4-bromophenyl)-1,3,5-cycloheptatriene
- Compound 96** 2-(4-(1,3,5-cycloheptatriene)phenyl)-(pinacolato)boron
- Compound 97** 1-(4-bromophenyl)-2,3,4,5-tetramethylcyclopent-2-enol
- Compound 98** 1-(4-bromophenyl)-2,3,4,5-tetramethylcyclopenta-1,3-diene
- Compound 99** (4-(3,4-dimethylcyclopenta-1,3-diene)phenyl)-(pinacolato)boron
- Compound 100** 4-bromo-8-(4-(1,3,6-cycloheptatriene)penyl)-1,1,3,3,5,5,7,7-octamethyl-s-hydrindacence

Chapter 1

Introduction to Nonlinear Optics

1.1 Nonlinear Optics Theory

1.1.1 Introduction

The use of nonlinear optical (NLO) materials has dramatically increased since their initial development to an estimated industry of 1.65 billion dollars today.¹ The properties of these materials makes them excellent candidates for use in the ever increasing complexity and function of modern technologies, such as employed in cell phones, optical communications, medical screening technologies,² and massive and rapid data storage.¹ Additionally, NLO materials have gained further recent widespread application due to their useful electromagnetic properties.^{3,4} With the increasing technological reliance upon such materials, the development of efficient and tunable NLO materials has become a requirement in order to achieve the necessary optical sensitivities and device specificities.

NLO materials are ‘nonlinear’ in the sense that under intense electromagnetic stimuli, they display a response that is not proportional to the incident electromagnetic field.⁵ In the case of second harmonic generation (SHG) NLO, the atomic response to an applied

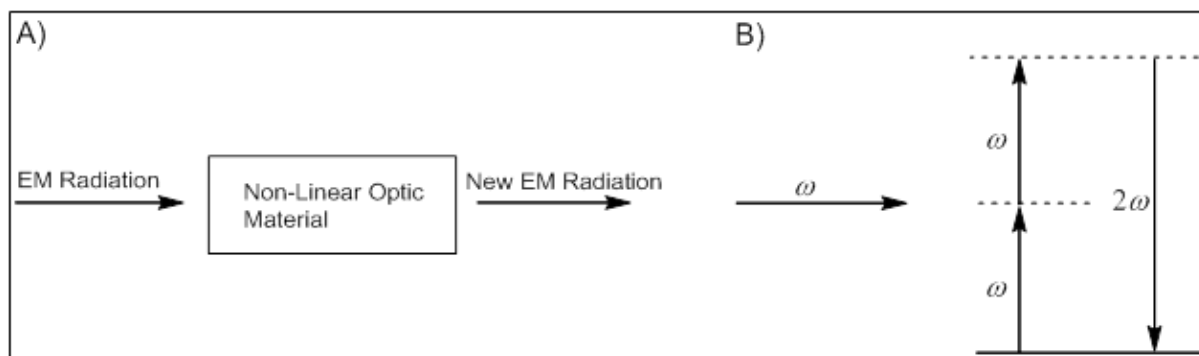


Figure 1 – A. Block diagram representation of a NLO system. B. Excitation diagram of a NLO compound.

electromagnetic field scales quadratically after an appropriate intensity of the irradiation is reached.⁵ This causes a doubling of the initial frequency. The NLO response in materials results in a redistribution of the electron density in the material. This electronic distribution change, or polarization, in a non-NLO molecule will remain linearly proportional to the electromagnetic field strength while in a NLO material the polarization response of the material will dramatically increase once a minimum excitation energy is reached. In response to an incident electromagnetic field, a NLO material will generate a new electromagnetic field with altered properties,⁶ allowing key features such as frequency and phase to be readily modulated.

The efficiency of NLO materials is an important concern due primarily to material cost and size. The efficiency of a molecular material for SHG is directly related to its molecular first hyperpolarizability (β), the second order electronic susceptibility per unit volume. The electronic susceptibility is a proportionality constant that indicates the amount of polarization in a material in response to an applied field. β represents the second order polarization of a material in a magnetic field. In this manner, Hyperpolarizability may be thought of as proportional to the second order deviation of a charge in an anharmonic field from equilibrium and is a measure of the nonlinear behavior of the system.⁵ For an efficient frequency doubling NLO material, a high β value is required. Many materials have the ability for hyperpolarization, however a material with a low β value will require a higher intensity of light for any NLO phenomena to occur.⁷ The value of β for a NLO material is based on the molecule's ability to redistribute electronic charge asymmetrically upon excitation.

$$\beta \propto (\mu_{ee} - \mu_{gg}) * \mu_{eg}^2 / \Delta E_{eg}^2 \text{ (Equation 1)}$$

The first hyperpolarizability of a molecule can be understood and estimated through a classical two-state model (Equation 1) which shows that, in order to achieve high β values, the difference in energies between the excited and ground states (ΔE_{eg}) must be small while the change in dipole moment ($\mu_{ee}-\mu_{gg}$), from ground to excited state, known as the transition dipole moment (μ_{eg}) from ground to excited state, must be large. This two-state model equation was formulated from experimental observations allowing correlations to be established between known structural features and high β value materials. Conjugated π -electron systems substituted with donor and acceptor groups, generating an asymmetric charge distribution, and with non-centrosymmetric crystal packing are among features that should yield good NLO materials (inversion symmetry will completely destroy a SHG NLO compounds efficiency).⁸⁻¹⁰

1.1.2 Push Pull Systems

The use of functional groups on a bridging unit to create an asymmetric molecular charge distribution have been described as a “push-pull” system.¹¹⁻¹⁴ This has been achieved in current molecular NLO materials through the use of a bridging subunit positioned between an electron donor and an electron acceptor. These systems contain a basic electron donating group, such as an alkyl or amino functional group, with an electron acceptor group, such as a

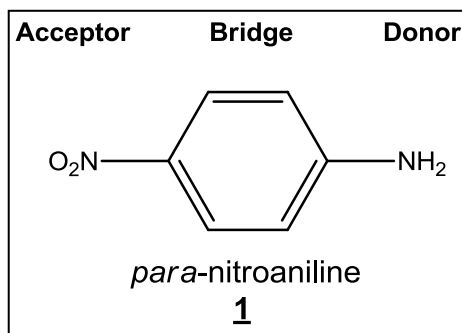


Figure 2 – *para*-nitroaniline, **1**, a simple push-pull NLO material.

nitro or cyano functionality, connected through a π -bridge, as shown by 1 in Figure 2.

The β values found for these types of systems are limited by the electronic distribution achieved through simple inductive effects. Increasing the β value in these systems requires either an increase in the electron donating/accepting potential difference between the acceptor and donor, or by lengthening the β -conjugated pathway.^{6,15,16} Lengthening the β -conjugated pathway is a reasonable approach unless the distance between the acceptor and donor becomes too great for sufficient electronic communication. Similarly, increasing the polarization effects from the donor and acceptor groups are limited by the chemically accessible units available. Additionally, molecular systems must form noncentrosymmetric arrangements when packing into a crystal system.

Most current molecular NLO materials are composed of “push-pull” organic molecular systems, such as found in *p*-nitroaniline. Due to issues with stability, robustness and low efficiencies, however, these compounds show smaller NLO effects in comparison to many extended lattice NLO materials, such as inorganic crystalline materials. Previous non-molecular efficient NLO materials, similar to those already discussed, employ extended lattice NLO materials such as inorganic crystalline materials as seen in neodymium or ytterbium-doped laser systems.^{17,18}

If a set of new, stable SHG NLO molecular materials could be created that meets the efficiency demands at multiple electromagnetic frequencies, as well as have reasonable synthetic costs, current technology prices could greatly decrease and the development of newly emerging fields of technologies would be fostered. It is hypothesized that molecular NLO

materials can be used to accomplish these goals. These molecular compounds may have ultra-fast response times, lower dielectric constants, improved processabilities and enhanced optical responses¹⁹ compared to extended lattice systems.

1.1.3 Calculations in Nonlinear Optics

To address the wide range of possible NLO material candidates computational methods were developed to examine β values without performing lengthy and costly synthesis. The development and application of perturbation theory in quantum mechanics allowed for various types of information to be calculated. Most important to the development of the methodology for calculating β was the ability to calculate the energy of a material in an applied magnetic field. Physics describes this by a Taylor expansion of the energy in the applied field, Equation 2.

$$E(F) = E(0) - \mu_i F_i - (1/2!) \alpha_{ij} F_i F_j - (1/3!) \beta_{ijk} F_i F_j F_k - (1/4!) \gamma_{ijkl} F_i F_j F_k F_l - \dots \text{ (Equation 2)}$$

Kurtz and coworkers¹⁰ reduced Equation 2 to a one dimensional form by assuming an applied magnetic field is applied only along one axis, Equation 3:

$$E(F) = E(0) - \mu_i F_i - (1/2!) \alpha_{ii} F_i^2 - (1/3!) \beta_{iii} F_i^3 - (1/4!) \gamma_{iiii} F_i^4 - \dots \text{ (Equation 3)}$$

Where $E(0)$ is the energy of the system with no applied field, μ is the dipole moment, α is the linear polarizability, β is the first hyperpolarizability and γ is the second hyperpolarizability.

Ending the expression after the 4th term and applying 4 field strengths ($\pm F$, $\pm 2F$) all constants can be solved. β in particular is solved through Equation 4.¹⁰

$$\beta_{iii} F_i^3 = [E(F_i) - E(-F_i)] - (1/2)[E(2F_i) - E(-2F_i)] \text{ (Equation 4)}$$

Using the calculated linear electric field values, multidimensional electric field values can be applied to solve for β in multiple dimensions.¹⁰

$$\beta_{ijj}F_iF_j^2 = (1/2)[E(-F_i, -F_j) - E(F_i, F_j) + E(-F_i, F_j) - E(F_i, -F_j)] + [E(F_i) - E(-F_i)] \quad \text{(Equation 5)}$$

$$\beta_{\text{total}} = [(\beta_{xxx} + \beta_{xyy} + \beta_{xzz})^2 + (\beta_{yyy} + \beta_{yzz} + \beta_{yxx})^2 + (\beta_{zzz} + \beta_{zxx} + \beta_{zyy})^2]^{1/2} \quad \text{(Equation 6)}$$

This leads to β being described by a 3x3x3 matrix (27 components) which is then reduced to ten components due to Kleinman symmetry.¹⁰ These ten components are calculated *via* computational program. The ten output components can then be inserted into Equation 6 to calculate the β_{total} of the material.

1.1.4 [5.6.7] Quinarene Derivatives

We have previously proposed a new class of proposed NLO materials involving an aromatic donor and acceptor design that is based on a series of [5.6.7] quinarene derivatives (Figure 3).²⁰ Quinarene, a known literature compound, has potentially interesting optical

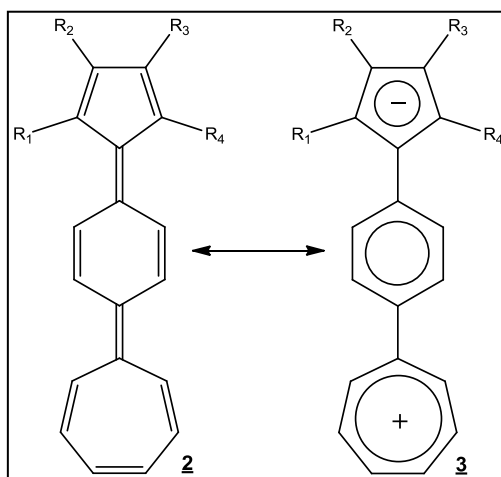


Figure 3 – [5.6.7] Quinarene in its resonance forms.

properties as a non-linear optic material based upon extensive calculations.²⁰ This parent compound was the starting point for our group's initial theoretical consideration of charged, rigid donor-acceptor NLO systems, such as those shown in Figure 4.²¹ Prior to our previous theoretical work, the use of charged aromatic donor and acceptor groups had not been explored. It was discovered that, although the non-coplanar form of quinarene was expected to be good NLO material, the difference in energy between its ground state and excited state is not large enough to foster a large β value. Most importantly, free rotation of the charged pendant groups around quinarene's center ring allows delocalization of the charge that greatly lowers the charge localization in the system (Figure 3). Attempts to minimize charge delocalization through simple pendant ring substitution have yielded compounds more, Figure 4, but not with improved NLO properties.²²⁻²⁵ It was, therefore, hypothesized that preventing charge delocalization by means of a boron cluster bridge or hindering the free rotation of the pendant charged aromatic groups would increase the β value.

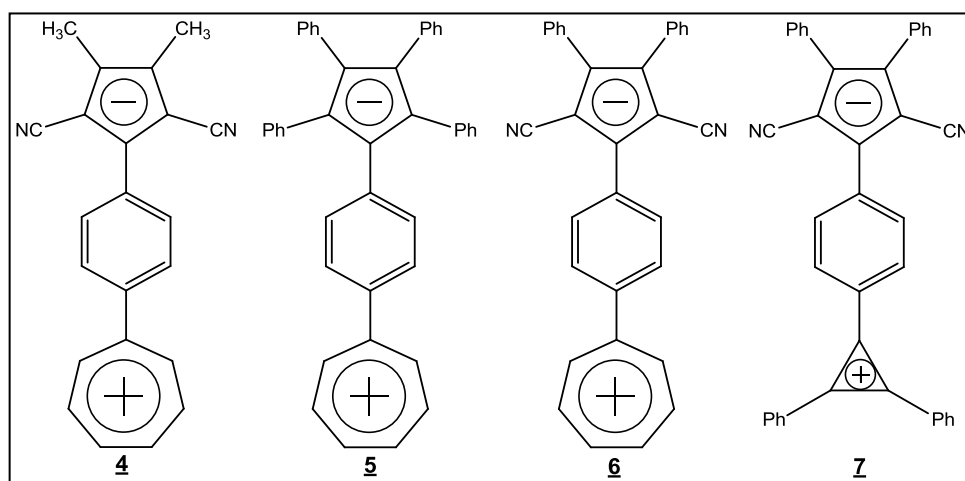


Figure 4 – Stabilized NLO compounds found in literature.²²⁻²⁵

1.2 Polyhedral NLO Compounds

1.2.1 Introduction

Initial work in new SHG NLO materials with charged aromatic donor and acceptor moieties focused initially on the use polyhedral-based systems. The polyhedral boron-based clusters display particularly attractive attributes for use in NLO materials such as: permanent dipole moments, three-dimensional aromatic molecular structures and a relatively large number of polarizable and delocalized electrons in a cluster framework. Beyond the electronic properties of borane clusters that make them potentially attractive as NLO materials, the polyhedral clusters display many desired physicochemical characteristics as well. These include high thermal and chemical stabilities while displaying synthetic properties similar to those of benzene, i.e. they undergo electrophilic substitution reactions as opposed to addition reactions and have synthetically “addressable” cage positions that can direct the site of cage substitution

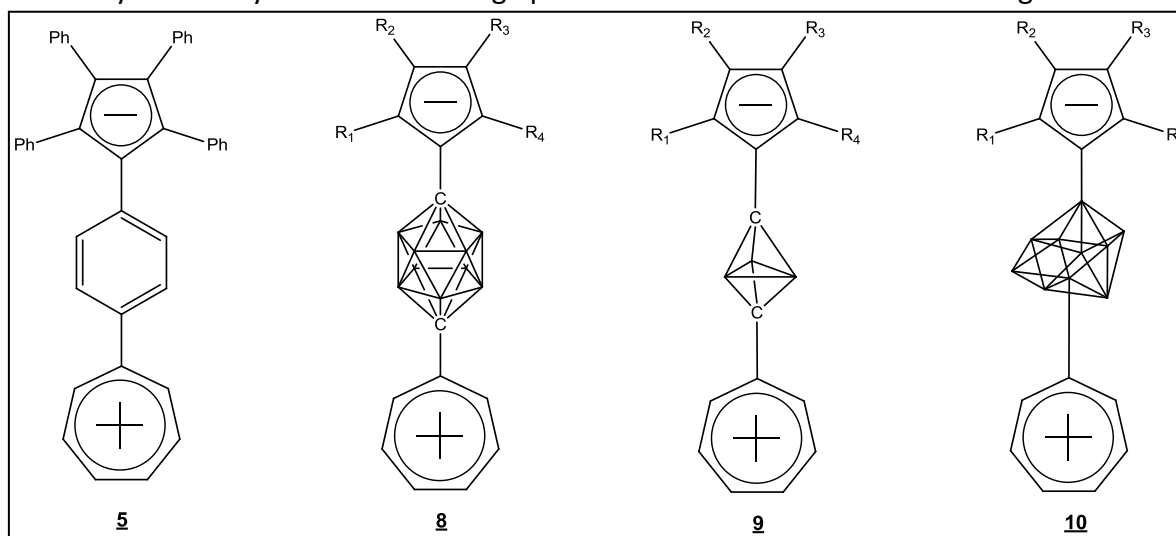


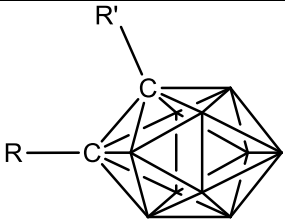
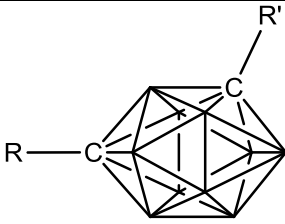
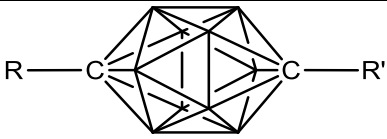
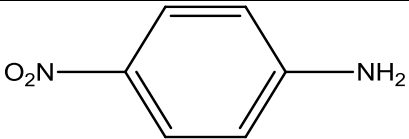
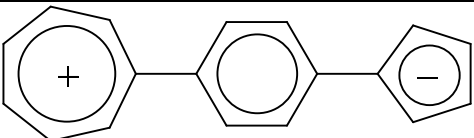
Figure 5 – 5 – [5.6.7] quinarene target from literature. **8** – *p*-carborane analog of **5**. **9** & **10** – Computationally calculated NLO carborane systems.

reactions.^{6,26,27}

Several boron polyhedral compounds have been explored computationally for their use in NLO materials, including C_2B_3 ,²⁸ C_2B_4 ,²⁹ and $B_{10}H_{10}$,⁶ but only those with a C_2B_{10} framework have been attempted synthetically to our knowledge. The icosahedral C_2B_{10} cluster framework has been examined as a NLO bridging unit both computationally and synthetically for several years with most work focusing on the *para*-substituted analog, **8**. The choice of the 1,12- C_2B_{10} cluster (*p*-carborane) is primarily due to its maximized dipole moment of the molecule and structural features in comparison to other icosahedral C_2B_{10} cluster isomers, 1,2-dicarborane (*o*-carborane) and 1,7-dicarborane (*m*-carborane).

The use of tropylium and cyclopentadienyl ions as the electron acceptor and donor units, respectively, were chosen for several reasons. The first is that these charged species may be ring-substituted to form a range of substituted compounds which may be used to fine tune the NLO compound's response. The charged nature of both rings also leads to the possibility of interaction with metal atoms of different natures which may also display interesting optical properties. The most important reason, however, for the choice is that these acceptors and donors are aromatic moieties and display aromatic π -stabilization leading to a stabilization of the maximum charge separation. This leads to highly desirable HOMO and LUMO molecular orbitals that facilitate large hyperpolarizabilities (*vide infra*). These factors combine with the permanent dipole arising from the use of polyhedral cage compounds has been hypothesized to significantly reduce potential delocalization of the charge within the molecule while allowing sufficient electronic communication.

Table 1 – A summary of computed hyperpolarizability values.³⁰

Carborane Based NLO Compounds	R, R'	β^a
 <p>1,2-(<i>ortho</i>)-dicarborane</p>	R = C ₇ H ₆ , R' = C ₅ H ₄	55.1
 <p>1,7-(<i>meta</i>)-dicarborane</p>	R = C ₇ H ₆ , R' = C ₅ H ₄	110.1
 <p>1,12-(<i>para</i>)-dicarborane</p>	R = C ₇ H ₆ , R' = C ₅ (CN) ₂ Me ₂ R = C ₇ H ₆ , R' = C ₅ (CN) ₂ Ph ₂ R = C ₇ H ₆ , R' = C ₅ H ₄ R = C ₇ H ₆ , R' = C ₅ Me ₄ R = C ₇ H ₆ , R' = C ₅ Et ₄	681.9 998.0 1063.5 1353.5 1783.1
Non-Carborane Based NLO Compounds		β
 <p><i>p</i>-nitroaniline</p>	<u>1</u>	5.3
	<u>3</u> *All co-planar	52.1

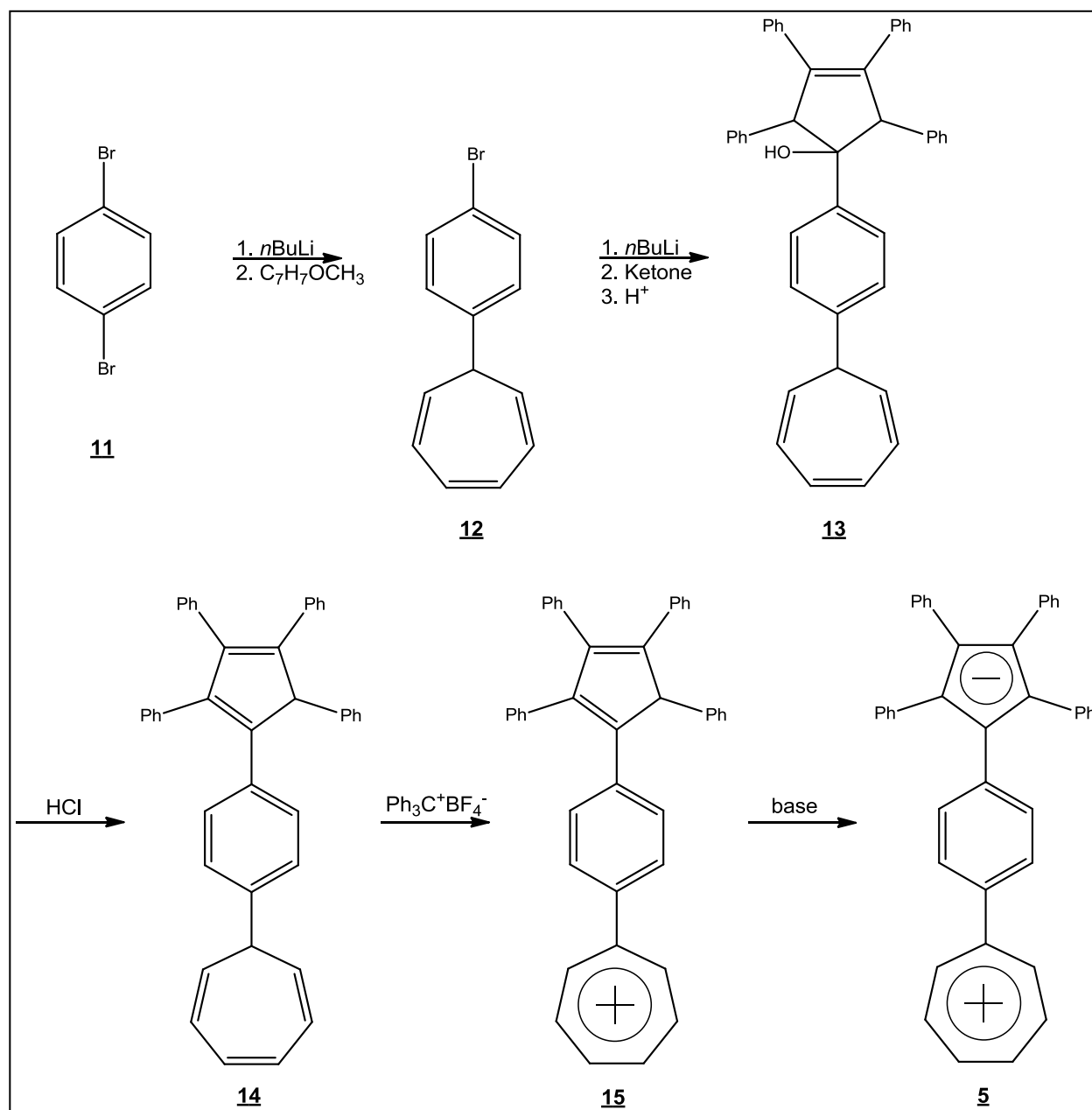
^a Calculated in units of $\times 10^{-30} \text{ cm}^5 \text{ esu}^{-1}$ at 0.5 eV using the E4 method.

Computational studies on icosahedral carborane compounds with pendant charged donor and acceptors have shown that they have very large β values, as illustrated in Table 1.⁶ First hyperpolarizability measurements of β are given in units of $\times 10^{-30} \text{ cm}^5 \text{ esu}^{-1}$ with materials typically having a values between 10 to 100 considered to be large, 100 to 500 very large and any value obtained over 500 is considered exceptional (at 1.0 eV excitation). As seen in Table 1, the previously mentioned [5.6.7] quinarene molecule (**3**) has a calculated β value of $52.1 \times 10^{-30} \text{ cm}^5 \text{ esu}^{-1}$ at 0.5 eV excitation.⁶ Although this is larger than the organic NLO benchmark compound of *p*-nitro aniline ($5.3 \times 10^{-30} \text{ cm}^5 \text{ esu}^{-1}$), it is still smaller than the calculated values for dicarborane based materials which range from $55.1 \times 10^{-30} \text{ cm}^5 \text{ esu}^{-1}$ (*ortho*-isomer) to $1783.1 \times 10^{-30} \text{ cm}^5 \text{ esu}^{-1}$ ($((\text{C}_7\text{H}_6)\text{-}p\text{-C}_2\text{B}_{10}\text{H}_{10}(\text{C}_5(\text{CN})_2\text{Ph}_2)$).⁶ It also shows another interesting point of comparison: the substituents located on the cyclopentadienyl ring greatly affect the β values of the compound. Due to the predicted NLO properties of the cluster-based compounds, much time and effort have been dedicated to their synthesis.

1.2.2 Previous Work in Polyhedral NLO Synthesis

Synthetic attempts to form carborane bridged NLO compounds have been met with mixed results. Niem's original synthetic pathway for the synthesis of the organic quinarene system, as shown in Scheme 1, was applied by analogy to the development of both *p*-carborane based and *m*-carborane based NLO materials.³¹ In the synthesis of quinarene, the starting material, 1,4-dibromobenzene, **11**, undergoes lithium-halide exchange to make the ring an nucleophile. Upon reaction with 7-methoxycycloheptatriene, the addition of the seven-

membered ring system occurs to the central benzene unit forming compound **12**. A second addition of lithium followed by addition of an α,β -unsaturated cyclopentenone forms a substituted tertiary alcohol, **13**. Removal of this alcohol through elimination creates a cyclopentadiene ring which has been shown to be very reactive even at subzero temperatures. Due to this reactivity, substitutions on the 2, 3, 4 and 5 positions of the cyclic ketone were explored by Niem.²⁵ Using phenyl substitution, dehydration of **13** through acid reflux produced **14**. The use of the Dauben reaction allows the removal of a hydride ion to convert **14** into compound **15**. Deprotonation of the cyclopentadiene in the final step in synthesis yields the target compound, **5**.



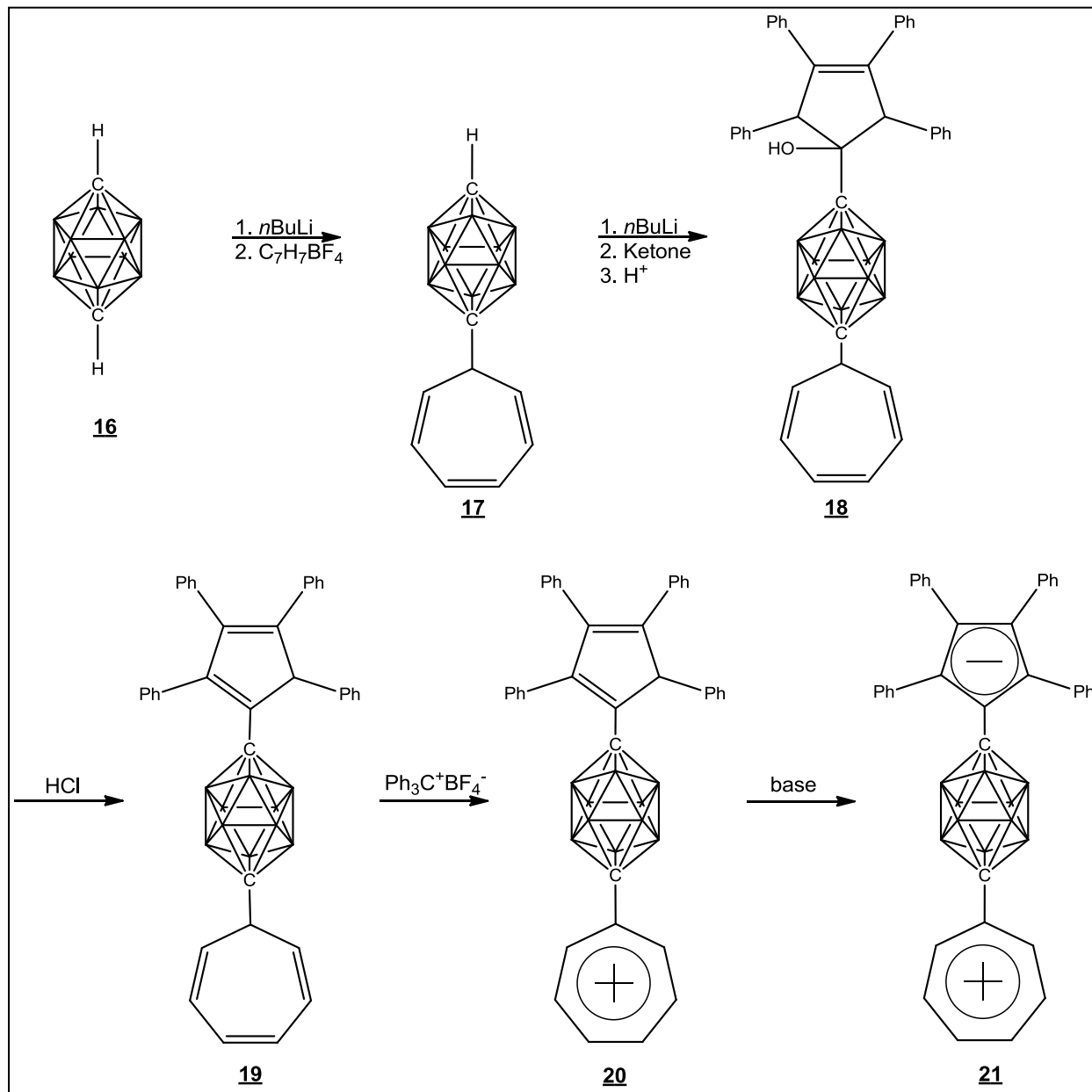
Scheme 1 – Neim’s synthetic pathway to **5**.

The proposed synthetic pathway for the carborane analog parallels the quinarene synthesis with an alteration in the initial metalation step. Instead of starting with a dibromo-carborane species, it is possible to use organolithium bases to deprotonate the carborane cages

at the carbon position to allow for nucleophilic substitution. Using this approach, the starting material is simply the appropriate carborane isomer instead of a dibromo-carborane compound (Scheme 2).

Synthetic problems arose, however, in previous work by former group members in the synthesis of the substituted *p*-carborane employing the above strategy.²⁹ For example, in the deprotonation of the cyclopentadiene ring after it had been attached to the cluster framework (formation of **21**), multiple attempts using a variety of bases were performed, however, none produced desired deprotonated compound. Several attempts were made to stabilize the target compound, **21**, through substitution on the cyclopentadienyl ring, although these also did not produce a stable anion.²⁹ A variety of schemes for the direct aromatic ring attachment and other approaches were unsuccessfully employed. Although a variety of new substituted carborane cages were achieved, no suitable materials with anticipated desirable NLO properties were produced. It has been hypothesized that the inability to detect a stabilized cyclopentadienyl ring has to do with the strength of the base produced.²⁹ The negatively charged ring is produced but easily protonated due to its high pK_a. Attempts to modify this with the addition of electron withdrawing groups on the ring, such as cyano groups, apparently were not sufficient to stabilize the anion.²⁹ Other approaches were also explored including Cp ring organometallic substitution, rearrangement of the cyclopentadiene starting system and

others. A new hypothesis for stabilizing the anion has now been developed and several new synthetic targets have been designed. This work will be discussed in chapter two of this thesis.



Scheme 2 – Paralleling Niem’s synthesis of **5**, the hypothesis for synthesized **21** proceeded in a similar fashion.

1.3 Rigid Organic NLO Compounds

1.3.1 Introduction

Both synthetic and theoretical work on the hypothesized polyhedral-based NLO compounds led to the consideration of several new potential organic NLO compounds. It is known that the separation of the two charged pendant groups' electronic properties is imperative to the effectiveness of the NLO optical compound. This separation would allow a localized charge on opposite ends of a molecule, giving a large transition dipole moment.

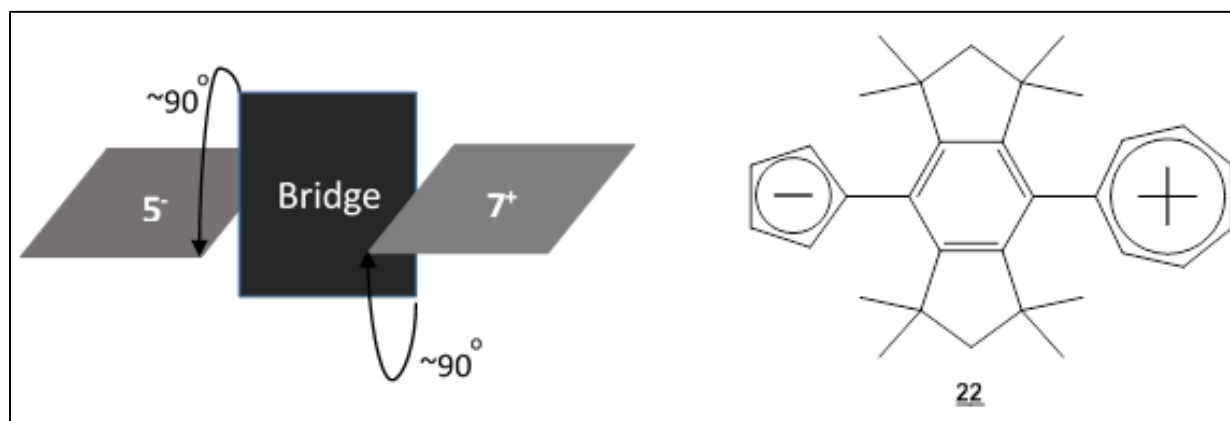


Figure 6 – A view of the hindered rotation and the target compound **22**.

Calculations of potential target compounds that could be pursued synthetically were performed. It was found that, as anticipated, having the donor and acceptor ring unable to delocalize their electrons through the bridging unit leads to increased β values. As shown in Figure 6, the redistribution of π -electrons is facile in a planar system but, if instead the three rings were not all coplanar, the delocalization of these electrons would be greatly reduced and potentially a large β value would be generated. To achieve this disruption of coplanarity, the

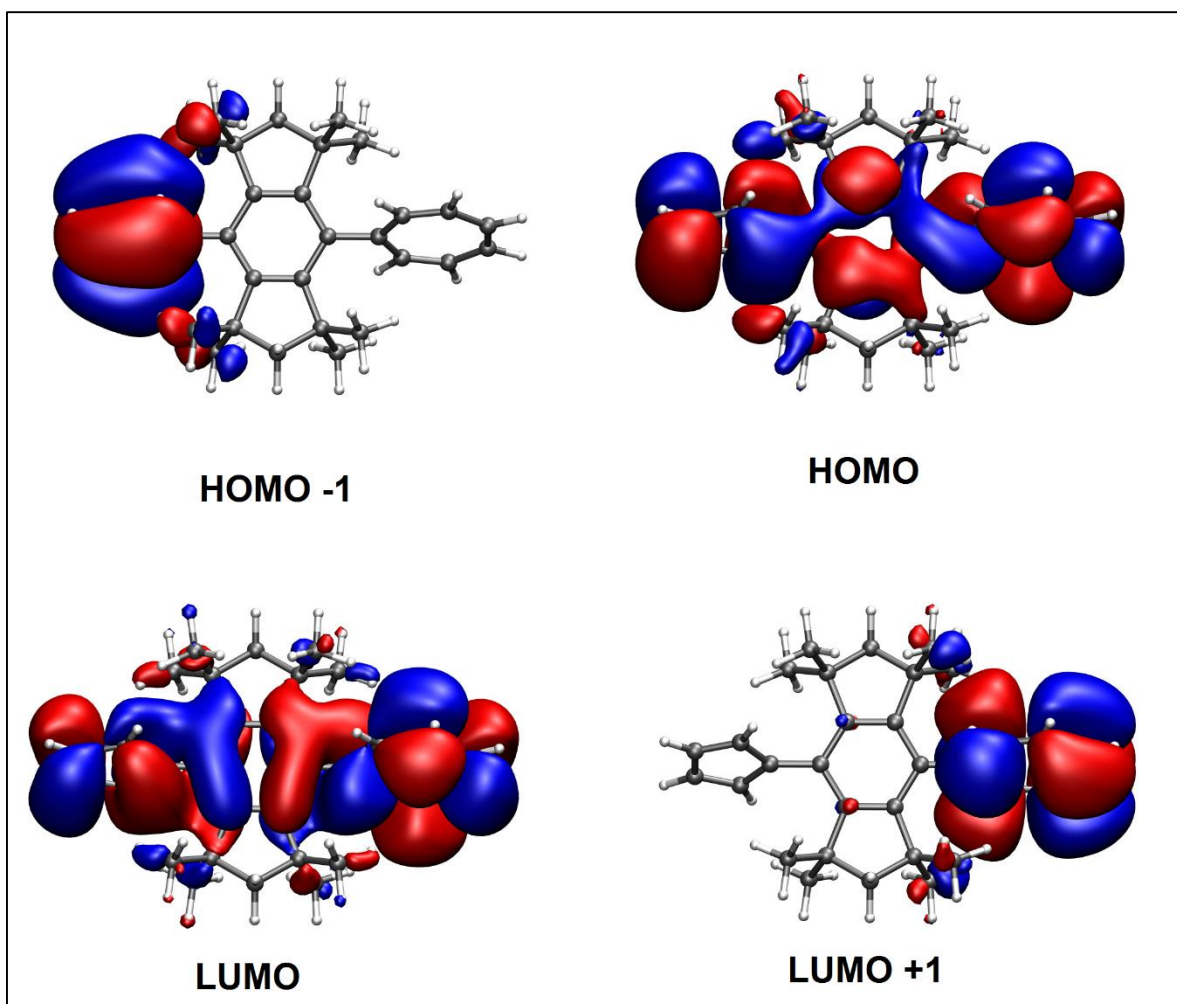
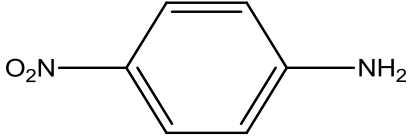
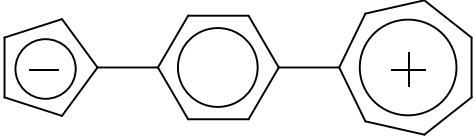
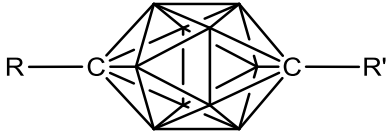
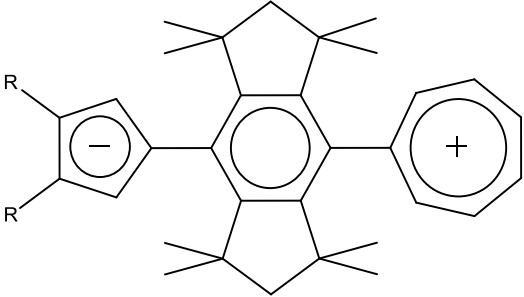


Figure 7 – Orbital diagrams for ideally-substituted hydrindacene bridge NLO compounds.

approach taken has been to construct a rigid and sterically demanding backbone small enough to allow the rings to be attached but sufficiently sterically encumbered to prevent rotation, all while allowing a necessary amount of communication between the two pendant rings. Based on previous computational work in group, the organic hydrindacene framework emerged as a promising bridging subunit for appending the charged aromatic subunits.^{6,21} Due to the steric bulk of the methyl groups of 1,1,3,3,5,5,7,7-octamethyl-*s*-hydrindacene, it was computed that the attached pendant aromatic charged species would be displaced well out of the plane of π -conjugation, approaching a 90° twist away from the bridging ring system. Semi-empirical

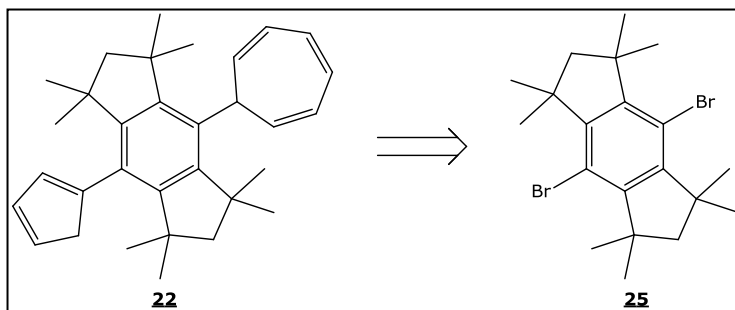
Table 2 – A comparison of different NLO materials to the hypothesized **23** and **24**.

Non-Linear Optic Material Structure	Compound: R, R'	β^a
	1	5.3
	3 *All rings coplanar	52.1
	6 R = C ₇ H ₆ , R' = C ₅ (CN) ₂ Ph ₂	1783.1
	23 R = CH ₃ 24 R = Ph	4049.8 4701.8

^a Calculated in units of $\times 10^{-30} \text{ cm}^5 \text{ esu}^{-1}$ at 0.5 eV using the E4 method. calculated orbitals show that this arrangements generates a charge density localized at the two distal regions in the compound as desired. The HOMO diagram shows the electron density all amongst the molecule. Upon excitation, the LUMO shows a nearly complete shift from bonding orbitals to antibonding orbitals. Further excitation to the LUMO+1 shows the electron density primarily centered around cyclopentadienyl (Figure 7). The large change in dipole between the ground state and excited state along with the excellent charge separation (26.93 Debye) results in a very large calculated β value. Comparing the predicted β values for this substituted hydrindacene compound to both the idealized substituted *p*-carborane cage and current standards, show a dramatic increase in the predicted β value.

1.3.2 Previous Synthetic Work in Rigid NLO Compounds

The theoretical treatment of the rigid organic NLO systems based upon the quinarene and hydrindacene systems has inspired several early attempts at the synthesis of these quinarene/s-hydrindacene compounds. The first synthetic attempts hypothesized that the formulation of the desired compound could parallel the pathway taken by Niem (Scheme 1), and pendant groups could be added to an already present bridging compound, as seen in Scheme 3. Problems in this synthetic pathway were discovered having to do with the size of the pendant group relative to the limited space for the approach of the nascent pendant groups to the bridging compound. An in depth examination and well as hypotheses on alternative synthetic methods are presented in chapter three. These include the use of a quinarene starting material followed by formation of the bridge as well as a 'partial construction' method in which part of the bridge is formed, then the donor and acceptor are attached followed by finishing the backbone.



Scheme 3 – The hypothesized retrosynthetic pathway of the target rigid organic NLO family of compounds.

Chapter 2

Synthesis towards Polyhedral Based NLO Materials

2.1 Introduction

The use of polyhedral compounds as bridging units for NLO materials has been of interest for many years. Multiple papers from our group have reported on the results of computational studies for these species, such as compounds **8** and **26** seen in Figure 8, and have indicated that they should provide new approaches to efficient NLO materials.^{6,29,30,32} However, synthetic work in the preparation of these compounds has proved to be more difficult than initially anticipated primarily due to problems in the functionalization of the donor ring.^{29,30,33} It has been hypothesized that the large pK_a of the donor ring may deprotonate other neighboring

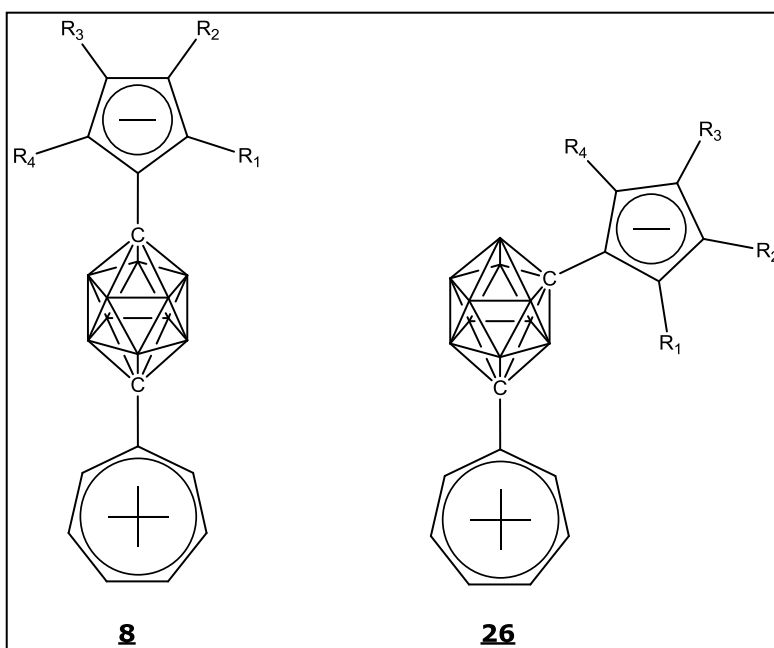


Figure 8 – Schematic drawing of compounds **8** and **26**, both *para* and *meta* carborane analogs of **3** have been explored in literature.^{29,30}

species, leaving it in an uncharged state and preventing the isolation of the aromatic Cp ring system.²⁹ Several attempts to stabilize the product by the addition of electron withdrawing groups and sterically bulky systems have likewise been unsuccessful.²⁹

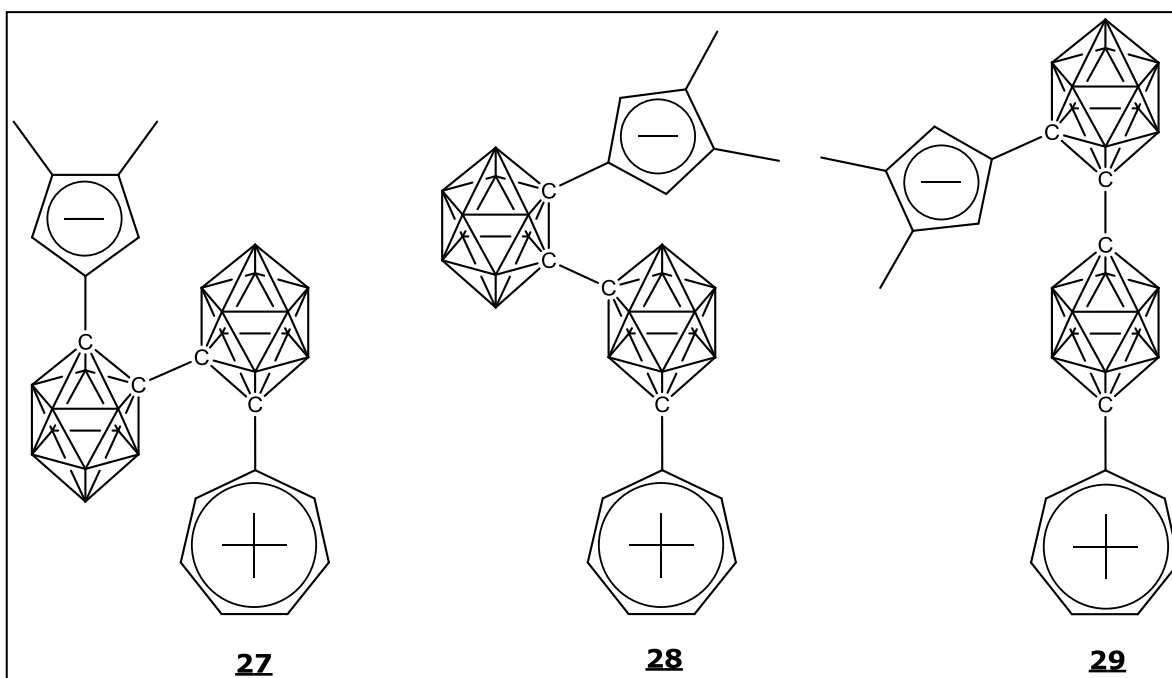


Figure 9 – Hypothesized multi cage systems for use as NLO materials.

It is hypothesized that the use of a linked, multi-cage system with the electron donor attached to one cage and the electron acceptor connected to the other linked cage, such as illustrated in Figure 9, might overcome the synthetic problems observed in previous work. *o*-Carborane, 1,2-C₂B₁₀H₁₂, is known to be an electron withdrawing group²⁶ and could be combined with other possible functional groups on the donor ring to stabilize the final charged species.^{20,25} Because of steric considerations, it is hypothesized that a multiple cage system would also be required in order to use *o*-carborane as a bridging unit. Previously reported calculations of *o*-carborane as a single bridge unit have resulted in a lower calculated β value relative to other cage configurations due to its overall lower dipole moment.⁶ It is hypothesized that by increasing the distance between the donor and acceptor groups through the addition of a larger bridging group may also result in an increased β value. This has been born out by

calculated β values for multi-cage systems (*vide infra*). The linked cage motif may also provide a more facile synthetic route by allowing the two “halves” of the final target molecule to be prepared independently and then conjoined at the end of the synthesis.

In the work reported here, several methods for the synthetic exploration of these multi-cage compounds has been examined and will be presented and discussed including convergent and linear synthetic approaches. Computational explorations into the optical properties of compounds **26** to **28** are reported using density functional theory to examine β values in a similar fashion to previous works.^{27,28,34} Although semi-empirical methods have been shown to provide a reliable computational method that has been used previously for carborane NLO calculations,⁶ problems have arisen regarding the intricate linked multi-carborane structures while optimizing geometries.

2.2 Experimental

2.2.1 Physical Measurements

All NMR spectra were recorded on samples dissolved in CDCl_3 , $\text{DMSO-}d_6$ or $\text{acetone-}d_6$, in 5 mm (o.d.) tubes. Proton (^1H), carbon (^{13}C) and boron (^{11}B) NMR spectra were recorded on either a Bruker DPX-300 spectrometer operating at 300.15 MHz for proton, 77.47 MHz for carbon, or a Bruker Ascend-400 with Prodigy CryoProb attachment operating at 400 MHz. Chemical shifts were referenced to either residual CHCl_3 ($\delta = 7.26$ ppm) or residual DMSO ($\delta = 2.50$ ppm) in the sample. The spectrometer was operated in the FT mode while locked on the deuterium resonance of the CDCl_3 or $\text{DMSO-}d_6$ solvent. The reference was set relative to tetramethylsilane from the known chemical shifts of the CDCl_3 ($\delta = 77.23$ ppm) and DMSO ($\delta = 39.52$ ppm) carbon atoms. All NMR data are reported in ppm. Unit resolution mass spectra were obtained on a Hewlett Packard model 5989B gas chromatograph/mass spectrometer (GC/MS) using an ionization potential of between 11 and 70 eV. FT-IR in the range of 400 to 4000 cm^{-1} were measured on a Mattson Galaxy 2020 spectrometer or a Perkin Elmer FT-IR Spectrometer Paragon 1000 and were referenced to the 1602.8 cm^{-1} band of polystyrene. All sonication was performed using a SONAER Model 241 running at 2.4 MHz. Silica used for column chromatography was Silicycle SiliaFlash P60 with a particle size of 40-63 μm (230-400 mesh).

2.2.2 Materials

All solvents used were reagent grade or better. Diethyl ether, tetrahydrofuran, toluene, benzene and hexanes were distilled from sodium prior to use with a benzophenone indicator. Dichloromethane, methanol and dioxane were distilled from calcium hydride before use. TLC plates were purchased from Sigma-Aldrich and used as received. Visualization of compounds on the TLC plates was performed using either ultraviolet light or 2% PdCl₂ in methanol. All organometallic reagents were titrated before use with a 1.0 M solution of diphenylacetic acid in dry tetrahydrofuran. *Ortho*-carborane (1,2-C₂B₁₀H₁₂), *meta*-carborane (1,7-C₂B₁₀H₁₂) and *para*-carborane (1,12-C₂B₁₀H₁₂) were purchased from either Katchem, Inc., Synthonix, Inc., or Sigma Aldrich and used as received. *n*BuLi (1.6 M in hexanes or 2.5 M in hexanes), *t*-butyllithium (1.7 M in pentane), and 2,3,4,5-tetramethyl-2-cyclopenten-1-one were purchased from Sigma Aldrich and used as received. Tropylium tetrafluoroborate was purchased from Alfa Aesar. 3,4-dimethyl-2-cyclopenten-1-one,⁴⁴ 3-methyl-2-cyclopenten-1-one,⁴⁵ and copper (I) chloride^{46,47} were synthesized according to appropriate literature methods. Deuterated solvents were purchased from Cambridge Isotopes and dried over 3Å molecular sieves before use. All other commercially available reagents were used as received.

2.2.3 Experimental Procedure

3-(1,12-C₂B₁₀H₁₃)-1,3,5-cycloheptatriene (30).²⁹ To a stirred solution of *p*-carborane (437 mg, 3.03 mmol, 1,12-C₂B₁₀H₁₂) in 10 mL of dry benzene at -78° C and under a dry N₂ atmosphere was added *n*BuLi (2.5 mL, 3.94 mmol) slowly dropwise. The solution was stirred for 30 minutes at -78° C then warmed slowly to room temperature. After 30 minutes at room temperature, the solution was cooled to -78° C and tropylium tetrafluoroborate (540 mg, 3.03 mmol) was added at once in a single portion. The reaction was slowly warmed to room temperature and stirred overnight. The reaction was quenched with 10 mL of 2 M HCl and the layers separated. The separated organic layer was washed with saturated aqueous NaHCO₃ solution (20 mL) followed by brine (20 mL). The removal of the solvent afforded a white semisolid that was purified through column chromatography and eluted with hexanes (R_f = 0.55). The residue was dissolved in toluene and refluxed for 4 hours. After cooling to room temperature, the solvent was removed through slow evaporation to dryness leaving large crystals of high quality for x-ray diffraction in 49% yield (2 steps, 0.35 g, 1.4 mmol.). R_f = 0.55 (hexanes). ¹H-NMR (CDCl₃): δ 1.5-3.2 (br m, 10H, HCB₁₀H₁₀-), 2.06 (t, 2H, C₇H₇, 7-CH₂), 2.74 (br s, 1H, HCB₁₀H₁₀C-), 5.25 (m, 1H, C₇H₇, 6-CH), 5.41 (m, 1H, C₇H₇, 2-CH), 5.95 (d, 1H, J = 8 Hz, C₇H₇, 2-CH), 6.04 (dd, 1H, J = 9.2 Hz, 6 Hz, C₇H₇, 5-CH), 6.55 (d, 1H, J = 6 Hz, C₇H₇, 4-CH). ¹³C-NMR (CDCl₃): δ 27.5, 59.6, 77.2, 119.8, 123.1, 125.5, 126.0, 130.2, 138.9. ¹¹B-NMR (CDCl₃): δ -15.2 (s, 5H, J = 513 Hz), -12.4 (s, 5H, J = 513).

1-(1,2-C₂B₁₀H₁₁)-3-methylcyclopenta-1,3-diene (32).^{29,30} To a stirred solution of *o*-carborane (0.22 g, 1.39 mmol, 1,2-C₂B₁₀H₁₂) in 2.0 mL of dried toluene at -78° C under a dry N₂

atmosphere was added *n*BuLi dropwise (0.95 mL, 1.52 mmol). The solution was then stirred for 30 minutes at -78° C and then warmed slowly to 0° C. After 30 minutes of stirring at room temperature, the solution was cooled to -78° C and 3-methyl-2-cyclopenten-1-one (0.13 g, 1.39 mmol) was added dropwise. After the addition was complete, the reaction was allowed to warm to 0° C. The reaction was then allowed to slowly warm to room temperature and stir overnight. The reaction was quenched with 1 M HCl (10 mL) that was added dropwise. The aqueous layer was separated and washed with diethyl ether (3 x 20 mL). The organic layer and the diethyl ether washes were combined and the solvent removed *via* rotoevaporation to leave a yellow oil. The yellow oil was dissolved in methanol (5 mL) and heated at reflux for 30 minutes. Concentrated HCl (1 mL) was added dropwise to the reflux solution. After 1 hour the reaction was cooled to room temperature and quenched with 10% NaHCO₃ (10 mL) and diethyl ether (10 mL). The aqueous layer was then extracted with diethyl ether (3 x 5 mL) and the organic layers were combined. Rotoevaporation of the organic layers left a yellow oil. The NMR data obtained for this product compound were not consistent with the 1,2-addition product. Purification through methods similar to literature did not provide the desired product.

1-(1,2-C₂B₁₀H₁₁)-2,3,4,5-tetramethyl-cyclopenta-2-en-1-ol (34).^{29,30} To a stirred solution of *o*-carborane (0.22 g, 1.4 mmol, 1,2-C₂B₁₀H₁₂) in 2 mL of dried toluene at -78° C under a dry N₂ atmosphere was added *n*BuLi (0.95 mL, 1.5 mmol) dropwise. The solution was stirred for 30 minutes then warmed to 0° C. After stirring for 30 minutes, the solution was cooled to -78° C and the 2,3,4,5-tetramethyl-2-cyclopenten-1-one (0.19 g, 1.4 mmol) was added dropwise. After the addition was complete, the reaction was allowed to slowly warm to 0° C. The reaction was then slowly warmed to room temperature and allowed to stir overnight. The reaction as

quenched with 1 M HCl (2 mL). The aqueous layer was separated and washed with diethyl ether (3 x 5 mL). The organic fractions were combined and the solvent removed *via* rotoevaporation to leave a yellow oil. The NMR of this compound again showed results inconsistent with 1,2-addition. Purification of this unknown compound was performed through chromatographic methods (5:1 hexanes: acetone) to produce an off white solid.

Recrystallization from 1:1 diethyl ether: hexanes produced white needles. The isolated product was found to be the product from a 1,4-addition process, (3-(1,2-C₂B₁₀H₁₁)-2,3,4,5-tetramethylcyclopentanone (**36**), instead of the 1,2-addition product, (1-(1,2-C₂B₁₀H₁₁)-2,3,4,5-tetramethylcyclopenta-2-en-1-ol, **34**). 15% yield, 0.21 mmol obtained. $R_f = 0.23$ (1:1 hexanes:acetone). mp. 130° - 132° C. ¹H-NMR (CDCl₃): δ 1.12 – 1.18 (ddd, 12H, C₅H₄O(CH₃)₄), 1.25 – 3.0 (br m, 10H, cage -BH) 1.81 – 1.93 (m, 2H, (O)C-CH₂), 2.425 (q, 1H, $J = 6.8$ Hz, (O)C-CH₂-CH), 3.79 (br s, 1H, cage, -CH). ¹³C-NMR (CDCl₃): δ 11.74, 13.8, 15.4, 17.5, 47.1, 48.2, 49.3, 55.5, 62.1, 85.3, 217.6. ¹¹B-NMR (CDCl₃): δ -3.2 (2B), -8.8 (2B), -10.7 (2B), -13.6 (4B).

1-(1,2-C₂B₁₀H₁₁)-3,4-dimethylcyclopenta-2-en-1-ol (37**)**.^{29,30} To a stirred solution of *o*-carborane (0.22 g, 1.4 mmol, 1,2-C₂B₁₀H₁₂) in 2 mL of dry toluene at -78° C under a dry N₂ atmosphere was added *n*-butyllithium (0.95 mL, 1.5 mmol) dropwise. The solution was stirred for 30 minutes at -78° C and then allowed to warm to 0° C. After 30 minutes at 0° C, the solution was cooled to -78° C and 3,4-dimethyl-2-cyclopenten-1-one (0.15 g, 1.4 mmol) was added dropwise after which the reaction was allowed to warm to 0° C. The reaction was then slowly warmed to room temperature and stirred overnight. The reaction was quenched with 1 M HCl (2 mL). The aqueous layer was separated and washed with diethyl ether (3 x 5 mL). The organic layers were combined and the solvent removed *via* rotoevaporation to leave a yellow

oil. Purification through chromatographic methods (5:1 hexanes: acetone) produced a yellow solid. Recrystallization from 1:1 hexanes/diethyl ether gave X-ray quality crystals. The product was found to be the 1,4-addition (3-(1,2-C₂B₁₀H₁₁)-3,4-(CH₃)-C₅H₅O, **39**) instead of the 1,2-addition product (1-(1,2-C₂B₁₀H₁₁)-3,4-(CH₃)-C₅H₃-1-(OH), **37**). 17% yield, 0.24 mmol obtained. R_f = 0.26 (5:1 hexanes: acetone). m.p. 115° C. ¹H-NMR (CDCl₃): δ 1.15-1.18 (m, 6H, 3,4-(CH₃)-C₅H₅O, -CH₃), 2.00-2.05 (m, 1H, (CH₃)CH-(CH₂)), 2.28 (d, 1H, J = 17.2 Hz, cage-CH₂-C(O)), 2.50-2.72 (m, 3H, CH₂-C(O)-CH₂), 3.75 (br s, 1H, cage, -CH). ¹³C-NMR (CDCl₃): δ 15.3, 21.7, 39.7, 45.0, 46.1, 57.7, 60.5, 83.3, 212.6. ¹¹B-NMR (CDCl₃): δ -3.2 (2B), -8.9 (2B), -10.5 (1B), -11.8 (1B), -13.1 (2H), -13.8 (2B).

1-(1,2-C₂B₁₀H₁₁)-3,4-dimethylcyclopenta-1,3-diene (38).³⁵ To a stirred solution of *o*-carborane (1.00 g, 6.90 mmol) in 18 mL of dry benzene at -78° C under a dry N₂ atmosphere was added *n*BuLi (3.46 mL, 6.9 mmol) dropwise. The solution was stirred for 30 minutes then was allowed to warm to 0° C. After 30 minutes the solution was transferred *via* a cannula into a stirred solution of CeCl₃ (1.70 g, 6.9 mmol) in dry toluene (7 mL). After 30 minutes at 0° C, the temperature was lowered to -78° C and 3,4-dimethyl-2-cyclopenten-1-one (0.76 g, 6.9 mmol) was added dropwise. After the addition was complete, the reaction was warmed to 0° C. The reaction was then slowly warmed to room temperature and stirred overnight. The reaction was quenched with 1 M HCl (15 mL). The aqueous layer was separated and washed with diethyl ether (3 x 20 mL). The organic layers were combined and the solvent removed *via* rotoevaporation to leave a yellow oil. This oil was then dissolved in hot methanol and refluxed for 10 min. An addition of concentrated HCl (12 M, 1 mL) was completed dropwise and the reaction was allowed to stir at room temperature for 1 hour. The reaction was then cooled to

0° C and quenched with aqueous NaHCO₃ (20 mL) and extracted with diethyl ether (3 x 20 mL). The organic layers were combined, washed with brine and dried with MgSO₄. After removal of the solvent, column chromatographic separation using 1:1 hexanes: acetone as an eluent afforded the desired compound **38** as a yellow oil. Recrystallization from 1:1 hexanes: diethyl ether gave X-ray quality crystals of **38** in a 5.8% yield (two steps). $R_f = 0.41$ (hexanes). m.p. 115° C. ¹H-NMR (CDCl₃): δ 1.5 – 3.1 (m, 10H, cage BH), 1.80 (d, 3H, $J = 0.6$ Hz, -CH₃), 1.89 (d, 3H, $J = 0.6$ Hz, -CH₃) 2.96 (t, 2H, $J = 1.2$ H, -CH₂), 3.70 (bs, 1H, cage -CH), 6.40 (s, 1H, -C=CH). ¹³C-NMR: δ (CDCl₃) δ 12.5, 13.4, 48.4, 62.1, 74.6, 134.4, 135.7, 138.7, 139.2. ¹¹B-NMR (CDCl₃): δ -13.0 (2B), -11.6 (2B), -10.8 (2B), -9.5 (2B), -5.4 (1B), -2.2 (1B).

3-[12-(2-(1,2-C₂B₁₀H₁₀)-3,4-dimethylcyclopenta-1,3-diene)-(1,12-C₂B₁₀H₁₀)]-1,3,5-cycloheptatriene (40**).**³⁶ To a stirred solution of compounds **30** (70 mg, 0.29 mmol) and **38** (69 mg, 0.29 mmol) in dry toluene (10 mL) at 0° C under a dry N₂ atmosphere was added *n*-butyllithium (1.16 mL, 0.73 mmol) dropwise. After stirring for 2 hours, the solution was allowed to warm to room temperature and stirred for another 22 hours. Copper (I) chloride (0.15 g, 1.5 mmol) was added to the reaction in a single portion and allowed to stir for a further 48 hours. The addition of 3 M HCl (5 mL) quenched the reaction. The aqueous layer was separated and extracted with diethyl ether (3 x 10 mL). The organic layers were combined and washed with a concentrated sodium chloride solution (10 mL). The organic layer was dried over MgSO₄. Removal of the solvent *via* rotoevaporation gave a brown solid. The NMR data obtained from this reaction showed the presence of only the starting materials. Spectroscopic data for the product have been reported previously for compounds **30** and **38**.

1,1'-bis(1,2-C₂B₁₀H₁₁) (41).³⁶ To a stirred solution of *o*-carborane (1.0 g, 3.5 mmol) in dry toluene (35 mL) at -78° C under a dry N₂ atmosphere was added *n*BuLi (11.2 mL, 7.0 mmol) dropwise. The solution was stirred at -78° C for 12 hours during which time a white precipitate formed. Copper (I) chloride (0.86 g, 8.8 mmol) was then added in a single portion to the reaction. The reaction was allowed to stir for a further 72 hours at room temperature. Addition of 3 M HCl (15 mL) quenched the reaction. The aqueous layer was separated and extracted with diethyl ether (3 x 20 mL). The organic layers were combined and washed with a saturated sodium chloride solution (20 mL). The organic layer was dried over MgSO₄. Removal of the solvent *in vacuo* provided a light green solid product. Purification through flash column chromatography (hexanes) produced a pure product as a white crystalline material in a 20% yield. Spectroscopic data matched that reported in literature.³⁶ ¹H-NMR (acetone-*d*₆): δ 1.43-2.70 (br m, 20H, cage -BH), 5.04 (br s, 2H, cage -CH) ¹³C-NMR (CDCl₃): δ 64.0, 72.3. ¹¹B-NMR (CDCl₃): δ -12.5 (2B), -10.0 (2B), -9.54 (2B), -2.8 (2B), -2.3 (2B).

7-[2-(1,2-C₂B₁₀H₁₀)-(1,2-C₂B₁₀H₁₁)]-1,3,5-cycloheptatriene (42).²⁹ To a stirred solution of 1,1-bis(*o*-carborane) (0.20 g, 0.69 mmol), **41**, in 7 mL of dry diethyl ether at -78° C under a dry argon atmosphere was added *n*BuLi (0.47 mL, 0.76 mmol) dropwise over 5 minutes. This solution was stirred for 1 hour at -78° C and then allowed to warm to room temperature. After stirring for 1 hour at room temperature, the solution was cooled to -78° C and tropylium tetrafluoroborate (0.14 g, 0.76 mmol) was added in a single portion. The reaction was allowed to stir overnight during which time the reaction changed in color from a cloudy colorless solution to clear and colorless solution. The reaction was quenched with saturated NH₄Cl (20 mL) solution. The layers were then separated and the aqueous layer was extracted with diethyl

ether (3 x 10 mL). The organic layers were combined, washed with brine and dried over MgSO₄. Removal of the solvent produced **42** as an off white solid (52 mg, 0.14 mmol, 20%). *R_f* = 0.56 (hexanes) ¹H-NMR (CDCl₃): δ 1.4 – 3.1 (br m, 20H, cage –BH), 2.50 (t, 1H, C₇H₇, 7-CH), 3.82 (s, 1H, cage –CH), 4.97 (dd, 2H, 1,6-CH), 6.31 (m, 2H, C₇H₇, 2,5-CH), 6.67 (t, 2H, C₇H₇, 3,4-CH). ¹³C-NMR (CDCl₃): δ 37.6, 61.5, 70.7, 106.5, 122.4, 125.4, 130.3. ¹¹B-NMR (CDCl₃): δ -12.6 (br s, 4B), -10.5 (6B), -9.2 (4B), -7.4 (2B), -2.5 (2B), -1.7 (2B).

3-[2-(2-(3,4-dimethyl-2-cyclopenten-1-ol)-)-(1,2-C₂B₁₀H₁₀)-(1,2-C₂B₁₀H₁₀)]-1,3,5-cycloheptatriene (43**).**³⁵ To a stirred solution of **42** in diethyl ether at 0° C under a dry Argon atmosphere was added *n*BuLi (0.10 mL, 0.16 mmol) dropwise over five minutes. The solution was stirred for an hour at 0° C and then allowed to warm to room temperature. After stirring for an hour at room temperature, the solution was cooled to 0° C and 3,4-dimethyl-2-cyclopenten-1-one (17 mg, 0.16 mmol) was added dropwise. The reaction was stirred overnight and checked periodically by TLC. After 12 hours of stirring the reaction was quenched with 1M HCl. The NMR data of the organic layer showed on the presence of unreacted starting material, **42**. Spectroscopic data for the starting material has been previously reported above.

2.2.4 Calculations

Calculations on multi-cage NLO compounds were run on a Processor: Intel(R) Core(TM) i5-2500 CPU @ 3.30 GHz and 16.0 Gb of RAM with a 64-bit Windows Enterprise operating system or a Gateway NV55C with an Intel® Pentium CPU P6100 @ 2.00GHz (x2) and 3.00 Gb of RAM with a 64-bit Windows 7 operating system. Either GaussView 5.0 or Avogadro was used

for molecule construction and Gaussian 09W was used for calculation processing. Cage-cage units were geometrically optimized through Density Functional Theory B3LYP 6-31G+ 2D2P. Addition of tropylium and cyclopentadienyl to the optimized cage-cage units were performed on GaussView 5.0. β were values calculated using semi-empirical methods with AM1 parameterization in the E4 method. Hyperpolarizabilities were calculated at both 0.0 eV and 0.5 eV (0.01837 Hartrees) and are reported in units of $\text{cm}^5\text{esu}^{-1}$. Molecular orbital images were created using Avogadro from data obtained from Gaussian 09W.

2.2.5 Crystallographic Studies

All crystals suitable for single crystal X-ray diffractometry were removed from a vial and immediately covered with a layer of silicone oil. For each compound investigated, a single crystal was selected, mounted on a glass rod on a copper pin and placed in the cold N_2 stream using an Oxford Cryosystems cryometer. XRD data collection was performed for compounds **30**, **36**, **38** and **39**, on a Bruker APEX II diffractometer using $\text{Mo K}\alpha$ radiation ($\lambda = 0.71073 \text{ \AA}$) equipped with a CCD area detector. Empirical absorption corrections were applied using SADABS.^{36,37} The structures were solved by using either direct methods or the Patterson option in SHELXS and refined by the full-matrix least-squares procedures in SHELXL.^{38,39} The space group assignments and structural solutions were evaluated using PLATON.^{40,41} The solvent of crystallization for compound **38** was removed from the refinement by using the “squeeze” option available in the PLATON program suite.⁴³ Non-hydrogen atoms were refined anisotropically. Hydrogen atoms were located in calculated positions corresponding to standard bond lengths and angles.

Crystallographic structures and data were submitted to The Cambridge Crystallographic Data Center. Each was assigned a unique number. Compound **30**: CCDC 1020287; Compound **36**: CCDC 1031408; Compound **37**: CCDC 1031529; Compound **38**: CCDC 1031532.

2.3 XRD Crystallographic Data and Tables

Table 3 – Crystallographic Parameters for compound **30**.

Compound	30
Formula	C ₃₀ H ₁₀ B ₁₀ O ₂
Fw (g mol ⁻¹)	510.48
<i>a</i> (Å)	6.9671 (19)
<i>b</i> (Å)	15.673 (4)
<i>c</i> (Å)	12.483 (3)
α (°)	90
β (°)	91.563 (5)
γ (°)	90
<i>V</i> (Å ³)	1362.6 (6)
<i>Z</i>	2
Crystal size (mm)	0.15 x 0.15 x 0.15
Crystal habit	Block
Crystal system	Monoclinic
Space group	P2 ₁ / <i>n</i>
<i>d</i> _{calc} (mg/m ³)	1.244
μ (mm ⁻¹)	0.07
<i>T</i> (K)	108
2 θ range (°)	2.1 to 28.3
<i>F</i> (000)	512
<i>R</i> _{int}	0.022
independent reflns	3373
No. of param.	244
R1, wR2 (>2 σ)	R1 = 0.039 wR2 = 0.106

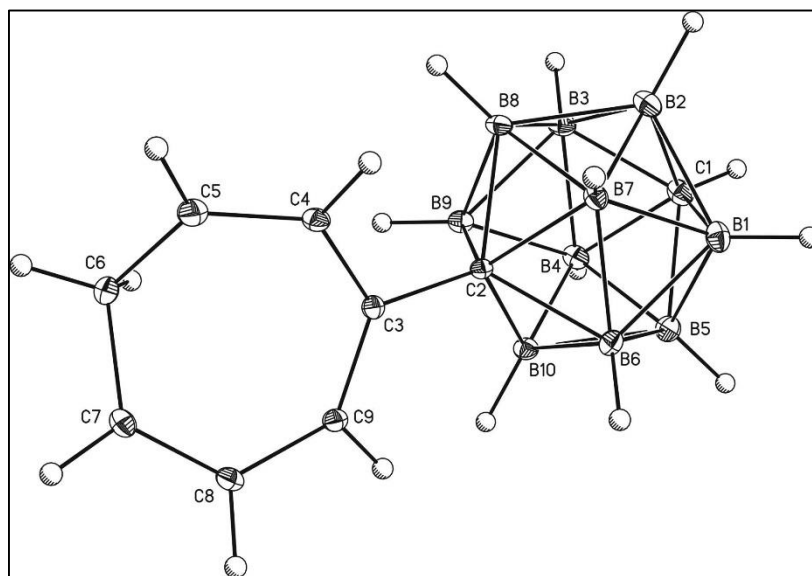


Figure 10 – ORTEP drawing of the crystallographically-determined molecular structures of compound **30**. Thermal ellipsoids are drawn with on all non-hydrogen atoms with a 30% probability.

Table 4 – Selected bond distances (Å) for **30** with estimated standard deviations in parentheses.

Bond	Distance	Bond	Distance
C3—C9	1.3573 (12)	B10—B4	1.7628 (15)
C3—C4	1.4651 (12)	B10—B9	1.7813 (15)
C3—C2	1.5173 (12)	B10—B6	1.7873 (15)
C4—C5	1.3363 (14)	B7—B1	1.7672 (15)
C2—B7	1.7218 (13)	B7—B2	1.7717 (15)
C2—B8	1.7248 (13)	B7—B8	1.7830 (15)
C2—B6	1.7293 (13)	B7—B6	1.7837(15)
C2—B10	1.7332 (14)	B9—B4	1.7668 (15)
C2—B9	1.7332 (14)	B9—B3	1.7668 (15)
C8—C7	1.3409 (13)	B9—B8	1.7829 (14)
C8—C9	1.4456 (12)	B4—B3	1.7812 (16)
C7—C6	1.4987 (13)	B4—B5	1.7833 (16)
C6—C5	1.5021 (13)	B8—B2	1.7627 (16)
C1—B3	1.7031 (15)	B8—B3	1.7683 (15)
C1—B4	1.7063 (14)	B6—B1	1.7684 (15)
C1—B5	1.7090 (15)	B6—B5	1.7732 (15)
C1—B2	1.7098 (14)	B2—B1	1.7823 (16)
C1—B1	1.7112 (15)	B2—B3	1.7859 (16)
B10—B5	1.7590 (15)	B5—B1	1.7835 (15)

Table 5 – Selected Bond Angles (°) for Compound **30** with estimated standard deviation in parentheses.

Angle	Value	Angle	Value
C9—C3—C4	123.01 (8)	C1—B4—B3	58.42 (6)
C9—C3—C2	119.19 (8)	B10—B4—B3	108.14 (7)
C4—C3—C2	117.52 (7)	B9—B4—B3	59.75 (6)
C5—C4—C3	124.83 (8)	C1—B4—B5	58.60 (6)
C3—C2—B7	118.60 (7)	B10—B4—B5	59.47 (6)
C3—C2—B8	117.54 (7)	B9—B4—B5	108.06 (7)
B7—C2—B8	62.30 (6)	B3—B4—B5 1	07.95 (7)
C3—C2—B6	119.59 (7)	C2—B8—B2	105.29 (7)
B7—C2—B6	62.30 (6)	C2—B8—B3 1	05.38 (7)
B8—C2—B6	113.47 (7)	B2—B8—B3	60.77 (6)
C3—C2—B10	119.33 (7)	C2—B8—B9	59.19 (5)
B7—C2—B10	113.33 (7)	B2—B8—B9	108.38 (7)
B8—C2—B10	112.90 (7)	B3—B8—B9	59.67 (6)
B6—C2—B10	62.28 (6)	C2—B8—B7	58.77 (5)
C3—C2—B9	117.64 (7)	B2—B8—B7	59.95 (6)
B7—C2—B9	113.48 (7)	B3—B8—B7	108.55 (7)
B8—C2—B9	62.07 (5)	B9—B8—B7 1	08.23 (7)
B6—C2—B9	113.46 (7)	C2—B6—B1	104.74 (7)
B10—C2—B9	61.92 (6)	C2—B6—B5	104.76 (7)
C7—C8—C9	125.34 (8)	B1—B6—B5	60.47 (6)
C3—C9—C8	126.83 (8)	C2—B6—B7	58.72 (5)
C8—C7—C6	121.51 (8)	B1—B6—B7	59.67 (6)
C7—C6—C5	107.90 (8)	B5—B6—B7	107.99 (7)
B3—C1—B4	62.99 (6)	C2—B6—B10	58.93 (5)
B3—C1—B5	115.33 (7)	B1—B6—B10	107.50 (7)

Table 6 – Crystallographic Parameters for Compounds **36**, **38** and **39**.

Compound	36	38	39
Formula	C ₁₁ H ₂₆ B ₁₀ O	C ₉ H ₂₀ B ₁₀	C ₉ H ₂₂ B ₁₀ O
Fw (g mol ⁻¹)	282.42	236.35	254.36
<i>a</i> (Å)	25.233 (2)	10.4735 (7)	9.2291 (8)
<i>b</i> (Å)	7.0791 (7)	10.8850 (9)	12.7531 (12)
<i>c</i> (Å)	19.8091 (18)	13.5894 (10)	12.8061(11)
α (°)	90	90	90
β (°)	109.983 (2)	110.763 (3)	103.354 (2)
γ (°)	90	90	90
<i>V</i> (Å ³)	3324.1 (5)	1448.63 (19)	1466.5 (2)
<i>Z</i>	8	4	4
Crystal size (mm)	0.15 x 0.15 x 0.15	0.25 x 0.20 x 0.15	0.25 x 0.19 x 0.15
Crystal habit	Block, white	Block, yellow	Block, yellow
Crystal system	Monoclinic	Monoclinic	Monoclinic
Space group	C2/c	P2 ₁ / <i>n</i>	P2 ₁ / <i>c</i>
<i>d</i> _{calc} (mg/m ³)	1.129	1.084	1.152
μ (mm ⁻¹)	0.06	0.05	0.06
<i>T</i> (K)	90	90	90
2 θ range (°)	2.2 to 30.6	2.5 to 26.4	2.3 to 28.3
<i>F</i> (000)	1200	496	536
<i>R</i> _{int}	0.031	0.029	0.039
independent reflns	5056	2866	3629
No. of params	270	252	227
R1, wR2 (>2 σ)	R1 = 0.042 wR2 = 0.119	R1 = 0.056 wR2 = 0.155	R1 = 0.044 wR2 = 0.122

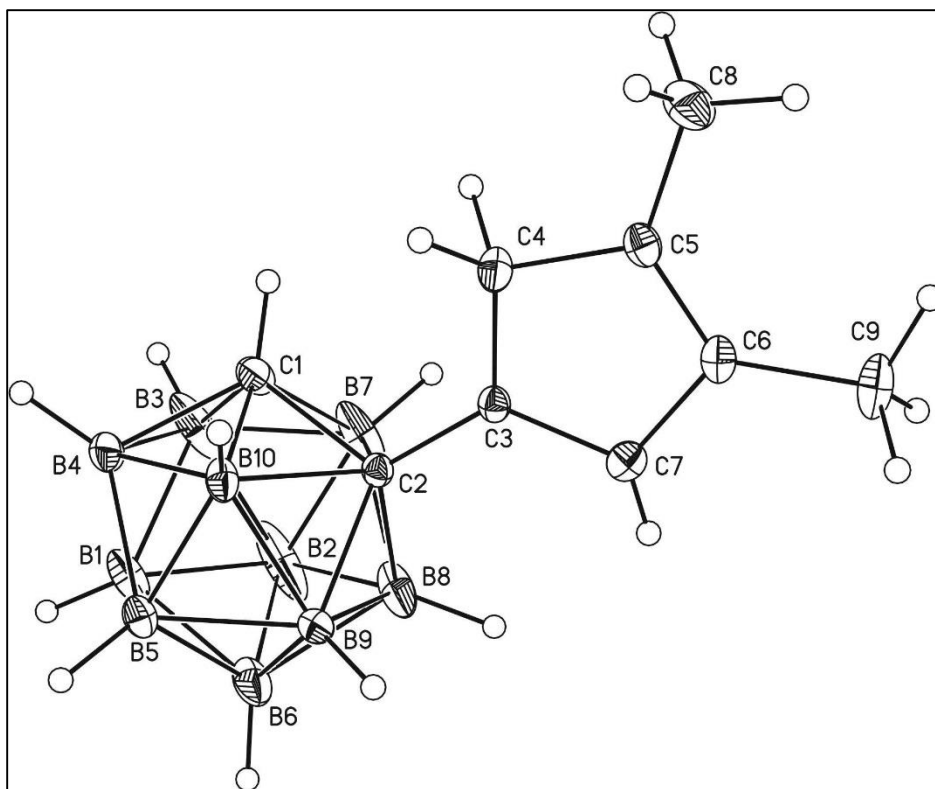


Figure 11 – ORTEP drawing of the crystallographically-determined molecular structures of compound **38**. Thermal ellipsoids are drawn on all non-hydrogen atoms with a 30% probability.

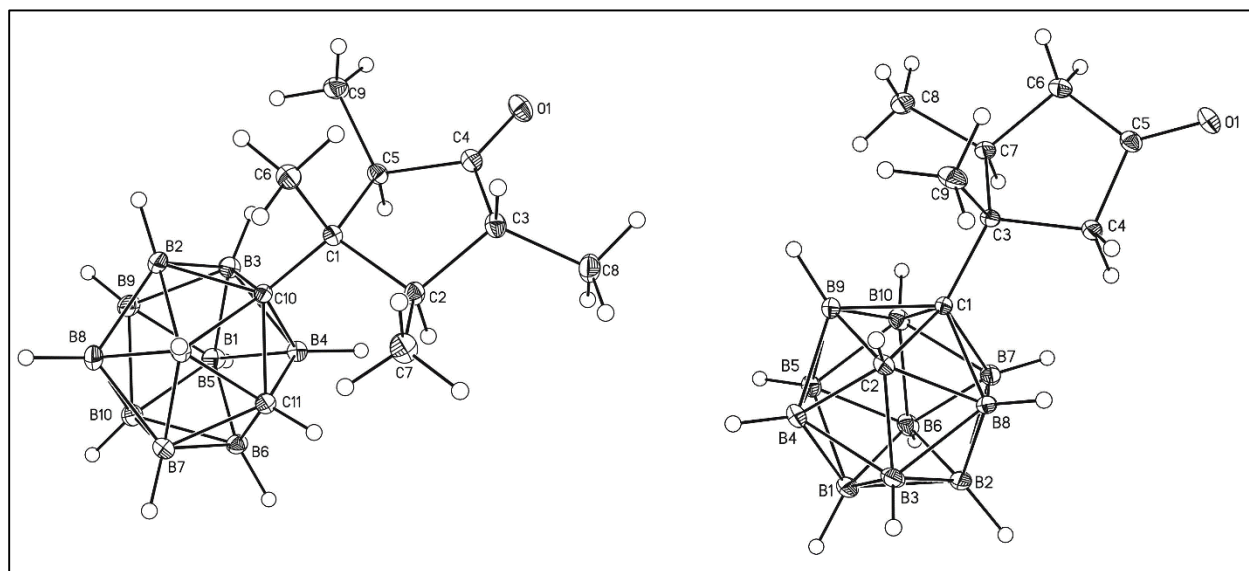


Figure 12 – ORTEP drawing of the crystallographically-determined molecular structures of **36** (L) and **39** (R). Thermal ellipsoids are drawn on all non-hydrogen atoms with a 30% probability.

Table 7 – Selected Bond Lengths (Å) for compound **38** with estimated standard deviation in parentheses.

Bond	Distance	Bond	Distance
B1—B4	1.758 (3)	B7—H16	1.08 (2)
B1—B5	1.766 (3)	B8—C2	1.690 (3)
B1—B3	1.772 (3)	B8—B9	1.777 (3)
B1—B6	1.775 (4)	B8—H15	1.09 (3)
B1—B2	1.778 (3)	B9—C2	1.709 (3)
B1—H5	1.097 (19)	B9—B10	1.754 (3)
B2—B7	1.749 (4)	B9—H6	1.14 (2)
B2—B3	1.762 (5)	B10—C1	1.709 (3)
B2—B8	1.766 (4)	B10—C2	1.736 (2)
B2—B6	1.787 (4)	B10—H1	1.13 (2)
B2—H18	1.06 (3)	C1—C2	1.635 (2)
B3—C1	1.685 (3)	C1—H2	0.98 (2)
B3—B4	1.768 (3)	C2—C3	1.489 (2)
B3—B7	1.771 (4)	C3—C7	1.409 (2)
B3—H19	1.10 (2)	C3—C4	1.426 (2)
B4—C1	1.693 (3)	C4—C5	1.490 (2)
B4—B5	1.763 (3)	C4—H10	0.93 (2)
B4—B10	1.766 (3)	C4—H29	1.15 (4)
B4—H9	1.05 (2)	C5—C6	1.336 (2)
B5—B10	1.748 (3)	C5—C8	1.494 (3)
B5—B9	1.775 (3)	C6—C7	1.476 (3)
B5—B6	1.776 (3)	C6—C9	1.504 (2)
B5—H3	1.092 (19)	C7—H17	0.82 (3)
B6—B9	1.768 (4)	C8—H7	0.97 (2)
B6—B8	1.777 (3)	C8—H11	1.00 (2)
B6—H12	1.05 (3)	C8—H13	0.98 (3)
B7—C1	1.714 (3)	C9—H4	1.02 (2)
B7—C2	1.728 (3)	C9—H8	1.02 (3)
B7—B8	1.754 (5)	C9—H14	0.97 (2)

Table 8 – Selected Bond Angles (°) for Compound **38** with estimated standard deviations in parentheses.

Angle	Value	Angle	Values
C3—C2—C1	117.58 (14)	C5—C4—H29	108.2 (16)
C3—C2—B8	122.77 (13)	H10—C4—H29	92 (2)
C1—C2—B8	109.50 (16)	C6—C5—C4	108.69 (16)
C3—C2—B9	122.91 (13)	C6—C5—C8	129.59 (17)
C1—C2—B9	109.26 (12)	C4—C5—C8	121.72 (16)
B8—C2—B9	63.06 (14)	C5—C6—C7	109.46 (15)
C3—C2—B7	116.36 (13)	C5—C6—C9	128.48 (18)
C1—C2—B7	61.19 (14)	C7—C6—C9	122.05 (17)
B8—C2—B7	61.76 (17)	C3—C7—C6	106.87 (16)
B9—C2—B7	113.79 (15)	C3—C7—H17	125 (2)
C3—C2—B10	117.27 (13)	C6—C7—H17	128 (2)
C1—C2—B10	60.82 (11)	C5—C8—H7	113.6 (15)
B8—C2—B10	113.05 (13)	C5—C8—H11	109.2 (14)
B9—C2—B10	61.22 (11)	H7—C8—H11	107.2 (19)
B7—C2—B10	113.53 (13)	C5—C8—H13	110.2 (17)
C7—C3—C4	108.78 (15)	H7—C8—H13	109 (2)
C7—C3—C2	125.02 (15)	H11—C8—H13	108 (2)
C4—C3—C2	126.20 (14)	C6—C9—H4	111.5 (12)
C3—C4—C5	106.19 (14)	C6—C9—H8	111.6 (14)
C3—C4—H10	119.6 (15)	H4—C9—H8	107.3 (19)
C5—C4—H10	117.4 (15)	C6—C9—H14	112.3 (13)
C3—C4—H29	112.6 (16)	H4—C9—H14	107.3 (17)
C1—B7—C2	56.74 (10)	H8—C9—H14	106.7 (19)

Table 9 – Selected Bond Lengths (Å) for compound **36** with estimated standard deviation in parentheses.

Bond	Distance	Bond	Distance
B1—C11	1.7126 (13)	B6—B7	1.7793 (15)
B1—C10	1.7353 (13)	B6—B10	1.7794 (14)
B1—B2	1.7649 (14)	B7—C11	1.7075 (13)
B1—B8	1.7700 (14)	B7—B8	1.7725 (15)
B1—B7	1.7788 (14)	B7—B10	1.7778 (15)
B2—C10	1.7068 (12)	B8—B9	1.7842 (17)
B2—B3	1.7603 (15)	B8—B10	1.7893 (16)
B2—B9	1.7678 (15)	B9—B10	1.7771 (15)
B2—B8	1.7679 (15)	C1—C6	1.5413 (11)
B3—C10	1.7305 (12)	C1—C5	1.5599 (11)
B3—B4	1.7598 (14)	C1—C2	1.5677 (11)
B3—B9	1.7639 (15)	C1—C10	1.5698 (11)
B3—B5	1.7716 (14)	C2—C7	1.5310 (12)
B4—C11	1.7130 (13)	C2—C3	1.5428 (12)
B4—C10	1.7376 (12)	C3—C4	1.5089 (12)
B4—B5	1.7725 (13)	C3—C8	1.5210 (13)
B4—B6	1.7815 (13)	C4—O1	1.2110 (11)
B5—B6	1.7728 (14)	C4—C5	1.5238 (11)
B5—B9	1.7861 (16)	C5—C9	1.5274 (12)
B5—B10	1.7896 (16)	C10—C11	1.6800 (11)
B6—C11	1.7032 (12)		

Table 10 – Selected Bond Angles (°) for compound **36** with estimated standard deviations in parentheses.

Angle	Value	Angle	Value
C11—B1—C10	58.31 (5)	C6—C1—C5	109.46 (7)
C11—B1—B2	104.01 (7)	C6—C1—C2	110.36 (6)
C10—B1—B2	58.36 (5)	C5—C1—C2	102.62 (6)
C11—B1—B8	104.63 (7)	C6—C1—C10	111.31 (6)
C10—B1—B8	106.02 (7)	C5—C1—C10	110.68 (6)
C11—B1—B7	58.52 (5)	C2—C1—C10	112.07 (6)
C10—B1—B7	106.33 (6)	C7—C2—C3	111.11 (7)
C10—B2—B3	59.86 (5)	C7—C2—C1	116.94 (7)
C10—B2—B1	59.95 (5)	C3—C2—C1	104.58 (7)
C10—B2—B9	107.21 (7)	C4—C3—C8	113.21 (8)
C10—B2—B8	107.36 (7)	C4—C3—C2	104.49 (6)
C10—B3—B4	59.71 (5)	C8—C3—C2	115.22 (7)
C10—B3—B2	58.54 (5)	O1—C4—C3	125.52 (8)
C10—B3—B9	106.35 (7)	O1—C4—C5	124.28 (8)
C10—B3—B5	107.00 (7)	C3—C4—C5	110.20 (7)
C11—B4—C10	58.26 (5)	C4—C5—C9	110.93 (7)
C11—B4—B3	104.93 (6)	C4—C5—C1	104.78 (6)
C10—B4—B3	59.31 (5)	C9—C5—C1	118.69 (7)
C11—B4—B5	104.76 (7)	C1—C10—C11	120.57 (6)
C10—B4—B5	106.65 (6)	C1—C10—B2	122.28 (6)
C11—B4—B6	58.30 (5)	C11—C10—B2	108.04 (6)
C10—B4—B6	106.15 (6)	C1—C10—B3	122.37 (6)
C11—B6—B5	105.16 (6)	C11—C10—B3	107.70 (6)
C11—B6—B7	58.67 (5)	B2—C10—B3	61.61 (6)
C11—B6—B10	104.88 (7)	C1—C10—B1	118.33 (6)
C11—B6—B4	58.84 (5)	C11—C10—B1	60.16 (5)
C11—B7—B8	104.73 (7)	B2—C10—B1	61.69 (6)
C11—B7—B10	104.77 (7)	B3—C10—B1	111.83 (6)
C11—B7—B1	58.80 (5)	C1—C10—B4	118.67 (6)
C11—B7—B6	58.44 (5)	C11—C10—B4	60.14 (5)
B6—C11—B7	62.89 (6)	B2—C10—B4	111.32 (6)
C10—C11—B1	61.52 (5)	B3—C10—B4	60.99 (5)
B6—C11—B1	114.72 (7)	B1—C10—B4	111.66 (6)
B7—C11—B1	62.68 (6)	C10—C11—B6	112.53 (6)
C10—C11—B4	61.60 (5)	C10—C11—B7	112.26 (6)
B6—C11—B4	62.87 (5)	B7—C11—B4	114.66 (7)
B1—C11—B4	114.03 (7)		

Table 11 – Selected Bond Lengths (Å) for compound **39**
 estimated standard deviation in parentheses.

Bond	Length	Bond	Length
B1—B4	1.773 (2)	B8—C1	1.7410 (17)
B1—B3	1.775 (2)	B8—H2	1.092 (14)
B1—B6	1.778 (2)	B9—C2	1.7055 (18)
B1—B5	1.787 (2)	B9—C1	1.7439 (18)
B1—B2	1.792 (2)	B9—B10	1.771 (2)
B1—H6	1.104 (17)	B9—H11	1.091 (15)
B2—B8	1.7618 (19)	B10—C1	1.7263 (17)
B2—B3	1.772 (2)	B10—H8	1.085 (16)
B2—B7	1.783 (2)	C1—C3	1.5646 (16)
B2—B6	1.789 (2)	C1—C2	1.6617 (15)
B2—H10	1.120 (17)	C2—H1	0.959 (16)
B3—C2	1.6951 (19)	C3—C9	1.5328 (15)
B3—B8	1.776 (2)	C3—C4	1.5488 (17)
B3—B4	1.777 (2)	C3—C7	1.5715 (15)
B3—H3	1.089 (17)	C4—C5	1.5087 (16)
B4—C2	1.6984 (18)	C4—H4A	0.9900
B4—B5	1.773 (2)	C4—H4B	0.9900
B4—B9	1.779 (2)	C5—O1	1.2132 (15)
B4—H4	1.078 (16)	C5—C6	1.5068 (17)
B5—B9	1.769 (2)	C6—C7	1.5363 (17)
B5—B10	1.779 (2)	C6—H6A	0.9900
B5—B6	1.789 (2)	C6—H6B	0.9900
B5—H5	1.074 (16)	C7—C8	1.5217 (17)
B6—B10	1.773 (2)	C7—H7A	1.0000
B6—B7	1.779 (2)	C8—H8A	0.9800
B6—H7	1.077 (16)	C8—H8B	0.9800
B7—C1	1.7167 (17)	C8—H8C	0.9800
B7—B8	1.7766 (19)	C9—H9A	0.9800
B7—B10	1.779 (2)	C9—H9B	0.9800
B7—H9	1.058 (16)	C9—H9C	0.9800

Table 12 – Selected Bond Angles (°) for Compound **39** with estimated standard deviations in parentheses.

Angle	Value	Angle	Values
C2—C1—B10	107.87 (9)	C5—C4—C3	105.89 (10)
B7—C1—B10	62.21 (8)	C5—C4—H4A	110.6
C3—C1—B8	116.20 (9)	C3—C4—H4A	110.6
C2—C1—B8	60.08 (7)	C5—C4—H4B	110.6
B7—C1—B8	61.83 (8)	C3—C4—H4B	110.6
B10—C1—B8	112.35 (9)	H4A—C4—H4B	108.7
C3—C1—B9	118.94 (9)	O1—C5—C6	125.99 (11)
C2—C1—B9	60.05 (7)	O1—C5—C4	125.06 (12)
B7—C1—B9	112.36 (9)	C6—C5—C4	108.90 (10)
B10—C1—B9	61.37 (7)	C5—C6—C7	105.21 (10)
B8—C1—B9	111.89 (9)	C5—C6—H6A	110.7
C1—C2—B3	113.39 (9)	C7—C6—H6A	110.7
C1—C2—B4	113.51 (9)	C5—C6—H6B	110.7
B3—C2—B4	63.16 (8)	C7—C6—H6B	110.7
C1—C2—B8	62.27 (7)	H6A—C6—H6B	108.8
B3—C2—B8	62.97 (8)	C8—C7—C6	111.94 (10)
B4—C2—B8	115.65 (10)	C8—C7—C3	117.82 (10)
C1—C2—B9	62.37 (7)	C6—C7—C3	103.81 (9)
B3—C2—B9	115.63 (10)	C8—C7—H7A	107.6
B4—C2—B9	63.02 (8)	C6—C7—H7A	107.6
B8—C2—B9	115.69 (9)	C3—C7—H7A	107.6
C1—C2—H1	116.7 (10)	C7—C8—H8A	109.5
B3—C2—H1	120.6 (10)	C7—C8—H8B	109.5
B4—C2—H1	118.7 (9)	H8A—C8—H8B	109.5
B8—C2—H1	117.6 (9)	C7—C8—H8C	109.5
B9—C2—H1	114.7 (10)	H8A—C8—H8C	109.5
C9—C3—C4	107.92 (9)	H8B—C8—H8C	109.5
C9—C3—C1	111.67 (9)	C3—C9—H9A	109.5
C4—C3—C1	112.09 (9)	C3—C9—H9B	109.5
C9—C3—C7	110.92 (10)	H9A—C9—H9B	109.5
C4—C3—C7	101.45 (9)	C3—C9—H9C	109.5
C1—C3—C7	112.29 (9)	H9A—C9—H9C	109.5

2.4 Results

2.4.1 Calculations

Given the synthetic difficulties encountered by previous groups forming the desired NLO carborane materials, it was determined that multi-cage systems might be an alternative. By separating the electron donating or electron withdrawing group it is hypothesized high β values can be obtained. Since these compounds have not been directly considered previously, coupled with the valuable information on such systems that can be gained by using previously reported calculational methods, calculations were performed on these systems to examine the first hyperpolarizability (β) values of these extended functional group compounds.

Due to limitations with geometric optimization of *o*-carborane compounds with AM1 parameter special procedures were performed for the calculation of molecular orbitals and β values. Compounds **27**, **28**, and **29** were optimized without pendant groups attached using Density Functional Theory at B3LYP 6-31G+ 2D2P level of theory. After optimization pendant groups were added and the compounds' molecular orbitals and β values were calculated using AM1 parametrization. Molecular orbitals of **27**, **28**, and **29** show great localization between

Table 13 - Calculated Mulicage hyperpolarizability values.

Compound	Cage-1	Cage-2	β^a
27	<i>ortho</i>	<i>ortho</i>	3.88×10^4
28	<i>meta</i>	<i>ortho</i>	164
29	<i>para</i>	<i>ortho</i>	788

^aCalculated in units of $\times 10^{-30} \text{cm}^5 \text{esu}^{-1}$

HOMO-1 and LUMO+1 orbitals and great localization between the HOMO and LUMO orbital of

27, Figure 13. This separation of charge between the HOMO-1 and LUMO+1 states was

expected due to literature precedent for carborane NLO compounds.⁶ Examining the calculated β values for **27**, **28** and **29** it was expected to see excellent responses do to each compounds ability to localize charge. The calculated β value for compound **27** was found to be enormous in comparison to compounds **28** and **29**. Compound **27** was calculated to have a β value of $38 \times 10^4 \times 10^{-30} \text{ cm}^5 \text{ esu}^{-1}$, Table 13. Compound **28** was calculated to have a β value of $164 \times 10^{-30} \text{ cm}^5 \text{ esu}^{-1}$ and compound **29** was calculated to have a β value of $788 \times 10^{-30} \text{ cm}^5 \text{ esu}^{-1}$. It was thought that compound **29** would have the largest β value due to the distance between the cyclopentadienyl ring and the tropylium ring. It is hypothesized the large β value in compound **27** arises from its parallel pendant groups. It has been shown in other scientific fields that parallel transition dipoles of the donor and acceptor groups are required for effective energy transfer between two molecules.⁴⁸ Furthermore, orbital mixing seen between the HOMO and LUMO orbitals of **28** and **29** is believed to decrease calculated β values. It is believed that this is why the observed value for **27** is much larger than that of **28** and **29**.

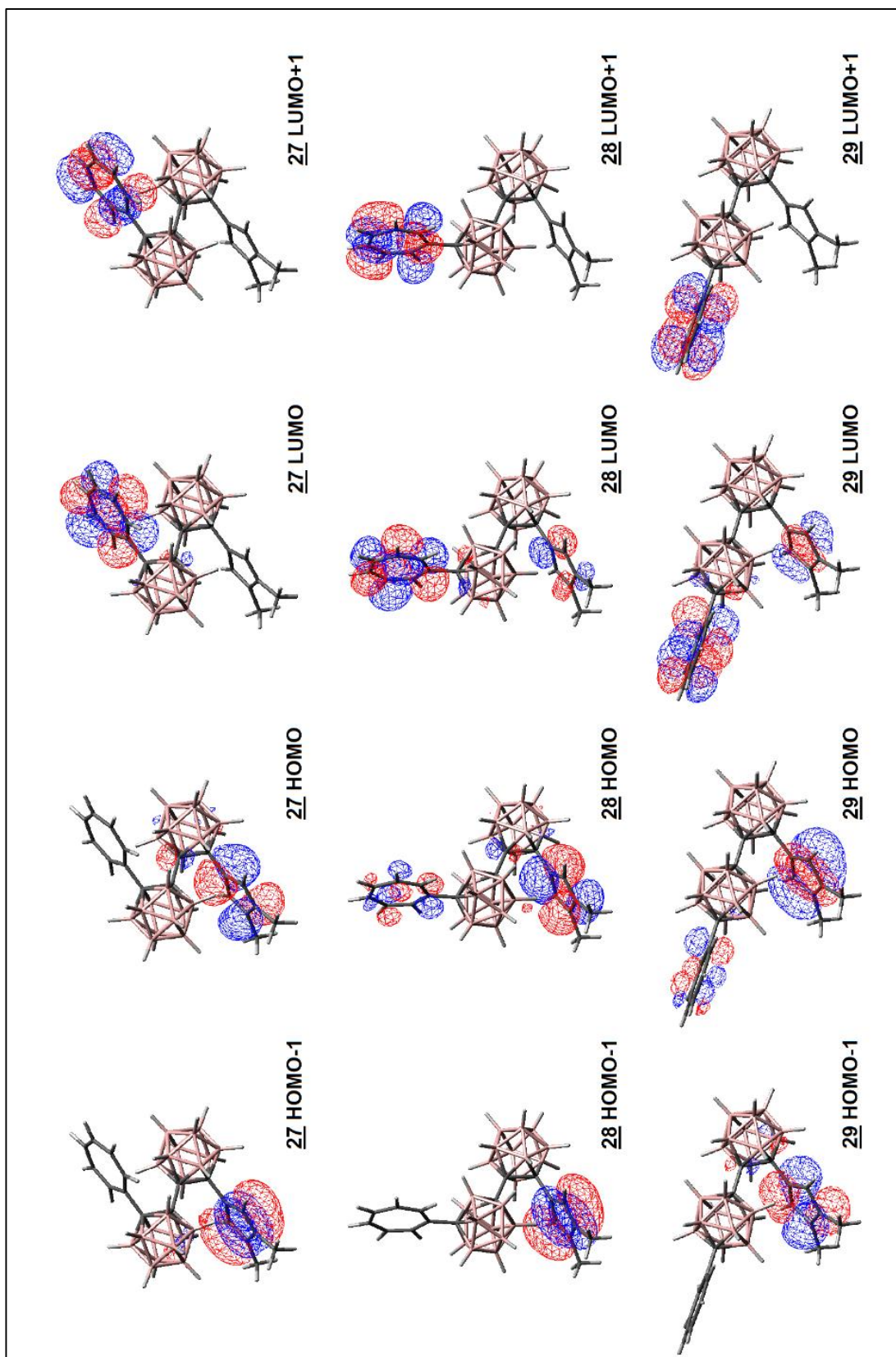


Figure 13 – HOMO-1, HOMO, LUMO and LUMO+1 molecular orbitals of compounds **27**, **28**, and **29**.

2.4.2 Synthesis

The initial target of the synthetic portion of the work began with the attempted formation of 3-[2-(2-(*o*-carborane)-3,4-dimethylcyclopenta-1,3-diene)-*p*-carborane]-1,3,5-cycloheptatriene, **40**, through a convergent synthetic pathway. It was believed that this

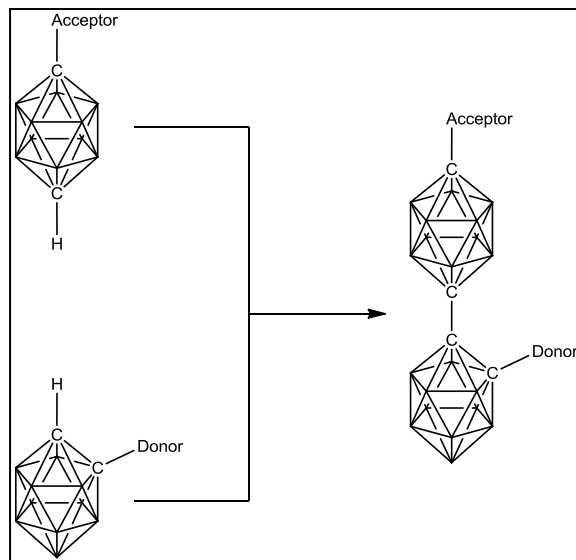
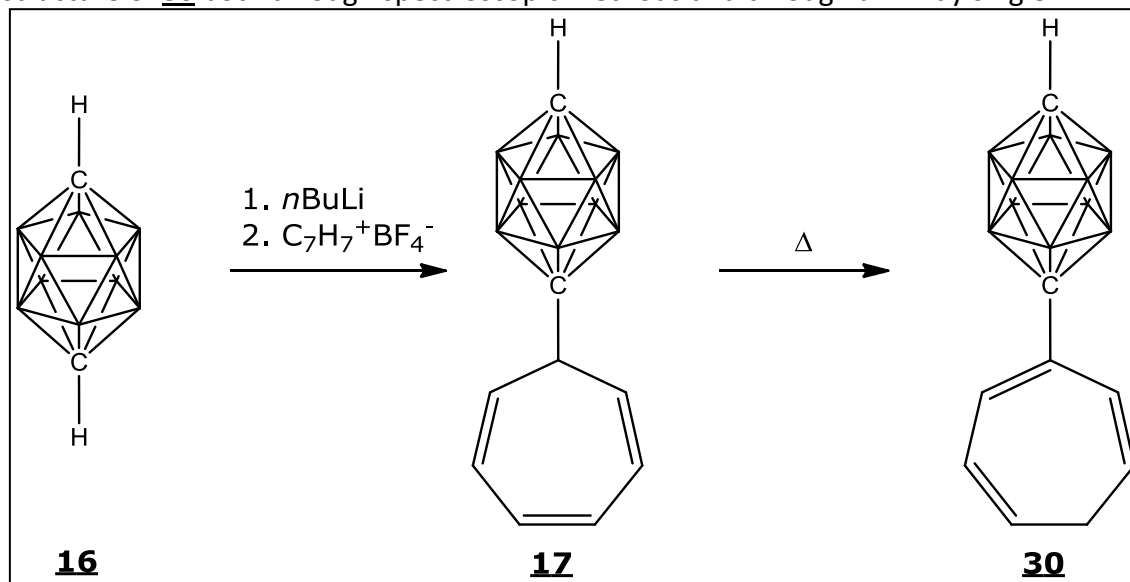


Figure 14 – Convergent Synthesis for a multi-cage NLO compound.

pathway, Figure 14, would yield the desired linked bis-carborane product with better yields compared to a linear synthesis methodology. The formation of 3-(*p*-carborane)-1,3,5-cycloheptatriene, **30**, as completed through similar methodology reported by our group in literature (Scheme 4).²⁹ In the first step, *p*-Carborane undergoes a lithium halide exchange reaction at cryogenic conditions followed by the reaction of tropylium tetrafluoroborate. Constant stirring while warming to room temperature overnight produced compound **37**, presumably through the nucleophilic addition of the troyl group to the cage framework. The impure product of this reaction was dissolved in toluene and refluxed in order to isomerize the

7-cycloheptatriene to the 3-cycloheptatriene isomer through a thermally induced [1,5]-hydrogen shift.⁴⁹ Purification through vacuum distillation of the product gave a white solid which was further recrystallized to obtain large colorless crystals. These were used to confirm the structure of **30** both through spectroscopic methods and through an X-ray single

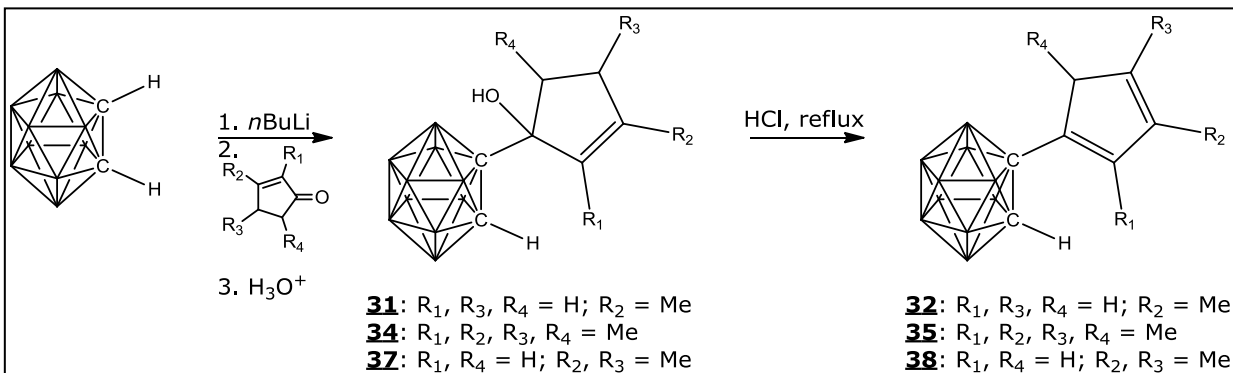


Scheme 4 – Synthesis of 3-(*p*-carborane)-1,3,5-cycloheptatriene (**30**).

crystal structural determination, Figure 10. Selected bond lengths and angles are reported in Table 4 and Table 5, respectively.

The synthesis of 1-(*o*-carborane)-3,4-dimethylcyclopenta-1,3-diene, compound **38**, was expected to follow similar procedures previously reported for the synthesis of the analogous *m*-carborane compound.³⁰ In this procedure, lithiation of the cage presumably produces a nucleophilic cage species that reacts with the carbonyl carbon of a ketone. Acidic workup followed by reflux of the impure product in an acidic medium should form the desired substituted diene. In the *m*-carborane analog, however, relatively low yields were observed from this reaction. Attempts to employ this procedure with use of *o*-carborane proved

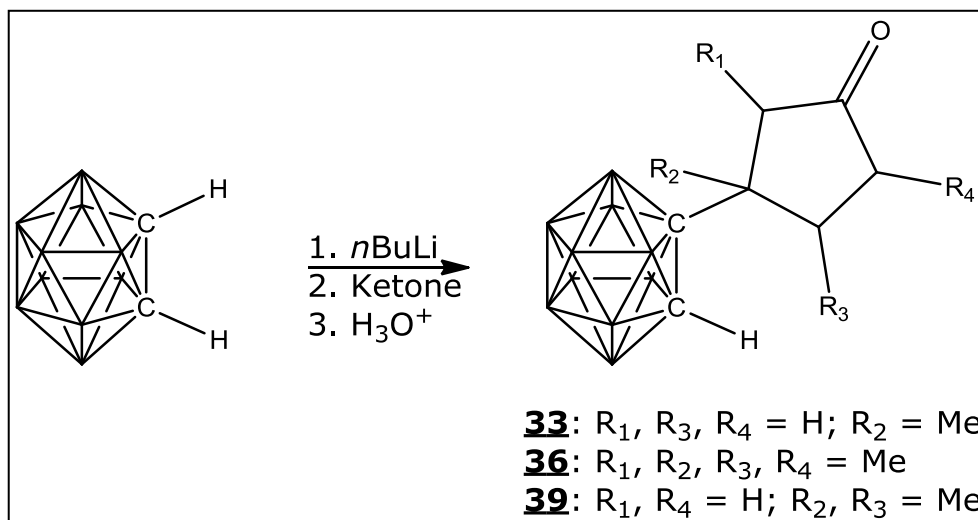
unsuccessful in forming any observed product. Multiple attempts varying the conditions and reactants similarly did not produce the desired product.



Scheme 5 – Initial Synthesis of cyclopentadiene substituted *o*-carborane cages.

In the formation of the *o*-carborane substituted species, it is hypothesized that the tertiary alcohol was not formed in the intermediate step from the addition of the ketone to the cage. Isolation of the intermediate compounds **31**, **34**, or **37**, shown in Scheme 5, would give insight into problems in the synthesis. In the literature procedure for the addition of 3-methyl-2-cyclopenten-1-one, 3,4-dimethyl-2-cyclopenten-1-one and 2,3,4,5-tetramethyl-2-cyclopenten-1-one to the *m*-carborane cage,^{29,30} the cage-substituted 1,2-ene-ol product was isolated while this was not observed for the *o*-carborane case. Purification of the product of the reaction of the cyclopent-2-ene-1-one with the lithiated *o*-carborane cage showed a different substitution pattern, yielding the 1,4-addition product instead of the 1,2- product for *m*-carborane, as shown in Scheme 6. Purification of these compounds through chromatographic methods and recrystallization allowed for the isolation of pure products. Spectroscopic data obtained for each new product confirmed the 1,4-addition product. Compounds **36** and **39** were further confirmed through their X-ray diffraction patterns, as shown in Figure 12. Selected bond lengths and angles are presented in Tables 9 – 12. Both compounds have proton spectra that

have clearly defined methyl peaks as expected with both compounds as well as less intense multiplets corresponding to the -CH and -CH₂ atoms on the rings of these compounds. In both



Scheme 6 – The observed 1,4-addition of α,β -unsaturated ketones to *o*-carborane.

compounds, the proton attached at the 2 position on the carborane cage is observed as a broad singlet (3.79 ppm for **36**, 3.75 ppm for **39**) as expected for this proton. No resonances were observed in the ¹H spectrum corresponding to an unsaturated proton. While this is typical for compounds such as **36**, this observation helped lead to the proposed conformation of compound **39** and therefore support the 1,4-conjugate addition hypothesis.

The carbon-13 NMR spectra for compounds **36** and **39** further supported the proposed formation of the 1,4- product. In the ¹³C spectra of both **36** and **39**, resonances were observed at 217.6 ppm and 212.6 ppm, respectively. These are representative of carbonyl carbons that are deshielded due to their proximity with oxygen. Furthermore, in both spectra the region between 90 ppm and 160 ppm is empty, suggesting that no unsaturated carbons are present in either molecule.

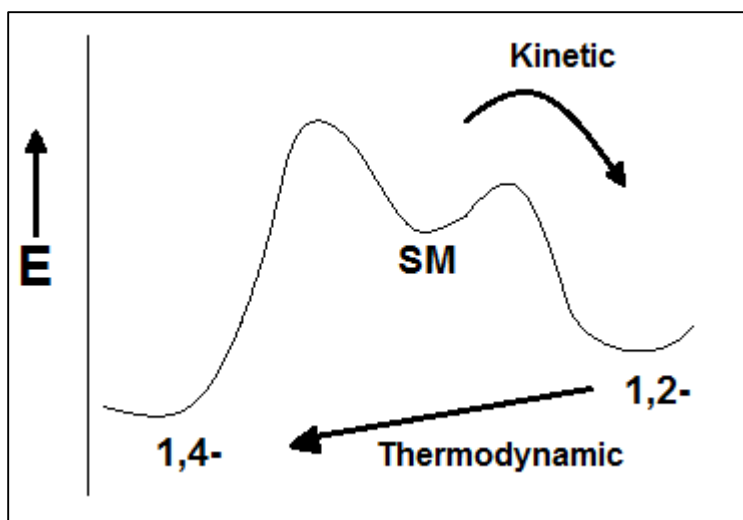


Figure 15 – Energy profile diagram for the kinetic vs thermodynamic product reaction.⁵⁰

The observation of a 1,4-addition of the α,β -unsaturated ketones onto the lithiated *o*-carborane was an unexpected observation. It is known that lithiated species kinetically favor 1,2-addition under most circumstances.⁵⁰ Generally, the 1,4-addition is the thermally favored product and may arise with longer reaction times or with stabilized nucleophiles, Figure 15. Monitoring the progress of the reaction of the lithiated *o*-carborane species and the α,β -unsaturated ketones using thin layer chromatography showed no immediate change and the reaction was therefore allowed to react longer, presumably aiding the formation of the thermodynamically favored species.

To promote the formation of the 1,2-addition product, a cerium intermediate was also explored.^{35, 50-52} In this reaction, the nucleophilic organic species is first lithiated and then allowed to react with anhydrous CeCl_3 to form the cerium (III) reagent. This complex is then allowed to react with the ketone to form the tertiary alcohol.³⁵ The use of a cerium intermediate generally promotes the formation of the 1,2- product because of cerium's oxophilic nature. Carrying out this strategy with *o*-carborane and 3,4-dimethyl-2-cyclopenten-

1-one formed the 1,2-addition product, as confirmed primarily by –OH stretch in the infrared spectrum, as previously reported in literature. Dehydration of this compound through acidic reflux successfully produced the desired diene, **38**. Purification of compound **38** was performed using chromatographic methods to produce a white solid. X-ray quality crystals were grown from a diethyl ether: hexane mixture and the structure was confirmed through spectroscopic data and x-ray diffraction structure, Figure 11. Full spectroscopic data is reported in Section 2.2.3 and selected bond lengths and angles are presented in Table 7 and Table 8.

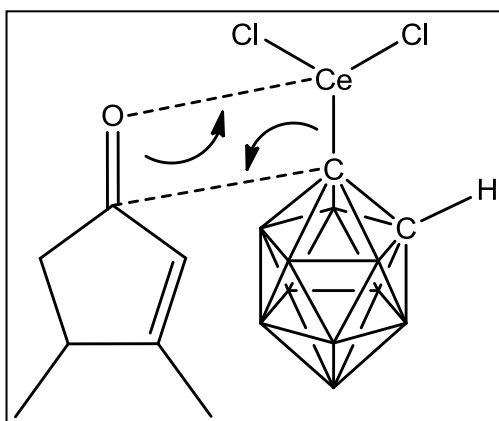
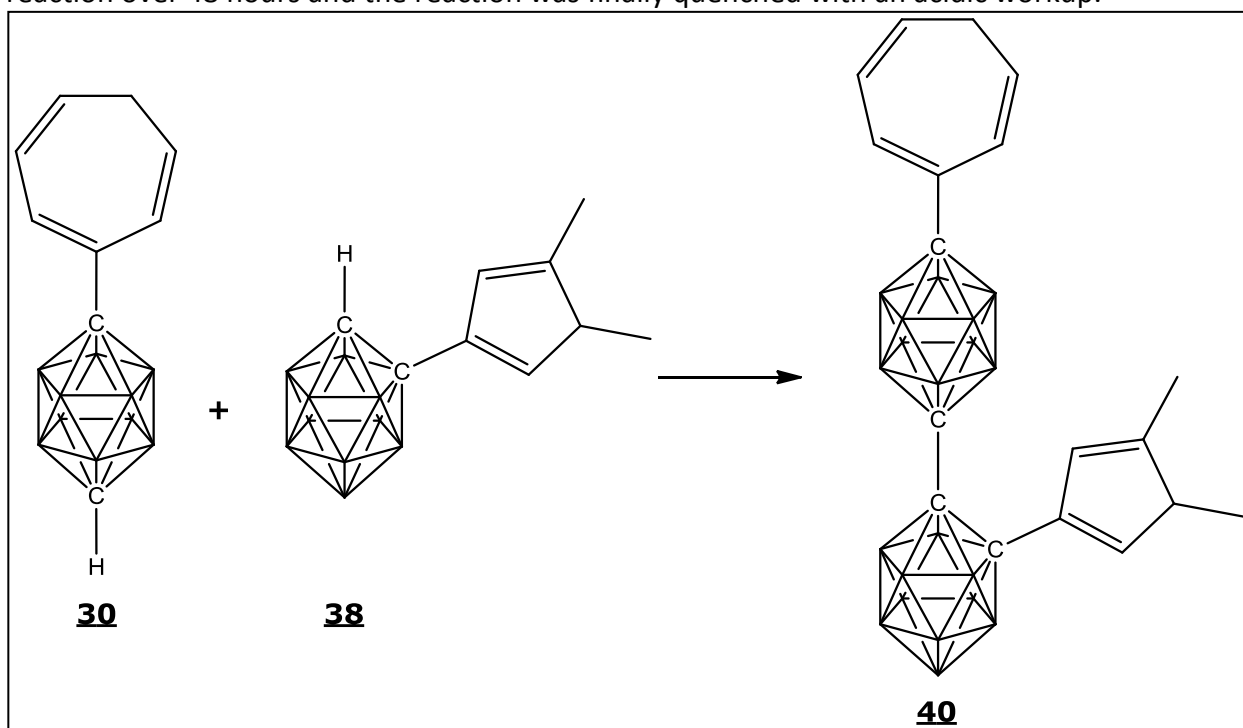


Figure 16 – Cerium intermediate coordination to oxygen promoting 1,2-addition.

The ^1H spectrum of compound **37** was shown to have peaks expected for a substituted 1,3-diene. The methyl groups at the 3,4- positions were seen as singlets at 1.80 ppm and 1.89 ppm with integration each corresponding their three protons. A small multiplet, observed at 2.97 ppm, is believed to correspond to the two protons at the C_5 position on cyclopentadiene ring. It is believed that the observed resonance is due to geminal splitting and its large coupling is due to the strain caused by the 1,3-cyclopentadiene ring. At 3.70 ppm, a broad singlet is observed corresponding to the carborane cage's framework –CH atom. Finally, at 6.40 ppm a singlet is seen corresponding to the unsaturated carbon at the 2 position. ^{13}C NMR confirms

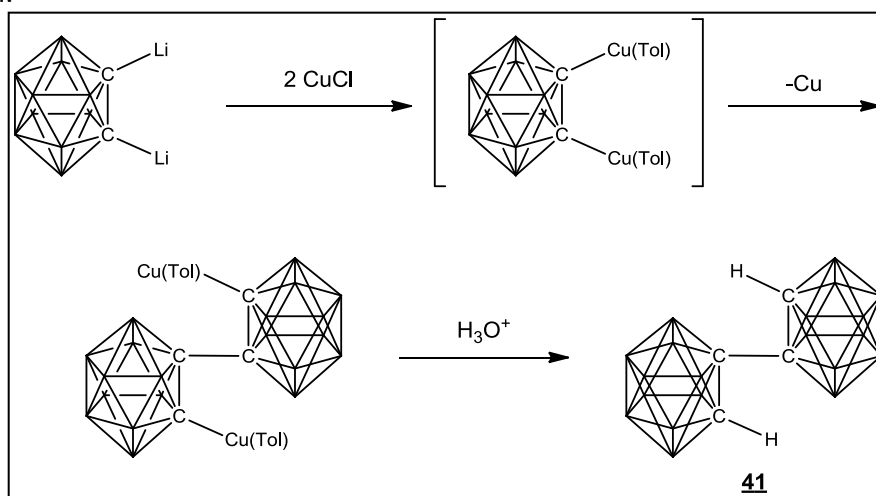
the presence of the diene by showing four resonances at 134.4 ppm, 135.7 ppm, 138.7 ppm, and 139.2 ppm.

Once the two prerequisite components had been synthesized, compounds **30** and **38**, the next step required the linking of the two cage units together to form the linked species, compound **40** shown in Scheme 7. Coupling of carborane cages through copper coupling has been demonstrated in literature.^{36, 52-55} Using two lithiated cages, a copper (I) or copper (II) salt is typically used to catalyze the cage-linking reaction, as illustrated in Scheme 8. In our work, equal amounts of compounds **30** and **38** were dissolved in dry diethyl ether under an inert atmosphere. The *n*-Butyllithium was added at 0° C followed by a total of 24 hours of stirring to form the active species. Copper (I) was added as a catalyst to perform a modified Ullmann reaction over 48 hours and the reaction was finally quenched with an acidic workup.



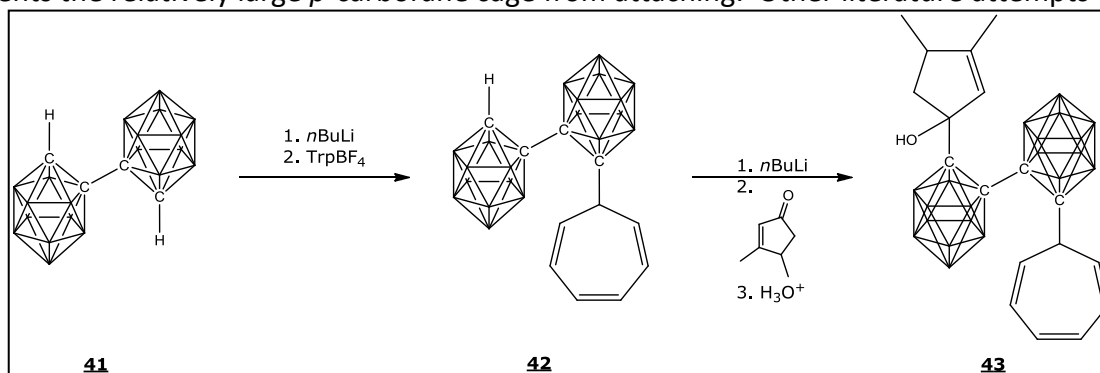
Scheme 7 – Attempt at the copper catalyzed addition of **30** onto **38** to form targeted compound **40**.

Examination of NMR data from the reaction did not show resonances expected for the desired cage-linked product. A successful coupling of the reactants would be expected to eliminate resonances observed at 2.67 ppm and 3.70 ppm. These two peaks correspond to the $-CH$ peaks in the carborane cages of compounds **30** and **38**. The actual observed presence and integration of these resonances, however, indicated the reaction did not proceed as expected. Proton resonances corresponding to the boron cage's carbons were still observed at 2.67 ppm and 3.70 ppm.



Scheme 8 – Literature example of copper catalyzed cage coupling.³⁶

Purification using chromatographic methods further confirmed that both starting materials remained in the reaction mixture. It is hypothesized the steric hindrance around *o*-carborane prevents the relatively large *p*-carborane cage from attaching. Other literature attempts



Scheme 9 – Synthesis attempt towards a dual substituted 1,1-bis-*o*-carborane.

to couple substituted *o*-carborane units have likewise been shown to be unsuccessful. For example, Ren and Xie unsuccessfully attempted the coupling of 1-methyl-*o*-carborane with itself using the same procedure attempted.³⁶ Although the coupling of two complete *o*-carborane units to form the final product proved unsuccessful, experimentation into alternate pathways was explored following a linear synthetic approach, as shown in Scheme 9.

In a second synthetic strategy for the formation of the desired compound, **27**, two carborane units would first be linked together and then differentially substituted with the diene and triene units towards the end of the synthetic pathway. This method would allow the two carborane units to rotate their unsubstituted (non-linked) carbon position away from each other opening the reaction site.

Following literature methods, 1,1-bis(*o*-carborane), **41**, was first synthesized as a synthetic starting unit following the procedures reported in literature and preformed for the attempted synthesis of **29**.³⁴ This pathway went through an initial deprotonation of the cage followed by a copper catalyzed coupling followed by an acidic quenching. Purification of this compound was accomplished following the literature methods using flash column chromatography with pure hexanes as an eluent. The ¹H and ¹¹B spectrum of this compound matched those reported in literature.³⁴

Paralleling the methodology describe above for the addition of tropylium tetrafluoroborate onto *p*-carborane, a cycloheptatriene unit was added onto 1,1-bis(*o*-carborane) forming **42**. This was performed through the deprotonation of compound **41** using *n*-butyllithium at 0° C followed by the addition of tropylium tetrafluoroborate *via* a dry addition

funnel in a single aliquot. Overnight stirring at room temperature was followed by an acidic workup, quenched any remaining active species. Purification of the product, **42**, was performed by silica gel column chromatography eluted with hexanes gave an off white solid in a low 20% yield. The structure was confirmed through proton, carbon and boron NMR.

The proton spectrum of **42** had showed resonances with shifts and splittings commonly seen with cycloheptatriene compounds. An upfield resonance at 2.41 ppm with a characteristic triplet splitting of H(7) was observed. More downfield, resonances are observed at 4.88 ppm (doublet of doublets), 6.22 ppm (a multiplet) and at 6.61 ppm (a triplet) representing H(1,6), H(2,5) and H(3,4), respectively. The characteristic broad multiplet carborane proton resonance, characteristic in carborane cage compounds from 1.5~3.2 ppm, was observed as well as a singlet a 3.74 ppm. All other of the resonances for this proton spectrum were also able to be identified through clean integration of peaks.

Using the compound **42** prepared above, the addition of the second pendant group was explored in hopes of forming **43**. Following the initial procedure used for the attempted addition of 3,4-dimethyl-2-cyclopenten-1-one to *o*-carborane, **42** underwent a deprotonation followed by addition of 3,4-dimethyl-2-cyclopenten-1-one. Following the reaction using chromatography, no change was observed from the spectrum for the starting material. After overnight stirring, the reaction was quenched through an acidic workup to view possible spectroscopic changes. No chromatographic changes were observed and the proton NMR of the reaction mixture only showed resonances for starting material.

2.5 Conclusions and Future Work

Work towards the synthesis of new multi-cage nonlinear optic compounds progressed. In the synthesis of 1-(*o*-carborane)-1,3-dienes, initially problems arose during the addition of the α,β -unsaturated ketones to the lithiated *o*-carborane. It was discovered through purification and spectroscopic analysis that 1,4-conjugate addition was occurring. Although the underlying cause of this was not explored, the use of a cerium intermediate promoted the addition of *o*-carborane to 3,4-dimethyl-2-cyclopenten-1-one at the 2 position allowing for the formation of **38**. For future 1,2-addition to *o*-carborane systems, cerium-based methods should be used to promote desired product formation.

The coupling of compounds **30** to **38** through use of a copper catalyst was shown to be ineffective in the synthesis of **40**. It is hypothesized that this is due to the steric hindrance around the lithiated carbon in **38**. Similar results were observed previously in the attempted synthesis of 2,2'-bis(1-methyl-*o*-carborane).³⁶ For this reason, it is believed that any multi-cage structure coupling *o*-carborane to another cage must have not have any substitutions near to the desired spot of substitution.

The attempted linear synthesis of compound **27** progressed to produce pure products but in low yields. Fine tuning of the reaction methods used may be helpful to increase yields. Following literature methods, 1,1'-bis(*o*-carborane), **41**, was synthesized and purified. Applying previously used methodology for the addition of tropylium rings, compound **42** was successfully formed. Purification using chromatographic methods yielded a pure compound with clean NMR spectra. More importantly, the successful formation of **42** revealed that the 2 and 2'

position in **41** are accessible and that complex materials might be made from carborane linked *o*-carboranes.

In the attempted synthesis of **43**, lithiation was done as previously mentioned followed by addition of 3,4-dimethylcyclopenten-1-one. Unlike the initial attempts with 1,2- addition in the synthesis of **38**, the 1,4-conjugate addition product was not observed. NMR spectroscopy showed, however, that no reaction had occurred.

Further work with multi-cage systems can examine a variety of different topics and not those solely related to NLO materials. There is a large variety of work to be done on examining the theoretical β values of different carborane to carborane isomers. Though only *o*-carborane donors were explored, potential new compounds using *m*-carborane, *p*-carborane or other polyhedral structures still exist.

Hetero-cage linking is in its infancy and must also be explored. Literature reports very little in terms of hetero-cage compounds. Examination of a one pot method in which both desired carborane isomers are lithiated together and undergo copper catalyzed metathesis would be the first step in such a project. Statistics dictates that in a reaction of one part *o*-carborane and one part *m*-carborane a 25:25:50 (*o*-carborane to *o*-carborane, *m*-carborane-*m*-carborane, *o*-carborane-*m*-carborane) mixture should occur however carboranes are unique in they do not always work in a desirable way. Continuation on the reaction factors of cage linking could examine substitutions on hetro-cage linking. Though 1-methyl-*o*-carborane was shown not to react with itself³⁶ it is still unknown if this applies to all substitute *o*-carboranes with all polyhedral materials.

Specific work on the formation of multi-cage based NLO materials can continue as planned with the formation of **43**. Another attempt using a cerium intermediate will promote the formation of the 1,2-addition product. Promotion of the 1,2-addition and attachment of the cyclopentene ring would mark a significant accomplishment. The ability to attach a second large hydrocarbon ring to the hindered 1,1-bis(*o*-caborane) system will be the first of its kind.

Chapter 3

Synthesis towards Rigid Organic Non-Linear Optic Materials

3.1 Introduction

The synthesis of a donor-acceptor, bis-olefin substituted compound containing a bulky bridge is a new and novel design for the construction of a new class of NLO compounds, Figure 17: rigid organic NLOs. This design potentially provides significant charge separation with localization, an expected large change in the dipole upon excitation, and a stable structural framework. This is similar in concept to the (C_7H_6) - $C_2B_{10}H_{10}$ - (C_5H_4) system described in Chapter

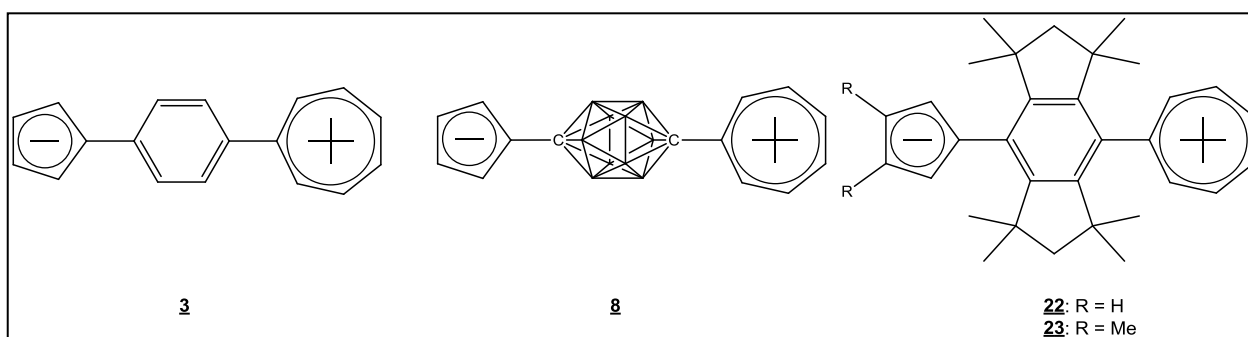


Figure 17 – Schematic showing several possible new nonlinear optical compounds based on charged aromatic donor-acceptor units bridged by aromatic units: compound **3**, a quinarene NLO; compound **8**, a quinarene NLO analog using *p*-carborane; **22/23** and the *s*-hydrindacene/quinarene molecule.

2 of this thesis.

The substituted hydrindacene family of compounds, including several examples that are shown in Figure 18, when linked to charged donor and acceptor units have been calculated to provide excellent bridging units in the new class of rigid organic NLO compounds. These compounds contain a three ring system in which substitutions on the outermost rings can form a sterically limited pocket around the substitution sites on the central ring. When methyl groups are substituted onto the neighboring rings, only compounds with specific geometries are able to be substituted on the central benzene ring due to the steric constraint. Using hydrindacenes as bridging subunits would force any pendant rings attached in the pocketed

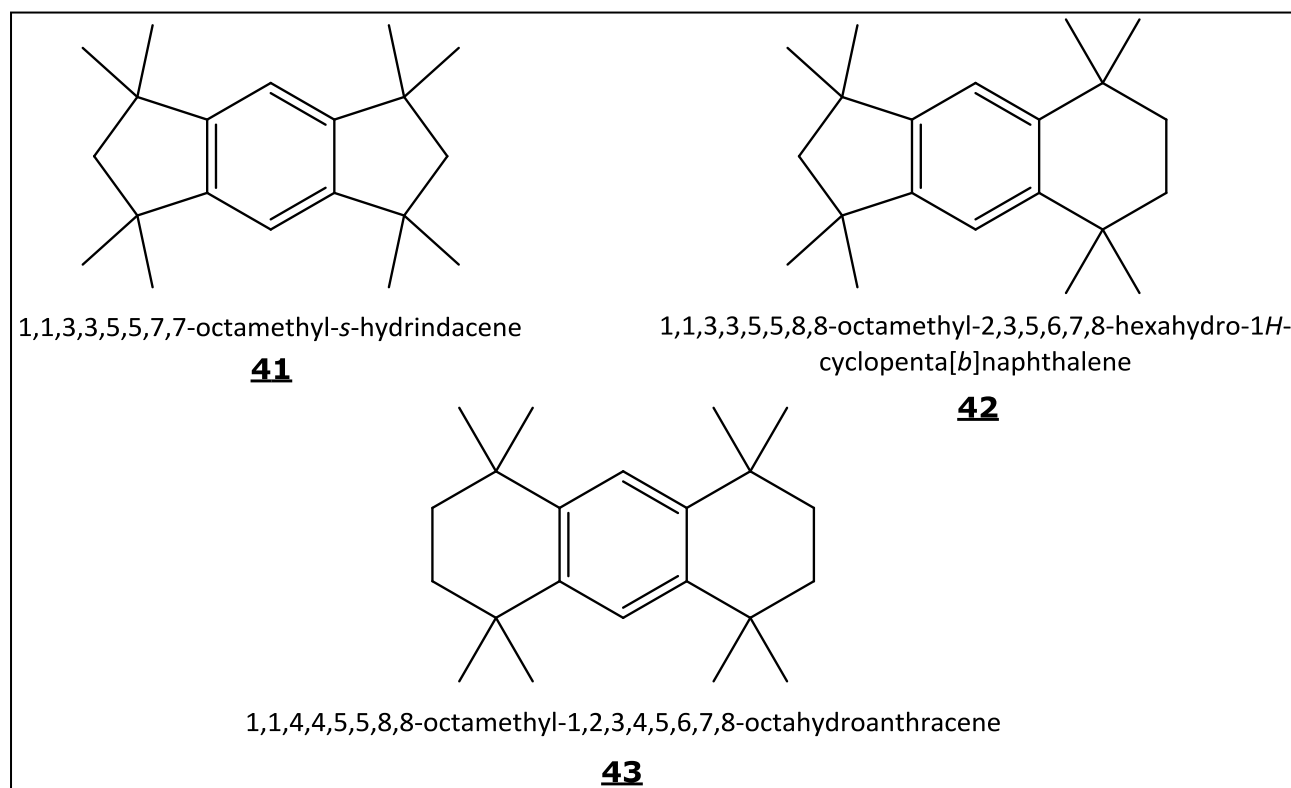


Figure 18 – Select members of the s-hydrindacene family of compounds from literatures.⁵⁶ with **41** being used as a bridge compound for calculation of β values.

positions to distort or “twist” away from being co-planar with the bridge in order to fit. This geometry distortion can be utilized to maintain opposing charged species on either side of the hydrindacene unit by minimizing delocalization throughout the entire molecule. The twist, preventing a co-planar species, thus prevents π -orbitals from delocalizing through the hydrindacene unit, thereby keeping the charges relatively localized. This concept for a twisted NLO system was first proposed by Albert and Marks⁵⁷ who calculated the NLO response for simple donor acceptor systems directly connected to each other containing pendant groups to prevent the π -overlap, as illustrated in Figure 19. The methyl groups on both the charged phenol and charged pyridine units prevent the two aromatic rings from becoming co-planar and, therefore, prevents significant charge delocalization.

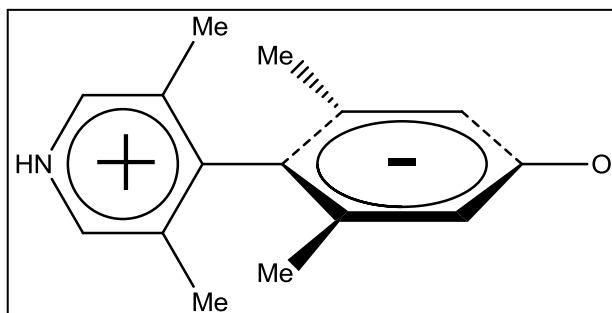
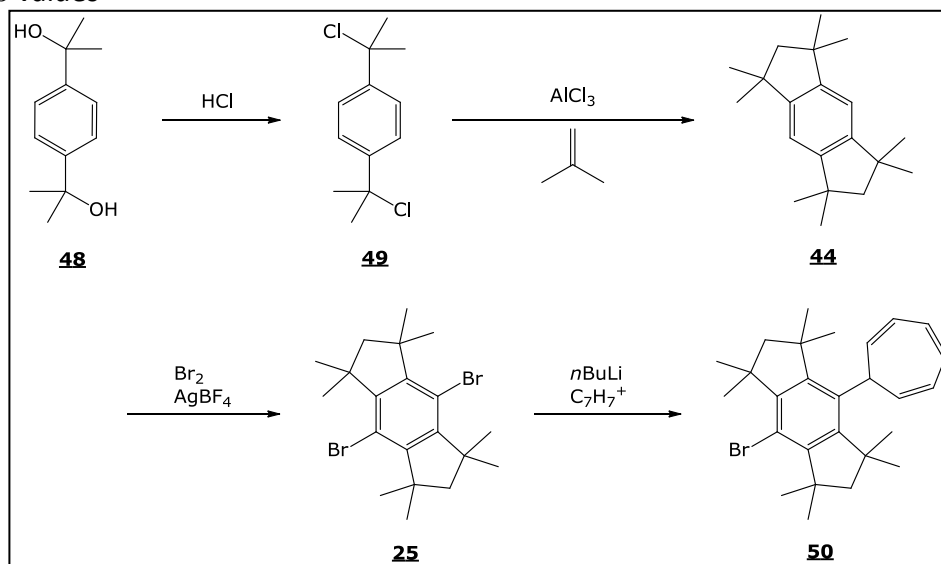


Figure 19 – The twisted zwitterionic compound explored in literature.⁵⁸

In our previous work, calculations have shown that the use of an octamethyl-*s*-hydrindacene bridge with pendant aromatic donor and acceptor groups produces very large first hyperpolarizability values (β), as shown in Table 2, with values exceeding $4000 \times 10^{-30} \text{cm}^5 \text{esu}^{-1}$. Tuning of the calculated β value has been shown to be readily achieved primarily through the simple modification of substitutions on the donor and acceptor rings. The calculated β values



Scheme 10 – Synthesis of compound **50** attempted previously in literature.³⁰

seen in this family of bridging compounds stems from their ability to keep a localized charge on the donor and acceptor rings while providing spatial separation. Structures built upon the framework of compound **41** were found to give larger calculated β values in comparison to

compounds derived from **42** and **43**. This was primarily due to increased rotation of the pendant groups relative to the central benzene ring allowed in the latter compounds.

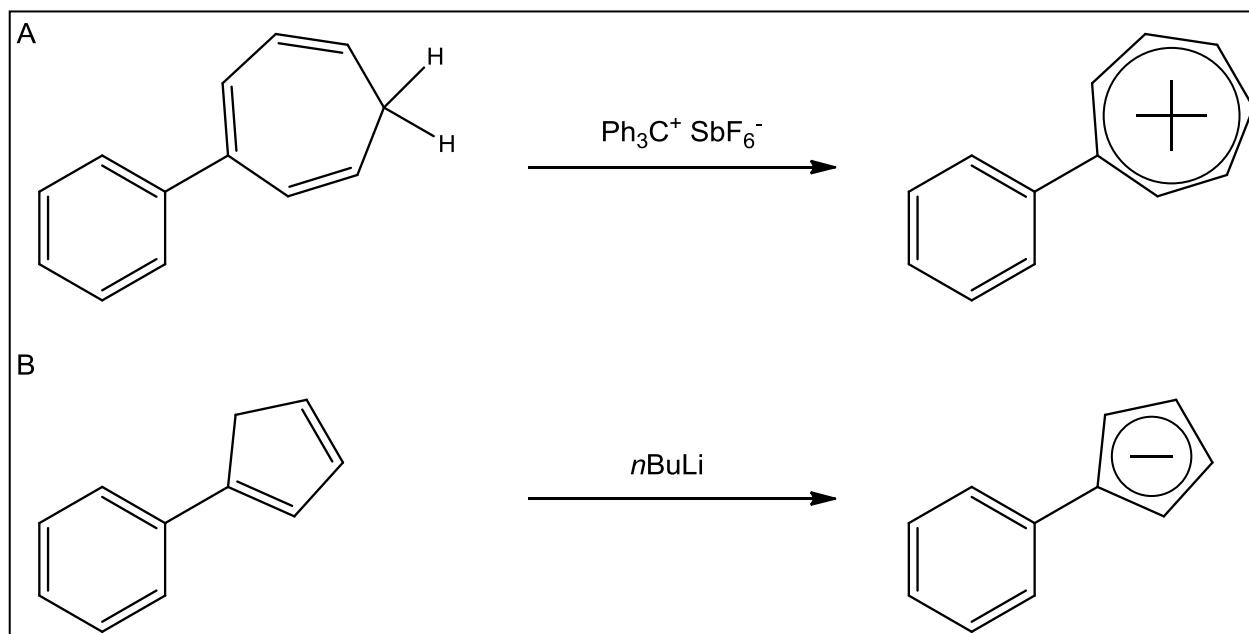


Figure 20 – The two reactions to turn precursor units in to the active charged species.

Given the interest in potentially significantly enhanced NLO properties of our proposed rigid organic NLOs compounds, the synthesis of a prototypic example was considered to be important. A number of synthetic approaches are possible for the preparation the key precursor of these systems that contain a hydrindacene bridge substituted with cyclopentadiene and cycloheptatriene units, Figure 20. Previous work in our group on the synthesis of **22** and its derivatives has examined the use of a brominated *s*-hydrindacene bridging unit in nucleophilic substitution reactions.³⁰ This synthesis began with the formation of *p*-dicumyl chloride, **49**, from *p*-bis(1-hydroxy-1-methylethyl)benzene, **48** through published methodology, Scheme 10.⁵⁹ This converted the hydroxyl functional group to an organic chloride. Once in the chloride form, a Friedel-Crafts alkylation was performed using isobutylene in the presence of boron trichloride.⁵⁹ Using the tertiary dichloride, compound **49**, the

isobutylene cyclization reaction formed the unsubstituted 1,1,3,3,5,5,7,7-octamethyl-*s*-hydrindacene product, compound **45**. Bromination of compound **45** was then performed through a silver tetrafluoroborate/acetic acid catalyzed reaction to produce di-substituted 4,8-dibromo-1,1,3,3,7,7,9,9-octamethyl-*s*-hydrindacene compound, **25**.⁵⁶ This dibromide compound was then used to attempt the nucleophilic addition of a 1,3,5-cycloheptatriene ring to form compound **50**. This last step, however, proved unsuccessful.³⁰ Possible products were observed but they were formed in very low yields and it was not possible to confirm their structures. It is speculated that the pocket of the octamethyl-*s*-hydrindacene is too sterically restricted to allow the direct attachment of a tropylium ring through a nucleophilic substitution process.

Given the problems encountered in the synthetic work on compound **22**, we have continued this synthetic work using other rational routes. This chapter details work involved in the synthesis towards compound **22** including the re-examination of ring addition to a completed bridge unit, an attempt at constructing the hydrindacene framework after ring attachment and a hybrid method in which partial bridge construction is followed by pendant ring addition. These various synthetic pathways are described and discussed as well as the problems faced in the various methods.

3.2 Experimental

3.2.1 Physical Measurements

All NMR spectra were recorded on samples dissolved in CDCl_3 or $\text{DMSO-}d_6$ in 5 mm (o.d.) tubes. Proton (^1H) and carbon (^{13}C) were recorded on either a Bruker DPX-300 spectrometer operating at 300.15 MHz for proton, 77.47 MHz for carbon; or a Bruker Ascend-400 with Prodigy CyroProb attachment operating at 400 MHz. Chemical shifts were referenced to either residual signals from CHCl_3 ($\delta = 7.26$ ppm) or residual DMSO ($\delta = 2.50$ ppm). The spectrometer was operated in the FT mode while locked on the deuterium resonance of the CDCl_3 or $\text{DMSO-}d_6$ solvent. The reference was set relative to tetramethylsilane from the known chemical shifts of the CDCl_3 ($\delta = 77.23$ ppm) and DMSO ($\delta = 39.52$ ppm) carbon atoms. All NMR units are reported in ppm. Unit resolution mass spectra were obtained on a Hewlett Packard model 5989B gas chromatograph/mass spectrometer (GC/MS) using an ionization potential of between 11 and 70 eV. FT-IR in the range of 400 to 4000 cm^{-1} were measured on a Mattson Galaxy 2020 spectrometer or a Perkin Elmer FT-IR Spectrometer Paragon 1000 and were referenced to the 1602.8 cm^{-1} band of polystyrene.

3.2.2 Materials

All solvents used were reagent grade or better. Diethyl ether, tetrahydrofuran, toluene, benzene and hexanes were distilled from sodium metal and benzophenone prior to use.

Dichloromethane, methanol and *n*-butanol were distilled from calcium hydride before use and stored over sodium hydroxide. 2,6-lutidine and pyridine were distilled from powdered

potassium hydroxide before use. TLC plates were purchased from Sigma-Aldrich and used as received. Visualization of compounds on the TLC plates was performed using ultraviolet light, potassium permanganate stain, *p*-anisole stain or bromine stain. All organometallic reagents were titrated before use using benzophenone. *p*-xylene, *n*-butyllithium (1.6 M in hexanes or 2.5 M in hexanes), *t*-butyllithium (1.7 M in pentane), methylmagnesium bromide (3 M in diethyl ether) and boron trichloride (1.0 M in CH₂Cl₂) were purchased from Sigma Aldrich. Tropylium tetrafluoroborate was purchased from Alfa Aesar and used as received. *tert*-Butyldimethylsilyl trifluoromethanesulfonate was purchased from TCI Chemicals used as received. 7-methoxy-1,3,5-cycloheptatriene,⁶⁰ 3,4-dimethyl-2-cyclopenten-1-one,⁴⁴ 3-methoxy-1,3,5-cycloheptatriene,⁶¹ 4,8-dibromo-1,1,3,3,7,7,9,9-octamethyl-*s*-hydrindacene,⁶² 2,5-dibromo-*p*-xylene,⁶³ and dimethyl-2,5-dibromo-terephthalate⁶³ were synthesized according to their literature methods. Deuterated solvents were purchased from Cambridge Isotopes and dried over 3Å molecular sieves before use. All other commercially available reagents were used as received. All sonication was performed using a SONAER Model 241 running at 2.4 MHz. Silica used for column chromatography was Silicycle SiliaFlash P60 with a particle size of 40-63 μm (230-400 mesh).

3.2.3 Synthesis

4-bromo-8-(7-(1,3,5-cycloheptatriene)-1,1,3,3,5,5,7,7-octamethyl-*s*-hydrindacene 50.⁶⁴

To a stirring solution of 4,8-dibromo-1,1,3,3,5,5,7,7-octamethyl-*s*-hydrindacene, **25**, (0.12 g, 0.28 mmol) in dry THF (6 mL) under N₂ at -78° C was added *n*-butyllithium (0.47 mL, 0.29 mmol)

dropwise over 15 minutes. The solution was stirred at -78°C for 1 hour. Tropylium tetrafluoroborate (68 mg, 0.38 mmol) was then added at -78°C and the solution was allowed to warm to room temperature. The reaction was quenched after 12 hours of stirring with a 2N (5 mL) solution of HCl. The layers were separated and the organic layer washed with a 10% NaHCO_3 solution (2 x 5 mL) and with a saturated sodium chloride solution (2 x 5 mL). The organic layer was dried over MgSO_4 , filtered and evaporated to dryness *in vacuo* to leave a white solid (90% yield, 90 mg, 0.25 mmol). The proton NMR of the obtained compound matched that previously reported for 4-bromo-1,1,3,3,5,5,7,7-octamethyl-s-hydrindacene (**53**). $^1\text{H-NMR}$ (CDCl_3) δ 1.30 (s, 12H, $-\text{CH}_3$), 1.51 (s, 12H, $-\text{CH}_3$), 1.91 (s, 2H, $-\text{CH}_2-$), 1.97 (s, 2H, $-\text{CH}_2-$), 6.81 (s, 1H, Ar-H) Literature: $^1\text{H-NMR}$ (CDCl_3): δ 1.27 (s, 12H, $-\text{CH}_3$), 1.51 (s, 12H, $-\text{CH}_3$), 1.93 (s, 4H, $-\text{CH}_2-$), 6.77 (s, 1H, Ar-H).

Alternate Synthesis: To a stirring solution of 4,8-dibromo-1,1,3,3,5,5,7,7-octamethyl-s-hydrindacene (127 mg, 0.30 mmol) in dry THF under dry N_2 at -78°C was added *n*-butyllithium (0.48 mL, 0.30 mmol) drop wise over 15 minutes. The solution was stirred for 1 hour. Freshly distilled 7-methoxy-1,3,5-cycloheptatriene (36 mg, 0.30 mmol) was added dropwise and the reaction was allowed to warm to room temperature. The reaction was quenched after 12 hours with a 2N (5 mL) solution of HCl. The layers were separated and the organic layer washed with a 10% NaHCO_3 solution (2 x 5 mL) and with brine (2 x 5 mL). The organic layer was dried over MgSO_4 and evaporated *in vacuo*. The proton NMR data for the compound obtained matched that of 4-bromo-1,1,3,3,5,5,7,7-octamethyl-s-hydrindacene reported previously in this section.

4-bromo-8-(3-(1,3,5-cycloheptatriene)-1,1,3,3,5,5,7,7-octamethyl-s-hydrindacene 50

To a stirring solution of 4,8-dibromo-1,1,3,3,5,5,7,7-octamethyl-s-hydrindacene (130 mg, 0.30 mmol) in dry THF (6 mL) under dry N₂ at -78° C was added *n*BuLi (0.48 mL, 0.30 mmol) drop wise over 15 minutes. The solution was stirred for 1 hour at -78° C. After which 3-methoxy-1,3,5-cycloheptatriene (36 mg, 0.30 mmol) was added dropwise and the reaction was allowed to warm to room temperature. The reaction was quenched after 12 hours of stirring with a 2 N solution (5 mL) of HCl. The layers were separated and the combined organic layer was washed with a 10% NaHCO₃ solution (2 x 5 mL) and with brine (2 x 5 mL). The organic layer was dried over MgSO₄ and evaporated *in vacuo*. The proton NMR data of the compound matched that of 4-bromo-1,1,3,3,5,5,7,7-octamethyl-s-hydrindacene previously reported.

5-bromo-2-(cyclohepta-2,4,6-triene)-*p*-xylene 58.⁶⁴ A stirring solution of 2,5-dibromo-*p*-xylene (1.0 g, 3.7 mmol) and diethyl ether (6.2 mL) under a dry N₂ atmosphere was cooled to 0° C and *n*BuLi (1.52 mL, 3.79 mmol) was added dropwise over a 30 minute period. After 1 hour stirring at 0° C, the solution was slowly cannulated into a flask containing tropylium tetrafluoroborate (0.23 g, 1.9 mmol) in diethyl ether (16mL) under a dry N₂ atmosphere at 0° C. The reaction was sonicated for 1 hour at room temperature and stirred for a further 24 hours. The reaction was quenched with 2 M HCl (5 mL) and extracted with diethyl ether (3 x 5 mL). Removal of the solvent produced a white powder (52%, 0.54 g, 1.9 mmol). ¹H-NMR (CDCl₃): δ 2.17 (s, 3H, aryl-CH₃), 2.42 (s, 3H, aryl-CH₃), 2.86 (t, *J* = 5.4 Hz, 1H, C₇H₇, 7-CH), 5.35 (dd, *J* = 18 Hz, *J* = 30 Hz, 2H, C₇H₇, 1,6-CH), 6.30 (ddd, *J* = 1.5 Hz, 2H, C₇H₇, 2,5-CH), 6.76 (d, *J* = 2.7 Hz, 2H, C₇H₇, 3,4-CH), 7.34 (s, 1H, aryl-H), 7.384 (s, 1H, aryl-H). ¹³C-NMR (CDCl₃): δ 19.2, 23.0, 41.7, 122.8, 125.2, 126.2, 129.7, 131.3, 134.3, 135.8, 135.9, 141.5.

2-bromo-5-(7-(1,3,5-cycloheptatriene))terephthalic acid 59.^{63, 65} To a stirring solution of 5-bromo-2-(cyclohepta-2,4,6-triene)-*p*-xylene (0.54 g, 1.9 mmol) in water was added potassium permanganate (1.73 g, 11.0 mmol). The reaction was brought to reflux (~120° C) and stirred for 8 hours. The reaction was allowed to cool to room temperature then quenched with 2M HCl (5 mL) followed by extraction with diethyl ether (3 x 5 mL). The organic layers were combined and washed with brine (7 mL) then dried over MgSO₄. The solvent was evaporated *in vacuo*. The ¹H-NMR of the impure product showed both methyl peaks intact and a lack of unsaturated peaks corresponding to 1,3,5-cycloheptatriene. Prominent peaks were observed as singlets in the ¹H-NMR spectrum. ¹H-NMR (DMSO-*d*₆): δ 1.78, 1.83, 2.26, 2.27, 2.38, 2.48, 2.53, 2.63, 4.05, 7.51, 7.68, 7.86, 7.93, 8.03, 8.26, 8.49.

2,5-Dibromo-4-methylbenzoic Acid 62. To nitric acid (50 mL of 70%) and water (50 mL) was added 2,5-dibromo-*p*-xylene (8.08 g, 30.6 mmol) and the mixture was heated to reflux for 6 d. During the reaction, sublimation of the starting material occurred and it was reintroduced into the reaction mixture through melting. The reaction was cooled and the precipitate was removed by filtration. The filtrate was extracted with ether (2 x 20 mL). The extracts were combined with the filtered solid and water (100 mL). The reaction was sonicated as sodium carbonate (2 g) was added slowly over several hours. The layers were separated and the aqueous layer was made acidic (pH ~1) with concentrated hydrochloric acid. To this was added ether and solid sodium chloride until saturation of the aqueous layer. The layers were separated and the aqueous layer was extracted with diethyl ether (3 x 15 mL) and all organic layers were combined. The solvent was removed *in vacuo* and the solid was recrystallized from hexane (150 mL) and ether (150 mL) to afford 4.974 g (55%). Further recrystallization afforded

0.040g (0.4%) for a total of ~56% of a fine white crystalline. m.p. 187-188° C (*literature mp*: 193-195° C); ¹H-NMR (300 MHz, DMSO-*d*₆) δ 2.30 (s, 3H), 7.75 (s, 1H), 7.93 (s, 1H).

2,5-dibromoterephthalic acid 61.⁶⁵ A stirring solution of 2,5-dibromo-*p*-xylene (10.38 g, 33.88 mmol) and potassium permanganate (11.70 g, 75.76 mmol) in water (50 mL) and pyridine (50 mL) was brought to reflux (~150° C) for 116 h. The reaction was allowed to cool and then filtered through a layer of celite (1 inch thick). The pad was washed with water and a saturated NaHCO₃ solution (50 mL). To the filtrate was added 12M HCl (25 mL) and then saturated with sodium chloride (25 g). The solution was extracted with ether (3 x 100 mL) and the organic layers combined and dried over magnesium sulfate. Evaporation of the solvent *in vacuo* yielded 2.57g (21%) of a white solid. ¹H-NMR (DMSO-*d*₆): δ 7.99 (s, 2H). *literature*: ¹H-NMR (DMSO-*d*₆): δ 5.06 (s, br, 2H), 8.02 (s, 2H).

Alternate synthesis:⁶³ 2,5-dibromo-*p*-xylene (20.0 g, 75.8 mmol) in 150 mL pyridine and 75 mL of H₂O was brought to reflux (~150° C) and potassium permanganate (59.9 g, 379 mmol) was added in a single portion. Every 30 minutes for 2 hours another portion of potassium permanganate (30 g, 126 mmol) in water (60 mL) was added. The reaction was kept at reflux overnight. After cooling to room temperature the reaction was filtered through a pad of celite. The reaction was acidified through addition of hydrochloric acid (1 M, 100 mL) then extracted with ethyl acetate (3 x 100 mL). The combined organic layers were dried over MgSO₄, filtered and dried to leave a white solid with a yield of 89% (21.8 g, 67.5 mmol). Spectroscopic data match that previously reported.

Di-*n*-butyl 2,5-dibromoterephthalate 63.⁶⁶ To a stirring solution of thionyl chloride (42.1 g, 194 mmol) was added 2,5-dibromo-terephthalic acid (2.67 g, 8.3 mmol). The mixture

was stirred at 80° C for 3 h. The thionyl chloride was removed *in vacuo* to obtain a colorless solid. To the solid was added dichloromethane (25 mL) and *n*-butanol (1.5 mL, 16 mmols) *via* an addition funnel and brought to reflux (~130° C). After 5 hours the reaction was cooled and ice water (50 mL) was added. The solution was separated and the organic layer was washed with a saturated aqueous NH₄Cl (3 x 15 mL). The solvent was evaporated *in vacuo* leaving a yellow oil. Recrystallization from ethanol yielded 1.60 g of a white solid (44%). m.p. 53° C. IR cm⁻¹ (KBr): 1119, 1466, 1721, 2858, 2927, 2972. ¹H-NMR (CDCl₃): δ 0.97 (t, *J* = 2.5 Hz, 6H, -CO₂(CH₂)₃CH₃), 1.49 (sextet, *J* = 2.5 Hz, 4H, -CO₂(CH₂)₂CH₂CH₃), 1.78 (quintet, *J* = 2.3 Hz, 4H, -CO₂CH₂CH₂-), 4.37 (t, *J* = 2.2 Hz, 4H, -CO₂CH₂-), 8.03 (s, 2H, aryl-H). ¹³C-NMR (CDCl₃): δ 14.1, 19.6, 30.9, 66.6, 120.4, 136.2, 136.8, 120.4.

Alternate Synthesis: A stirring solution of *n*-butanol (116 mL), thionyl chloride (4.76 g, 40.0 mmol) and 2,5-dibromo-terephthalic acid (2.57 g, 8.00 mmol) was refluxed (~130° C) for 12 hours under a N₂ atmosphere. The reaction was allowed to cool to room temperature and quenched with 3 M NaOH (30 mL). The layers were separated and the aqueous layer was extracted with diethyl ether (3 x 30 mL). The organic layers were combined, washed with brine (20 mL) and the solvent removed *in vacuo* to leave a yellow oil. Recrystallization from methanol yielded white crystals. (73%). Spectroscopic data matched that as reported above for compound **63**.

2,5-dibromo-1,4-bis-(2-hydroxy-2-propyl)benzene 64.⁶⁷ To a stirring solution of di-*n*-butyl-2,5-dibromo terephthalate (0.60 g, 1.3 mmol) at 0° C under N₂ was added methylmagnesium bromide in diethyl ether (3.50 mL, 10.5 mmol). The reaction was stirred at 0° C for 1 hour and then allowed to warm to room temperature. The reaction was quenched

slowly with 2M HCl until no more precipitate formed (pH 2~3). The layers were separated and the organic layer was washed with brine (15 mL). Evaporation of the solvent yielded a pale yellow solid. The impure product was filtered through a layer of silica gel with a solution of MeOH:DCM (1:100) to yield 240 mg of a white crystalline solid (53%). m.p. 220°-223° C. IR cm^{-1} (KBr): 851, 953, 1362, 1465, 2964, 3381. $^1\text{H-NMR}$ (DMSO- d_6): δ 1.59 (s, 12H, C- CH_3), 5.40 (s, 2H, -OH), 7.96 (s, 2H, aryl-H). $^{13}\text{C-NMR}$ (DMSO- d_6): δ 29.4, 72.0, 119.4, 134.5, 148.8.

2,5-dibromo-1,4-bis-(2-(dimethyl-*t*-butyl silyl ether)-2-propyl)benzene 65.⁶⁸ To a stirring solution of 2,5-dibromo-1,4-bis-(2-hydroxy-2-propyl)benzene (3.48 g, 9.89 mmol) in dichloromethane (30 mL) was added 2,6-lutidine (4.56 mL, 39.3 mmol) and *t*-butyldimethylsilyl trifluoromethanesulfonate (5.45 mL, 23.8 mmol). The solution was stirred overnight then quenched with deionized water (10 mL). The layers were separated and the aqueous layer was extracted with DCM (3 x 15 mL). The organic extracts were combined and washed with 10% CuSO_4 (15 mL) and brine (20 mL). Evaporation of the solvent produced an off white solid in a 70% yield (4.02g, 6.92 mmol). Purification was performed through chromatographic methods to produce white crystals. $R_f = 0.98$ (hexanes). $^1\text{H-NMR}$ (DMSO- d_6): δ 0.19 (s, 12H, Si- CH_3), 1.01 (s, 18H, C-(CH_3)₃), 1.76 (s, 12H, C- CH_3), 8.12 (s, 2H, aryl-H). $^{13}\text{C-NMR}$ (DMSO- d_6): δ -2.0, 18.5, 26.0, 30.2, 76.2, 118.6, 134.8, 148.1.

1,4-bis-(2-(dimethyl-*t*-butylsilyl ether)-2-propyl)-2-bromo-5-cyclohepta-1,3,5-triene-benzene 66. Tropylium tetrafluoroborate (0.44 g, 2.4 mmol) was placed in a 100 mL Schlenk flask with an addition funnel attachment and septa. To this was added 8mL of dry THF. In a separate round bottom 50 mL Schlenk flask was added 2,5-dibromo-1,4-bis-(2-(dimethyl-*t*-butyl

silyl ether)-2-propyl)benzene (0.39 g, 1.1 mmol) under dry Argon. Diethyl ether (10 mL) and THF (10 mL) were added and the temperature lowered to -78° C. The *n*BuLi (1.5 mL, 2.5 mmol) was added slowly dropwise over 30 minutes. The reaction was stirred for 30 minutes at -78° C and then allowed to warm to room temperature. The lithiated intermediate was cannulated into the addition funnel and slowly added to the tropylium tetrafluoroborate slurry dropwise at -78° C. The reaction was sonicated for 10 minutes and allowed to stir overnight slowly warming to room temperature. The solution was quenched with a 10% NaHCO₃ solution (15 mL) and then washed with brine (20 mL). Evaporation of the solvent *in vacuo* left a yellow solid. Proton NMR of this impure product did not show any proton resonances corresponding to the spectrum expected for the 1,3,5-cycloheptatriene subunit but that of compound **68**.

1,4-dibromo-2,5-diisopropenyl-benzene 70. A stirring solution of 2,5-dibromo-1,4-bis-(2-hydroxy-2-propyl)benzene (11.1 g, 31.5 mmol), *p*-toluenesulfonic acid (1.0 g, 5.8 mmol) in 60 mL of toluene was brought to reflux (~125° C) in a 250 mL round bottom flask equipped with a Dean-Stark apparatus. After 12 hours, the reaction was allowed to cool to room temperature and quenched with 1 M NaOH (10 mL). The aqueous layer was extracted with diethyl ether (3 x 15 mL), washed with brine and dried over MgSO₄. Evaporation of the solvent *in vacuo* produced a brown oil. The product was purified through column chromatography with hexanes ($R_f = 0.67$) and produced a clear oil which crystallized to white crystals over a 2 hour period at room temperature in a 45% yield (14.2 mmol). $R_f = 0.67$. m.p. 48° – 50° C. IR cm⁻¹ (KBr): 541, 890, 906, 1052, 1256, 1470, 1639, 2967, 3078. ¹H-NMR (CDCl₃): δ 2.12 (m, 6H, HHC=CCH₃), 5.00 (m, 2H, HHC=CCH₃), 5.27 (m, 2H, HHC=CCH₃), 7.43 (s, 2H, aryl-H). ¹³C-NMR (CDCl₃): δ 23.7, 117.3, 120.7, 133.9, 144.7, 145.2.

7-(4-bromo-2,5-diisopropenylphenyl)-1,3,5-cycloheptatriene 71. To a stirring solution of **66** (1.58 g, 5.00 mmol) in diethyl ether (50 mL) at -78° C was added *n*BuLi (5.0 mmol) over a 10 minute period. After stirring for 1 hour at -78° C, tropylium tetrafluoroborate (0.89 g, 5.0 mmol) was added in a single portion and stirred overnight at -78° C. The reaction was warmed to room temperature and quenched with 1 M HCl (5 mL). The organic and aqueous layers were separated and the organic layer was washed with 10% NaHCO₃ brine and dried over MgSO₄. Evaporation of the solvent *in vacuo* left a yellow oil. Purification by column chromatography using hexanes produced a light yellow oil which solidified at subzero temperatures and remained a semisolid crystal at room temperature. *R*_f = 0.49. m.p. 41° C. IR cm⁻¹ (KBr): 3080, 3011, 2969, 1637, 904, 705. ¹H-NMR (CDCl₃): δ 1.97 (d, 3H, HHC=CCH₃), 2.21 (d, 3H, HHC=CCH₃), 3.03 (br m, 1H, C₇H₇, 7-CH), 4.85 (s, 1H, HHC=CCH₃), 5.07 (s, 1H, HHC=CCH₃), 5.13 (d, 1H, HHC=CCH₃), 5.31 (d, 1H, HHC=CCH₃), 5.36 (dd, 2H, C₇H₇, 1,6-CH), 6.27 (m, 2H, C₇H₇, 2,5-CH), 6.75 (m, 2H, C₇H₇, 3,4-CH), 7.43 (s, 1H, aryl-H), 7.44 (s, 1H, aryl-H). ¹³C-NMR (CDCl₃): δ 23.6, 24.9, 41.4, 116.1, 116.2, 118.9, 124.4, 127.1, 128.8, 130.8, 131.9, 140.6, 143.5, 143.8, 144.2, 145.6.

1-(4-(1,3,5-cycloheptatriene)-2,5-diisopropenylphenyl)-3,4-dimethylcyclopent-2-enol 72. To a stirring solution of 7-(4-bromo-2,5-diisopropenylphenyl)-1,3,5-cycloheptatriene (0.31g, 0.94 mmol) in 16 mL of a 2:3 diethyl ether and toluene solution at -78° C was added *t*-BuLi (2.06 mmol, 1.22 mL) dropwise over a 10 minute period at -78° C. The reaction was stirred for 1 hour at -78° C and then 3,4-dimethyl-2-cyclopenten-1-one was added dropwise over a 10 minute period. The reaction was warmed slowly to room temperature overnight and then quenched with saturated aqueous NH₄Cl. The layers were separated and the aqueous layer was extracted

with diethyl ether (3x). The organic fractions were combined and washed with brine then dried over MgSO₄. Evaporation of the solvent *in vacuo* left a yellow oil. Proton NMR spectra of the impure product showed a singlet at 5.47 ppm hypothesized to correspond to the proton on the unsaturated carbon. Purification through column chromatography (100:1 hexanes: ethyl acetate) produced a yellow oil (79% yield, 0.25 g, 0.74 mmol). Proton NMR spectra of the purified product showed a new compound. ¹H-NMR (CDCl₃): δ 1.79 (dd, 3H, -C₅H₃(CH₃)₂), 1.82 (dd, 3H, -C₅H₃(CH₃)₂), 1.87 (d, 3H, HHC=CCH₃), 1.90 (dd, 3H, HHC=CCH₃), 2.87 (m, 1H, C₇H₇, H, 7-CH), 3.17 (s, 2H, -C₅H₃(CH₃)₂, 5-CH₂), 4.68 (m, 1H, HHC=CCH₃), 4.94 (m, 1H, HHC=CCH₃), 4.97 (m, 1H, HHC=CCH₃), 5.03 (m, 1H, HHC=CCH₃), 5.28 (m, 2H, C₇H₇, 1,6-CH), 6.20 (m, 2H, C₇H₇, 2,5-CH), 6.56 (s, 1H, -C₅H₃(CH₃)₂, 2-CH), 6.69 (t, 2H, C₇H₇, 4,3-CH), 6.99 (s, 1H, aryl-H), 7.22 (s, 1H, aryl-H). ¹³C-NMR (CDCl₃): δ 12.6, 13.3, 23.8, 25.1, 41.6, 47.5, 115.1, 115.2, 124.1, 127.6, 127.7, 128.5, 130.6, 132.8, 135.0, 135.3, 135.8, 138.9, 141.3, 142.2, 142.5, 144.8, 148.0.

4-(3,4-dimethyl-1,3-cyclopentadiene)-8-(1,3,5-cycloheptatriene)-1,1,3,3,5,5,7,7-octamethyl-s-hydrindacene, 51.⁶² Compound **73** was placed in a 250 mL 3-necked round bottom flask equipped with a nitrogen inlet, gas condenser and an oil bubbler. To this was added CH₂Cl₂ (12 mL) under a dry argon atmosphere and the temperature lowered to -78° C. Dry ice was placed in the gas condenser and isobutene was condensed into the reaction (excess). BCl₃ in CH₂Cl₂ (0.16 mL, 0.16 mmol) was added dropwise. The yellow color of the reaction changed to a grey color. The reaction was allowed to warm to room temperature overnight. The reaction was quenched with H₂O (5 mL) and NaOH (1 M, 5 mL). The layers were separated and the aqueous layer was extracted with CH₂Cl₂ (3 x 10 mL). The organic fractions were combined and dried over MgSO₄. Removal of the solvent produced a sticky solid. ¹H-

NMR of the impure product showed aryl proton peaks and peaks unsaturated proton region.

Both characteristics of the starting material. $^1\text{H-NMR}$ (CDCl_3): δ 0.77-0.79 (9H), 1.03 (8H), 1.18 (6H), 1.34 (3H), 1.68 (2.5H), 1.84 (3H), 2.02 (2H), 4.66 (1H), 4.8 (0.5H), 4.87 (0.14H), 4.9 (1H), 5.9 (0.5H), 6.1 (2H), 6.6 (2H), 6.96 (0.5H), 7.27 (0.5H).

3.2.4 Crystallographic Studies

All crystals suitable for single crystal X-ray diffractometry were removed from a vial and immediately covered with a layer of silicone oil. A single crystal was selected, mounted on a glass rod on a copper pin, and placed in the cold N_2 stream provided by an Oxford Cryosystems cryometer. XRD data collection was performed for compounds **63**, **64**, **65**, **70**, and **71**, on a Bruker APEX II diffractometer with use of Mo $\text{K}\alpha$ radiation ($\lambda = 0.71073 \text{ \AA}$) and a CCD area detector. Empirical absorption corrections were applied using SADABS.^{36,37} The structures were solved with use of either direct methods or the Patterson option in SHELXS and refined by the full-matrix least-squares procedures in SHELXL.^{38,38} The space group assignments and structural solutions were evaluated using PLATON.^{40,41} Non-hydrogen atoms were refined anisotropically. Hydrogen atoms were located in calculated positions corresponding to standard bond lengths and angles. Crystallographic data and structures were submitted to The Cambridge Crystallographic Database Center. Each compound was assigned a unique identifying number. Compound **63**: CCDC1031528; Compound **64**: CCDC 1020280; Compound **65**: CCDC 1031527; Compound **70**: CCDC1020281; Compound **71**: CCDC1031530. Data for the compounds crystallographically studied in this work are presented in Tables 14 through 25.

3.3 XRD Crystallographic Data and Tables

Table 14 – Crystallographic XRD data and details of measurements for compounds **63** and **64**.

Compound	63	64
Formula	C ₁₆ H ₂₀ Br ₂ O ₄	C ₁₂ H ₁₆ Br ₂ O ₂
Fw (g mol ⁻¹)	436.14	352.07
<i>a</i> (Å)	7.077 (3)	7.8950 (8)
<i>b</i> (Å)	8.091 (3)	17.9970 (18)
<i>c</i> (Å)	8.190 (3)	9.0940 (9)
α (°)	111.352 (8)	90
β (°)	91.676 (9)	90.730 (2)
γ (°)	105.701 (8)	90
<i>V</i> (Å ³)	416.2 (3)	1292.0 (2)
<i>Z</i>	1	4
Crystal size (mm)	-	0.22 x 0.06 x 0.06
Crystal habit	Block	Block
Crystal system	Triclinic	Monoclinic
Space group	P1	P2(1)/c
<i>d</i> _{calc} (mg/m ³)	1.740	1.810
μ (mm ⁻¹)	4.88	6.258
<i>T</i> (K)	73	83(2)
2 θ range (°)	2.7 to 26.7	2.5 to 25.9
<i>F</i> (000)	218	296
<i>R</i> _{int}	0.035	0.0277
independent reflns	1712	2979
No. of params	101	151
R1, wR2 (>2 σ)	R1 = 0.019 wR2 = 0.0449	R1 = 0.0337 wR2 = 0.0603

Mo K α ($\lambda=0.71073\text{\AA}$). $R_1 = \sum / |F_o| - |F_c| / \sum |F_o|$; $wR2 = [\sum_w(F_o^2 - F_c^2)^2 / \sum_w(F_o^2)^2]^{1/2}$

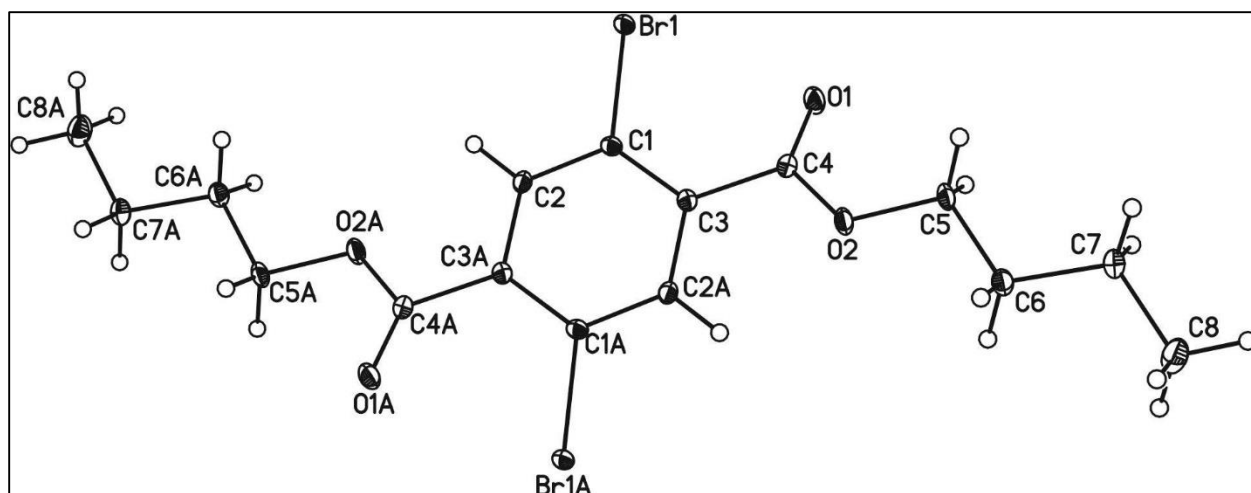


Figure 21 – ORTEP drawing of the crystallographically-determined molecular structures of compound **63**. Thermal ellipsoids are drawn with on all non-hydrogen atoms with a 30% probability.

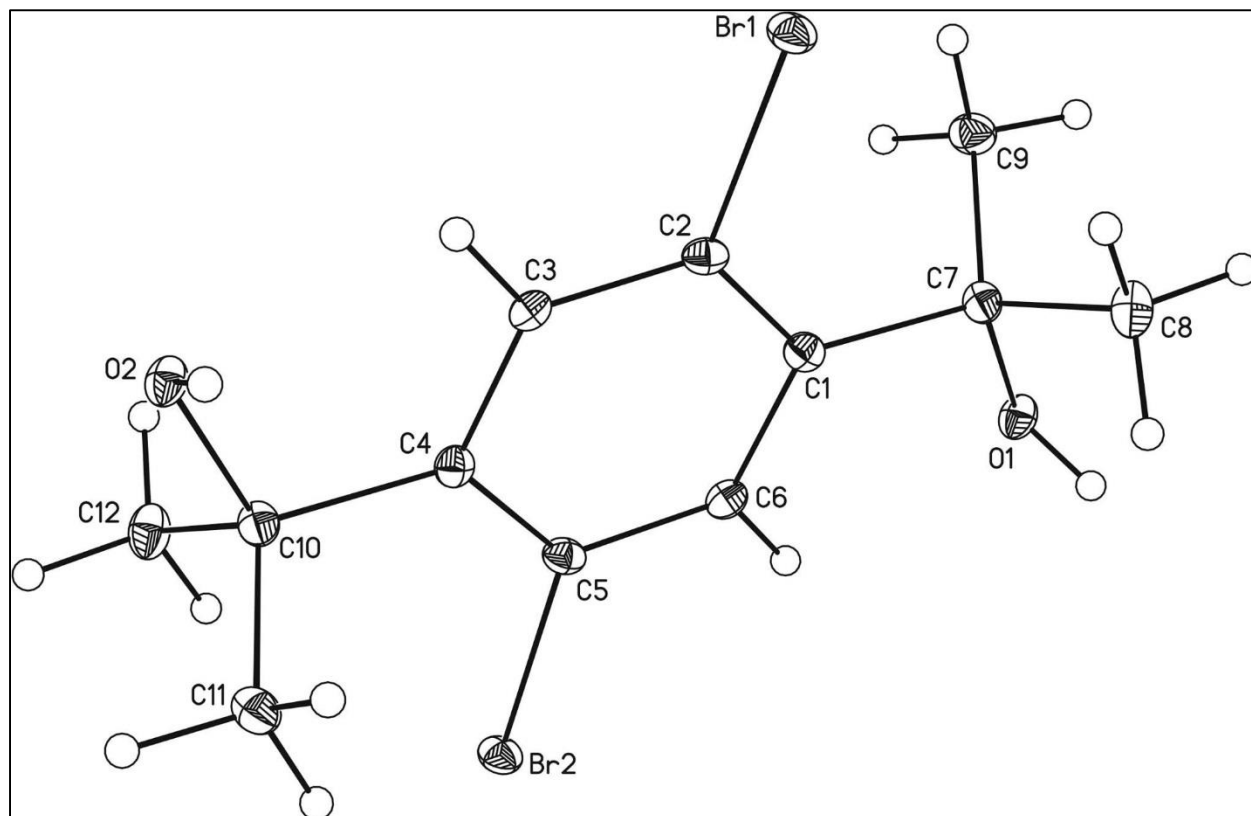


Figure 22 – ORTEP drawing of the crystallographically-determined molecular structures of compound **64**. Thermal ellipsoids are drawn with on all non-hydrogen atoms with a 30% probability.

Table 15 – Selected Bond Lengths (Å) for compound **63** with estimated standard deviation in parentheses.

Bond	Length	Bond	Length
Br1—C1	1.8924 (17)	C4—O1	1.198 (2)
C1—C2	1.382 (3)	C4—O2	1.339 (2)
C1—C3	1.403 (2)	C5—O2	1.457 (2)
C2—C3 ⁱ	1.397 (2)	C5—C6	1.505 (3)
C3—C2 ⁱ	1.397 (2)	C6—C7	1.525 (3)
C3—C4	1.504 (2)	C7—C8	1.522 (3)

Table 16 – Selected Bond Angles (°) for compound **63** with estimated standard deviation in parentheses.

Angle	Value	Angle	Value
C2—C1—C3	120.57 (15)	O1—C4—O2	123.76 (17)
C2—C1—Br1	116.30 (13)	O1—C4—C3	125.51 (16)
C3—C1—Br1	123.13 (13)	O2—C4—C3	110.72 (14)
C1—C2—C3 ⁱ	122.05 (16)	O2—C5—C6	107.24 (14)
C2 ⁱ —C3—C1	117.38 (16)	C5—C6—C7	111.92 (14)
C2 ⁱ —C3—C4	118.78 (15)	C4—O2—C5	116.25 (13)
C1—C3—C4	123.83 (15)	C8—C7—C6	111.63 (15)

Table 17 – Selected Bond Lengths (Å) for compound **64** with estimated standard deviation in parentheses.

Bond	Length	Bond	Length
Br(1)-C(2)	1.909(2)	C(4)-C(10)	1.540(3)
Br(2)-C(5)	1.915(2)	C(9)-C(7)	1.528(3)
O(2)-C(10)	1.445(3)	C(7)-O(1)	1.441(3)
C(8)-C(7)	1.526(3)	C(7)-C(1)	1.547(3)
C(3)-C(2)	1.389(3)	C(10)-C(12)	1.524(3)
C(3)-C(4)	1.390(3)	C(10)-C(11)	1.534(3)
C(2)-C(1)	1.399(3)	C(6)-C(5)	1.386(3)
C(4)-C(5)	1.400(3)	C(6)-C(1)	1.392(3)

Table 18 – Selected Bond Angles (°) for compound **64** with estimated standard deviation in parentheses.

Angle	Value	Angle	Value
C(2)-C(3)-C(4)	123.1(2)	C(3)-C(4)-C(5)	115.0(2)
C(3)-C(2)-C(1)	121.8(2)	C(3)-C(4)-C(10)	119.1(2)
C(3)-C(2)-Br(1)	114.10(17)	C(5)-C(4)-C(10)	125.9(2)
C(1)-C(2)-Br(1)	124.10(18)	C(6)-C(5)-C(4)	122.1(2)
C(5)-C(6)-C(1)	122.8(2)	C(6)-C(5)-Br(2)	113.95(17)
C(8)-C(7)-C(1)	110.8(2)	C(4)-C(5)-Br(2)	123.93(17)
C(9)-C(7)-C(1)	111.0(2)	O(1)-C(7)-C(8)	109.19(19)
O(2)-C(10)-C(12)	104.65(19)	O(1)-C(7)-C(9)	104.68(19)
O(2)-C(10)-C(11)	107.65(19)	C(8)-C(7)-C(9)	112.4(2)
C(12)-C(10)-C(11)	113.1(2)	O(1)-C(7)-C(1)	108.52(18)
O(2)-C(10)-C(4)	109.75(18)	C(6)-C(1)-C(2)	115.2(2)
C(12)-C(10)-C(4)	111.5(2)	C(6)-C(1)-C(7)	118.9(2)
C(11)-C(10)-C(4)	109.97(19)	C(2)-C(1)-C(7)	125.9(2)

Table 19 – Crystallographic data and details of measurements for compounds **65**, **70** and **71**.

Compound	65	70	71
Formula	C ₂₄ HBr ₂ O ₂ Si ₂	C ₁₂ H ₁₂ Br ₂	C ₁₉ H ₁₉ Br
Fw (g mol ⁻¹)	580.59	316.04	327.25
<i>a</i> (Å)	6.3501(16)	7.1259(10)	9.214(2)
<i>b</i> (Å)	8.940(2)	8.3976(12)	8.815(2)
<i>c</i> (Å)	12.787(3)	10.6249 (15)	19.903(5)
α (°)	84.588(3)	80.718(3)	90.0
β (°)	80.250(3)	76.621(3)	95.296(6)
γ (°)	88.817(3)	81.670(3)	90
<i>V</i> (Å ³)	712.2(3)	606.60(15)	1609.62
<i>Z</i>	1	2	4
Crystal size (mm)	0.34 x 0.16 x 0.08	0.20 x 0.20 x 0.21	0.30 x 0.31 x 0.28
Crystal system	Triclinic	Triclinic	Monoclinic
Space group	P-1	P1	P 2 ₁ /n
<i>d</i> _{calc} (mg/m ³)	1.354	1.810	1.350
μ (mm ⁻¹)	2.947	6.258	2.542
<i>T</i> (K)	83(2)	83(2)	90
2 θ range (°)	1.62 to 24.96	2.0 to 26.6	24.633
<i>F</i> (000)	302	308	672.0
<i>R</i> _{int}	0.0277	0.020	
independant reflns	2488	2501	
No. of params	143	175	183
R1, wR2 (all data)	R1 = 0.0440 wR2 = 0.1178	R1 = wR2 =	R1 = 0.0916 wR2 = 0.2487
R1, wR2 (>2 σ)	R1 = 0.0535 wR2 = 0.1235	R1 = wR2 =	R1 = wR2 =

Mo K α ($\lambda=0.71073\text{\AA}$). $R_1 = \sum |F_o| - |F_c| / \sum |F_o|$; $wR_2 = [\sum_w(F_o^2 - F_c^2)^2 / \sum_w(F_o^2)^2]^{1/2}$

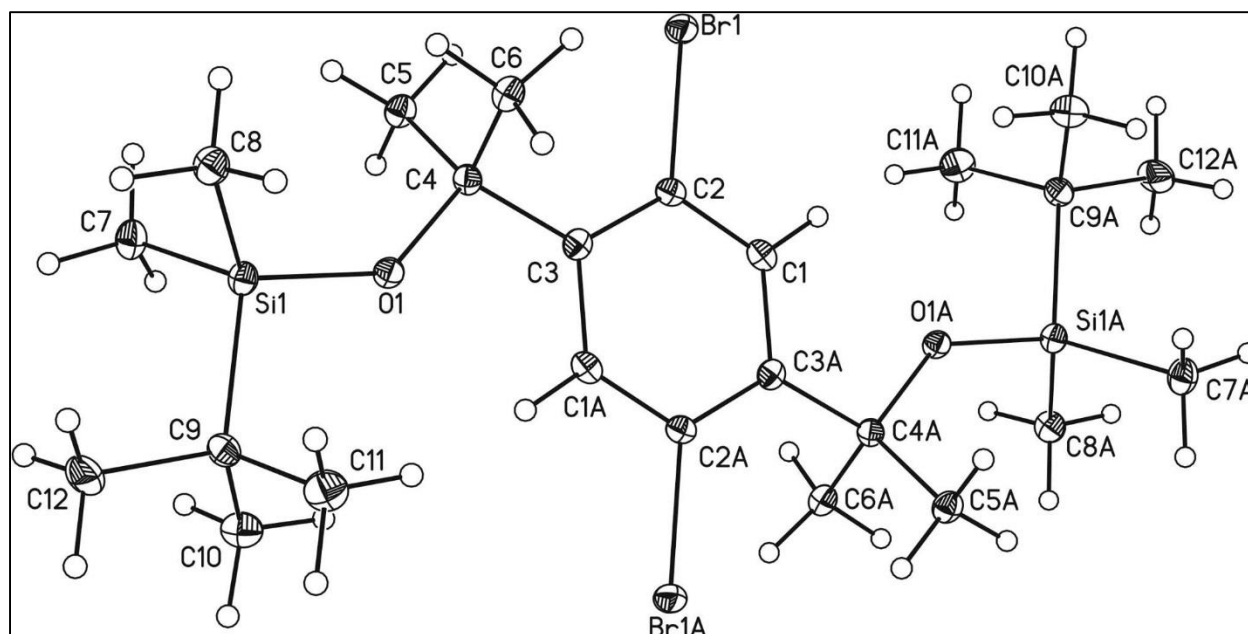


Figure 23 – ORTEP drawing of the crystallographically-determined molecular structures of compound **65**. Thermal ellipsoids are drawn with on all non-hydrogen atoms with a 30% probability.

Table 20 – Selected Bond Lengths (Å) for compound **65** and estimated standard deviations in parentheses.

Bond	Length	Bond	Length
Br(1)-C(2)	1.924(4)	C(3)-C(4)	1.545(5)
Si(1)-O(1)	1.652(3)	C(2)-C(1)	1.384(6)
Si(1)-C(8)	1.863(4)	C(1)-C(3)#1	1.393(5)
Si(1)-C(7)	1.871(4)	C(4)-C(5)	1.531(5)
Si(1)-C(9)	1.888(4)	C(4)-C(6)	1.539(5)
O(1)-C(4)	1.425(4)	C(9)-C(10)	1.534(6)
C(3)-C(1)#1	1.393(5)	C(9)-C(12)	1.541(6)
C(3)-C(2)	1.401(5)	C(9)-C(11)	1.543(6)

Table 21 – Selected Bond Angles (°) for compound **65** and estimated standard deviations in parentheses.

Angle	Value	Angle	Value
O(1)-Si(1)-C(8)	112.23(17)	O(1)-C(4)-C(5)	108.6(3)
O(1)-Si(1)-C(7)	112.76(17)	O(1)-C(4)-C(6)	108.7(3)
C(8)-Si(1)-C(7)	107.60(19)	C(5)-C(4)-C(6)	111.6(3)
O(1)-Si(1)-C(9)	102.96(16)	O(1)-C(4)-C(3)	106.4(3)
C(8)-Si(1)-C(9)	110.65(19)	C(5)-C(4)-C(3)	111.7(3)
C(7)-Si(1)-C(9)	110.65(19)	C(6)-C(4)-C(3)	109.6(3)
C(4)-O(1)-Si(1)	135.4(2)	C(10)-C(9)-C(12)	108.8(4)
C(1)#1-C(3)-C(2)	114.6(3)	C(10)-C(9)-C(11)	109.2(3)
C(1)#1-C(3)-C(4)	118.5(3)	C(12)-C(9)-C(11)	108.3(4)
C(2)-C(3)-C(4)	126.9(3)	C(10)-C(9)-Si(1)	110.2(3)
C(1)-C(2)-C(3)	122.5(3)	C(12)-C(9)-Si(1)	109.8(3)
C(1)-C(2)-Br(1)	113.7(3)	C(11)-C(9)-Si(1)	110.5(3)
C(3)-C(2)-Br(1)	123.8(3)	C(2)-C(1)-C(3)#1	123.0(4)

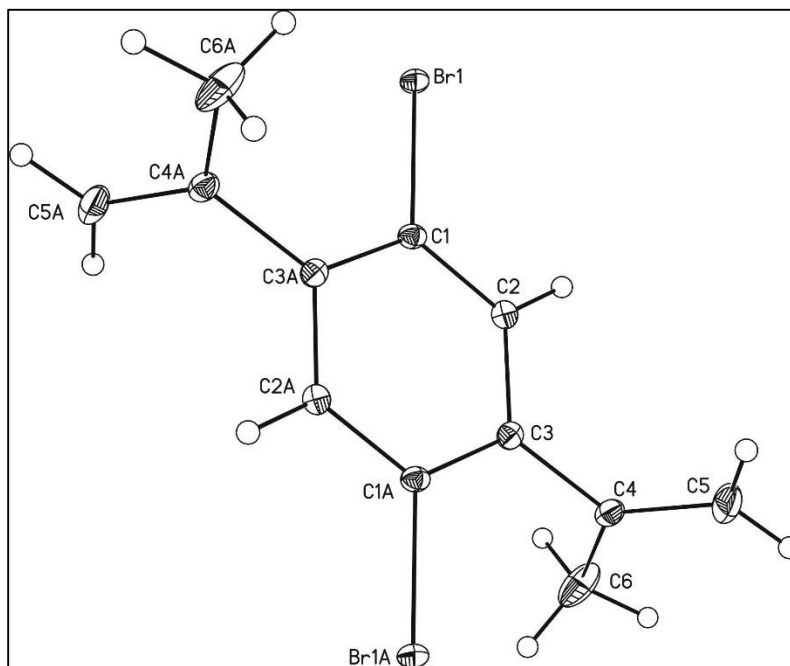


Figure 24 – ORTEP drawing of the crystallographically-determined molecular structures of compound **70**. Thermal ellipsoids are drawn with on all non-hydrogen atoms with a 30% probability.

Table 22 – Selected Bond Lengths (Å) for Compound **70** and estimated standard deviation in parentheses.

Bond	Length	Bond	Length
Br(1)-C(7)	1.8995 (16)	C(6)-C(7)ii	1.396 (2)
Br(2)-C(9)	1.899 (16)	C(6)-C(A)	1.495 (2)
C(3)-C(5)	1.395 (2)	C(7)-C(6)ii	1.396 (2)
C(3)-C(9)	1.394 (2)	C(8)-C(C)	1.377 (2)
C(3)-C(8)	1.496 (2)	C(8)-C(B)	1.446 (2)
C(4)-C(7)	1.387 (2)	C(9)-C(5)i	1.39 (2)
C(4)-C(6)	1.393 (2)	C(A)-C(D)	1.367 (3)
C(5)-C(9)i	1.39 (2)	C(A)-C(E)	1.438 (3)

Table 23 – Selected Bond Angles (°) for Compound **70** and estimated standard deviations in parentheses.

Angle	Value	Angle	Value
C(5)-C(3)-(9)	117.06 (14)	C(6)ii-C(7)-Br(1)	120.77 (12)
C(5)-C(3)-C(8)	119.54 (14)	C(C)-C(8)-C(B)	123.93 (16)
C(9)-C(3)-C(8)	123.4 (14)	C(C)-C(8)-C(3)	119.01 (15)
C(7)-C(4)-(6)	121.2 (15)	C(B)-C(8)-C(3)	117.02 (15)
C(3)-C(5)-C(9)i	120.91 (15)	C(3)-C(9)-C(5)i	122.03 (15)
C(4)-C(6)-C(7)ii	116.95 (14)	C(3)-C(9)-Br(2)	120.04 (12)
C(4)-C(6)-C(A)	119.07 (14)	C(5)i-C(9)-Br(2)	117.85 (12)
C(7)ii-C(6)-C(A)	123.98 (15)	C(D)-C(A)-C(E)	123.69 (18)
C(4)-C(7)-C(6)ii	121.85 (15)	C(D)-C(A)-C(6)	118.67 (16)
C(4)-C(7)-Br(1)	117.35 (12)	C(E)-C(A)-C(6)	117.57 (16)

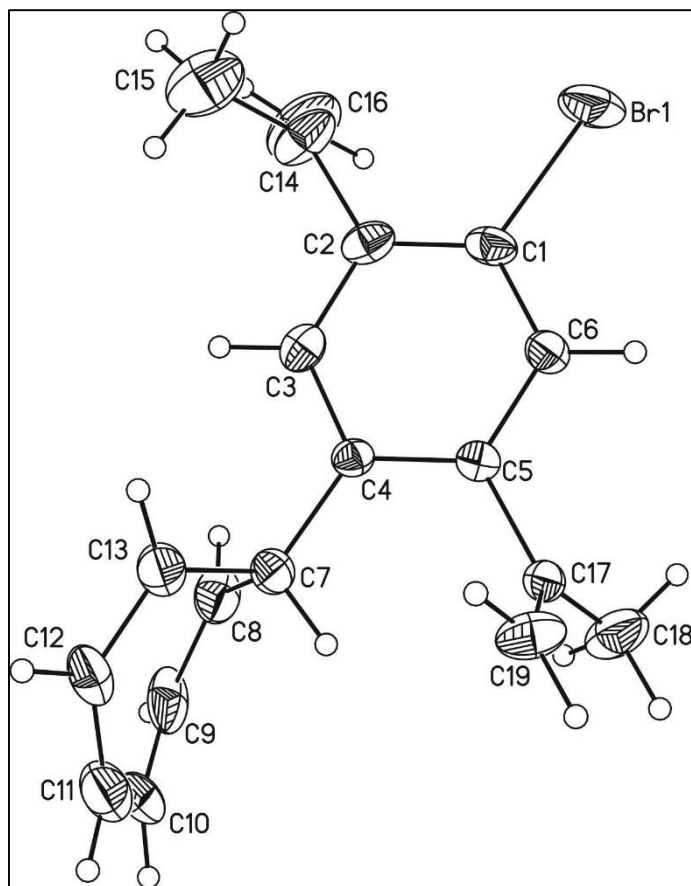


Figure 25 – ORTEP drawing of the crystallographically-determined molecular structures of compound **71**. Thermal ellipsoids are drawn with on all non-hydrogen atoms with a 30% probability.

Table 24 – Selected Bond Lengths for compound **71** and estimated standard deviations in parentheses.

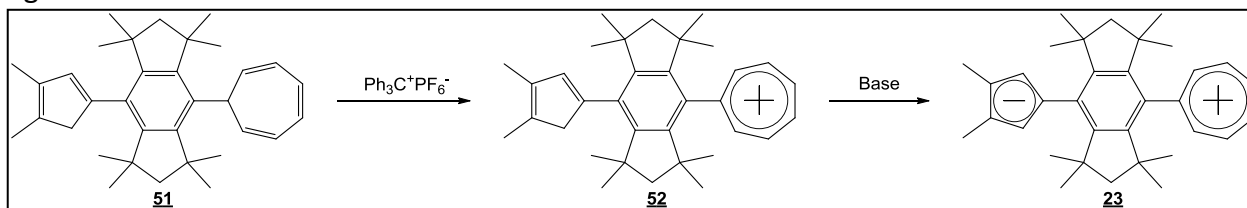
Bond	Length	Bond	Length
Br1-C1	1.903 (7)	C7-C8	1.512 (11)
C1-C6	1.376 (11)	C7-C13	1.518 (12)
C1-C2	1.386 (11)	C8-C9	1.349 (13)
C2-C3	1.374 (11)	C9-C10	1.446 (15)
C2-C14	1.496 (11)	C10-C11	1.308 (14)
C3-C4	1.389 (10)	C11-C12	1.412 (15)
C4-C5	1.388 (10)	C12-C13	1.345 (12)
C4-C7	1.510 (10)	C14-C16	1.360 (16)
C5-C6	1.396 (10)	C14-C15	1.407 (15)
C5-C17	1.505 (10)	C17-C19	1.380 (11)
		C17-C18	1.408 (12)

Table 25 – Selected Bond Angles for compound **71** and estimated standard deviations in parentheses.

Angle	Value	Angle	Value
C6—C1—C2	121.8 (7)	C4—C7—C8	114.0 (7)
C6—C1—Br1	117.6 (6)	C4—C7—C13	114.4 (7)
C2—C1—Br1	120.6 (6)	C8—C7—C13	105.0 (6)
C3—C2—C1	116.6 (7)	C9—C8—C7	120.7 (10)
C3—C2—C14	118.1 (8)	C8—C9—C10	124.6 (9)
C1—C2—C14	125.3 (8)	C11—C10—C9	127.1 (10)
C2—C3—C4	123.5 (7)	C10—C11—C12	125.2 (11)
C5—C4—C3	118.7 (7)	C13—C12—C11	125.0 (10)
C5—C4—C7	122.0 (6)	C12—C13—C7	122.7 (9)
C3—C4—C7	119.2 (7)	C16—C14—C15	115.3 (10)
C4—C5—C6	118.8 (7)	C16—C14—C2	120.2 (9)
C4—C5—C17	122.1 (6)	C15—C14—C2	118.6 (8)
C6—C5—C17	119.1 (6)	C19—C17—C18	123.2 (8)
C1—C6—C5	120.6 (7)	C19—C17—C5	119.8 (7)
		C18—C17—C5	117.0 (7)

3.4 Results and Discussion

Initial work in the synthesis of the key intermediate for a 5.6.7-quinarene/hydrindacene hybrid NLO compound, **51**, began by reinvestigating the work and observations previously reported in our group. The formation of **51** is a key intermediate in the total synthesis of **23**, as illustrated in Scheme 11. Compound **51** is the uncharged species in which pendant rings are attached in the sterically hindered pockets of the hydrindacene framework. From this point only two steps would remain; removal of a hydride group from the cycloheptatriene ring (a Dauben reaction) and removal of a proton from the cyclopentadiene ring *via* strong base, Scheme 11. The Dauben reaction has been shown in the literature to be an effective reaction for removal of a hydride to form the tropylium group.^{69,70} The reaction uses a triphenylcarbenium salt at room temperature and an inert atmosphere to remove a hydride group from cycloheptatrienes.^{69,70} Similarly the deprotonation of cyclopentadienes to form cyclopentadienyls is a well-documented process commonly used to form organometallic ligands.^{71,72} This



Scheme 11 – The remaining synthesis from key intermediate **51**.

deprotonation reaction typically requires the use of a strong base such as *n*-butyllithium and proceeds in high yields.

The key intermediate in this approach is the 4,8-dibromo-1,1,3,3,7,7,9,9-octamethyl-*s*-hydrindacene compound, **25**, that was synthesized using a recent literature methodology.⁶²

The bromide substituted carbon of the aromatic ring provides a reactive center from which the diene and triene subunits might be appended. In our work here, the addition of the tropylium precursor triene was first investigated. Addition of a 1,3,5-cycloheptatriene unit was first attempted *via* dry addition of tropylium tetrafluoroborate to the framework of compound **24**. This pathway began with the addition of a single equivalent of *n*-butyllithium followed by the addition of the tropylium ion. This method proved unsuccessful in the attachment of the triene unit to the hydrindacene structure, as seen through the NMR data obtained from the reaction. It was observed, however, that lithium halide exchange had occurred through the appearance of a singlet in the aromatic region at 6.78 ppm while the rest of the spectrum showed little change. The observed spectrum matched that of literature values for the 4-bromo-1,1,3,3,5,5,7,7-octamethyl-*s*-hydrindacene's, **53**, aromatic proton.⁶²

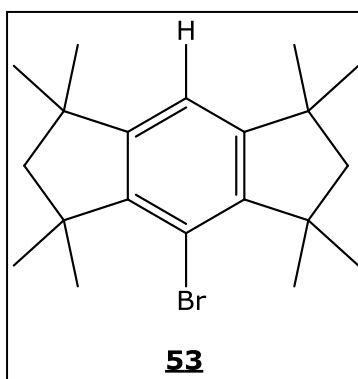


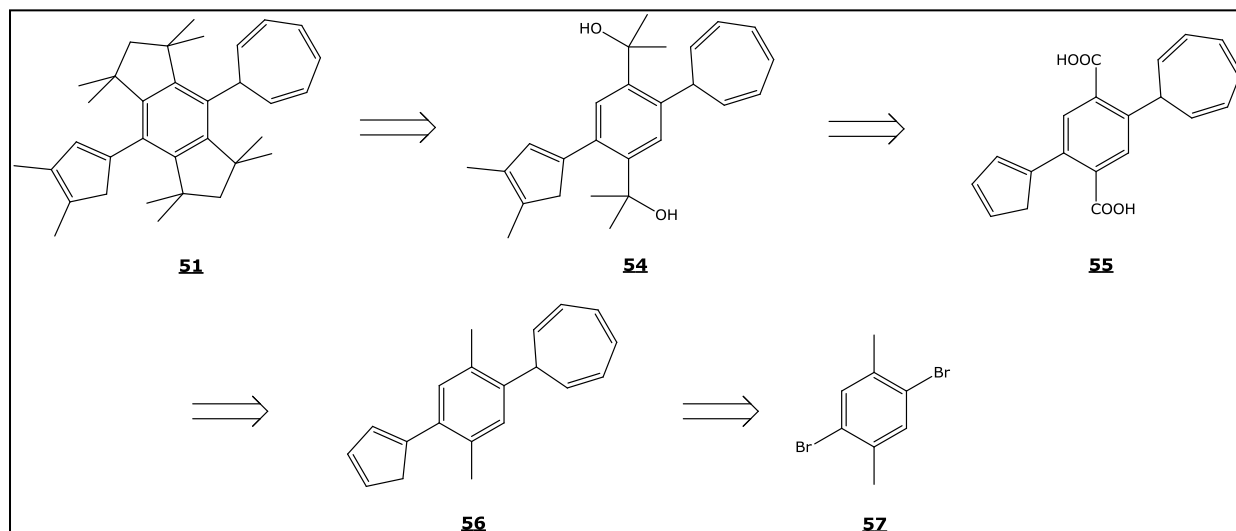
Figure 26 – 4-Bromo-1,1,3,3,5,5,7,7-octamethyl-*s*-hydrindacene.

One possibility for the observed failure of the ring substitution reaction could be the relatively low solubility of the nucleophilic agent, tropylium tetrafluoroborate. The experiment was performed using another reagent that also has the potential to add 1,3,5-cycloheptatriene to the nucleophilic bridge but was much more soluble in organic solvents, 7-methoxy-1,3,5-

cycloheptatriene.^{73,74} 7-Methoxy-1,3,5-cycloheptatriene, a derivative from tropylium tetrafluoroborate, was used in a similar manner to that employed with tropylium tetrafluoroborate. The reaction began with the lithiation of **25** to form the lithiated nucleophile at -78° C. Slow addition of 7-methoxy-1,3,5-cycloheptatriene at -78° C followed by slow warming overnight resulted in ¹H-NMR spectra showing the proton same peak at 6.78 ppm, presumably arising from the hydrogen at the 8-position of **53**, Figure 26.

These observations led to a hypothesis about the synthetic limitations imposed on any substitution reaction by the steric requirements of octamethyl-*s*-hydrindacene “pocket” around the 1,4-ring sites. Both previously attempted 1,3,5-cycloheptatriene addition reactions would form a sp³ center which could be too bulky for the restricted space available in the hydrindacene pocket.

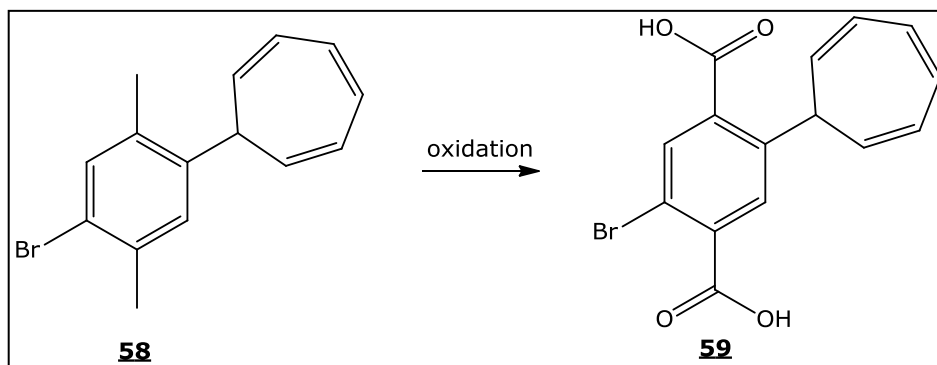
It was believed that, based upon the experiments described above, the formation of the two tetramethylpropyl bridging units on the central benzene ring of the hydrindacene framework before the nucleophilic addition of the donor and acceptor rings sterically blocks the substitution reactions and yields an ineffective method to produce the desired substituted compound. It was, therefore, hypothesized that the addition of the donor and acceptor rings onto a central benzene unit followed by building of the two methyl-substituted bridging units of the hydrinadacene framework should be an improved method for the synthesis of compound **22**, as illustrated in Scheme 12. Starting with 2,5-dibromo-*p*-xylene, compound **57**, and proceeding through a lithiated intermediate, the reactant tropylium tetrafluoroborate should add to the benzene ring *via* the reaction with tropylium tetrafluoroborate. The choice of tropylium tetrafluoroborate over 7-methoxy-1,3,5-cycloheptatriene was due to an



Scheme 12 – The retrosynthesis of key intermediate **51** via a pendant ring first method.

observation in the long term stability and storage of 7-methoxy-1,3,5-cycloheptatriene. It was discovered that the compound's reactivity decreased significantly after 24 hours, even under an inert atmosphere along with UV free and frigid conditions. Using this approach, the 5-bromo-2-(1,3,5-cycloheptatriene)-*p*-xylene compound, **58**, was formed in high yields, ~70%, after purification using standard chromatographic methods. The formation of this product was confirmed through ^1H and ^{13}C spectra. The most upfield peaks in both the proton and carbon spectrum correspond to the two methyl groups of the compound at the 1 and 4 positions. These peaks are seen at 2.17 ppm and 2.42 ppm in the proton spectrum and at 19.17 ppm and 22.99 ppm on the carbon-13 spectrum. Moving downfield in both spectra, peaks corresponding to the 1-CH on the pendant ring are observed at 2.86 ppm and 41.73 ppm. The peak at 2.86 ppm is a triplet due to splitting by its neighboring protons, 2-CH and 7-CH. Multiplets at 5.35 ppm, 6.30 ppm and 6.76 ppm represent the remaining protons on the cycloheptatriene ring, 2,7-CH, 3,6-CH and 4,5-CH respectively. Their corresponding ^{13}C peaks are observed at 125.24 ppm, 126.25 ppm and 129.68 ppm respectively.

Literature precedent shows that an unsubstituted 1,3,5-cycloheptatriene has the ability to oxidize under relatively mild conditions through the use of selenium dioxide to form a tropone⁷⁵ while the use of strong oxidizing agents are required for the oxidation of the methyl groups on 5-bromo-2-(2,4,6-cycloheptatriene)-*p*-xylene.^{63,65}

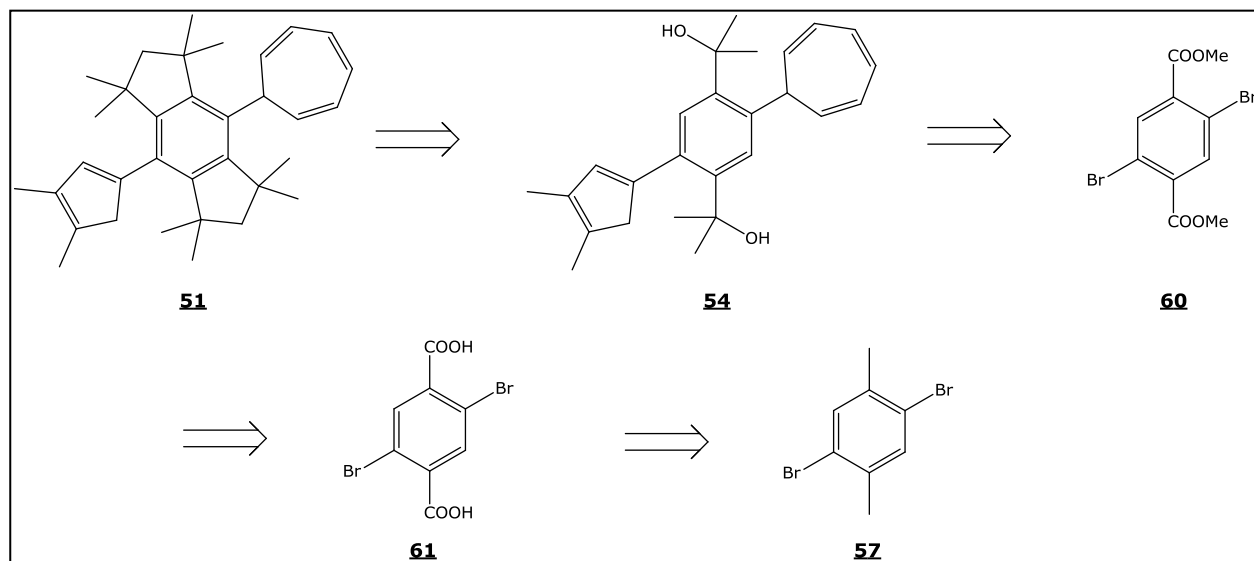


Scheme 13 – The potential oxidation reaction of **58** to **59**.

Attempts at the oxidation of compound **58** to form compound **59** was carried out using both literature methods described to test the reactivity of both the methyl groups and the pendant cycloheptatriene ring. Oxidation through use of SeO₂ began with dissolving 5-bromo-2-(2,4,6-cycloheptatriene)-*p*-xylene, **58**, and KH₂PO₄ (20% molar equivalent) in a 10:1 mixture of dioxane and water (0.1 M) and heating the mixture to 90°-100° C. Once the target temperature was reached, the SeO₂ was added in a single aliquot to the reaction. The reaction was maintained at 100° C with stirring for a further 24 hours followed by quenching and work up. What was observed were NMR resonances corresponding only to the starting material, **58**. The conditions necessary to oxidize 1,3,5-cycloheptatriene were presumably not strong enough to form the desired material.

To increase the probability of oxidation of compound **58**, a stronger oxidant was explored. Potassium permanganate was refluxed with **58** in a 1:1 water/ pyridine mixture for 6 days. After this time, the reaction was allowed to cool to room temperature and was then quenched with an acidic medium. Extraction *via* ethyl acetate produced a dark brown product. Spectroscopic analysis was performed through the use of $^1\text{H-NMR}$. Resonances corresponding to the starting material's cycloheptatriene unit were not present in the spectrum. Instead, several sets of singlets were observed in the upfield portion of the spectrum. It is hypothesized that KMnO_4 was too strong of an oxidizing agent and not surprisingly oxidized the compound beyond what was desired.

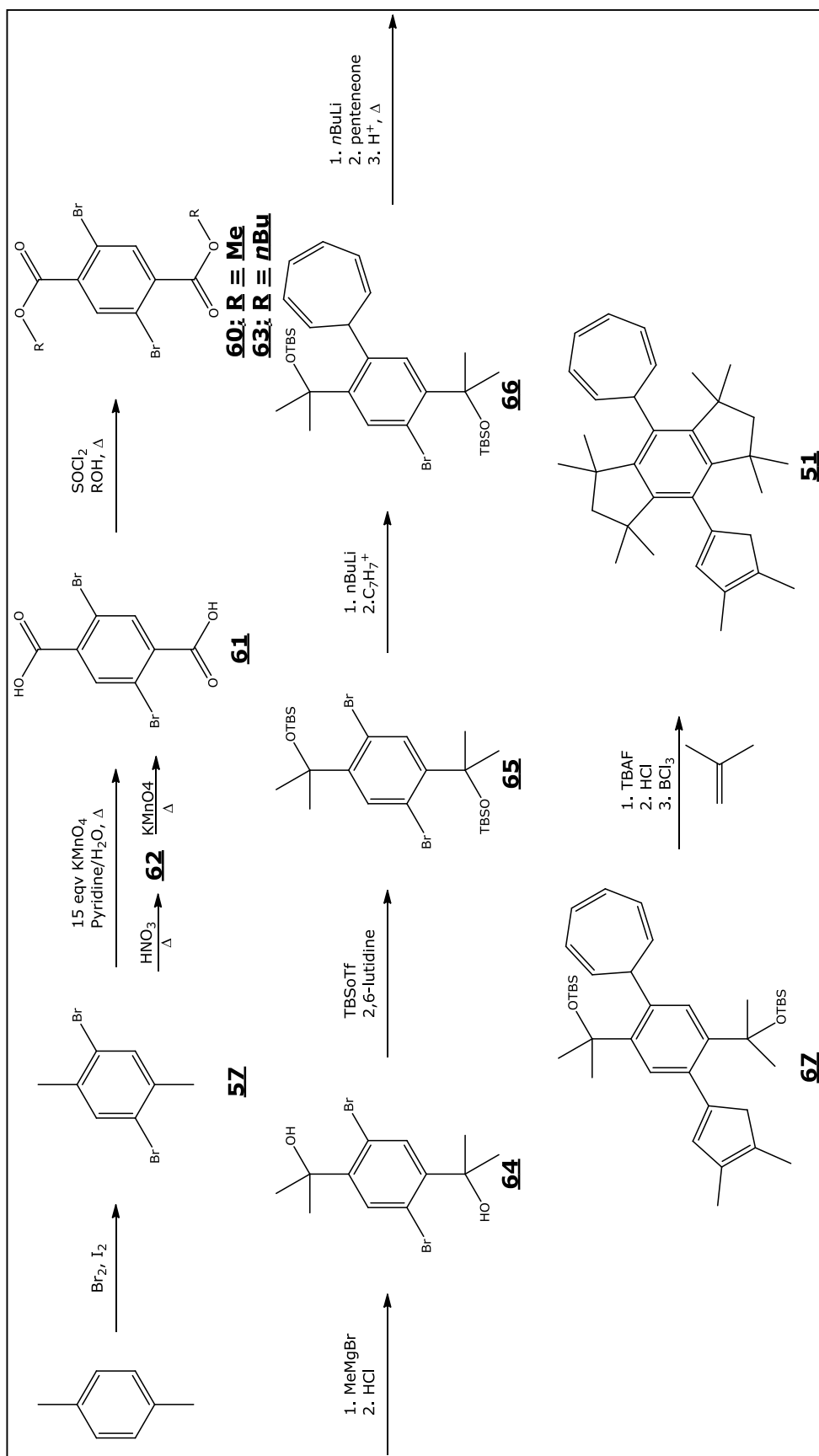
Since the pendant cycloheptatriene ring apparently did not survive the oxidation attempts of the methyl groups, our second approach for the total synthesis of **65** through prior



Scheme 14 – The retrosynthetic approach for the preparation of **51** via the partial hydrindacene framework construction method. ring addition before adding the bridging group was also unsuccessful.

Reworking the synthetic approach to compound **51** provided a new direction in its preparation. In this revised synthetic approach, shown in Scheme 14, the synthesis of compound **51** may be accomplished through an initial partial bridge construction method. Constructing an octamethyl-s-hydrindacene precursor, followed by attaching the pendant rings to the central benzene ring, and finally closing the preformed bridge fragment could provide the necessary order of synthesis to yield the desired product. This method would first require the preparation of the brominated compound **60** before closure of the bridge, as illustrated in the retrosynthetic pathway in Scheme 14. After the formation of compound **60**, the two olefinic groups, 1,3,5-cycloheptatriene and 1,3-cyclopentadiene, could be added and then the final hydrindacene ring system completed. The final steps would include the Dauben reaction to for the tropylium ring formation and a deprotonation reaction to form the cyclopentadienyl group. Both of these reactions are known to be successful in similar systems from previous work in our group as discussed previously.^{29,30}

Previous work in the bromination of 1,4-bis(2-hydroxyisopropyl)benzene, had been shown, however, to proceed in low yield with complex product mixtures.³⁷ Due to this, the synthesis was started from 2,5-dibromo-*p*-xylene (**57**). Compound **57**, was synthesized in high yields *via* electrophilic aromatic substitution. Using iodine as a catalyst led to an uncomplicated workup and purification through recrystallization from methanol with clean spectral data and melting point consistent with the literature. Literature reports for **57** report a melting range between 73.5-74.0° C with ¹H-NMR peaks reported at 7.39 ppm and 2.33 ppm.^{63,76} Experimental data in our work were observed to have similar results with a melting point at 73.8° C and ¹H-NMR peaks at 7.38 ppm and 2.32 ppm.



Scheme 15 – The synthetic pathway towards the synthesis of **51** via partial backbone construction.

Oxidation of compound **57** had been described previously in literature as best accomplished in high yield through a two-step process.⁷⁷ The first step in this process is oxidation using nitric acid at reflux over six days. This reaction proved to be experimentally troublesome due to the physical properties of **57**. For example, at reflux temperatures, compound **57** sublimates out of the reaction mixture, leading to clogged condensers and pressurized reaction flasks. Once the reaction was complete, however, the literature workup and purification of the product led to 2,5-dibromo-4-methyl-benzoic acid, **62**, as a clean product and produced good yields ~70%. Spectral data for this compound matched those reported previously in literature.³⁷ The second step in the oxidation used 2.6 equivalents of potassium permanganate in an aqueous solution. This reaction required reflux for 3 days and produced lower yields of the desired product **61**, approximately 40% yield, with large impurities seen in the spectra of compound **62**.

The problems associated with the complete oxidation of **57** to form compound **61** and the purification of **61** led us to search for an alternative method of oxidation for compound **57**. At the time, literature for alternative methods were limited to the patent literature that did not provide sufficiently detailed information on reaction concentrations, solvents employed and oxidant quantities used.^{63,78} Considering the basic information provided in these patent accounts, a methodology for the marco-scale synthesis of compound **61** was discovered with yields exceeding those described in the literature.^{63,78} Using pyridine as a co-solvent with water provided the necessary organic media to help redissolve any sublimed starting material, **57**, as well as maintain a basic pH sufficient to keep the product deprotonated. Excess use of potassium permanganate coupled with relatively high temperatures (150~160° C) gave the

excess oxidative force needed to drive the reaction to completion in shorter amounts of time. Following the discovery of our new conditions, other literature was published detailing a very similar method to that which we employed.^{63,65} Work up of the reaction was accomplished through filtration followed by acidification of the solution to form a precipitate. It was found that extraction of the aqueous layer with ethyl acetate would dissolve the precipitate most efficiently in comparison to other polar organic solvents, such as diethyl ether or tetrahydrofuran. Infrared spectra of the product showed the distinct characteristics of the main functional group on **61** at 2800-3100 cm⁻¹ (-COOH), 1703 cm⁻¹ (-COOH) and 1297 cm⁻¹ (-COOH). The ¹H-NMR spectrum obtained for the compound showed two peaks at 8.02 ppm (aryl-*H*) and 13.93 ppm (-COOH). Some literature sources report the carboxylic acid proton much more upfield at 5.06 ppm.⁶³ After the completion of the work up, the compound was used as is without any further purification, with low solubility as a limitation.

Conversion of the carboxyl groups in compound **61** to esters to produce compounds **60** and **63** was first done through a Fischer esterification process. Following literature procedures,³⁷ reflux using a Soxhlet extractor containing a thimble of desiccant was performed to form the methyl ester, dimethyl-2,5-dibromo-terephthalate (**60**), that was confirmed through observed changes in IR and NMR spectra of the reaction. The infrared spectra showed the broad hydroxyl peak of the starting material disappear while the NMR spectra showed the appearance of a strong singlet at 3.93 ppm. Recrystallization of the material gave high yields of crystalline material. It was discovered, however, that impurities carried over from the prior oxidation of 2,5-dibromo-*p*-xylene and co-crystallized with the desired product.

Because of the purification difficulties, it was decided to explore the esterification of **61** to form the di-*n*-butyl-2,5-dibromo-terephthlate (**63**) as the primary product. The large aliphatic side chains were expected create a compound with significantly different solubility properties so as to not co-crystallize with the desired compound **63**. Di-*n*-butyl-2,5-dibromo-terephthlate (**63**) was synthesized *via* an acid chloride intermediate. The starting 2,5-dibromo-terephthlic acid (**61**) was refluxed in 1-butanol under dry argon and thionyl chloride was slowly added. This method did not require the use of a Soxhlet extractor since water was not a byproduct in this reaction. Reflux overnight produced the desired ester in comparable yields to the Fischer method and crystallized out into pure white needles with a melting point of 53° C. The infrared spectrum of the material confirmed removal of the carboxylic acid groups (no broad peak around 3000 cm⁻¹) but still had peaks relating to ester functional groups at 1721⁻¹ and 1234 cm⁻¹. New peaks are seen corresponding to saturated hydrocarbons as well around 2900 cm⁻¹.

Examining the ¹H-NMR spectrum shows five sets of peaks; four corresponding to the aliphatic chains and 1 to the aryl protons. Most upfield resonances at 0.98 ppm are believed to correspond to the methyl hydrogens on the hydrocarbon chain furthest away from the ester functional group. The more downfield, and the less shielded, the protons correspond to protons closer to the ester group with peaks at 1.47 ppm (γ carbon), 1.76 ppm (β carbon) and 4.36 ppm (α carbon). ¹³C-NMR also confirmed the product to be **61** and displayed eight peaks; the first four at 13.90 ppm, 19.41 ppm, 30.73 ppm and 66.44 ppm representing the aliphatic chain; three resonances at 120.24 ppm, 136.01 ppm, and 136.64 ppm representing the aromatic carbons and finally the resonance at 164.58 ppm corresponding to the carbonyl

carbon. The crystal structure of **61** confirmed the presence of ester groups in para geometry on a benzene ring. It was also observed that the *n*-butyl group is oriented unfolded when crystallized. Complete spectral data of di-*n*-butyl-2,5-dibromo-terephthlate (**61**) is given in section 3.2.3 and selected bond distances and angles are listed in Table 15 and Table 16.

With the successful formation of the ester product, compound **63**, the nucleophilic addition of the hydrindacene ring precursor subunits *via* organometallic reagent was performed in the attempted synthesis of compound **64**. The slow addition of compound **63** to a cold solution of methyl magnesium bromide Grignard reagent followed by overnight stirring and acidic work up produced the desired 2,5-dibromo-1,4-bis(2-hydroxyisopropyl)benzene, **64**. Purification was performed through column chromatography with an extremely polar mobile phase (100:1 DCM: MeOH) to give the product as crystals in 53% yield and a melting range of 220-223° C. Infrared spectroscopy showed the functional group transformation for this reaction. The disappearance of the compound **63** ketone peak and the formation of an –OH stretch at 3381 cm⁻¹ corresponds to a complete functional group transformation. The ¹H-NMR spectrum displayed three singlets at 1.59 ppm, 5.44 ppm and 7.98 ppm from the primary carbon protons, the hydroxyl protons and the aryl protons, respectively. The ¹³C-NMR spectrum was relatively simple with five peaks at 28.58 ppm (primary carbons), 71.15 ppm (tertiary carbon), 118.57 ppm, 133.64 ppm and 147.94 ppm (aryl carbons). The crystallographic structure of **64** confirmed the proposed structure and shows the hydroxyl groups oriented in the same direction, eliminating the possibility of an inverse center. Furthermore, the crystal structure shows no bending between the bromine atoms and the phenyl ring. Spectral data (¹H-NMR, ¹³C-NMR and IR) and crystallographic structure confirmed

the assigned structure, Figure 22. Complete spectral data is reported in section 3.2.3 and selected bond lengths and angles are reported in Table 17 and Table 18.

Once compound **64** had been successfully prepared, it was decided to protect the hydroxyl groups due to their relative sensitivity to the strong bases required in the subsequent step. The use of a silyl protection group was employed because of their robust nature to the conditions necessary for the synthesis of compound **66**, ease of attachment and ease of removal. Use of 2,6-lutidine and *tert*-butyldimethylsilyl triflate in dichloromethane produced the desired silyl ester, compound **65**, in a nearly quantitative overall yield. Purification of this compound was performed through chromatographic methods using silica gel and eluting with pure hexanes. Evaporation of the solvent produced large clear crystals. ¹H-NMR of the pure structure showed four resonances. The three large peaks were upfield at 0.19 ppm, 1.01 ppm and 1.78 ppm corresponding to silyl-methyl protons, *t*-butyl-protons and methyl protons in close proximity to the ring, respectively. The final smaller peak at 8.12 ppm corresponds to the two aryl protons. Crystallographic data of the compound was obtained and further confirmed the protection of the hydroxyl group through silyl ether protection, as shown in Figure 23. It can be seen that the *t*-butylsilyl portion of the compound does not extend out but folds back towards the center of the compound to make a more compact molecule. This may be the reason crystallization occurs so readily with the compound. Spectral data is reported in section 3.2.3 and selected bond lengths are reported in Table 20 & Table 21.

With the base sensitive hydroxide groups protected, attempts at the addition of the 1,3,5-cycloheptatriene group were performed. As stated previously, *n*-butyllithium was used at low temperatures to form the reactive substituted benzene nucleophile. Addition of tropylium

tetrafluoroborate to form the desired product compound **66** did not, however, proceed as desired. The spectra from the reaction mixture did not show any peaks corresponding to a 1,3,5-cycloheptatriene-substituted compound but instead showed new aromatic peaks consistent with *ortho*-proton ring splitting. The reaction was repeated several times using different addition methods, electrophiles and conditions, yielding the same results in all instances. It is hypothesized that the bulkiness of the silyl group prevented the bulky tropylium ring from adding. It is hypothesized from $^1\text{H-NMR}$ data that lithiation of **65** occurred, however, and nucleophilic addition did not occur. This is consistent with the peaks seen in the aromatic region of the unpurified spectra which have three sets of peaks, two of which are doublets split by each other. Successful lithiation followed by quenching would produce a compound three

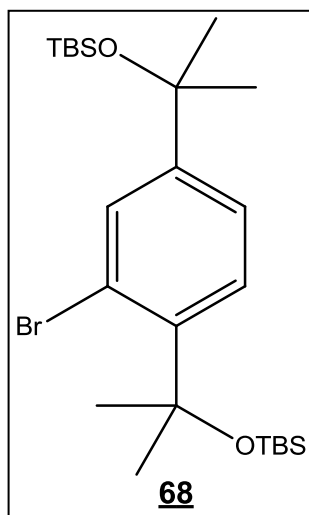


Figure 27 – Compound **68**.

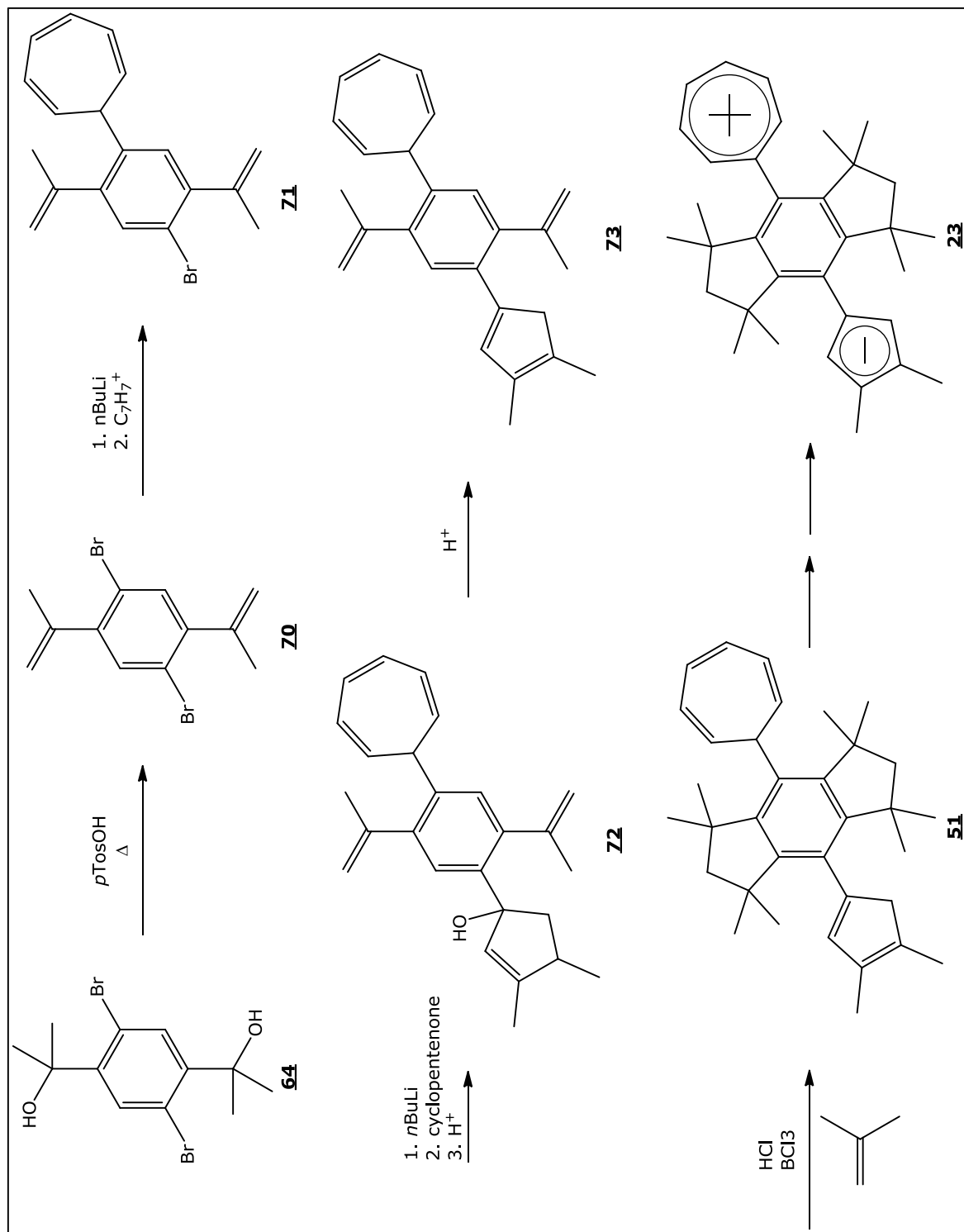
aryl hydrogens all electronically different in $^1\text{H-NMR}$ spectra.

Given these results, an attempt was also made to replace the hydroxyl groups with chlorine on compound **64**. Although alkyl chlorines also have the ability to undergo lithium halide exchange, the reaction would presumably still proceed at the aromatic bromines. This is

due to the stability of the corresponding anion. The negative charge on the aromatic ring is significantly more stable than that at a tertiary carbon, making lithium halide exchange at the phenyl ring to generally occur first⁷⁹. In this reaction, the 2,5-dibromo-1,4-bis(2-hydroxyisopropyl)benzene **64** was dissolved in dry DCM at 0° C and hydrochloric acid was bubbled through the solution for four hours. NMR data were collected on the reaction mixture throughout the reaction to monitor the expected shift of the methyl peaks closest to the reaction site. After four hours there was no observation of a secondary peak so it was concluded that the typical reaction conditions for conversion of a hydroxyl group to a chloride were not sufficient for the chlorination of compound **64**. Another attempt was made at chlorination through use of thionyl chloride at 0° C and reflux conditions for conversion to **69** but what was observed was either no reaction or dehydration of the hydroxyl groups.

The failure of a chlorination reaction for compound **64** led to an attempt involving the dehydration reaction of compound **64** to form an alkene, compound **70**. Reflux in toluene in the presence of *p*-toluenesulfonic acid with a Dean-Stark apparatus was used for this reaction. The *p*-toluenesulfonic acid was chosen primarily for its solubility and relatively limited ability to form oxidized side products. The use of a Dean-Stark apparatus helps prevent conversion of the product back to starting material by removing the water formed in the synthesis. Limiting reaction time further helped to prevent the possible formation of any polymeric compounds reported for other systems in literature.⁸¹ Purification of the product was performed through chromatographic methods by pure hexanes to leave white crystals.

The formation of pure 1,4-dibromo-2,5-di(prop-1-en-2-yl)benzene, **70**, was confirmed using a number of different methods. The ¹H-NMR spectrum of the compound presented four



Scheme 16 – Partial bridge construction via dehydration of **64**.

unique sets of resonances: a doublet at 2.11 ppm, a multiplet at 5.00 ppm, a multiplet at 5.27 ppm and a singlet at 7.43 ppm. The doublet at 2.11 ppm, corresponding to the methyl groups, was shown to have been split by the peak at 5.00 ppm. Long range split (4J) is known to occur on the allylic protons due to a π -orbital promotion factor known as allylic coupling.⁸²

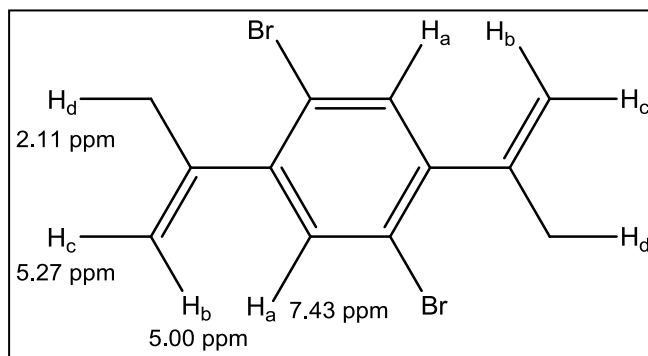


Figure 28 – Compound **70** with $^1\text{H-NMR}$ shifts.

When the allylic C-H bond is perpendicular to the carbon double bond (parallel to the π orbital) the bond helps transmit spin information.⁸³ This peak at 5.00 ppm corresponds to the hydrogen *cis*- to the methyl group which feels a larger effect of 4J coupling.⁸⁴ Further structural conformation was obtained using x-ray crystallography, Figure 24. From this structure, it is observed that the two pendant allylic groups are not coplanar with that of the central benzene ring but instead skewed almost perpendicular to relieve strain caused by atoms in too close proximity. Complete spectral data is reported in section 3.2.3, selected bond lengths and angles are presented in Table 22 and Table 23.

The synthesis of compound **71** was then explored starting with compound **70**. Compound **70** was dissolved in diethyl ether under argon and the temperature lowered to -78°C . Addition of *n*-butyllithium followed by the addition of 1 equivalent of tropylium tetrafluoroborate was successful in forming compound **71**. Purification through column

chromatography *via* hexanes produced a yellow oil. This oil slowly solidified to very fine yellow crystals. $^1\text{H-NMR}$ spectrum of the purified product showed two doublets at 1.96 ppm and 2.21 ppm both integrating to 3 protons each. These two peaks correspond to the two allylic methyl groups. At 3.02 ppm a broad multiplet represents the 1-*CH* proton. Protons peaks at 4.85 ppm and 5.13 ppm have fine splitting from geminal coupling and long range coupling from the allylic methyl at 1.96 ppm. Proton peaks at 5.07 ppm and 5.31 ppm are both multiplets split by each other and by the allylic group at 2.21 ppm. Multiplets at 5.36 ppm, 6.26 ppm and 6.75 ppm all integrate to two protons each and correspond to the protons around the cycloheptatriene ring. The final two singlet peaks at 7.43 ppm and 7.44 ppm correspond to the aryl protons. These assignments helped confirm **71**. Further confirmation was done through IR spectroscopy, $^{13}\text{C-NMR}$ and x-ray crystallography. Full spectroscopic data is reported in section 3.2.3 and selected bond lengths and angles are reported in Table 24 and Table 25. The crystal structure for the compound shows large thermal ellipsoids for all non-hydrogen atoms as well as the boat conformation of the cycloheptatriene unit, Figure 25. This unit is also twisted out of plane of the bridging unit, relieving the steric interaction.

Attempts at the addition of a 2-cyclopenten-1-one unit to compound **71** to form the bis-olefin substituted compound **72** employed similar reaction conditions as that used in the addition of 1,3,5-cycloheptatriene to compound **70**. Compound **71** was first treated with a lithiating reagent at subzero temperatures and then treated with 3,4-dimethyl-2-cyclopenten-1-one via a dropwise addition before being allowed to stir overnight. The NMR of the reaction mixture, however, showed only the presence of the starting material compound **71**. Repeated attempts employing varying conditions yielded the same results with only the starting material

recovered. The lithiation was also tried using a stronger lithiating reagent, *tert*-butyllithium. Addition of 3,4-dimethyl-2-cyclopenten-1-one to the reaction gave a promising NMR spectrum. Upon attempted purification of **72** through chromatographic methods, it was noticed that the cyclopentene ring's unsaturated proton at the 5 position (5.61 ppm) had disappeared and a new peak had arisen at 6.56 ppm. Comparison of the NMR with that of the obtained product, Figure 29, shows a large shift in the proton associated with the cyclopentene ring. Initially the peak starts out at ~5.6 ppm (blue peaks in Figure 29) and upon dehydration/rearrangement, shifts downfield (red peaks). Through a comparison of the NMR data for compound **72** before and after chromatographic methods, is believe that the dehydration reaction occurs in the presence of silica gel to form **73**. It is thought that the silica gel is a strong enough acid to react with the tertiary alcohol group on **72**, producing **73**.

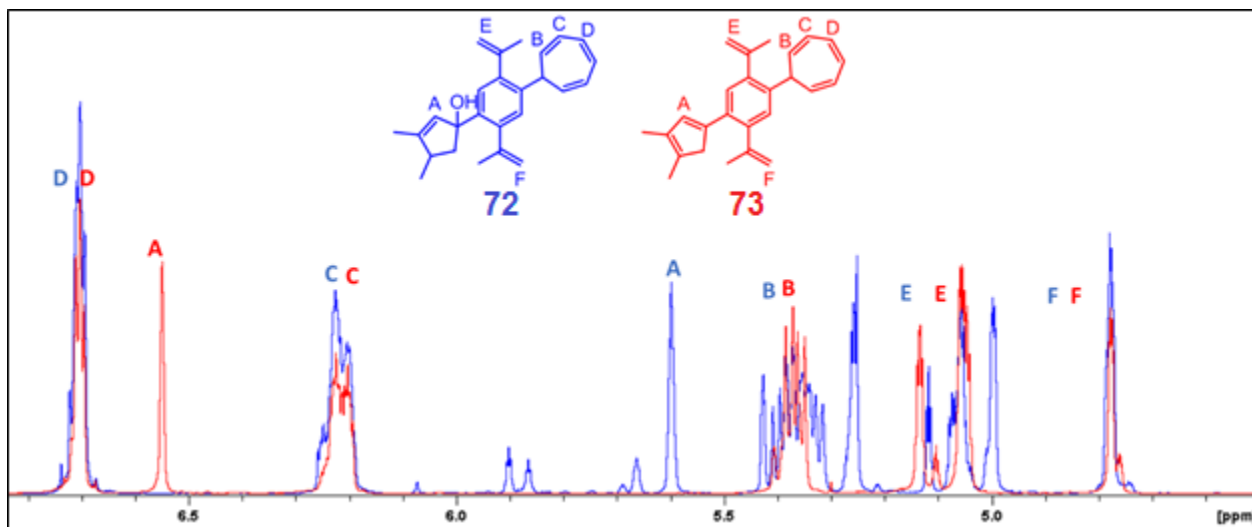


Figure 29 – A NMR comparison between the crude **72** product, blue, and its purified form **73** in red.

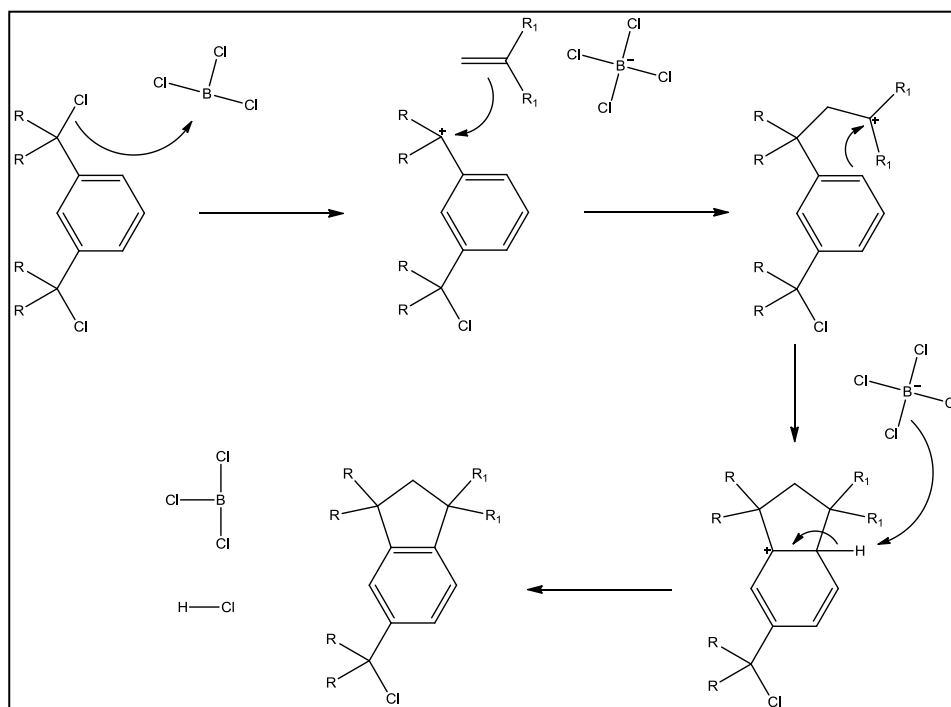


Figure 30 – Mechanism of the Friedel-Craft alkylation ring closure.

Compound **73** was then used to attempt at a Friedel-Crafts alkylation comparable to literature methods to form compound **51**, the key intermediate in the synthesis.^{62,85} Literature methods for the closure of the hydrindacene ring system involve using a Lewis acid catalyst to promote the formation of a 2° carbocation on the alkane group. The carbocation is then presumably attacked by isobutene forming a longer alkene chain with another 2° carbocation. The electron density of the phenyl ring interacts with this carbon ultimately forming the five membered ring. The final step had the removal of the 3° proton to reform the phenyl double bond and create hydrochloric acid, Figure 30. In our work, compound **73** in dichloromethane at low temperatures was added to condensed isobutylene, hydrochloric acid and boron trichloride. This reaction differs from literature methods used for the formation of hydrindacene previously performed with the addition of the hydrochloric acid. This was used to help create the tertiary carbocation on the isopropenyl side chain. This tertiary carbocation was then expected to be

able to go through the Friedel-Crafts alkylation described by Chang and Kennedy.⁸⁵ The NMR spectra of the reaction mixture showed resonances shifted upfield as well as aromatic resonances near that of the starting material. The presence of these aryl peaks showed that the closure of the small five membered rings on the bridge did not occur. Large peaks in the hydrocarbon region were observed leading to a hypothesis of what had occurred. It is hypothesized that some isobutene addition did occur at various places on molecule but did not close to form the five membered ring. Other possible products formed may involve closure onto the 5 and 7 membered ring.

3.5 Conclusions and Future Work

Although the synthesis of 51 did not occur, a number of important discoveries about the nature of the synthesis of this compound were learned. Attempted ring addition of tropylium and 7-methoxycycloheptatriene through nucleophilic addition proved unsuccessful. It is hypothesized the bulk of the ring prevented this from occurring. Forcing the ring into a pocket was not accomplished. In initial attempt to attach the pendant rings followed by construction of the bridge's backbone, we observed preferential oxidation of the backbone due to the harsh conditions required for oxidation of methyl groups. Using gentler oxidative conditions, however, did not produce the cycloheptatriene ring substitution.

The failure to build the bridge and then attach the pendant rings as well as the failure to attach rings then build the bridge led to a hypothesized synthetic pathway which hybridized the two methods. Bridge construction proceeded first through the oxidation step to form 61.

Proceeding to a compound which could withstand the use of organometallic reagents needed for addition of pendant rings, compound 61 was first transformed to an ester and then a Grignard reaction to form a diol, 64. Protection of the hydroxyl groups on 64 was done with the silyl ether TBS. These protective groups, however, presumably proved to be too large, hindering the addition of tropylium to the bridge.

Transforming the hydroxyl to a chloride proved ineffective as well. Using normal conditions for the transformation showed no reaction. Using more reactive compounds to drive the chlorination showed the formation of an unsaturated compound through dehydration of 64. The ease of dehydration was used with *p*-toluenesulfonic acid to form the unsaturated compound 70. With no appropriate functional groups and hindrance from bulky substituents, addition of tropylium to form cycloheptatriene proceeded to form 71. Lithiation followed by addition of 3,4-dimethyl-2-cyclopenten-1-one was successful in the formation of 72. Attempted purification of 72 through use of column chromatography produced 73. The acidity of the silica gel dehydrated 72.

The final reaction in the formation of 51 used an altered literature method. Hydrochloric acid in dichloromethane was added to 72 and stirred followed by addition of isobutene and boron trichloride. Examination of the reactions ¹H-NMR showed side reactions had dominated the mixture and product was not formed.

Synthesis of compound 51 might still be possible. A second attempt at Friedel-Crafts alkylation on a prechlorinated compound might yield better results. This can be done through bubbling dry HCl through 72 in DCM for short periods of time. Though it should be noted that

attempts do this with compound **64** and **70** had failed previously. Literature has also shown that a Friedel-Crafts alkylation will cyclize better when warmed to room temperature quicker. It has also been shown a shorter amount of time at low temperature can promote the cyclization of s-hydrindacene.⁵⁹

A possible method for development of **51** could be from addition of small building blocks into the pocket of **25**. Using chemistries discussed in chapter four, planner compounds can be coupled into the 4- position of **25**.

Chapter 4

Synthesis towards Rigid Non-Linear Optic Materials through Organometallic Catalysts

4.1 Introduction

The challenges encountered in previous work towards the synthesis of the target compound **51** prompted the search for a new methodology that could be used in place of the bridge closure methods explored. Several recent papers have been published describing synthetic access to the 4 and 8-positions in *s*-hydrindacene derivatives by a several methods.⁸⁵⁻⁸⁸ Literature reports also describe substitution reactions of larger alkyl groups at these hindered positions.⁸⁷ One particular communication in the literature described a new synthetic route of potential promise for the continuation of organic hydrindacene based NLOs project.⁸⁶

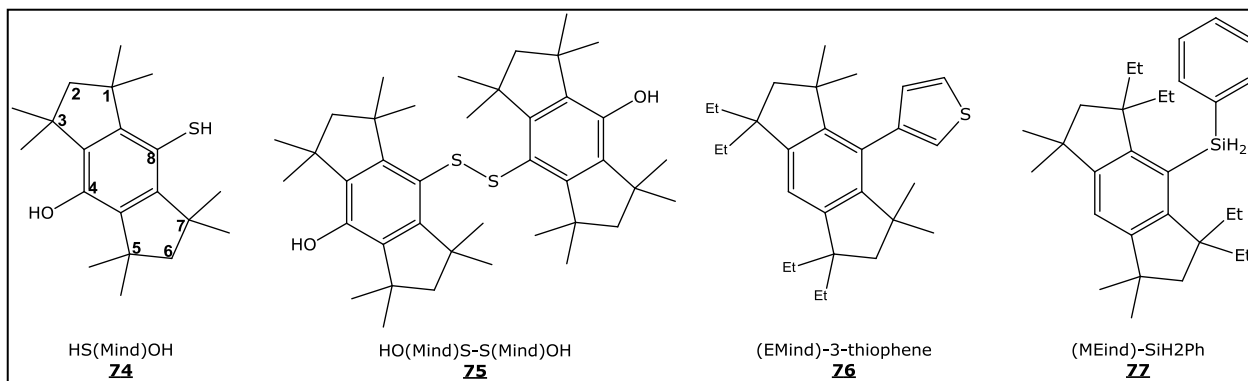


Figure 31 – Substituted hydrindacene compounds from literature⁸⁵⁻⁸⁸ with the numbering scheme for *s*-hydrindacene compound on compound **74**.

In this work, a palladium metathesis pathway was employed that added planner ring systems onto the central hydrindacene benzene bridge unit.⁸⁶ This was accomplished by treating 4-bromo-1,1,7,7-tetraethyl-3,3,5,5-tetramethyl-*s*-hydrindacene in 1,4-dioxane with 3-thienylboronic acid in the presence of potassium phosphate. The organometallic reagents 2-dicyclohexylphosphino-2',6'-diisopropoxybiphenyl (RuPhos), and Tris(dibenzylideneacetone)dipalladium(0) (Pd₂(dba)₃) were used as catalysts at reflux temperatures, as shown in Figure 32.⁸⁶

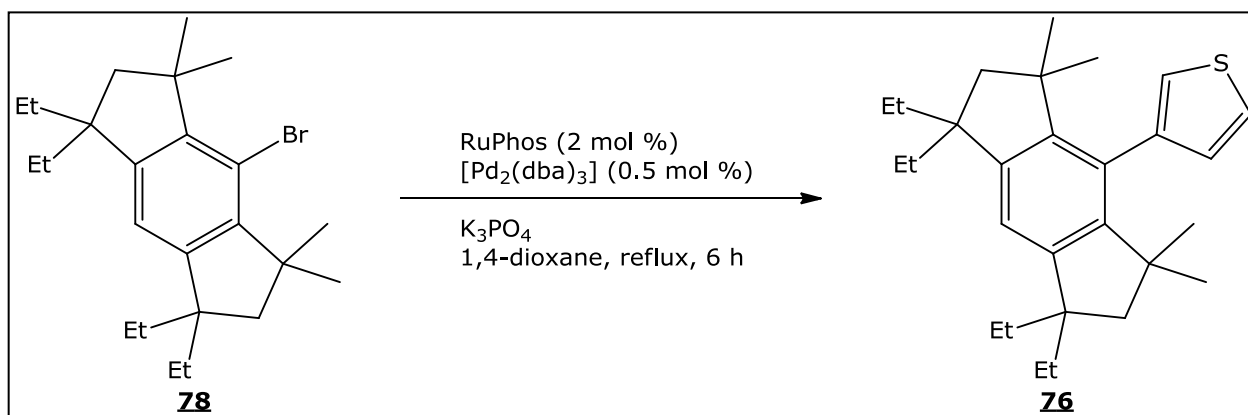


Figure 32 – Literature method for the palladium catalyzed ring structure into an s-hydrindacene backbone.⁸⁷

In an attempt to employ a similar methodology for the synthesis of a hydrindacene donor-acceptor NLO using the palladium metathesis route in our work, several new coupling reagents for the pendant groups must first be made. These reagents are derivatives of cyclopentadiene and cycloheptatriene ring systems that have a unit attached that is able to undergo an oxidative addition reaction onto a palladium catalyst. Examples of this include, but are not limited to borates, cyclopentadiene and cycloheptatriene substituted alkyl tin and triflate compounds.^{89,90} The synthesis of these required subunits in itself presents a difficult synthetic challenge due to the lack of literature of synthetic methods required for the substitution of 1,3,5-cycloheptatriene and cyclopentadienyl compounds. It was also thought of value to examine the theoretical β values of extended quinarene hydrindacene-based compounds, as shown in Figure 30. The addition of an “extra” aromatic linker between each charged aromatic unit and the hydrindacene framework may have a higher probably of synthetic success but would not be productive is the observed β value were decreased.

This chapter details the work involving the attempted synthesis of cyclopentadiene coupling agents in order to form stable cyclopentadiene units able to undergo palladium

catalyzed coupling reactions. Also discussed are theoretical calculations for several possible NLO extended-framework structures, Figure 32, and how they might relate to previously calculated compounds in terms of hyperpolarizability. Finally, the synthesis towards the formation of these extended structures is discussed. Various approaches for the synthesis of these compounds are discussed and their effectiveness to the overall synthetic strategy is discussed.

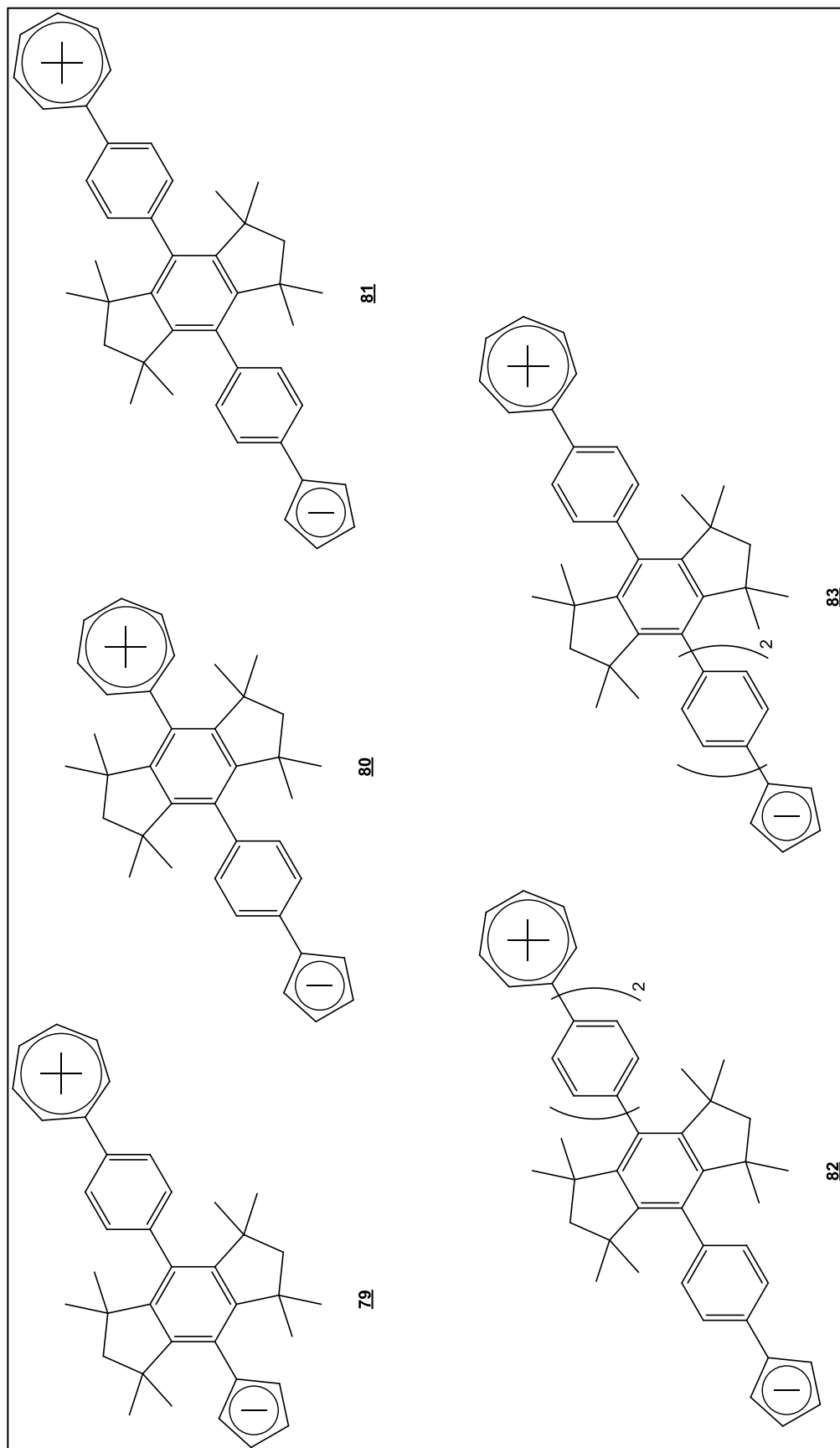


Figure 32 – Extended Quinarene/*s*-Hydrindacene targets to be examined computationally and synthetically.

4.2 Experimental

4.2.1 Physical Measurements

All NMR spectra were recorded on samples dissolved in dry CDCl_3 or $\text{DMSO-}d_6$, in 5 mm (o.d.) tubes. Proton (^1H) and carbon (^{13}C) spectra were recorded on either a Bruker DPX-300 spectrometer operating at 300.15 MHz for proton, 77.47 MHz for carbon; or a Bruker Ascend-400 with Prodigy CyroProb attachment operating at 400 MHz. Chemical shifts referenced to either residual CHCl_3 ($\delta = 7.26$ ppm) or residual DMSO ($\delta = 2.50$ ppm). The spectrometer was operated in the FT mode while locked on the deuterium resonance of the CDCl_3 or $\text{DMSO-}d_6$ solvent. The reference was set relative to tetramethylsilane from the known chemical shifts of the CDCl_3 ($\delta = 77.23$ ppm) and DMSO ($\delta = 39.52$ ppm) carbon atoms. All NMR data are reported in ppm. Unit resolution mass spectra were obtained on a Hewlett Packard model 5989B gas chromatograph/mass spectrometer (GC/MS) using an ionization potential of between 11 and 70 eV. FT-IR in the range of 400 to 4000 cm^{-1} were measured on a Mattson Galaxy 2020 spectrometer or a Perkin Elmer FT-IR Spectrometer Paragon 1000 and were referenced to the 1602.8 cm^{-1} band of polystyrene.

4.2.2 Materials

All solvents used were reagent grade or better. Diethyl ether, tetrahydrofuran, and 1,4-dioxane were distilled from sodium prior to use. TLC plates were purchased from Sigma-Aldrich and used as received. Visualizations of TLC fractions were performed using ultraviolet light, potassium permanganate stain, *p*-anisole stain or bromine stain. All organometallic reagents

were purchased from Sigma Aldrich and titrated before use including: *n*-butyllithium (1.6 M in hexanes or 2.5 M in hexanes), *t*-butyllithium (1.7 M in pentane), methylmagnesium bromide (3 M in diethyl ether) and boron trichloride (1.0 M in CH₂Cl₂). Tropylium tetrafluoroborate was purchased from Alfa Aesar and used as received. [1,2-Bis(diphenylphosphino)ethane] dichloronickel(II),⁹¹ Tris(dibenzylideneacetone) dipalladium(0),⁹² 7-(4-bromophenyl)cyclohepta-1,3,5-triene,³¹ Comin's Reagent,⁹³ 2-dicyclohexylphosphino-2',6'-diisopropoxybiphenyl,⁹⁴ and 4,8-dibromo-1,1,3,3,5,5,7,7-octamethyl-*s*-hydrindacene,⁶² were all synthesized according to literature methods. Silica used for column chromatography was Silicycle SiliaFlash P60 with a particle size of 40-63 μm (230-400 mesh).

4.2.3 Synthesis

3,4-dimethyl-2-cyclopenten-1-trimethyltin 86.⁸⁹ To a stirring solution of diisopropyl amine (5.0 mmol) in dry, degassed THF (15 mL) at 0° C in a 50 mL Schlenk flask was added *n*-butyllithium (5.0 mmol) dropwise over 5 minutes. The reaction was stirred for 10 minutes at 0° C and then a solution of tributyl tin chloride was added dropwise over 2 minutes and allowed to react for 10 minutes at 0° C. The reaction was then cooled to -78° C and the 3,4-dimethyl-2-cyclopenten-1-one (0.55 g, 5.0 mmol) was added. This mixture was allowed to react for 30 minutes at -78° C before the addition of triethyl amine (3.9 g, 5.5 mL) and methane sulfonyl chloride (MsCl) (2.4 g, 1.6 mL, 20 mL). The reaction was allowed to warm to room temperature, then hexanes were added (15 mL) and the reaction extracted with acetonitrile (3 x 10 mL).

Removal of solvent through rotoevaporation left an impure solid. The NMR of the product showed that no reaction had occurred and only NMR resonances for the starting material were observed.

3,4-dimethylcyclopenta-1,3-dien-1-yl diphenyl phosphate 88.⁹⁵ To a stirring solution of lithium diisopropyl amine (LDA) (5.7 mmol) in dry, degassed THF (10 mL) at -78° C and under an N₂ atmosphere was added 3,4-dimethyl-2-cyclopenten-1-one (5.2 mmol) dropwise over 5 minutes. After 30 minutes of stirring at -78° C, the diphenyl chlorophosphate (5.7 mmol) was added in one portion and the reaction was allowed to warm to 0° C. The solution was stirred at 0° C for 50 minutes and then allowed to warm to room temperature. After 10 minutes at room temperature, the solvent was removed through rotoevaporation and the residue was dissolved in Et₂O (15 mL), washed with water (2x 10 mL), dried over MgSO₄, filtered and the solvent removed *in vacuo*. Purification using silica gel column chromatography (5:1 Hexanes: EtOAc) produced the compound as a yellow oil (1.3 g, 3.7 mmol) in a 65% yield. ¹H-NMR and ¹³C-NMR were obtained. After approximately 1 hour at room temperature, the oil turned to a dark black solid showing a new NMR spectrum that did not match that expected for the product, 88.
Observed data: ¹H-NMR (CDCl₃): δ 1.81 (s, 3H, C₅H₄(CH₃)₂, 4-CCH₃), 1.84 (s, 3H, C₅H₄(CH₃)₂, 3-CCH₃), 3.03 (s, 2H, C₅H₄(CH₃)₂, 5-CH₂), 5.85 (s, 1H, 2-CH), 7.24-7.38 (m, 10H, OP(O)(OPh)₂, aryl-H). ¹³C-NMR (CDCl₃): 13.2, 13.3, 43.9, 117.8, 120.4, 120.5, 125.9, 127.5, 130.2, 132.7, 150.8.

3,4-dimethyl-2-cyclopenten-1-ethertriflate 90.⁹⁰ To a stirring solution of 3,4-dimethyl-2-cyclopenten-1-one (0.11 g, 1.0 mmol), THF (16 mL), and N-(5-chloro-2-pyridyl)bis(trifluoromethanesulfonimide) (Comin's reagent) (0.79 g, 2.0 mmol) in a 100 mL Schlenk flask was added potassium bis(trimethylsilyl) amide (KHMDs, (1.1 mmol, 1.1 mL, 0.21 g)

in diethyl ether (7.7 mL) at -78° C under an argon atmosphere. This reaction was stirred for 30 minutes at -78° C and then a second portion of KHMDS (0.55 mmol, 0.11 g, in 1.1 mL THF) was added at -78° C. After another 30 minute increment, another portion of KHMDS in THF was added to the reaction at -78° C (0.25 mmol, 0.049 g, in 0.5 mL THF). Monitoring the reaction through TLC showed no change in the reaction throughout these additions. Three hours after the last addition was complete, the reaction was quenched with 10% aqueous NaHCO₃ (10 mL) and extracted with diethyl ether (3 x 10 mL). The organic layers were combined and washed with saturated NaCl solution (10 mL) and dried over MgSO₄. Removal of the solvent *via* rotoevaporation produced an impure solid. The NMR of the product showed that no reaction had occurred and only NMR resonances for the starting material were observed.

4-bromophenyl-boronic acid 93.⁹⁶ To a stirring solution of 1,4-dibromobenzene (4.75 g, 20.0 mmol) in diethyl ether (100 mL) at -78° C under an argon atmosphere was added *n*-butyllithium (21.0 mmol) over a period of 15 minutes. The solution was warmed to room temperature after 1 hour at -78° C and stirred for an additional hour. The solution was cooled to -78° C and the triethylborate (5.1 mL, 30 mmol) was added dropwise and stirred for 15 minutes. The reaction was allowed to warm to room temperature then quenched with 3 M HCl (20 mL). The layers were separated and the aqueous layer was extracted with diethyl ether (3 x 25 mL). The combined organic layer was washed with a saturated NaCl solution (50 mL) and then dried over NaSO₄. Removal of the solvent *via* rotoevaporation produced 1.2 g, (6.2 mmol), 31% of a white crystalline solid. m.p. 282°-284° C. literature m.p. 284°-288° C.

4,8-(4-bromobenze-1-nyl)-1,1,3,3,5,5,7,7-octamethyl-s-hydrindacene 92.⁹⁷ Solid 4,8-dibromo-1,1,3,3,5,5,7,7-octamethyl-s-hydrindacene (0.43 g, 1 mmol), 4-bromophenyl-boronic

acid (0.60 g, 3 mmol), palladium (II) acetate (4 mol%, 8.9 mg, 0.040 mmol) and triphenyl phosphine (4 mol%, 10 mg, 0.040 mmol) were placed in a 10 mL Schlenk tube and evacuated for 30 minutes. Dioxane (2.0 mL) and potassium phosphate (2.0 mmol) were added and the solution was refluxed ($\sim 110^\circ$) for 6 hours. After cooling to room temperature, the reaction was filtered and washed with water (2 mL) and diethyl ether (2 mL). The aqueous layer was extracted with diethyl ether (3 x 5 mL). The NMR of the organic layer showed the probable metathesis of 4-bromophenyl-boronic acid with other units of 4-bromophenyl-boronic acid along with unreacted starting material.

Alternate Synthesis: Solid 4,8-dibromo-1,1,3,3,5,5,7,7-octamethyl-s-hydrindacene (0.43 g, 1.0 mmol), 4-bromophenyl-boronic acid (0.60 g, 3.0 mmol), Pd₂(dba)₃ (4.0 mol%, 36 mg, 0.040 mmol) and RuPhos (4.0 mol%, 19 mg, 0.040 mmol) were placed in a 10 mL Schlenk tube and placed under vacuum for 30 minutes. Dioxane (2.0 mL) and potassium phosphate (2.0 mmol) were added and the reaction was brought to reflux ($\sim 110^\circ$ C) for 6 hours. After cooling to room temperature, the reaction was filtered and washed with water (2 mL) and diethyl ether (2 mL). The aqueous layer was extracted with diethyl ether (3 x 5 mL). ¹H-NMR spectra of the product showed the broad peaks in the phenyl-*H* region.

3-(4-bromophenyl)cycloheptatriene 95.³¹ To a stirring solution of 1,4-dibromobenzene (8.0 g, 34 mmol) in diethyl ether (50 mL) at -78° C under an argon atmosphere was added *n*-butyllithium (34 mmol) dropwise over 15 minutes. After stirring for 1 hour, tropylium tetrafluoroborate was added and the reaction was warmed to 0° C and stirred overnight, slowly warming to room temperature. The reaction was quenched with 2 M HCl (15 mL) and the layers were separated. The organic layer was washed with 10% NaHCO₃ (2 x 15 mL) and brine

(2 x 15 mL). Removal of the solvent *via* rotoevaporation produced a yellow oil. This product was distilled to yield a compound with a b.p. at 204° C. This distilled compound was identified as the isomerized product of the initial substitution product and obtained as a yellow oil in 55% yield (18.86 mmol). b.p. 135° C (0.1 torr). IR (KBr): 716 735, 768, 823, 1008, 1074, 1486, 2924, 2959, 3022.32. ¹H-NMR (CDCl₃): δ 2.26 (t, 2H, *J* = 6.8, C₇H₇, 7-CH), 5.39-5.50 (m, 2H, C₇H₇, 1,6-CH), 6.20 (m, 2H, C₇H₇, 2,5-CH), 6.81 (d, 1H, *J* = 6.0, C₇H₇, 4-CH), 7.24 (d, 2H, *J* = 2.4, 2,6-aryl-H), 7.39 (d, 2H, *J* = 2.4, 3,5-aryl-H). ¹³C-NMR (CDCl₃): δ 28.2, 122.2, 122.4, 126.9, 127.1, 128.7, 128.8, 129.2, 131.7, 141.4, 142.0.

3-(4-(pinocolatoboron)-phenyl)cycloheptatriene 96. To dry 100 mL Schlenk flask was added 3-(4-bromophenyl)cycloheptatriene (0.99 g, 4.0 mmol), bis(pinacolato)diboron (1.2 g, 4.8 mmol), potassium acetate (1.2 g, 12 mmol), palladium (II) acetate (5.0 mol%, 44 mg, 0.2 mmol), and triphenylphosphine (0.13 g, 0.5 mmol) and the mixture was placed under vacuum for 30 minutes. Under a dry nitrogen atmosphere, dioxane (14 mL) was added and the reaction was warmed to 90° C for 9 hours then cooled to room temperature. The reaction was filtered and deionized (DI) water (5 mL) added. This solution was extracted with ethyl acetate (3 x 5 mL). The organic layer was separated and washed with a saturated NaCl solution, dried over MgSO₄ and reduced to produce an impure product. Purification was performed using silica gel chromatographic methods with a hexanes:EtOAc gradient (20:1 → 10:1 → 5:1) to produce the produce as a yellow oil, 70% yield. *R_f* = 0.49 (10:1 Hex:EtOAc). IR (KBr): 741, 1091, 1144, 1360, 1937, 1608, 2977, 3413.03. ¹H-NMR (CDCl₃): δ 1.38 (s, 12H. pinocolate, -CH₃), 2.37 (m, 2H, C₇H₇, 7-CH), 5.56 (m, 2H, C₇H₇, 1,6-CH), 6.32 (m, 1H, C₇H₇, 5-CH), 6.39 (m, 1H, C₇H₇, 2-CH), 7.01 (m,

¹H, C₇H₇, 4-CH), 7.50 (d, 2H, *J* = 10, 2,6-aryl-H), 7.82 (d, 2H, *J* = 10, 3,5-aryl-H). ¹³C-NMR (CDCl₃): δ 24.8, 27.9, 83.7, 121.6, 122.0, 126.2, 126.6, 126.7, 127.3, 128.7, 134.9, 142.4, 145.0.

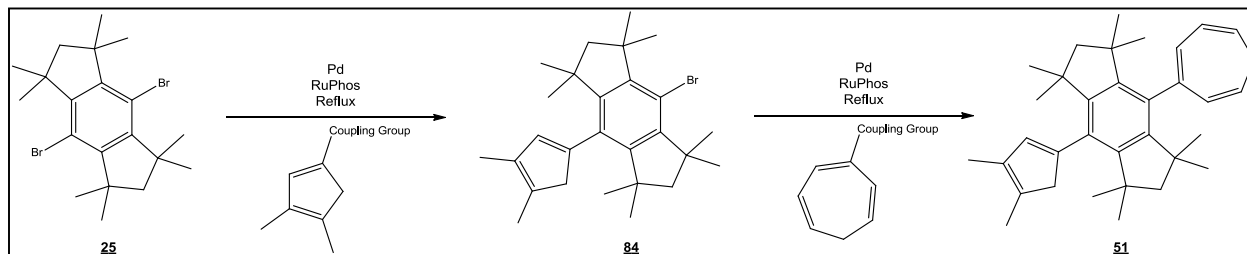
1-(4-bromophenyl)-2,3,4,5-tetramethylcyclopentene-1-ol 97.⁹⁸ To a stirring solution of 1,4-dibromobenzene (2.6 g, 11 mmol) in diethyl ether (15 mL) at -78° C under an argon atmosphere was added *n*-butyllithium (12 mmol) dropwise over 15 minutes. The solution was allowed to warm to room temperature and stir for 30 minutes. The solution was then cooled to -78° C and the 2,3,4,5-tetramethyl-2-cyclopenten-1-one (3.8 g, 27 mmol) was added dropwise over 15 minutes. The solution was allowed to warm to room temperature and stirred for 1 hour. The reaction was quenched with ice (10 mL) and the layers were separated. The aqueous layer was extracted with diethyl ether (3 x 10 mL). The organic fractions were combined and washed with brine (15 mL) and dried over MgSO₄. Removal of the solvent *via* rotoevaporation produced the impure product as a brown oil. Purification using silica gel chromatographic methods (5:1 hexanes: Et₂O) produced a light yellow oil. *R_f* = 0.31 (5:1 Hex:Et₂O). IR(KBr): 911, 1483, 2870, 2927, 2961, 3481.37. ¹H-NMR (CDCl₃): δ 0.87 (d, 3H, *J* = 7.2, C₅H₂(CH₃)₄OH, 5-CCH₃), 1.02 (d, 3H, *J* = 7.2, C₅H₂(CH₃)₄OH, 4-CCH₃), 1.42 (s, 3H, C₅H₂(CH₃)₄OH, 3-CCH₃), 1.74 (s, 3H, C₅H₂(CH₃)₄OH, 2-CCH₃), 2.16 (s, 1H, C₅H₂(CH₃)₄OH, 1-COH), 2.23 (m, 1H, C₅H₂(CH₃)₄OH, 4-CH), 2.51 (m, 1H, C₅H₂(CH₃)₄OH, 5-CH), 7.21 (dd, 2H, *J* = 6.9, 1.8, 2,6-aryl-H), 7.43 (dd, 2H, *J* = 6.6, 1.8, 3,5-aryl-H). ¹³C-NMR (CDCl₃): δ 8.3, 10.1, 13.0, 16.1, 45.3, 48.1, 88.9, 120.1, 128.8, 130.8, 134.3, 143.6, 145.2.

4.2.4 Calculations

Calculations on extended quinarene/*s*-hydrindacene hybrid compounds were run on a Gateway NV55C with an Intel® Pentium CPU P6100 @ 2.00GHz (x2) and 3.00 Gb of RAM with a 64-bit Windows 7 operating system. Either GaussView 5.0 or Avogadro were used for molecule construction and Gaussian 09W was used for calculation processing. Compounds were geometrically optimized through semi-empirical methods (AM1) and β values calculated using semi-empirical methods with AM1 parameterization in the E4 method. Hyperpolarizabilities were calculated at both 0.0 eV and 0.5 and are reported in units of $\text{cm}^5\text{esu}^{-1}$. Molecular orbital images were created using Avogadro from data obtained from Gaussian 09W.

4.3 Results and Discussion

4.3.1 Coupling Agents



Scheme 17 – The synthetic strategy for the formation of **51** through coupling methodology.

The revised strategy for the synthesis of the key compound **51** involved the formation of a suitable coupling reagent compounds that could link the donor and acceptor subunits to the hydrindacene framework. The work employing this synthetic approach began with the attempted synthesis of the necessary coupling agents for the cyclopentadiene groups, compounds **86**, **88** and **90**, shown in Scheme 18. The methodology explored was analogous to the literature procedure for the formation of vinylstannanes from ketones using lithium trialkyltin reagents, shown in Figure 33.⁸⁹ Trialkyltin compounds were chosen for this work as viable reactant compounds because of their potential use in Stille coupling reactions involving a type of palladium metathesis.⁹⁹

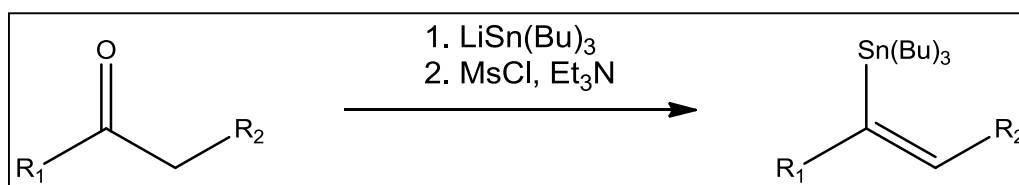
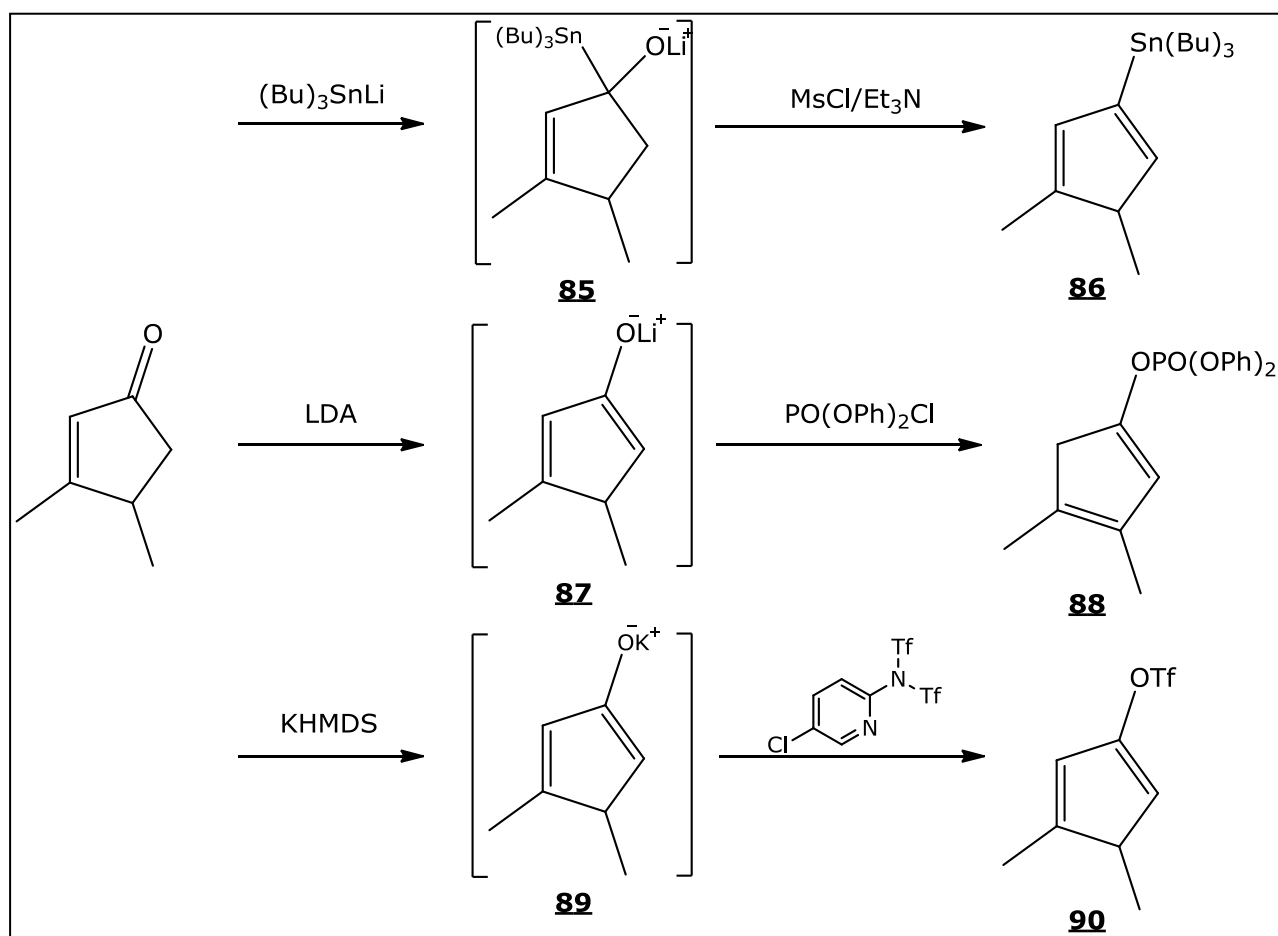


Figure 33 – Formation of vinylstannanes from ketones.⁸⁹

In the first approach, aimed at the preparation of compound **86**, freshly made lithium diisopropylamine was used to form LiSn(Bu)₃ to be added to the α,β -unsaturated ketone. The

mixing of $\text{LiSn}(\text{Bu})_3$ with 3,4-dimethyl-2-cyclopenten-1-one formed the intermediate **85**. Under typical circumstances, protonation of **85** would be performed to form the tertiary alcohol. Instead of protonation, however, a one-pot method was performed in which methane sulfonylchloride and triethyl amine were added to **85** in order to attempt the elimination reaction thereby forming **86**.⁸⁹ After work up of the reaction mixture, however, the NMR data did not show the formation of the desired product, compound **86**. It was hypothesized that compound **86** either did not form or was too unstable to be purified.



Scheme 18 – Attempted synthesis of a cyclopentadiene coupling agents, compounds **86**, **88** and **90**, from 3,4-dimethyl-2-cyclopenten-1-one.

The second approach for the synthesis of the key cyclopentadiene coupling compound involved the formation of a diphenylphosphate compound **88**. Diphenylphosphate compounds have been shown to undergo nickel catalyzed reactions with Grignard reagents to form metathesis products.⁹⁵ The reaction employed freshly prepared LDA at -78° C that was mixed with 3,4-dimethyl-2-cyclopenten-1-one. This reaction was hoped to form the lithium enolate that was then added, without isolation, to diphenyl chlorophosphate and warmed. Purification of this compound using silica gel chromatographic methods, in this case, was found to produce the desired compound **88** as a yellow oil in good yield. The ¹H-NMR spectrum of the obtained compound displayed a series of resonances expected based on the proposed structure of compound **88**. Two singlets at 1.81 ppm and 1.84 ppm were observed which corresponded to the two methyl groups on the cyclopentadiene unit. A singlet at 3.03 ppm, with a relative integration of two protons, corresponds to the saturated carbon on the cyclopentadiene ring. These data led to the belief the double bonds had rearranged in the product to a 1,3-diene instead of a 1,4-diene. The resonance for the relatively deshielded 2-CH proton was observed at 5.85 ppm as a singlet. Conformation of the phenyl phosphate groups was observed through multiplets found between 7.24-7.38 ppm, integrating to the ten protons. Although the synthesis of this compound was successful, it was found to decompose extremely rapidly into a dark black solid, making it unsuitable as an intermediate in the next step of the proposed synthesis of compound **84**.

Given the rapid decomposition of **88**, an additional attempt was made for the formation of a stable coupling agent. This reaction involving the addition of potassium bis(trimethylsilyl)amide to 3,4-dimethyl-2-cyclopenten-1-one, to presumably form the

intermediate, compound **89**. The formation of this compound (**89**), in the presence of Comin's reagent, was the hoped to form **90**. After aqueous quenching, extraction with Et₂O and removal of the solvent produced a red oil. This compound was found to be unstable and rapidly turned black. The NMR data obtained was not, however, consistent with that expected for the desired product, compound **90**.

From the observations obtained from the three routes we employed here to prepare the key intermediary cyclopentadiene compounds **86**, **88** and **90**, it was believed that, while they may initially be formed, they are not sufficiently stable to be useful in our synthetic strategy. One hypothesis is that these compounds undergo self-dimerization as seen with other cyclopentadienes.¹⁰⁰ This dimerization could be proceeding through Diels-Alder reaction, accelerated by the electron withdrawing groups used to form coupling reagents.

4.3.2 Extended Quinarene/Hydrindacene Calculations

Given the synthetic difficulties encountered on forming the desired coupling agents for the direct palladium catalyzed coupling of the pendant group to the hydrindacene backbone, it was determined that an extended aryl systems might be a viable alternative. By separating the electron donating or electron withdrawing groups further from the coupling reagent's functional group for attachment to the hydrindacene core, the possibility of creating larger addition units that can still meet the requirements for a rigid, charged NLO species would still be met. Since these compounds have not been directly considered previously, coupled with the valuable information on such systems that can be gained by using previously reported

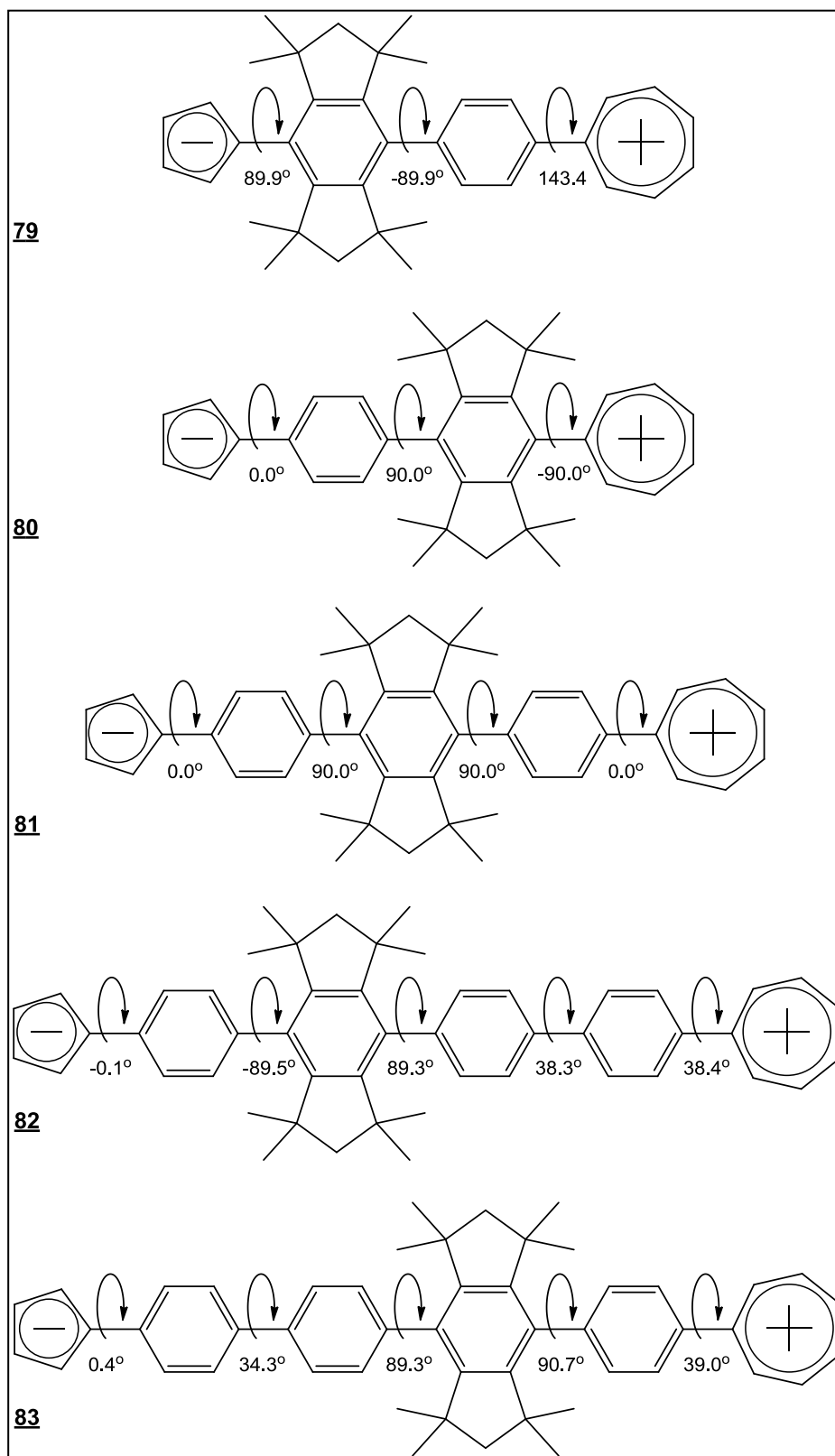


Figure 34 – Twist angles calculated in extended pendant group compounds **79** through **83**. AM1 parameterization utilized.

calculational methods, calculations were performed on these systems to examine the first hyperpolarizability (β) values of these extended functional group compounds.

Results of the computational studies for several extended hydrindacene framework compounds showed the ground state conformation to have occupied molecular orbitals largely surrounding the donor ring and any bridging phenyls while the excited states were shown to shift these occupied orbitals to the acceptor side of the molecule. The calculations also showed various geometry 'twists' between pendant rings and β values for compounds **79** – **83**, shown in Figure 34. These 'twists' refer to the angle created by two rings, connected by a single bond, on different planes. Two of the five calculated compounds, compounds **80** and **81**, had optimized ground state geometries in which the pendant rings lie in the same plane with each other but approximately 90 degrees to the central benzene ring of the bridge. The remaining three compounds, compounds **79**, **82** and **83**, show slight twists between the bridge and at least one of their pendant groups. In compound **79**, for example, a 36.6° twist is observed between the phenyl ring and the cycloheptatriene unit. The larger extended compounds, **82** and **83** are seen to have more sets of twists between rings, Figure 34.

The twists in the extended pendant group compounds were shown to have significant differences between the HOMO and LUMO orbitals, as illustrated in Figure 35 in the calculated molecular orbitals (MOs) for compound **79** – **81**. This collection of MOs shows the majority of the electron density in the HOMO -1 localized on the cyclopentadienyl ring. The HOMO, however, shows the electron density distributed throughout the pendant groups. In the LUMO orbital, it is seen that the bonding and anti-bonding orbitals from the HOMO have been completely reversed. Finally, in the LUMO +1 orbital it is calculated that the molecular orbitals

are localized primarily around the tropylium ring; a complete reversal from where the electron density started. It is this significant change in the expected electron density between the HOMO and LUMO, leading to a large change in dipole moment upon excitation, that is largely responsible for the large calculated β values for these compounds.

Table 26 – Calculated β values for extended rigid NLO systems.

Compound	M =	N =	Beta (β) ^{α}
<u>23</u>	0	0	4049.87 ^{β}
<u>79</u>	0	1	1064.28
<u>80</u>	1	0	183.37
<u>81</u>	1	1	1111.53
<u>82</u>	1	2	1726.76
<u>83</u>	2	1	1920.53

^{α} Calculated in units of $\times 10^{-30} \text{ cm}^5 \text{ esu}^{-1}$ at 0.5 eV using the E4 method. ^{β} Value reported in previous group calculations.

Calculated β values are an important part to the research since they help to focus synthetic work towards the compounds with greatest promise. As shown in Table 26, the β values of the extended structures are not quite as large as those calculated for the originally proposed Tp-Hydrindacene-Cp structures. Although the extended compounds show somewhat lower hyperpolarizabilities, their values are still considered very large and therefore are of interest. Insertion of a phenyl group in between the bridge and acceptor lowers the β value

approximately 4-fold from $4049.87 \times 10^{-30} \text{ cm}^5\text{esu}^{-1}$ to $1064.28 \times 10^{-30} \text{ cm}^5\text{esu}^{-1}$ while insertion of the aromatic group between the hydrindacene and the donor, compound **80**, has a more drastic effect lowering the β value by a factor of approximately 22x to $183.37 \times 10^{-30} \text{ cm}^5\text{esu}^{-1}$. Extending both groups pendant on the hydrindacene framework, however, increased the calculated β value relative to those found for inserting the extension on one side only. Having both sides equidistant from the hydrindacene framework (**81**) is shown to increase the calculated β to $1111.53 \times 10^{-30} \text{ cm}^5\text{esu}^{-1}$. Further, extending both sides beyond a single phenyl group is shown to increase the β even further with the first hyperpolarizability of compound **82** calculated to be $1726.76 \times 10^{-30} \text{ cm}^5\text{esu}^{-1}$ and **83** $1920.53 \times 10^{-30} \text{ cm}^5\text{esu}^{-1}$. The insights from these calculations provide valuable information on possible targets for synthetic construction.

Increasing the distance between a donor group and acceptor group increases the dipole moment of the compound. The increase in dipole moment should increase the overall β value as observed in literature.⁶ This trend is not observed when comparing compound **23** to any of the extended systems. It is hypothesized the added phenyl groups allows for greater delocalization over these extended pendant groups. This makes the charge more diffuse and lowers the magnitude of the dipole moment on excitation.

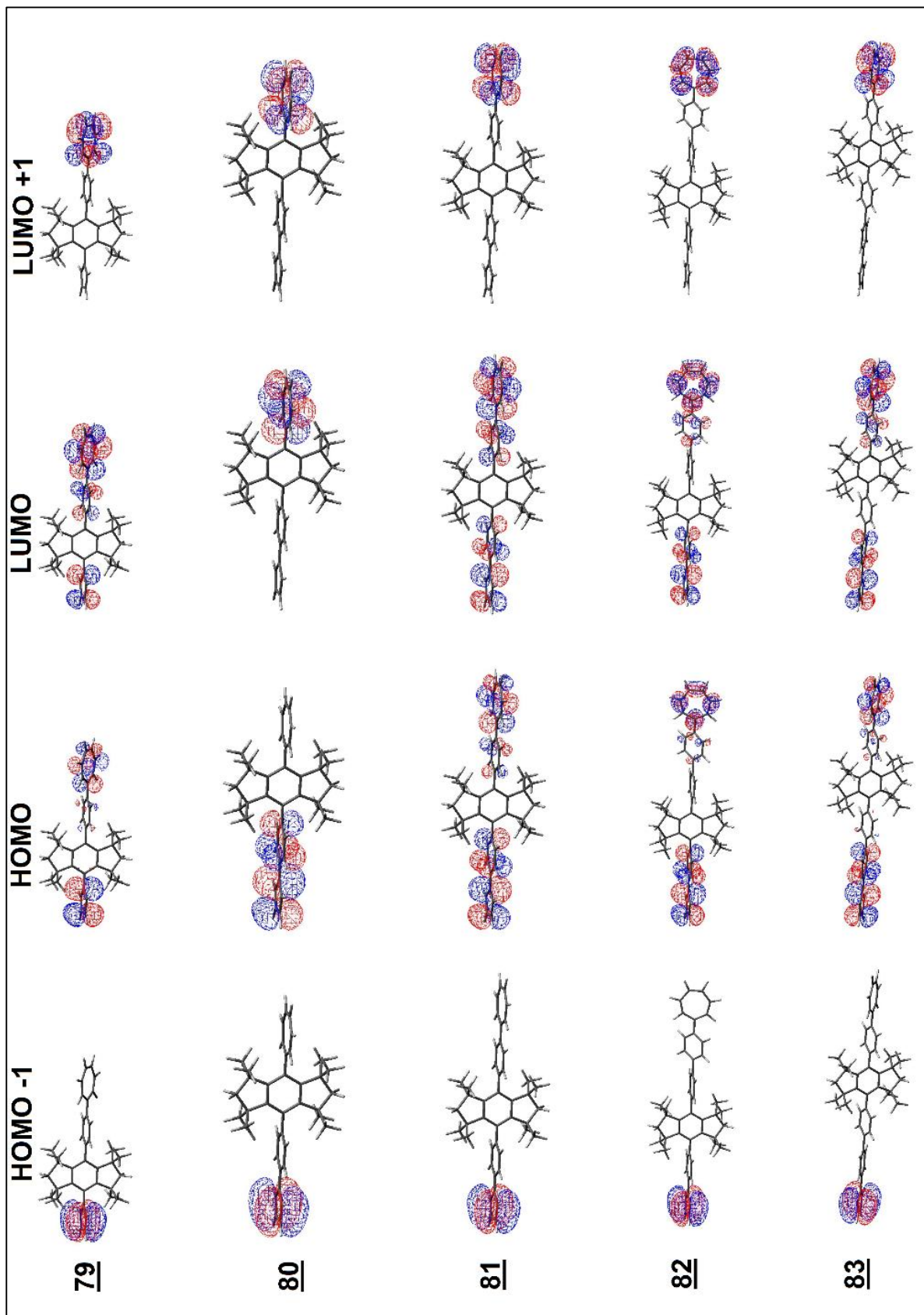
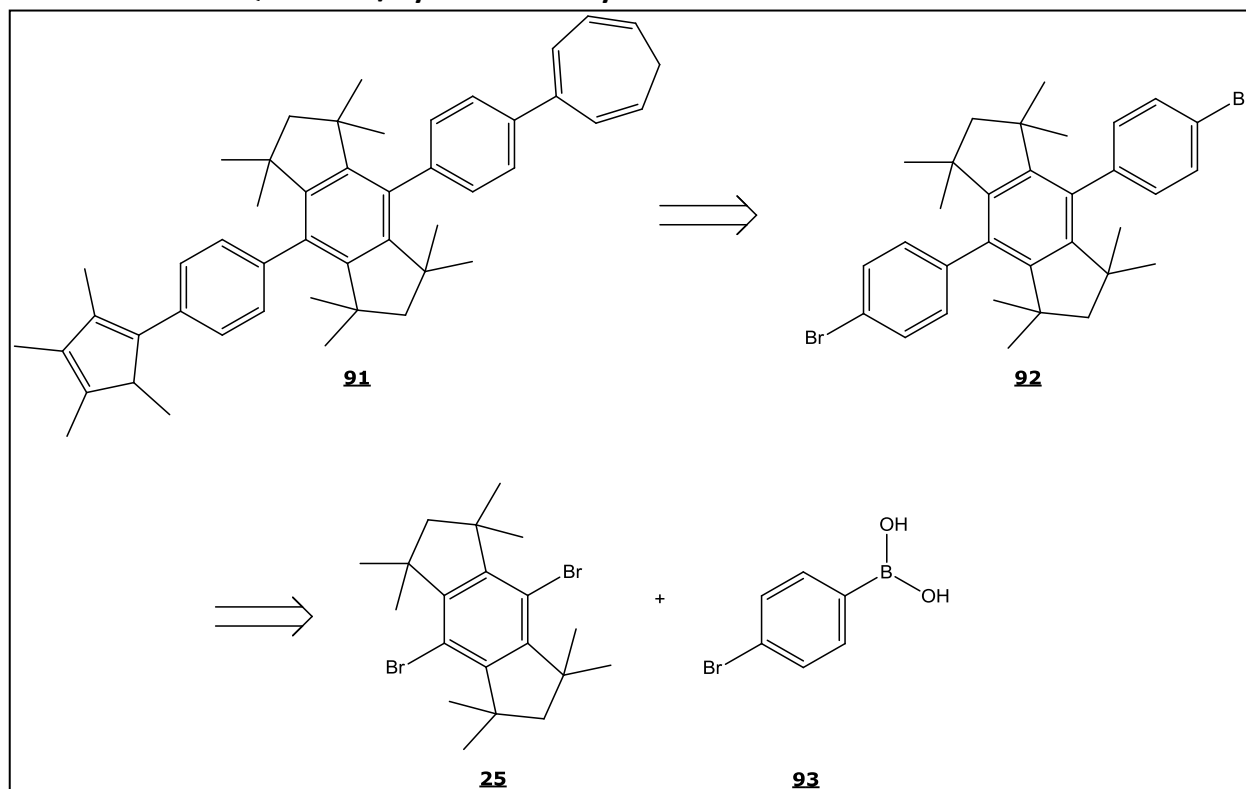


Figure 35 – Calculated HOMO -1, HOMO, LUMO and LUMO +1 diagrams of compounds 79 – 83.

4.3.3 Extended Quinarene/Hydrindacene Synthesis



Scheme 19 – The retrosynthesis of an extended quinarene/hydrindacene compound, **91**.

The initial concept for the synthesis of an extended pendant system was that compound **91** might be formed from a phenyl precursor, **92**, as illustrated in the retrosynthetic pathway shown in Scheme 19. Compound **92** could be used for the formation of multiple derivatives of extended pendant systems due to the large variety of reactions that could be asymmetrically performed on its halide substituted sites. One synthetic route to compound **92** might be through a Negishi-type coupling involving the previously synthesized compound **25**. To explore this, 1,4-dibromobenzene, **11**, was reacted with *n*-butyllithium at -78°C to undergo a lithium halide exchange. The reaction of this lithium intermediate with triethyl borate was used

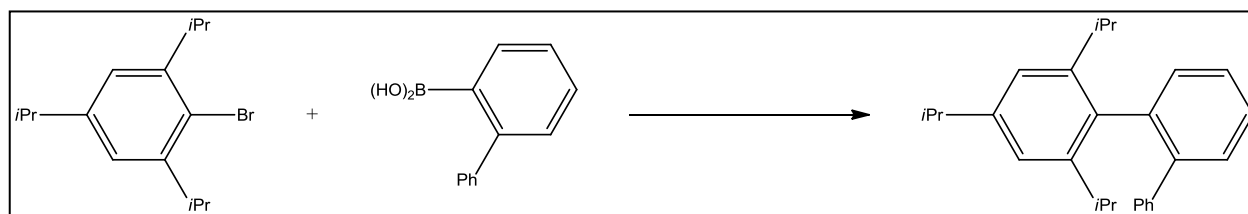
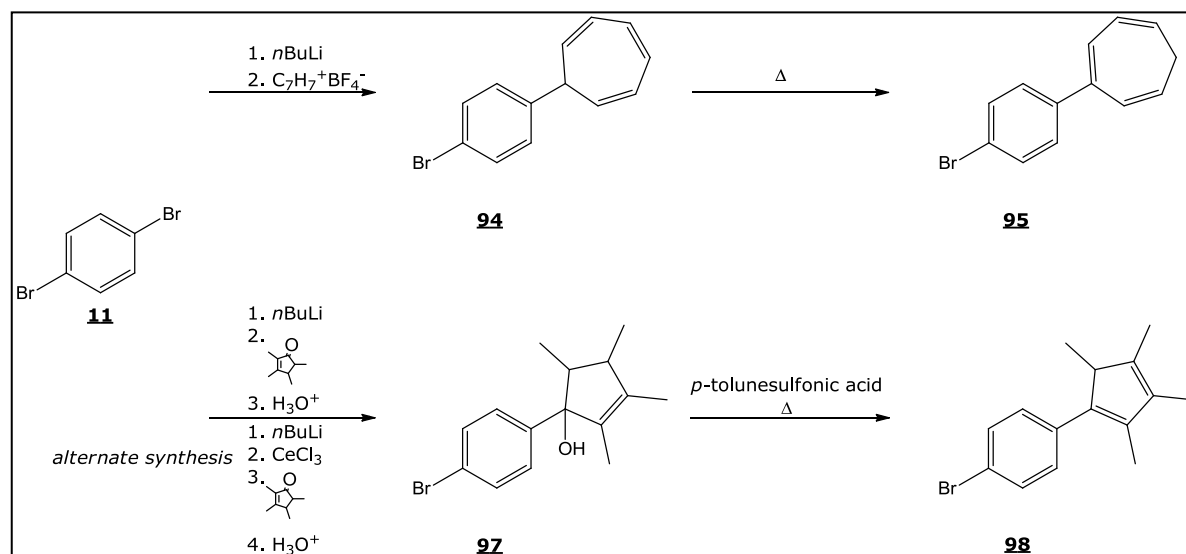


Figure 36 – Literature metathesis of hindered compounds using RuPhos.¹⁰²

to form the nucleophilic addition product. Acidic workup of the reaction with HCl produced the boric acid derivative, compound **93**, in good yield. Compound **93** was then refluxed with 4,8-dibromo-1,1,3,3,5,5,7,7-octamethyl-*s*-hyrindacene in the presence of Pd₂(dba)₂, K₃PO₄, and 2-Dicyclohexylphosphino-2',6'-diisopropoxybiphenyl (RuPhos). RuPhos was selected as the phosphine ligand of choice because of literature precedence for its use coupling in hindered systems, as seen in Figure 36.^{86,101,102} The reaction produced a slightly soluble compound for which the ¹H-NMR showed relatively deshielded broad proton resonances. All attempts at the purification of this compound proved unsuccessful, largely due to its poor solubility. It is believed that, while the palladium catalyzed polymerization occurred, the reaction formed a polyarylene oligomer compound rather than the desired substitution monomeric product.

To avoid the presumed oligomerization of **93** required the development of an alternate synthetic route for the preparation of compound **91**. In this alternate strategy, the synthesis of the complete donor and acceptor units with the phenyl extender units in place prior to coupling them onto the backbone was explored in our work. In this approach, 1,4-dibromobenzene was first lithiated using the typical conditions and tropylium tetrafluoroborate was added to form the 7-substituted intermediate, compound **94**. Vacuum distillation of compound **94** was found to isomerize it to **95** and purify the newly formed **95**. The spectroscopic analysis compound **95** was supported the proposed structure. ¹H-NMR shows the expected



Scheme 20 – Initial synthesis towards coupling agents.

resonances corresponding to the protons on **95**. At 2.25 ppm, a triplet representing 7-CH₂ was observed with a relative integration on two. At approximately 5.4 ppm, two sets of overlapping multiplets were observed corresponding to protons 1-CH and 6-CH, the two protons closest to the point of substituted carbon. At around 6.20 ppm we observed another set of overlapping resonances corresponding to 2-CH and 5-CH. The final cycloheptatriene ring proton was observed as a doublet at 6.83 ppm since it is expected to be the most deshielded of all the protons due to its proximity to a tertiary carbon. Two sets of doublets corresponding to the two sets of protons on the phenyl ring were observed at 7.24 ppm and 7.39 ppm with coupling constants of 2.4 Hz (split by each other). Full spectroscopic data of **95** is reported in section 4.2.3.

The formation of the boronic ester species, compound **96**, was completed through the palladium catalyzed cross-coupling reaction of **95** with bis(pinacolato)diboron using conditions similar to those previously reported.^{103,104} After reflux and standard workup, the resulting compound **96** was purified using chromatographic methods to give a yellow oil in a 70% yield.

$^1\text{H-NMR}$ and $^{13}\text{C-NMR}$ spectral data were similar to those observed for **95** with the exception of the distinct resonances corresponding to the pinacolato group in both the carbon and proton spectra. In the $^1\text{H-NMR}$ for compound **96**, protons from the pinacolato unit were observed at 1.38 ppm that integrated to the expected 12 protons corresponding to the four

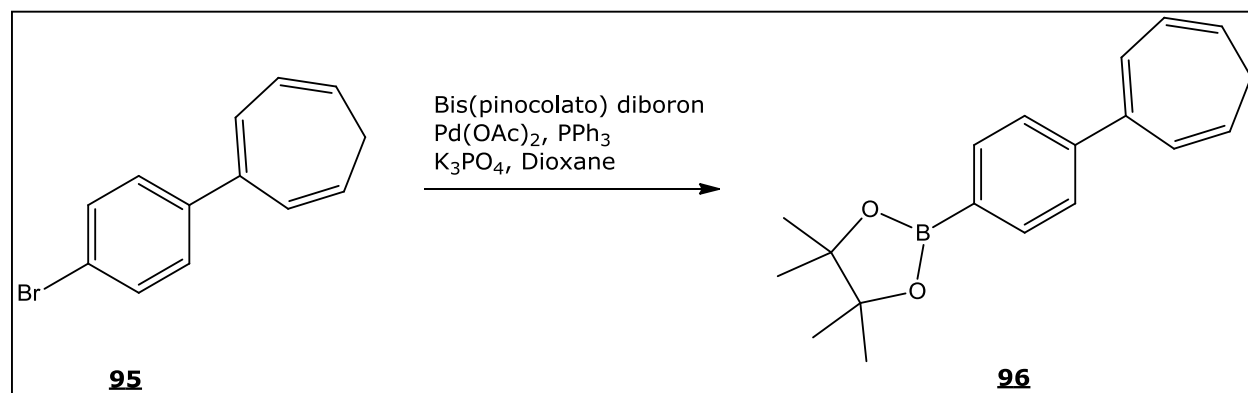


Figure 37 – Formation of the boronic ester, **96**.

magnetically equal methyl groups. The carbon-13 NMR spectrum shows two distinct resonances corresponding to the boron pinacolato group at 24.84 ppm and 83.73 ppm. The upfield peak corresponds to the four primary carbons on the pinacolato group while the peak downfield is that of the deshielded quaternary carbons. Full spectroscopic data for this compound is reported in section 4.2.3.

Using 1,4-dibromobenzene as a starting material, progress was made towards the extended donor precursor: the cyclopentadiene coupling agent. Attempts to add various substituted 2-cyclopenten-1-one rings were made using a lithium intermediate followed by the addition of the α,β -unsaturated ketone, 2,3,4,5-tetramethyl-2-cyclopentene-1-one. Quenching and attempted purification of these reactions produced a high yield of an undesired, unidentified byproduct and relatively little of **97**. The byproduct was assumed to be the 1,4-

addition product, so in order to promote the formation of **97**, the reaction time after the addition of the α,β -unsaturated ketone was reduced to 1 hour and cerium (III) was employed to promote the formation of 1,2-substituted species.⁸¹ Using this alternate method, the formation of compound **97** was achieved in moderate yields. Using silica gel column chromatography, the product was purified and its structure supported *via* spectroscopic data. In the infrared spectra of the compound, a broad peak was seen from 3200 cm^{-1} to 3500 cm^{-1} , corresponding to the hydroxyl group of **97**. The $^1\text{H-NMR}$ spectrum of the compound displayed resonances characteristic of the alkane groups on **97**. Doublets corresponding to 4- CCH_3 and 5- CCH_3 were observed at 0.86 ppm and 1.03 ppm. The remaining two methyl groups are observed at 1.42 ppm and 1.74 ppm, shifted downfield due to their proximity to the alkene bond. The two saturated protons, 4- CH and 5- CH , are seen as multiplets at 2.23 ppm and 2.51 ppm respectively. NMR resonances corresponding to the aryl protons are observed at 7.22 ppm and 7.44 ppm as doublets.

4.4 Conclusions and Future Work

Exploration into organometallic catalyzed addition chemistry towards the synthesis of new nonlinear optic compounds was explored. The initial attempts at the formation of a stable coupling agent version of a cyclopentadiene unit proved to be unsuccessful. The synthesis of a vinylstannane, **86**, and vinyl triflate, **90**, version proved unsuccessful since they were too unstable to be isolated and later employed in subsequent synthetic steps. The synthesis of the

acyclic dienyl phosphate reagent, **88**, however, proved successful but was relatively short-lived due to the instability of the compound.

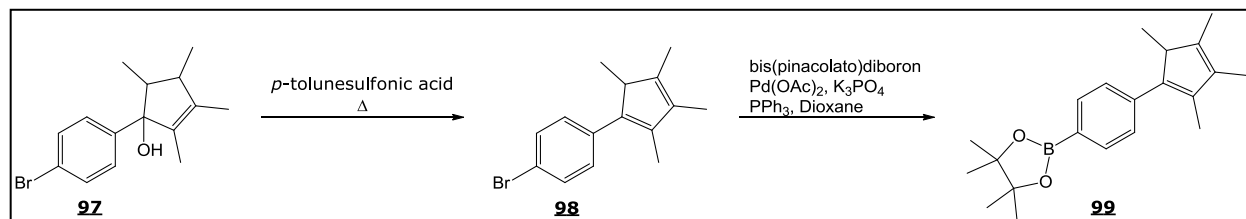
Calculations examining the effectiveness of an extended pendant group system showed promise in the design of new hydrindacene-based nonlinear optic compounds. It was shown through the calculations that the addition of a single phenyl “extender” group would, however, reduce the β values in comparison to **23**. It was interesting to note how the position of the phenyl group affected the calculated β value. If placed in between the donor and the hydrindacene bridge, the decrease in the β value was calculated to be much larger in comparison with placing a phenyl group between the acceptor and the bridge. It is hypothesized the difference in β values has to do with the relative rotations of the ring planes (“twists”) between the ring structures. Compound **79** was shown to display a calculated 36° twist between its phenyl group and tropylium ring, preventing some delocalization of electrons whereas in compound **80** the phenyl and cyclopentadienyl ring remain co-planar allowing for significant delocalization of the negative charge over more atoms.

Increasing the pendant group distance by adding additional phenyl units proved to have a greater β value than those calculated for a single phenyl addition. Compounds **81**, **82** and **83** were all seen to display a calculated increase in β values in comparison to **79** and **80**. This is presumed due to the larger distance between the dipoles of the HOMO and LUMO. When comparing compounds **81**, **82** and **83**, it was seen that **81** displayed the lowest calculated β value, followed by **82** with compound **83** displaying the largest value. In examining the

calculated structures, compounds in which smaller twists were observed between phenyl and Cp or phenyl and Tp rings showed lower β values.

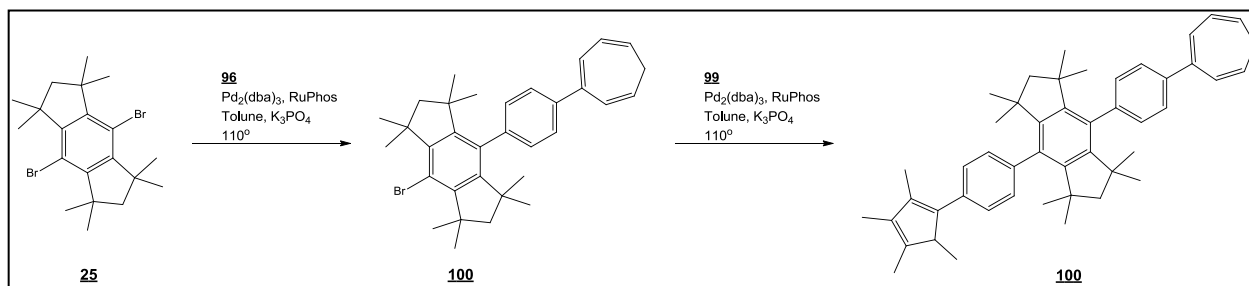
Progress in the synthesis towards these extended systems was made. The successful formation of an extended acceptor unit was completed through the addition of 1,3,5-cycloheptatriene onto 1,4-dibromobenzene to form **94**. Purification of this compound through vacuum distillation both isomerized and purified the compound to produce **95**. Compound **95** was used in a Suzuki coupling in a cross metathesis reaction with bis(pinacolato)diboron forming **96**. Progress in the preparation of the extended donor unit was reached through the successful addition of 2,3,4,5-tetramethyl-2-cyclopenten-1-one to 1,4-dibromobenzene to form **97**. To increase the yields of this reaction, the time for nucleophilic addition was shortened and a cerium intermediate was used to promote 1,2-addition.

Future work towards the synthesis of **91** should extend the methodology for the synthesis and purification of most precursors has been reported here. The first compound to complete is the donor Suzuki reagent, **99**, as seen in Scheme 21.



Scheme 21 – Synthesis of the donor Suzuki reagent, **99**.

Upon successful synthesis of **99** both **96** and **99** could be coupled onto **25** to form **91**, Scheme 22. This is expected to need methodology required to maximize overall yields of these syntheses. This is due to the possible dual coupling of the initial agent. Although a small fraction of the reaction would be expected to still go to this unwanted side product, method development and reaction monitoring should be able to reduce this pathway. Upon formation of compound **91**, the Dauben reaction and deprotonation would be expected to occur to form an important compound in the synthetic pathway to new hydrindacene-based NLO compounds.



Scheme 22 – Formation of **91** and **100** through palladium catalyzed coupling using RuPhos.

Appendix A
Crystallographic Data

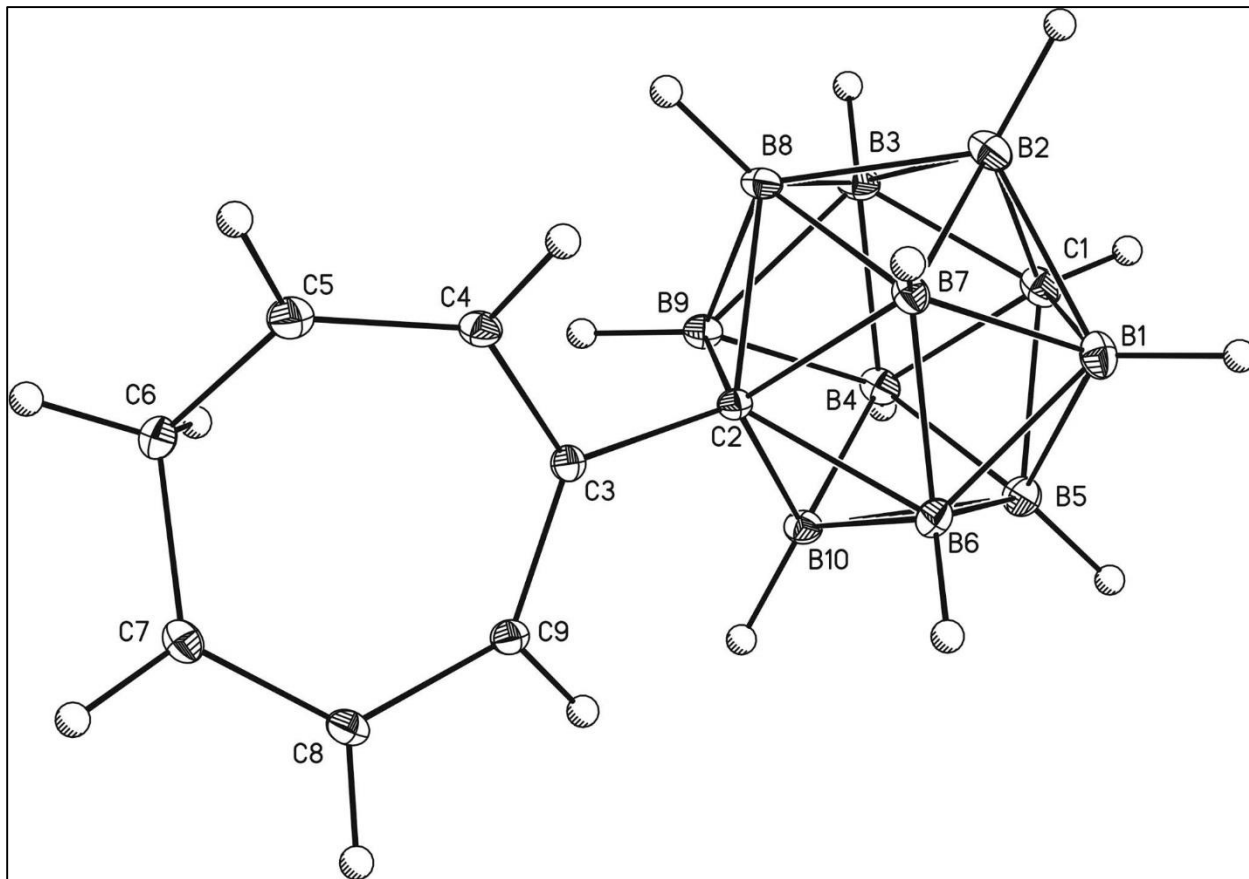


Figure 38 – Crystal data and structure refinement of **30**.

Table 27 – Atomic coordinates and equivalent isotropic displacement parameters (\AA^2) for **30**.

	x	y	z	Uiso*/Ueq
C3	0.79584 (12)	0.13607 (5)	0.10568 (7)	0.01168 (17)
C4	0.65868 (12)	0.09821 (6)	0.17882 (7)	0.01362 (18)
C2	0.73279 (12)	0.21514 (5)	0.04405 (7)	0.01099 (17)
C8	1.06621 (13)	0.03647 (6)	0.15376 (7)	0.01462 (18)
C9	0.97965 (12)	0.10843 (6)	0.09845 (7)	0.01358 (18)
C7	0.97456 (13)	-0.03538 (6)	0.18039 (7)	0.01572 (19)
C6	0.76873 (13)	-0.05036 (6)	0.14770 (8)	0.01720 (19)
C1	0.59532 (14)	0.37465 (6)	-0.08441 (8)	0.01731 (19)
C5	0.64902 (14)	0.01525 (6)	0.20275 (8)	0.0189 (2)
B10	0.87179 (14)	0.25209 (6)	-0.05883 (8)	0.0139 (2)
B7	0.61847 (14)	0.29532 (6)	0.11176 (8)	0.0141 (2)
B9	0.64685 (14)	0.20155 (7)	-0.08643 (8)	0.0142 (2)
B4	0.70836 (15)	0.29637 (7)	-0.15371 (8)	0.0164 (2)
B8	0.49009 (14)	0.22873 (7)	0.01881 (8)	0.0142 (2)
B6	0.85525 (14)	0.30984 (6)	0.06403 (8)	0.0145 (2)
B2	0.45400 (15)	0.34005 (7)	0.01668 (8)	0.0175 (2)
B5	0.83679 (15)	0.36323 (7)	-0.06106 (8)	0.0170 (2)
B3	0.47198 (15)	0.28212 (7)	-0.10584 (8)	0.0172 (2)
B1	0.67962 (16)	0.39017 (7)	0.04416 (9)	0.0179 (2)
H1	0.550 (2)	0.4238 (9)	-0.1241 (11)	0.028 (3)*
H2	0.5739 (18)	0.1360 (8)	0.2121 (11)	0.022 (3)*
H3	1.0649 (18)	0.1420 (8)	0.0562 (10)	0.018 (3)*
H4	0.5948 (18)	0.2886 (8)	0.1964 (11)	0.023 (3)*
H5	0.732 (2)	0.3026 (8)	-0.2396 (11)	0.028 (3)*
H6	1.0033 (19)	0.2213 (8)	-0.0803 (11)	0.024 (3)*
H7	1.0473 (19)	-0.0792 (9)	0.2219 (10)	0.024 (3)*
H8	0.6471 (19)	0.1387 (9)	-0.1193 (11)	0.025 (3)*
H9	0.3950 (18)	0.1821 (8)	0.0481 (10)	0.022 (3)*

H10	1.2019 (19)	0.0415 (8)	0.1695 (10)	0.022 (3)*
H11	0.9763 (19)	0.3122 (8)	0.1203 (11)	0.023 (3)*
H12	0.349 (2)	0.2795 (9)	-0.1609 (12)	0.032 (4)*
H13	0.729 (2)	-0.1072 (9)	0.1674 (11)	0.028 (3)*
H14	0.752 (2)	-0.0419 (9)	0.0693 (12)	0.033 (4)*
H15	0.558 (2)	-0.0032 (9)	0.2619 (11)	0.029 (3)*
H16	0.6817 (19)	0.4533 (8)	0.0773 (11)	0.028 (3)*
H17	0.320 (2)	0.3721 (9)	0.0344 (12)	0.032 (4)*
H18	0.935 (2)	0.4116 (9)	-0.0914 (11)	0.030 (3)*

Table 28 – Atomic displacement parameters (\AA^2) for **30**.

	U11	U22	U33	U12	U13	U23
C3	0.0124 (4)	0.0114 (4)	0.0113 (4)	0.0001 (3)	0.0003 (3)	-0.0002 (3)
C4	0.0112 (4)	0.0163 (4)	0.0136 (4)	0.0013 (3)	0.0024 (3)	0.0007 (3)
C2	0.0095 (4)	0.0122 (4)	0.0113 (4)	-0.0002 (3)	0.0011 (3)	-0.0002 (3)
C8	0.0116 (4)	0.0163 (4)	0.0159 (4)	0.0027 (3)	-0.0001 (3)	-0.0012 (3)
C9	0.0112 (4)	0.0144 (4)	0.0151 (4)	-0.0007 (3)	0.0006 (3)	0.0009 (3)
C7	0.0159 (4)	0.0145 (4)	0.0168 (4)	0.0037 (3)	0.0017 (3)	-0.0007 (3)
C6	0.0164 (4)	0.0125 (4)	0.0227 (5)	-0.0015 (3)	0.0000 (3)	-0.0013 (3)
C1	0.0185 (4)	0.0171 (4)	0.0164 (4)	0.0040 (3)	0.0027 (3)	0.0049 (3)
C5	0.0148 (4)	0.0194 (4)	0.0225 (5)	-0.0001 (3)	0.0019 (3)	0.0030 (4)
B10	0.0124 (4)	0.0161 (4)	0.0134 (4)	0.0000 (3)	0.0026 (3)	0.0017 (3)
B7	0.0152 (4)	0.0133 (4)	0.0139 (4)	0.0020 (3)	0.0021 (3)	-0.0002 (3)
B9	0.0131 (4)	0.0176 (5)	0.0119 (4)	0.0002 (3)	-0.0008 (3)	-0.0003 (3)
B4	0.0164 (5)	0.0192 (5)	0.0139 (4)	0.0027 (4)	0.0017 (4)	0.0029 (4)
B8	0.0095 (4)	0.0175 (5)	0.0155 (4)	0.0012 (3)	0.0002 (3)	0.0017 (4)
B6	0.0150 (4)	0.0132 (4)	0.0154 (4)	-0.0025 (3)	0.0006 (3)	0.0009 (3)
B2	0.0166 (5)	0.0187 (5)	0.0174 (5)	0.0053 (4)	0.0035 (4)	0.0037 (4)
B5	0.0173 (5)	0.0160 (5)	0.0178 (5)	-0.0010 (4)	0.0027 (4)	0.0036 (4)
B3	0.0138 (4)	0.0217 (5)	0.0160 (5)	0.0024 (4)	-0.0014 (4)	0.0031 (4)
B1	0.0228 (5)	0.0135 (5)	0.0174 (5)	0.0017 (4)	0.0030 (4)	0.0016 (4)

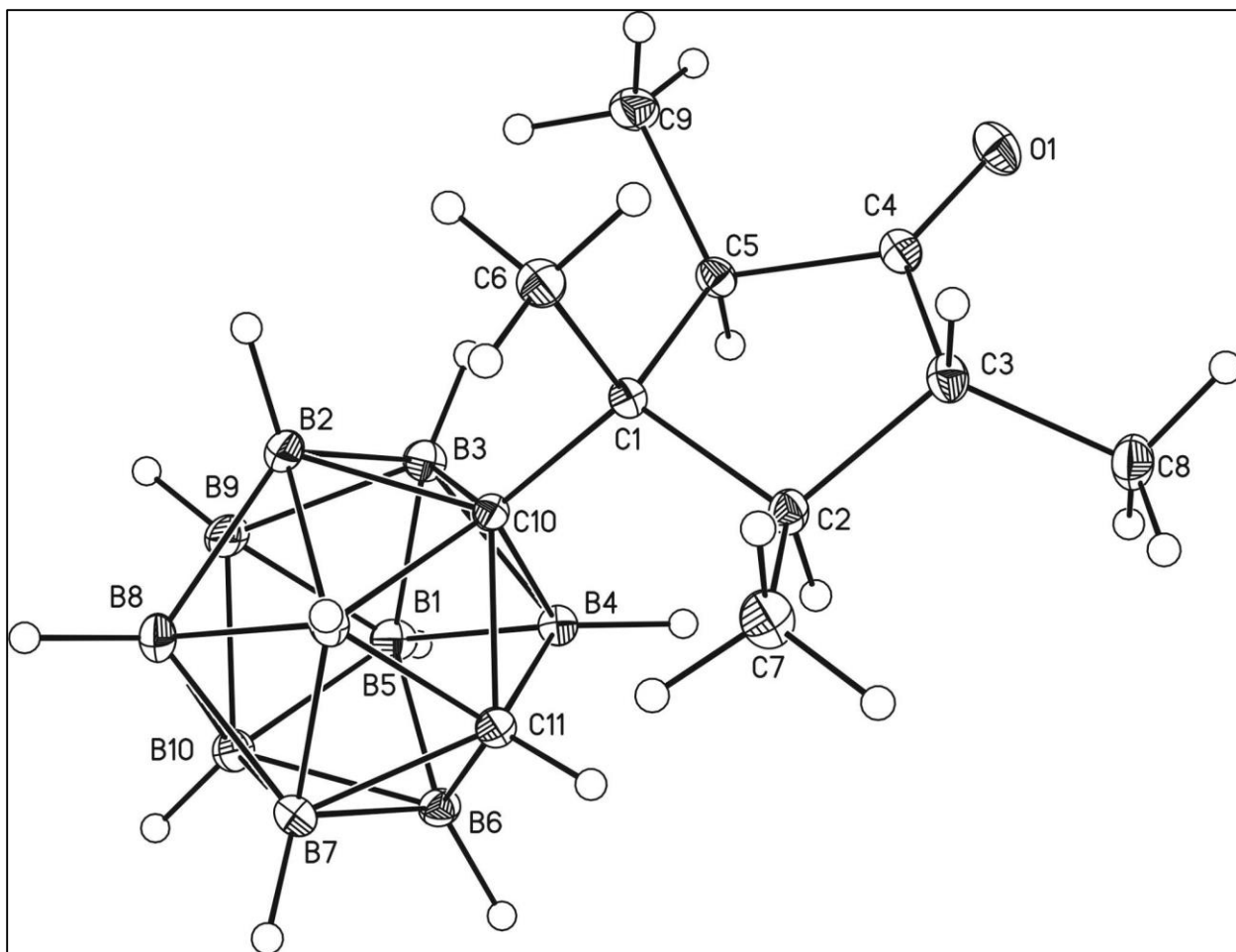


Figure 39 – Crystal data and structure refinement of 36.

Table 29 – Atomic coordinates and equivalent isotropic displacement parameters (\AA^2) for **36**.

	x	y	z	Uiso*/Ueq
B1	0.63130 (4)	1.09137 (13)	0.74037 (5)	0.01963 (18)
B2	0.58873 (4)	0.95076 (15)	0.77493 (5)	0.02168 (19)
B3	0.61894 (4)	0.72439 (15)	0.79481 (5)	0.02046 (18)
B4	0.68052 (4)	0.72153 (13)	0.77200 (5)	0.01731 (17)
B5	0.68580 (4)	0.74578 (16)	0.86313 (5)	0.02251 (19)
B6	0.72883 (4)	0.88651 (14)	0.82867 (5)	0.01942 (18)
B7	0.69818 (4)	1.11533 (14)	0.80928 (5)	0.02158 (19)
B8	0.63557 (5)	1.11757 (16)	0.83094 (6)	0.0258 (2)
B9	0.62796 (4)	0.88921 (17)	0.86464 (5)	0.0256 (2)
B10	0.69620 (4)	0.99068 (16)	0.88629 (5)	0.0238 (2)
C1	0.58923 (3)	0.78964 (11)	0.64218 (4)	0.01461 (15)
C2	0.62826 (4)	0.78716 (12)	0.59529 (4)	0.01775 (16)
C3	0.59967 (4)	0.64639 (12)	0.53423 (4)	0.01978 (17)
C4	0.57066 (4)	0.50625 (12)	0.56732 (4)	0.01843 (16)
C5	0.57003 (3)	0.57944 (11)	0.63938 (4)	0.01696 (15)
C6	0.53736 (4)	0.91620 (13)	0.60714 (5)	0.02098 (17)
C7	0.63919 (5)	0.97682 (14)	0.56529 (5)	0.02620 (19)
H7A	0.6674	0.9600	0.5419	0.039*
H7B	0.6532	1.0681	0.6046	0.039*
H7C	0.6040	1.0238	0.5302	0.039*
C8	0.63876 (4)	0.55387 (16)	0.50011 (5)	0.0276 (2)
H8A	0.6685	0.4846	0.5369	0.041*
H8B	0.6558	0.6513	0.4790	0.041*
H8C	0.6171	0.4661	0.4625	0.041*
C9	0.51382 (4)	0.53549 (14)	0.64919 (5)	0.02560 (19)
H9A	0.4828	0.5854	0.6082	0.038*
H9B	0.5130	0.5945	0.6936	0.038*
H9C	0.5096	0.3984	0.6521	0.038*

C10	0.62196 (3)	0.85172 (11)	0.72164 (4)	0.01456 (15)
C11	0.68670 (3)	0.94694 (12)	0.74412 (4)	0.01801 (16)
H2	0.6645 (5)	0.7298 (16)	0.6244 (6)	0.015 (2)*
H3	0.5689 (6)	0.712 (2)	0.4946 (7)	0.033 (3)*
H5	0.6012 (5)	0.5098 (17)	0.6748 (6)	0.021 (3)*
H11	0.7027 (5)	0.9603 (19)	0.7040 (7)	0.028 (3)*
H12	0.6151 (5)	1.1862 (18)	0.6964 (6)	0.024 (3)*
H13	0.7237 (6)	1.234 (2)	0.8070 (7)	0.033 (3)*
H14	0.6940 (5)	0.6059 (19)	0.7468 (7)	0.025 (3)*
H15	0.5928 (6)	0.604 (2)	0.7851 (7)	0.036 (4)*
H16	0.7740 (6)	0.861 (2)	0.8387 (7)	0.031 (3)*
H17	0.7035 (6)	0.632 (2)	0.8994 (7)	0.034 (3)*
H18	0.7219 (6)	1.040 (2)	0.9400 (8)	0.037 (4)*
H19	0.6061 (6)	0.869 (2)	0.9016 (8)	0.039 (4)*
H21	0.6199 (6)	1.242 (2)	0.8474 (8)	0.046 (4)*
H22	0.5440 (6)	0.965 (2)	0.7517 (7)	0.035 (4)*
H6A	0.5486 (5)	1.0456 (19)	0.6050 (7)	0.028 (3)*
H6B	0.5166 (6)	0.8686 (19)	0.5595 (7)	0.030 (3)*
H6C	0.5120 (6)	0.912 (2)	0.6337 (7)	0.033 (3)*
O1	0.55059 (3)	0.35683 (9)	0.54102 (4)	0.02595 (15)

Table 30 – Atomic displacement parameters (\AA^2) for **36**.

	U11	U22	U33	U12	U13	U23
B1	0.0198 (4)	0.0156 (4)	0.0231 (4)	0.0012 (3)	0.0069 (3)	-0.0029 (3)
B2	0.0179 (4)	0.0279 (5)	0.0213 (4)	-0.0007 (3)	0.0095 (3)	-0.0053 (3)
B3	0.0219 (4)	0.0244 (4)	0.0156 (4)	-0.0031 (3)	0.0072 (3)	0.0009 (3)
B4	0.0180 (4)	0.0170 (4)	0.0162 (4)	0.0017 (3)	0.0048 (3)	0.0018 (3)
B5	0.0229 (4)	0.0290 (5)	0.0148 (4)	-0.0032 (4)	0.0054 (3)	0.0025 (3)
B6	0.0162 (4)	0.0248 (4)	0.0166 (4)	-0.0012 (3)	0.0049 (3)	-0.0006 (3)
B7	0.0210 (4)	0.0202 (4)	0.0235 (4)	-0.0041 (3)	0.0076 (3)	-0.0052 (3)
B8	0.0239 (5)	0.0290 (5)	0.0258 (5)	0.0008 (4)	0.0101 (4)	-0.0108 (4)
B9	0.0226 (5)	0.0391 (6)	0.0182 (4)	-0.0050 (4)	0.0111 (3)	-0.0050 (4)
B10	0.0222 (4)	0.0319 (5)	0.0181 (4)	-0.0037 (4)	0.0080 (3)	-0.0059 (4)
C1	0.0163 (3)	0.0139 (3)	0.0134 (3)	0.0002 (3)	0.0047 (3)	0.0005 (2)
C2	0.0215 (4)	0.0182 (4)	0.0156 (3)	-0.0011 (3)	0.0090 (3)	0.0000 (3)
C3	0.0224 (4)	0.0209 (4)	0.0155 (3)	0.0016 (3)	0.0059 (3)	-0.0010 (3)
C4	0.0194 (4)	0.0164 (4)	0.0174 (3)	0.0025 (3)	0.0036 (3)	0.0001 (3)
C5	0.0193 (4)	0.0148 (3)	0.0165 (3)	-0.0019 (3)	0.0057 (3)	0.0001 (3)
C6	0.0194 (4)	0.0196 (4)	0.0208 (4)	0.0037 (3)	0.0028 (3)	0.0012 (3)
C7	0.0372 (5)	0.0236 (4)	0.0217 (4)	-0.0060 (4)	0.0150 (4)	0.0028 (3)
C8	0.0265 (4)	0.0370 (5)	0.0204 (4)	0.0033 (4)	0.0093 (3)	-0.0060 (4)
C9	0.0241 (4)	0.0282 (5)	0.0264 (4)	-0.0089 (3)	0.0111 (3)	-0.0027 (3)
C10	0.0143 (3)	0.0146 (3)	0.0152 (3)	0.0003 (3)	0.0055 (3)	-0.0003 (2)
C11	0.0168 (3)	0.0182 (4)	0.0187 (3)	0.0003 (3)	0.0057 (3)	-0.0010 (3)
O1	0.0326 (4)	0.0169 (3)	0.0248 (3)	-0.0003 (2)	0.0052 (3)	-0.0038 (2)

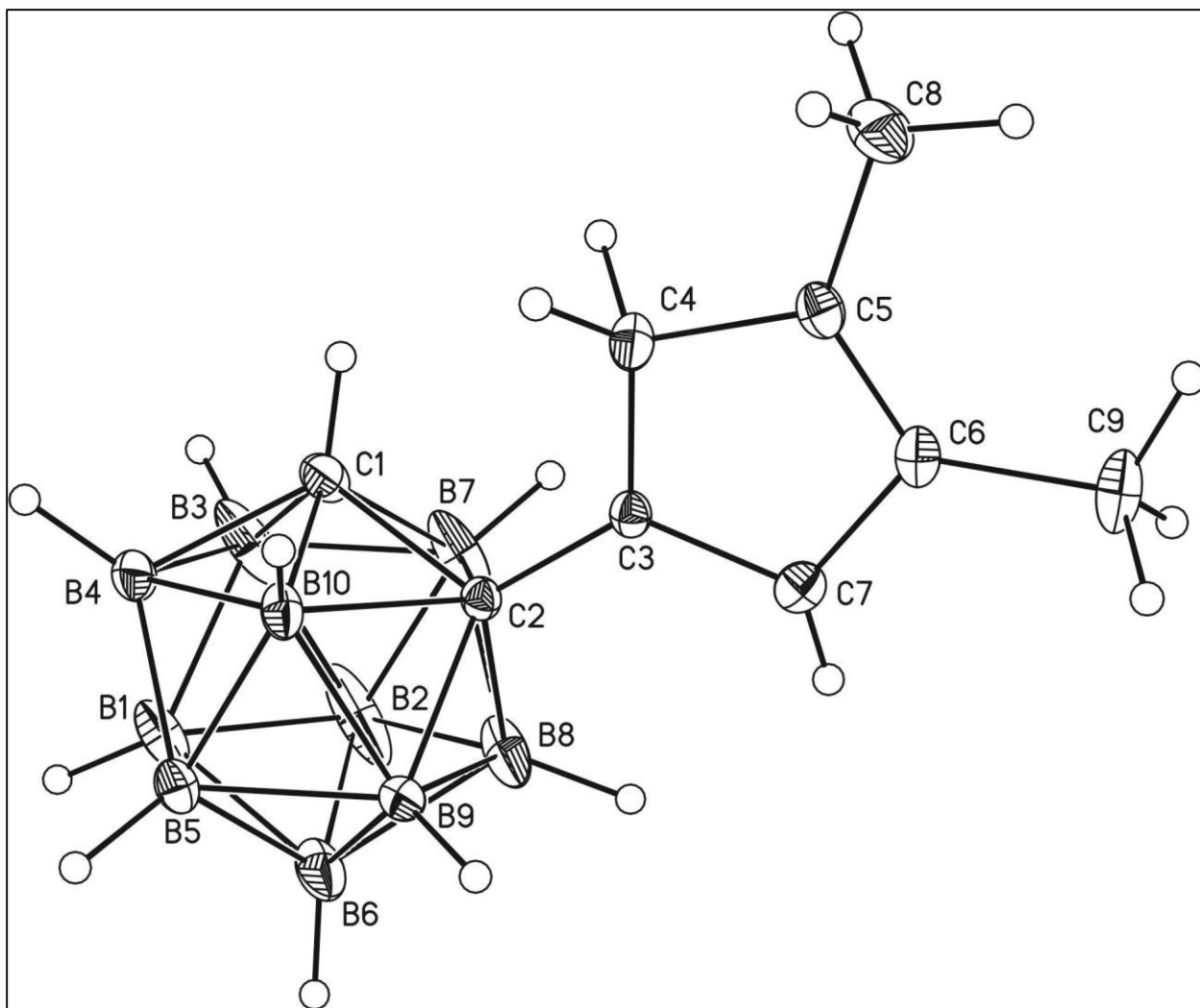


Figure 40 – Crystal data and structure refinement of **38**.

Table 31 – Atomic coordinates and equivalent isotropic displacement parameters (\AA^2) for **38**.

	x	y	z	Uiso*/Ueq
B1	0.37109 (19)	0.2102 (2)	0.74114 (18)	0.0364 (6)
B2	0.2084 (2)	0.2112 (3)	0.6386 (3)	0.0704 (11)
B3	0.2504 (3)	0.3263 (3)	0.7361 (2)	0.0606 (10)
B4	0.4249 (2)	0.3634 (2)	0.76862 (15)	0.0328 (5)
B5	0.49209 (18)	0.27186 (19)	0.69150 (15)	0.0250 (5)
B6	0.3585 (3)	0.1769 (2)	0.6101 (2)	0.0466 (7)
B7	0.1616 (2)	0.3634 (3)	0.6023 (2)	0.0501 (8)
B8	0.2295 (2)	0.2738 (2)	0.5254 (2)	0.0478 (7)
B9	0.4049 (2)	0.3111 (2)	0.55753 (15)	0.0307 (5)
B10	0.44740 (18)	0.42452 (19)	0.65554 (14)	0.0248 (5)
C1	0.29974 (19)	0.4463 (2)	0.67984 (13)	0.0335 (5)
C2	0.28646 (14)	0.41873 (15)	0.55830 (12)	0.0192 (4)
C3	0.24657 (14)	0.52280 (15)	0.48237 (11)	0.0194 (4)
C4	0.25517 (18)	0.65019 (17)	0.50838 (13)	0.0262 (4)
C5	0.20609 (16)	0.71773 (16)	0.40642 (12)	0.0249 (4)
C6	0.16931 (15)	0.63603 (17)	0.32799 (12)	0.0242 (4)
C7	0.19318 (16)	0.51058 (18)	0.37199 (13)	0.0250 (4)
C8	0.2044 (2)	0.8548 (2)	0.40202 (19)	0.0411 (5)
C9	0.1138 (2)	0.6595 (2)	0.21137 (14)	0.0383 (5)
H1	0.508 (2)	0.5086 (19)	0.6518 (15)	0.041 (5)*
H2	0.275 (2)	0.530 (2)	0.6925 (17)	0.057 (7)*
H3	0.5984 (19)	0.2415 (18)	0.7219 (15)	0.040 (5)*
H4	0.181 (2)	0.633 (2)	0.1766 (16)	0.053 (6)*
H5	0.4053 (19)	0.1409 (18)	0.8037 (14)	0.037 (5)*
H6	0.448 (2)	0.3204 (19)	0.4918 (17)	0.052 (6)*
H7	0.163 (2)	0.888 (2)	0.331 (2)	0.063 (7)*
H8	0.094 (3)	0.750 (3)	0.1951 (19)	0.076 (9)*
H9	0.477 (2)	0.405 (2)	0.8419 (18)	0.060 (7)*

H10	0.333 (2)	0.680 (2)	0.5610 (18)	0.062 (7)*
H11	0.150 (2)	0.887 (2)	0.4443 (17)	0.054 (7)*
H12	0.379 (2)	0.088 (2)	0.5902 (19)	0.072 (8)*
H13	0.298 (3)	0.887 (3)	0.433 (2)	0.088 (9)*
H14	0.029 (2)	0.616 (2)	0.1764 (16)	0.048 (6)*
H15	0.171 (3)	0.259 (3)	0.442 (2)	0.080 (8)*
H16	0.064 (2)	0.408 (2)	0.5687 (16)	0.055 (6)*
H17	0.175 (3)	0.445 (3)	0.340 (2)	0.097 (11)*
H18	0.135 (3)	0.145 (2)	0.641 (2)	0.080 (8)*
H19	0.209 (3)	0.349 (2)	0.7979 (19)	0.070 (7)*
H29	0.187 (4)	0.677 (3)	0.555 (3)	0.116 (11)*

Table 32 – Atomic displacement parameters (\AA^2) for **38**.

	U11	U22	U33	U12	U13	U23
B1	0.0200 (9)	0.0381 (14)	0.0506 (13)	0.0030 (9)	0.0120 (9)	0.0254 (11)
B2	0.0224 (11)	0.0555 (19)	0.110 (2)	-0.0116 (12)	-0.0060 (13)	0.0580 (18)
B3	0.0414 (13)	0.086 (2)	0.0729 (18)	0.0358 (14)	0.0427 (13)	0.0614 (18)
B4	0.0437 (12)	0.0346 (13)	0.0189 (10)	0.0143 (10)	0.0099 (9)	0.0071 (9)
B5	0.0187 (9)	0.0291 (12)	0.0259 (9)	0.0011 (8)	0.0062 (7)	0.0054 (8)
B6	0.0505 (14)	0.0190 (12)	0.0460 (14)	0.0023 (10)	-0.0130 (11)	-0.0014 (10)
B7	0.0187 (10)	0.0579 (18)	0.0738 (17)	0.0063 (10)	0.0167 (11)	0.0449 (14)
B8	0.0413 (13)	0.0198 (12)	0.0517 (14)	-0.0082 (10)	-0.0212 (11)	0.0037 (10)
B9	0.0348 (11)	0.0334 (13)	0.0226 (10)	0.0150 (9)	0.0084 (8)	0.0012 (9)
B10	0.0218 (9)	0.0249 (11)	0.0221 (9)	-0.0035 (8)	0.0009 (7)	0.0037 (8)
C1	0.0451 (11)	0.0386 (12)	0.0232 (9)	0.0211 (9)	0.0199 (8)	0.0109 (8)
C2	0.0165 (7)	0.0203 (9)	0.0190 (8)	0.0000 (6)	0.0043 (6)	0.0000 (6)
C3	0.0162 (7)	0.0234 (9)	0.0183 (8)	0.0003 (6)	0.0058 (6)	0.0012 (7)
C4	0.0268 (9)	0.0281 (10)	0.0201 (8)	-0.0034 (7)	0.0038 (7)	0.0021 (7)
C5	0.0235 (8)	0.0262 (10)	0.0249 (8)	0.0006 (7)	0.0084 (7)	0.0058 (7)
C6	0.0170 (7)	0.0345 (11)	0.0209 (8)	-0.0022 (7)	0.0065 (6)	0.0049 (7)
C7	0.0232 (8)	0.0283 (11)	0.0254 (9)	-0.0025 (7)	0.0111 (7)	-0.0016 (8)
C8	0.0525 (13)	0.0272 (12)	0.0440 (12)	0.0041 (10)	0.0177 (11)	0.0094 (10)
C9	0.0296 (10)	0.0604 (16)	0.0204 (9)	-0.0090 (10)	0.0033 (8)	0.0074 (9)

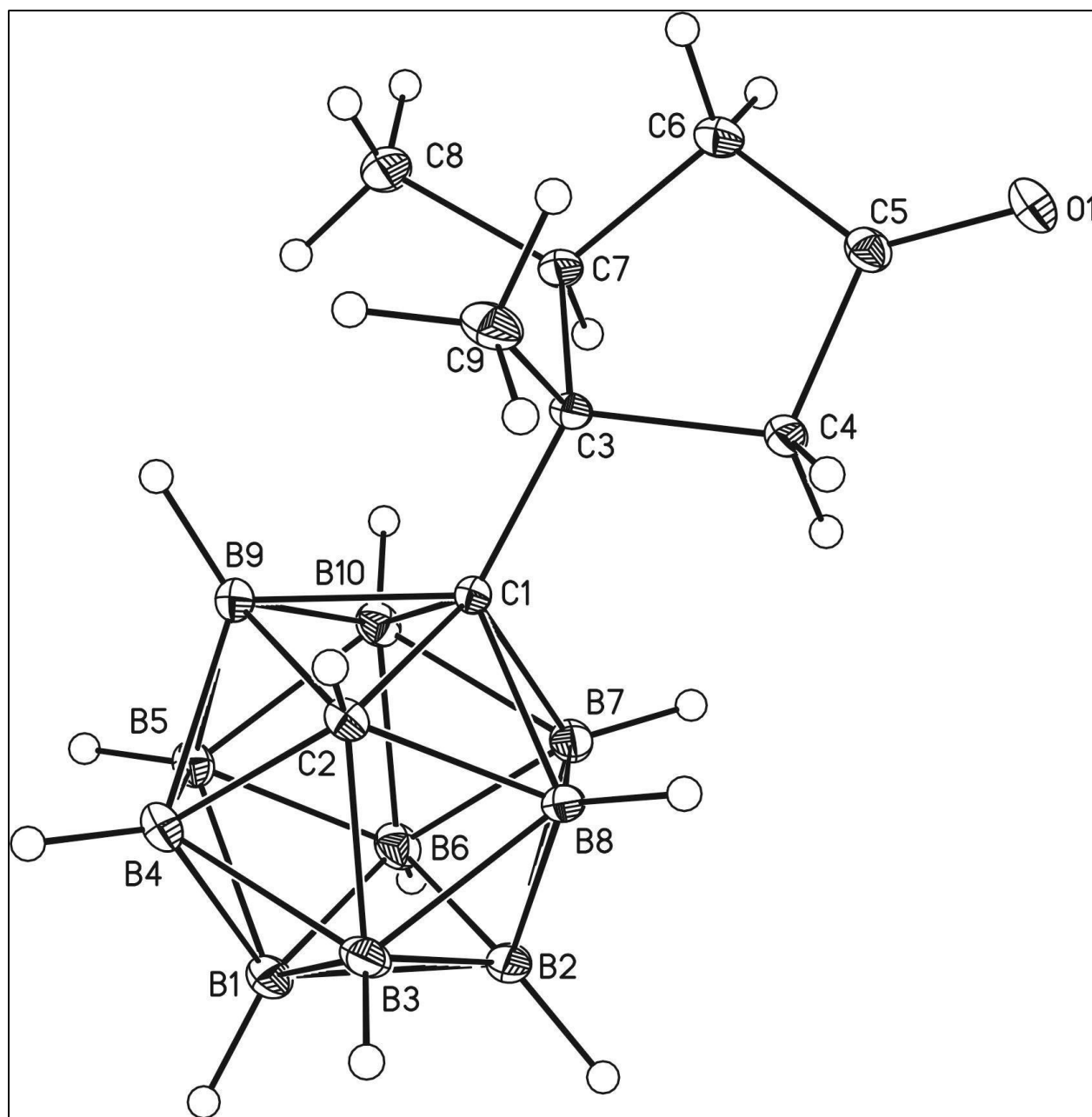


Figure 41 – Crystal data and structure refinement of **39**.

Table 33 – Atomic coordinates and equivalent isotropic displacement parameters (\AA^2) for **39**.

	x	y	z	Uiso*/Ueq
B1	0.55077 (16)	0.60151 (11)	0.23781 (11)	0.0225 (3)
B2	0.53361 (16)	0.74142 (12)	0.23032 (12)	0.0227 (3)
B3	0.47930 (16)	0.67159 (11)	0.33468 (11)	0.0219 (3)
B4	0.39531 (17)	0.55173 (11)	0.28145 (11)	0.0219 (3)
B5	0.39689 (16)	0.54566 (11)	0.14337 (11)	0.0219 (3)
B6	0.48311 (17)	0.66324 (12)	0.11142 (12)	0.0229 (3)
B7	0.36980 (16)	0.77128 (11)	0.13022 (11)	0.0194 (3)
B8	0.36873 (15)	0.77667 (11)	0.26867 (11)	0.0183 (3)
B9	0.23179 (16)	0.58218 (11)	0.18188 (11)	0.0195 (3)
B10	0.28647 (16)	0.65103 (11)	0.07719 (11)	0.0199 (3)
C1	0.22394 (12)	0.71869 (9)	0.17499 (8)	0.0141 (2)
C2	0.29202 (13)	0.65981 (9)	0.29178 (9)	0.0174 (2)
C3	0.06882 (12)	0.77404 (9)	0.15673 (8)	0.0155 (2)
C4	0.08351 (13)	0.89491 (9)	0.16471 (9)	0.0196 (3)
H4A	0.0940	0.9183	0.2398	0.024*
H4B	0.1716	0.9188	0.1395	0.024*
C5	-0.05758 (13)	0.93814 (10)	0.09390 (9)	0.0191 (3)
C6	-0.13771 (14)	0.85107 (10)	0.02427 (10)	0.0222 (3)
H6A	-0.1661	0.8733	-0.0518	0.027*
H6B	-0.2287	0.8303	0.0475	0.027*
C7	-0.02605 (13)	0.75989 (9)	0.03878 (9)	0.0184 (3)
H7A	0.0414	0.7723	-0.0109	0.022*
C8	-0.10306 (16)	0.65500 (11)	0.00891 (11)	0.0285 (3)
H8A	-0.1652	0.6385	0.0593	0.043*
H8B	-0.0279	0.6000	0.0122	0.043*
H8C	-0.1657	0.6589	-0.0641	0.043*
C9	-0.01859 (14)	0.73770 (11)	0.23841 (10)	0.0248 (3)
H9A	0.0346	0.7589	0.3107	0.037*

H9B	-0.0285	0.6612	0.2354	0.037*
H9C	-0.1177	0.7698	0.2214	0.037*
H1	0.2296 (19)	0.6591 (12)	0.3422 (13)	0.033 (4)*
H2	0.3392 (17)	0.8456 (11)	0.3099 (11)	0.026 (4)*
H3	0.525 (2)	0.6820 (13)	0.4203 (13)	0.039 (4)*
H4	0.3894 (19)	0.4874 (13)	0.3348 (13)	0.035 (4)*
H5	0.4016 (18)	0.4716 (12)	0.1043 (12)	0.032 (4)*
H6	0.6605 (19)	0.5627 (13)	0.2602 (13)	0.038 (4)*
H7	0.5441 (18)	0.6639 (12)	0.0492 (12)	0.032 (4)*
H8	0.2160 (18)	0.6462 (12)	-0.0032 (12)	0.031 (4)*
H9	0.3512 (19)	0.8407 (12)	0.0838 (12)	0.034 (4)*
H10	0.6297 (19)	0.7974 (13)	0.2469 (13)	0.036 (4)*
H11	0.1276 (17)	0.5398 (12)	0.1768 (11)	0.025 (4)*
O1	-0.09627 (10)	1.02921 (7)	0.09120 (7)	0.0248 (2)

Table 34 – Atomic displacement parameters (\AA^2) for **39**.

	U11	U22	U33	U12	U13	U23
B1	0.0170 (7)	0.0199 (7)	0.0293 (7)	0.0050 (5)	0.0027 (5)	-0.0018 (5)
B2	0.0124 (7)	0.0193 (7)	0.0353 (7)	0.0014 (5)	0.0033 (5)	-0.0017 (6)
B3	0.0164 (7)	0.0222 (7)	0.0238 (6)	0.0053 (5)	-0.0018 (5)	-0.0016 (5)
B4	0.0217 (7)	0.0161 (7)	0.0265 (7)	0.0049 (5)	0.0028 (6)	0.0027 (5)
B5	0.0221 (7)	0.0159 (7)	0.0267 (7)	0.0040 (5)	0.0034 (5)	-0.0035 (5)
B6	0.0198 (7)	0.0223 (7)	0.0282 (7)	0.0051 (5)	0.0089 (6)	0.0006 (5)
B7	0.0158 (7)	0.0185 (7)	0.0256 (6)	0.0010 (5)	0.0079 (5)	0.0022 (5)
B8	0.0129 (6)	0.0161 (7)	0.0237 (6)	0.0001 (5)	-0.0001 (5)	-0.0033 (5)
B9	0.0185 (7)	0.0135 (6)	0.0244 (6)	0.0001 (5)	0.0012 (5)	-0.0006 (5)
B10	0.0205 (7)	0.0198 (7)	0.0194 (6)	0.0040 (5)	0.0044 (5)	-0.0028 (5)
C1	0.0137 (5)	0.0122 (5)	0.0152 (5)	0.0000 (4)	0.0013 (4)	-0.0004 (4)
C2	0.0165 (6)	0.0173 (6)	0.0174 (5)	0.0024 (4)	0.0019 (4)	0.0021 (4)
C3	0.0117 (5)	0.0161 (6)	0.0179 (5)	0.0011 (4)	0.0016 (4)	-0.0008 (4)
C4	0.0162 (6)	0.0167 (6)	0.0239 (5)	0.0024 (4)	0.0004 (4)	-0.0039 (4)
C5	0.0169 (6)	0.0200 (6)	0.0217 (5)	0.0033 (5)	0.0071 (5)	0.0007 (4)
C6	0.0162 (6)	0.0237 (7)	0.0239 (6)	0.0021 (5)	-0.0013 (5)	0.0007 (5)
C7	0.0150 (6)	0.0190 (6)	0.0186 (5)	-0.0002 (4)	-0.0014 (4)	-0.0012 (4)
C8	0.0219 (7)	0.0237 (7)	0.0342 (7)	-0.0021 (5)	-0.0050 (5)	-0.0053 (5)
C9	0.0169 (6)	0.0327 (7)	0.0259 (6)	0.0058 (5)	0.0073 (5)	0.0053 (5)
O1	0.0252 (5)	0.0210 (5)	0.0288 (5)	0.0089 (4)	0.0077 (4)	0.0008 (3)

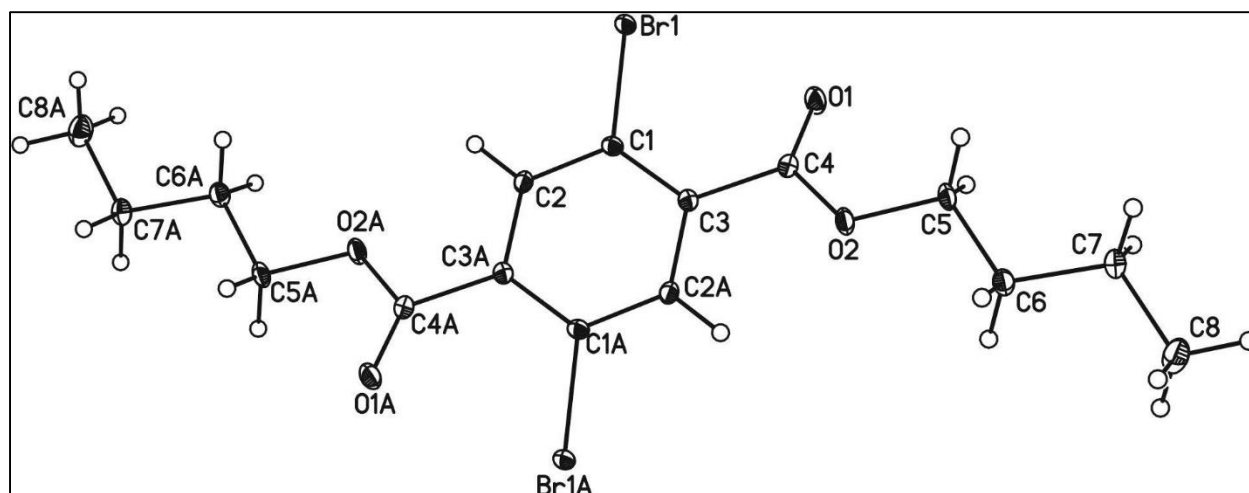


Figure 42 – Crystal data and structure refinement of 63.

Table 35 – Atomic coordinates and equivalent isotropic displacement parameters (\AA^2) for **63**.

	x	y	z	Uiso*/Ueq
Br1	0.06956 (2)	0.74104 (2)	1.03303 (2)	0.01866 (8)
C1	0.3203 (2)	0.8837 (2)	1.0106 (2)	0.0146 (3)
C2	0.3579 (2)	1.0747 (2)	1.0806 (2)	0.0160 (3)
H2	0.2589	1.1251	1.1362	0.019*
C3	0.4631 (2)	0.8042 (2)	0.9277 (2)	0.0157 (3)
C4	0.4334 (3)	0.5980 (2)	0.8475 (2)	0.0182 (4)
C5	0.5558 (3)	0.3640 (2)	0.6534 (2)	0.0226 (4)
H5A	0.4382	0.2942	0.5613	0.027*
H5B	0.5464	0.3076	0.7429	0.027*
C6	0.7428 (3)	0.3570 (2)	0.5718 (2)	0.0197 (4)
H6A	0.8589	0.4273	0.6655	0.024*
H6B	0.7523	0.4180	0.4858	0.024*
C7	0.7482 (3)	0.1578 (3)	0.4776 (2)	0.0210 (4)
H7A	0.7288	0.0938	0.5612	0.025*
H7B	0.6380	0.0900	0.3780	0.025*
C8	0.9440 (3)	0.1523 (3)	0.4070 (3)	0.0311 (5)
H8A	0.9649	0.2178	0.3262	0.047*
H8B	0.9404	0.0226	0.3434	0.047*
H8C	1.0527	0.2130	0.5061	0.047*
O1	0.3110 (2)	0.48241 (18)	0.87840 (19)	0.0315 (4)
O2	0.56473 (19)	0.55924 (16)	0.73624 (16)	0.0218 (3)

Table 36 – Atomic displacement parameters (\AA^2) for **63**.

	U11	U22	U33	U12	U13	U23
Br1	0.01499 (11)	0.01380 (11)	0.02551 (11)	0.00256 (7)	0.00723 (7)	0.00667 (8)
C1	0.0137 (7)	0.0145 (8)	0.0158 (7)	0.0025 (6)	0.0023 (6)	0.0071 (6)
C2	0.0161 (8)	0.0150 (8)	0.0191 (8)	0.0073 (6)	0.0048 (6)	0.0068 (6)
C3	0.0162 (8)	0.0134 (8)	0.0178 (7)	0.0049 (7)	0.0030 (6)	0.0062 (7)
C4	0.0172 (8)	0.0157 (9)	0.0224 (8)	0.0074 (7)	0.0040 (6)	0.0064 (7)
C5	0.0250 (9)	0.0100 (8)	0.0313 (9)	0.0062 (7)	0.0096 (7)	0.0051 (7)
C6	0.0231 (9)	0.0150 (8)	0.0207 (8)	0.0066 (7)	0.0050 (7)	0.0058 (7)
C7	0.0263 (9)	0.0165 (9)	0.0205 (8)	0.0095 (7)	0.0046 (7)	0.0053 (7)
C8	0.0365 (11)	0.0309 (11)	0.0344 (10)	0.0192 (9)	0.0155 (9)	0.0149 (9)
O1	0.0280 (7)	0.0141 (7)	0.0528 (9)	0.0065 (6)	0.0215 (6)	0.0123 (6)
O2	0.0264 (6)	0.0114 (6)	0.0276 (6)	0.0071 (5)	0.0122 (5)	0.0061 (5)

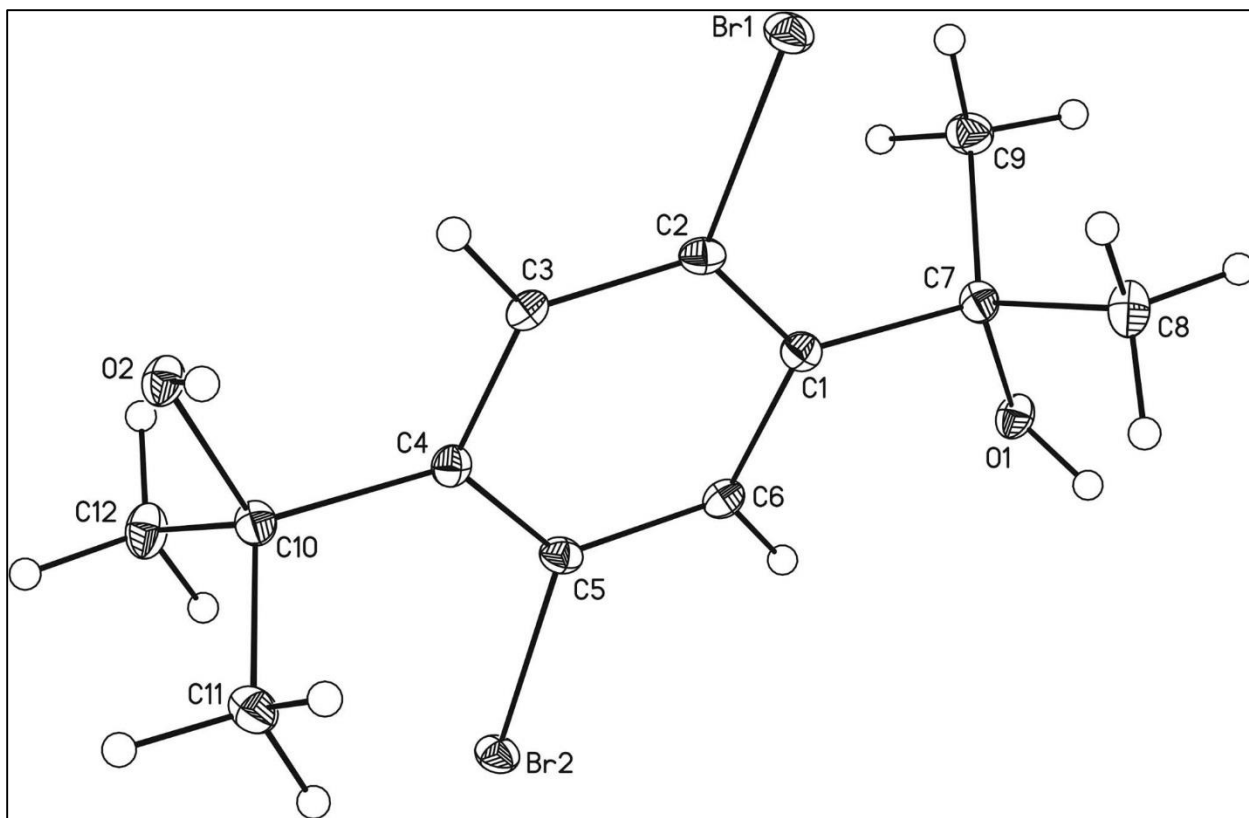


Figure 43 – Crystal data and structure refinement of **64**.

Table 37 – Atomic coordinates and equivalent isotropic displacement parameters (\AA^2) for **64**.

	x	y	z	Uiso*/Ueq
Br1	0.10309 (3)	0.439039 (12)	0.63773 (3)	0.01936 (8)
Br2	0.23619 (3)	0.083766 (12)	0.74478 (3)	0.01956 (8)
O2	-0.2608 (2)	0.21019 (9)	0.56136 (18)	0.0184 (4)
H2	-0.3020	0.2371	0.6274	0.028*
C8	0.4454 (3)	0.40939 (14)	0.8705 (3)	0.0239 (6)
H8A	0.4281	0.3798	0.9594	0.036*
H8B	0.3450	0.4401	0.8513	0.036*
H8C	0.5446	0.4415	0.8843	0.036*
C3	0.0220 (3)	0.28860 (13)	0.6324 (2)	0.0160 (5)
H6	-0.0815	0.3092	0.5971	0.019*
C2	0.1567 (3)	0.33625 (12)	0.6617 (3)	0.0162 (5)
C6	0.3247 (3)	0.23320 (13)	0.7290 (2)	0.0161 (5)
H3	0.4291	0.2124	0.7618	0.019*
C4	0.0316 (3)	0.21214 (13)	0.6524 (2)	0.0155 (5)
C5	0.1887 (3)	0.18604 (13)	0.7032 (3)	0.0166 (5)
C9	0.5276 (3)	0.39970 (14)	0.6022 (3)	0.0227 (5)
H9A	0.6349	0.4255	0.6217	0.034*
H9B	0.4402	0.4361	0.5752	0.034*
H9C	0.5422	0.3645	0.5212	0.034*
C7	0.4739 (3)	0.35773 (13)	0.7401 (3)	0.0171 (5)
C10	-0.1276 (3)	0.16451 (13)	0.6238 (3)	0.0173 (5)
C1	0.3149 (3)	0.30977 (13)	0.7088 (3)	0.0161 (5)
C11	-0.1921 (3)	0.13262 (13)	0.7691 (3)	0.0207 (5)
H11A	-0.2196	0.1734	0.8361	0.031*
H11B	-0.1041	0.1013	0.8141	0.031*
H11C	-0.2938	0.1028	0.7501	0.031*
C12	-0.0959 (3)	0.10506 (14)	0.5080 (3)	0.0232 (6)
H12A	-0.1971	0.0739	0.4967	0.035*

H12B	0.0003	0.0742	0.5389	0.035*
H12C	-0.0706	0.1289	0.4139	0.035*
O1	0.6140 (2)	0.30893 (9)	0.77334 (18)	0.0192 (4)
H1	0.6335	0.3092	0.8644	0.029*

Table 38 – Atomic displacement parameters (\AA^2) for **64**.

	U11	U22	U33	U12	U13	U23
Br1	0.02004 (14)	0.01313 (12)	0.02488 (15)	0.00233 (9)	-0.00046 (10)	0.00210 (9)
Br2	0.02002 (14)	0.01365 (13)	0.02499 (15)	0.00213 (9)	-0.00039 (10)	0.00328 (9)
O2	0.0144 (9)	0.0190 (8)	0.0218 (9)	0.0036 (7)	-0.0032 (7)	-0.0027 (7)
C8	0.0210 (14)	0.0255 (13)	0.0250 (15)	-0.0001 (10)	-0.0026 (11)	-0.0070 (10)
C3	0.0149 (12)	0.0184 (12)	0.0145 (12)	0.0024 (9)	-0.0018 (9)	0.0012 (9)
C2	0.0185 (13)	0.0146 (11)	0.0155 (12)	0.0033 (9)	0.0021 (9)	0.0018 (9)
C6	0.0143 (12)	0.0188 (12)	0.0154 (12)	0.0039 (9)	0.0000 (9)	0.0006 (9)
C4	0.0175 (12)	0.0162 (11)	0.0129 (12)	0.0005 (9)	0.0011 (9)	-0.0024 (9)
C5	0.0202 (13)	0.0129 (11)	0.0167 (12)	0.0015 (9)	0.0019 (10)	0.0006 (9)
C9	0.0199 (14)	0.0234 (13)	0.0247 (14)	-0.0017 (10)	0.0011 (11)	0.0050 (10)
C7	0.0133 (12)	0.0163 (11)	0.0216 (13)	0.0015 (9)	-0.0016 (10)	-0.0008 (9)
C10	0.0153 (12)	0.0157 (11)	0.0209 (13)	0.0011 (9)	-0.0009 (10)	-0.0011 (9)
C1	0.0169 (12)	0.0168 (11)	0.0147 (12)	-0.0001 (9)	0.0027 (9)	-0.0001 (9)
C11	0.0186 (13)	0.0170 (12)	0.0263 (14)	-0.0003 (10)	0.0013 (10)	0.0021 (10)
C12	0.0205 (13)	0.0221 (13)	0.0270 (14)	0.0030 (10)	-0.0038 (11)	-0.0081 (10)
O1	0.0144 (9)	0.0228 (9)	0.0204 (9)	0.0031 (7)	-0.0034 (7)	-0.0020 (7)

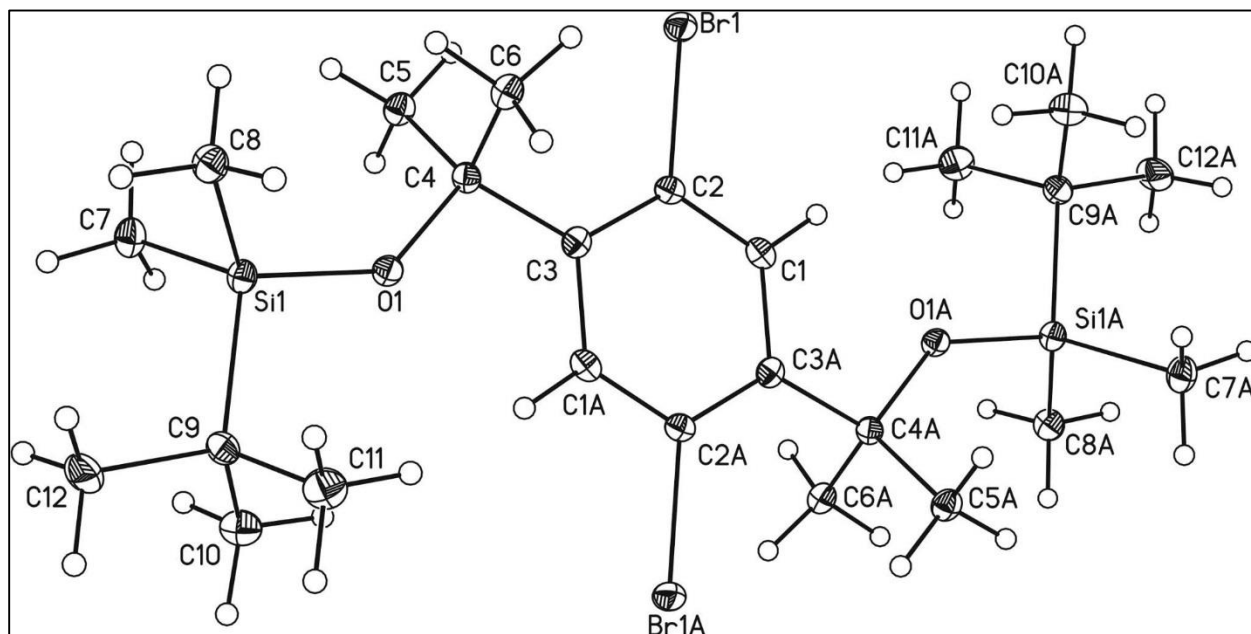


Figure 44 – Crystal data and structure refinement of 65.

Table 39 – Atomic coordinates and equivalent isotropic displacement parameters (\AA^2) for **65**.

	x	y	z	Uiso*/Ueq
Br	1 0.29241 (7)	0.21033 (4)	1.18883 (3)	0.02610 (19)
Si1	0.14470 (17)	0.33827 (11)	0.71848 (9)	0.0187 (3)
O1	0.2327 (4)	0.2373 (3)	0.8174 (2)	0.0186 (6)
C3	0.3659 (6)	0.1235 (4)	0.9692 (3)	0.0182 (8)
C2	0.4077 (6)	0.0937 (4)	1.0732 (3)	0.0181 (8)
C1	0.5357 (6)	-0.0248 (4)	1.1023 (3)	0.0181 (8)
H1	0.5571	-0.0392	1.1727	0.022*
C4	0.2181 (6)	0.2475 (4)	0.9289 (3)	0.0174 (8)
C5	0.2902 (7)	0.4044 (4)	0.9461 (3)	0.0219 (9)
H5A	0.4324	0.4221	0.9079	0.033*
H5B	0.2885	0.4110	1.0208	0.033*
H5C	0.1948	0.4784	0.9205	0.033*
C6	-0.0142 (6)	0.2167 (4)	0.9833 (3)	0.0222 (9)
H6A	-0.1040	0.2982	0.9629	0.033*
H6B	-0.0218	0.2079	1.0593	0.033*
H6C	-0.0617	0.1249	0.9618	0.033*
C8	-0.1499 (6)	0.3688 (5)	0.7465 (3)	0.0251 (9)
H8A	-0.2204	0.2737	0.7656	0.038*
H8B	-0.1965	0.4171	0.6840	0.038*
H8C	-0.1846	0.4311	0.8042	0.038*
C7	0.2738 (7)	0.5271 (4)	0.6871 (3)	0.0266 (9)
H7A	0.2163	0.5913	0.7411	0.040*
H7B	0.2463	0.5705	0.6191	0.040*
H7C	0.4252	0.5163	0.6849	0.040*
C9	0.2195 (7)	0.2194 (4)	0.6032 (3)	0.0222 (9)
C11	0.1184 (7)	0.0621 (5)	0.6307 (4)	0.0314 (10)
H11A	0.1588	0.0029	0.5716	0.047*
H11B	-0.0343	0.0717	0.6453	0.047*

H11C	0.1680	0.0137	0.6924	0.047*
C10	0.4632 (7)	0.2028 (5)	0.5766 (4)	0.0298 (10)
H10A	0.5154	0.1508	0.6363	0.045*
H10B	0.5271	0.3005	0.5611	0.045*
H10C	0.4997	0.1467	0.5156	0.045*
C12	0.1369 (8)	0.2943 (5)	0.5043 (4)	0.0337 (11)
H12A	0.2041	0.3903	0.4837	0.051*
H12B	-0.0151	0.3079	0.5208	0.051*
H12C	0.1702	0.2316	0.4468	0.051*

Table 40 – Atomic displacement parameters (\AA^2) for **65**.

	U11	U22	U33	U12	U13	U23
Br1	0.0358 (3)	0.0238 (3)	0.0198 (3)	0.00580 (17)	-0.00628 (18)	-0.00618 (16)
Si1	0.0186 (6)	0.0186 (5)	0.0200 (6)	-0.0006 (4)	-0.0067 (4)	-0.0007 (4)
O1	0.0221 (15)	0.0172 (12)	0.0184 (14)	-0.0005 (11)	-0.0071 (11)	-0.0040 (10)
C3	0.017 (2)	0.0153 (17)	0.022 (2)	-0.0053 (15)	-0.0034 (16)	-0.0015 (15)
C2	0.017 (2)	0.0188 (18)	0.018 (2)	-0.0031 (15)	-0.0023 (16)	-0.0039 (15)
C1	0.0178 (19)	0.0218 (19)	0.016 (2)	-0.0078 (16)	-0.0044 (16)	-0.0026 (15)
C4	0.022 (2)	0.0165 (18)	0.0155 (19)	-0.0022 (15)	-0.0068 (16)	-0.0027 (15)
C5	0.024 (2)	0.0185 (19)	0.024 (2)	-0.0020 (16)	-0.0072 (17)	-0.0032 (16)
C6	0.023 (2)	0.0190 (19)	0.025 (2)	0.0000 (16)	-0.0067 (17)	-0.0015 (16)
C8	0.021 (2)	0.029 (2)	0.025 (2)	0.0028 (17)	-0.0072 (17)	-0.0010 (18)
C7	0.030 (2)	0.024 (2)	0.027 (2)	-0.0009 (17)	-0.0106 (18)	0.0015 (17)
C9	0.026 (2)	0.024 (2)	0.017 (2)	0.0002 (17)	-0.0072 (17)	-0.0038 (16)
C11	0.035 (3)	0.029 (2)	0.032 (3)	-0.0053 (19)	-0.009 (2)	-0.0079 (19)
C10	0.026 (2)	0.034 (2)	0.030 (3)	0.0008 (19)	-0.0045 (19)	-0.0083 (19)
C12	0.041 (3)	0.043 (3)	0.019 (2)	0.008 (2)	-0.011 (2)	-0.0052 (19)

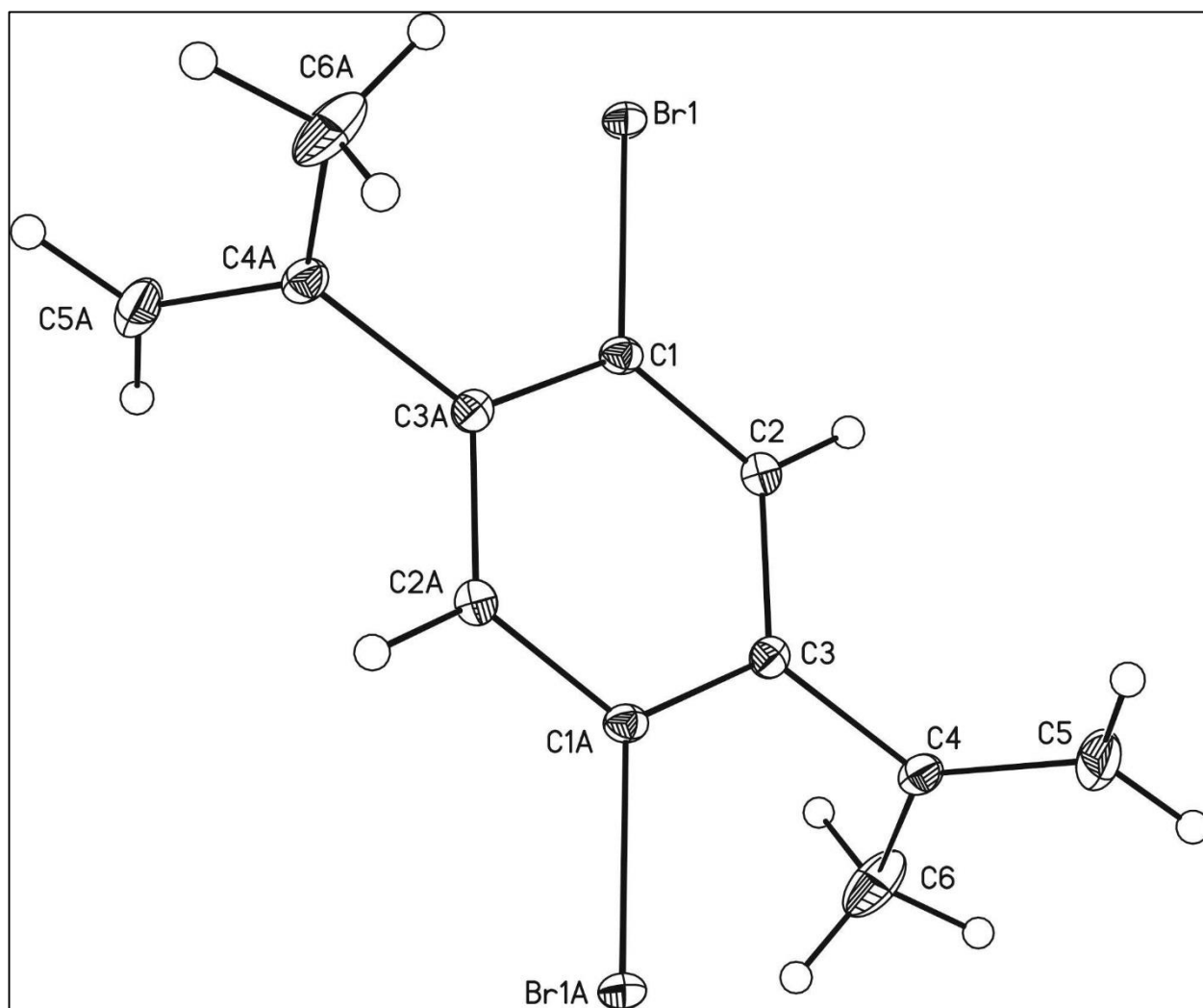


Figure 45 – Crystal data and structure refinement of 70.

Table 41 – Atomic coordinates and equivalent isotropic displacement parameters (\AA^2) for **70**.

	x	y	z	Uiso*/Ueq
Br1	0.26640 (2)	0.79139 (2)	0.36410 (2)	0.01758 (6)
Br2	0.06891 (2)	1.18481 (2)	1.21572 (2)	0.02176 (6)
C3	-0.1523 (2)	1.40004 (19)	1.05216 (15)	0.0121 (3)
C4	0.3017 (2)	1.03192 (19)	0.51168 (16)	0.0133 (3)
C5	-0.1720 (2)	1.5326 (2)	0.95656 (16)	0.0138 (3)
C6	0.3924 (2)	1.12350 (19)	0.57329 (15)	0.0122 (3)
C7	0.4070 (2)	0.91176 (19)	0.44010 (15)	0.0123 (3)
C8	-0.3173 (2)	1.29995 (19)	1.10633 (16)	0.0143 (3)
C9	0.0229 (2)	1.37000 (19)	1.09368 (15)	0.0129 (3)
CA	0.2722 (2)	1.2513 (2)	0.64946 (17)	0.0150 (3)
CB	-0.4265 (3)	1.3201 (3)	1.23669 (19)	0.0248 (4)
CC	-0.3608 (3)	1.1994 (2)	1.0293 (2)	0.0261 (4)
CD	0.2107 (4)	1.3955 (3)	0.5832 (2)	0.0356 (5)
CE	0.2204 (4)	1.2119 (3)	0.7890 (2)	0.0360 (5)
H1	0.165 (3)	1.053 (2)	0.517 (2)	0.016 (5)*
H2	-0.289 (3)	1.557 (2)	0.9268 (19)	0.015 (5)*
H3	-0.467 (4)	1.140 (3)	1.068 (2)	0.037 (7)*
H4	0.130 (4)	1.477 (3)	0.633 (3)	0.040 (7)*
H5	-0.528 (3)	1.251 (3)	1.271 (2)	0.032 (6)*
H6	0.176 (4)	1.109 (3)	0.822 (3)	0.044 (7)*
H7	0.135 (4)	1.297 (3)	0.829 (3)	0.042 (7)*
H8	0.219 (4)	1.410 (3)	0.497 (3)	0.049 (8)*
H9	-0.354 (4)	1.318 (3)	1.302 (3)	0.047 (8)*
H10	-0.280 (4)	1.170 (3)	0.961 (3)	0.046 (8)*
H11	-0.484 (5)	1.440 (4)	1.242 (3)	0.066 (9)*
H12	0.340 (8)	1.185 (6)	0.824 (5)	0.15 (2)*

Table 42 – Atomic displacement parameters (\AA^2) for **70**.

	U11	U22	U33	U12	U13	U23
Br1	0.01840 (9)	0.01607 (9)	0.02190 (10)	-0.00342 (6)	-0.00807 (7)	-0.00634 (7)
Br2	0.01627 (9)	0.02093 (10)	0.02579 (11)	-0.00574 (7)	-0.00851 (7)	0.01274 (7)
C3	0.0119 (7)	0.0120 (7)	0.0118 (7)	-0.0017 (6)	-0.0005 (6)	-0.0022 (6)
C4	0.0120 (7)	0.0139 (7)	0.0131 (8)	-0.0019 (6)	-0.0014 (6)	-0.0005 (6)
C5	0.0120 (7)	0.0157 (8)	0.0135 (8)	-0.0018 (6)	-0.0036 (6)	-0.0004 (6)
C6	0.0150 (7)	0.0108 (7)	0.0098 (7)	-0.0013 (6)	-0.0016 (6)	-0.0001 (5)
C7	0.0151 (7)	0.0112 (7)	0.0116 (7)	-0.0038 (6)	-0.0041 (6)	-0.0007 (6)
C8	0.0121 (7)	0.0136 (7)	0.0166 (8)	-0.0028 (6)	-0.0045 (6)	0.0029 (6)
C9	0.0149 (7)	0.0119 (7)	0.0108 (7)	-0.0014 (6)	-0.0027 (6)	0.0015 (6)
CA	0.0137 (7)	0.0137 (7)	0.0184 (8)	-0.0021 (6)	-0.0023 (6)	-0.0059 (6)
CB	0.0179 (8)	0.0373 (11)	0.0186 (9)	-0.0129 (8)	-0.0034 (7)	0.0058 (8)
CC	0.0200 (9)	0.0222 (9)	0.0372 (12)	-0.0077 (7)	-0.0028 (8)	-0.0076 (8)
CD	0.0500 (13)	0.0253 (10)	0.0319 (12)	0.0177 (9)	-0.0170 (10)	-0.0131 (9)
CE	0.0493 (13)	0.0241 (10)	0.0261 (11)	-0.0027 (10)	0.0135 (10)	-0.0108 (8)

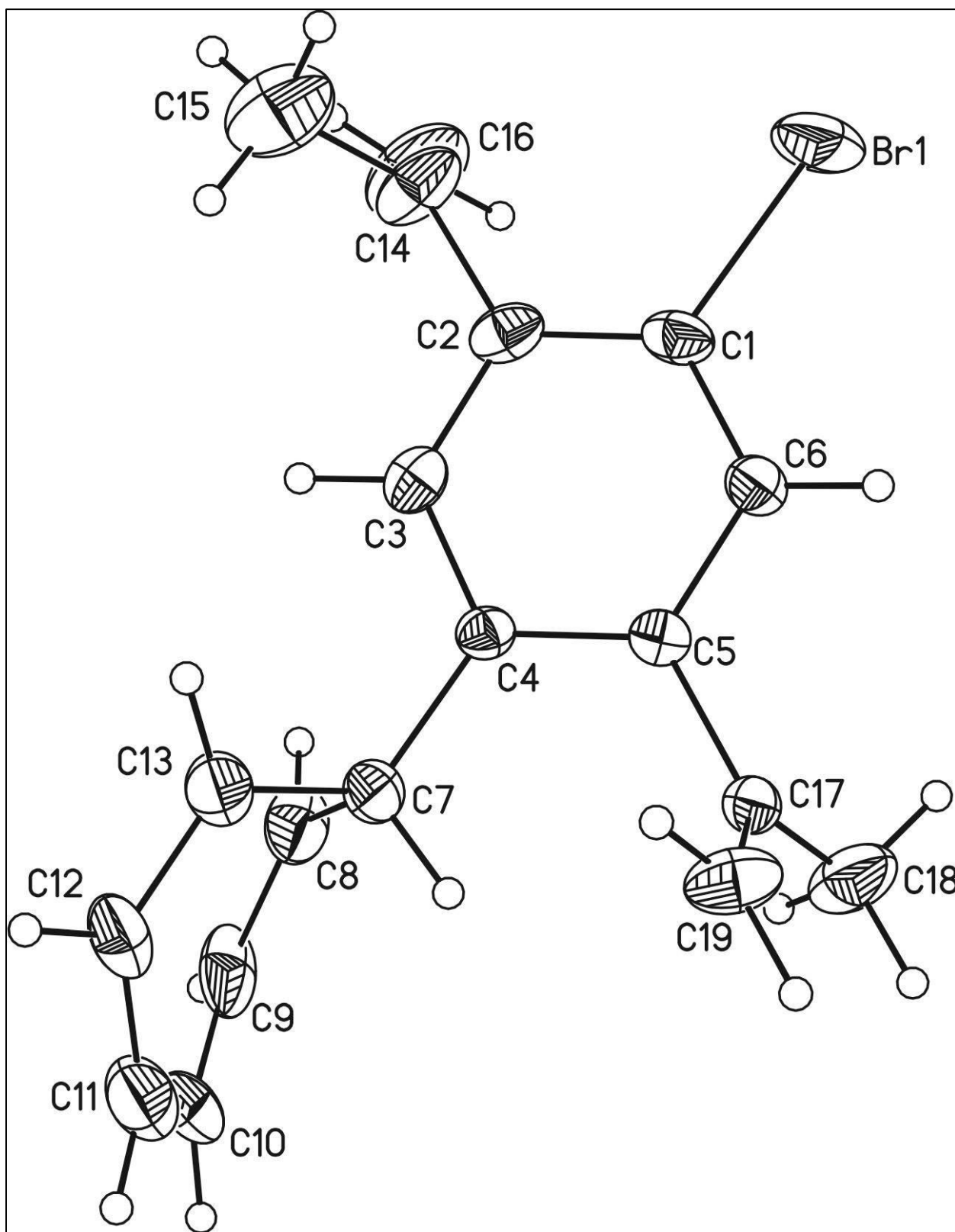


Figure 46 – Crystal data and structure refinement of **71**.

Table 43 – Atomic coordinates and equivalent isotropic displacement parameters (\AA^2) for **71**.

	x	y	z	Uiso*/Ueq
Br1	0.55528 (12)	0.70141 (12)	0.59789 (6)	0.0791 (5)
C1	0.7244 (8)	0.5766 (9)	0.6072 (4)	0.0442 (19)
C2	0.8354 (9)	0.6048 (9)	0.6575 (4)	0.0449 (19)
C3	0.9525 (9)	0.5075 (9)	0.6610 (4)	0.0415 (18)
H3	1.0308	0.5256	0.6946	0.050*
C4	0.9623 (8)	0.3843 (8)	0.6182 (3)	0.0335 (16)
C5	0.8497 (8)	0.3585 (8)	0.5683 (3)	0.0334 (16)
C6	0.7304 (8)	0.4567 (9)	0.5633 (4)	0.0400 (17)
H6	0.6526	0.4406	0.5292	0.048*
C7	1.0935 (8)	0.2813 (9)	0.6280 (4)	0.0428 (18)
H7	1.0776	0.1955	0.5953	0.051*
C8	1.1185 (10)	0.2141 (10)	0.6980 (5)	0.059 (2)
H8	1.0684	0.2549	0.7335	0.071*
C9	1.2112 (10)	0.0969 (11)	0.7105 (5)	0.070 (3)
H9	1.2117	0.0477	0.7530	0.084*
C10	1.3099 (10)	0.0409 (12)	0.6638 (6)	0.067 (3)
H10	1.3291	-0.0650	0.6650	0.081*
C11	1.3756 (11)	0.1200 (13)	0.6200 (6)	0.071 (3)
H11	1.4392	0.0672	0.5932	0.085*
C12	1.3596 (9)	0.2778 (12)	0.6094 (5)	0.065 (3)
H12	1.4419	0.3322	0.5967	0.078*
C13	1.2368 (9)	0.3569 (11)	0.6157 (4)	0.054 (2)
H13	1.2398	0.4643	0.6125	0.065*
C14	0.8360 (11)	0.7295 (12)	0.7085 (5)	0.069 (3)
C15	0.9466 (16)	0.8399 (15)	0.7098 (7)	0.103 (4)
H15A	1.0388	0.7915	0.7012	0.154*
H15B	0.9573	0.8888	0.7542	0.154*
H15C	0.9208	0.9163	0.6750	0.154*

C16	0.7784 (16)	0.7062 (16)	0.7681 (7)	0.110 (5)
H16A	0.8133	0.7628	0.8069	0.132*
H16B	0.7032	0.6334	0.7710	0.132*
C17	0.8508 (8)	0.2261 (9)	0.5205 (4)	0.0375 (17)
C18	0.7586 (11)	0.1034 (12)	0.5321 (6)	0.075 (3)
H18A	0.7897	0.0573	0.5759	0.113*
H18B	0.7639	0.0276	0.4964	0.113*
H18C	0.6581	0.1397	0.5322	0.113*
C19	0.9387 (11)	0.2300 (10)	0.4681 (4)	0.059 (2)
H19A	0.9390	0.1470	0.4376	0.071*
H19B	0.9990	0.3156	0.4624	0.071*

Table 44 – Atomic displacement parameters (\AA^2) for **71**.

	U11	U22	U33	U12	U13	U23
Br1	0.0692 (7)	0.0587 (7)	0.1108 (10)	0.0311 (5)	0.0161 (6)	-0.0123 (6)
C1	0.038 (4)	0.038 (4)	0.060 (5)	0.009 (3)	0.018 (4)	0.000 (4)
C2	0.054 (5)	0.037 (4)	0.047 (5)	-0.006 (4)	0.021 (4)	-0.007 (4)
C3	0.049 (4)	0.039 (4)	0.037 (4)	-0.011 (4)	0.007 (3)	0.003 (3)
C4	0.038 (4)	0.028 (4)	0.034 (4)	0.000 (3)	0.003 (3)	0.002 (3)
C5	0.036 (4)	0.034 (4)	0.031 (4)	0.002 (3)	0.008 (3)	0.002 (3)
C6	0.038 (4)	0.042 (4)	0.040 (4)	0.006 (3)	0.003 (3)	0.000 (3)
C7	0.047 (4)	0.040 (4)	0.039 (4)	0.004 (4)	-0.008 (3)	0.005 (3)
C8	0.064 (6)	0.051 (5)	0.059 (6)	-0.010 (5)	-0.016 (4)	0.015 (5)
C9	0.063 (6)	0.065 (6)	0.074 (7)	-0.015 (5)	-0.037 (5)	0.031 (5)
C10	0.045 (5)	0.064 (6)	0.089 (7)	0.020 (5)	-0.017 (5)	0.002 (6)
C11	0.048 (5)	0.074 (7)	0.090 (8)	0.008 (5)	-0.007 (5)	0.006 (6)
C12	0.032 (4)	0.075 (7)	0.085 (7)	0.004 (4)	-0.002 (4)	0.000 (6)
C13	0.046 (5)	0.052 (5)	0.062 (5)	0.000 (4)	-0.002 (4)	0.003 (4)
C14	0.069 (6)	0.065 (6)	0.079 (7)	-0.024 (5)	0.043 (5)	-0.038 (5)
C15	0.133 (12)	0.086 (9)	0.094 (9)	-0.013 (8)	0.032 (8)	-0.019 (7)
C16	0.131 (12)	0.108 (11)	0.097 (10)	-0.027 (9)	0.050 (9)	-0.053 (8)
C17	0.039 (4)	0.040 (4)	0.033 (4)	0.007 (3)	-0.002 (3)	-0.004 (3)
C18	0.072 (6)	0.066 (7)	0.092 (8)	-0.008 (5)	0.029 (6)	-0.038 (6)
C19	0.087 (7)	0.044 (5)	0.048 (5)	0.006 (5)	0.025 (5)	-0.004 (4)

Appendix B

Input Data for Calculations

Input Data for 27

%Chk=checkpoint.chk

#n AM1 Polar CPHF=RdFreq

(CH3)2-5007

O 1

H	-1.66640	-3.73411	-1.48235
H	-0.76125	-1.05095	-2.34708
H	-0.76125	-1.05095	2.34712
H	-1.66640	-3.73411	1.48238
H	0.71655	-5.13648	0.00002
H	1.26812	-3.40245	-2.48036
H	2.09216	-0.59677	-1.47922
H	2.09216	-0.59677	1.47925
H	1.26812	-3.40245	2.48039
B	0.88495	-2.96451	-1.45106
B	1.40984	-1.35782	-0.89104
B	0.56320	-3.96388	0.00002
B	1.40984	-1.35782	0.89108
B	0.88495	-2.96451	1.45109
B	1.91877	-2.80701	0.00002
B	-0.78473	-3.21905	-0.89034
B	-0.25471	-1.62352	-1.45643
B	-0.25471	-1.62352	1.45646
B	-0.78473	-3.21905	0.89037
C	-1.14670	-1.81443	0.00002
H	3.05540	-3.13534	0.00002
C	-0.28505	0.77010	0.00002
B	-1.61074	1.40580	0.89108
B	0.05380	1.67151	1.45646
B	-1.61074	1.40580	-0.89104
B	0.05380	1.67151	-1.45643
H	-2.29306	0.64475	1.47925
B	-2.11968	2.85499	0.00002
B	-1.08586	3.01249	1.45109
H	0.56035	1.09893	2.34712
B	0.58383	3.26703	0.89037
H	-2.29306	0.64475	-1.47922
B	-1.08586	3.01249	-1.45106
B	0.58383	3.26703	-0.89034
H	0.56035	1.09893	-2.34708
H	-3.25630	3.18333	0.00002
H	-1.46903	3.45043	2.48039
H	1.46550	3.78209	1.48238
H	-1.46903	3.45043	-2.48036
H	1.46550	3.78209	-1.48235
C	0.08415	-0.72211	0.00002

B	-0.76410	4.01187	0.00002
H	-0.91745	5.18447	0.00002
C	0.94580	1.86241	0.00002
C	-2.56237	-1.20823	0.00002
C	-3.19446	-0.93756	-1.24092
C	-3.19446	-0.93756	1.24095
C	-4.42150	-0.41213	-1.53697
H	-2.60969	-1.18796	-2.15060
C	-4.42150	-0.41214	1.53700
H	-2.60969	-1.18797	2.15063
C	-5.45562	0.03069	-0.68029
H	-4.65528	-0.31203	-2.61831
C	-5.45562	0.03068	0.68032
H	-4.65528	-0.31203	2.61834
H	-6.35930	0.41765	-1.19332
H	-6.35931	0.41765	1.19335
C	2.36147	1.25621	0.00002
C	3.22650	0.88576	1.17992
C	3.22652	0.88583	-1.17989
H	2.89382	1.02798	2.20562
C	4.40778	0.38061	0.73585
H	2.89389	1.02803	-2.20560
C	4.40783	0.38066	-0.73592
C	5.59593	-0.12751	-1.57364
H	6.38178	0.59843	-1.55513
H	5.95245	-1.04960	-1.16431
H	5.27906	-0.28446	-2.58352
C	5.59600	-0.12770	1.57333
H	5.82538	-1.13444	1.29271
H	6.44845	0.49463	1.39745
H	5.33975	-0.09645	2.61172

0.01837

Input Data for 28

%Chk=checkpoint.chk

#n AM1 Polar CPHF=RdFreq

(CH3)2-5OM7

O 1

H	-4.43247	2.06208	1.48437
H	-1.83426	1.02546	2.35424
H	-1.83426	1.02546	-2.35427
H	-4.43247	2.06208	-1.48440
H	-3.95531	4.78620	-0.00002
H	-2.27377	4.07294	2.47968
H	0.38100	2.89912	1.49167
H	0.38100	2.89912	-1.49170
H	-2.27377	4.07294	-2.47971
B	-2.19285	3.50069	1.44768
B	-0.62914	2.85559	0.89078
B	-3.16259	3.90816	-0.00002
B	-0.62914	2.85559	-0.89082
B	-2.19285	3.50069	-1.44771
B	-1.40303	4.18434	-0.00002
B	-3.47138	2.40022	0.88774
B	-1.91380	1.76370	1.44907
B	-1.91380	1.76370	-1.44910
B	-3.47138	2.40022	-0.88777
C	-2.63717	1.21025	-0.00002
H	-0.91283	5.26147	-0.00002
C	-0.06063	0.17177	-0.00002
B	-0.71088	-1.43833	-0.00002
B	0.10399	-0.80002	-1.45039
B	0.10399	-0.80002	1.45036
B	1.40862	0.25059	0.89746
H	-1.88145	-1.59057	-0.00002
B	0.44531	-2.45071	0.89376
B	0.44531	-2.45071	-0.89379
H	-0.49230	-0.52423	-2.42223
B	1.76502	-1.39399	-1.44083
H	-0.49230	-0.52423	2.42220
B	1.76502	-1.39399	1.44080
H	1.79764	1.21761	1.43422
H	0.09147	-3.38069	1.53209
H	0.09147	-3.38069	-1.53212
H	2.44690	-1.52496	-2.39476
H	2.44690	-1.52496	2.39472
C	-0.98988	1.42132	-0.00002
B	1.97824	-2.41684	-0.00002
H	2.82094	-3.24304	-0.00002

C	2.42299	-0.76212	-0.00002
B	1.40862	0.25059	-0.89749
H	1.79764	1.21761	-1.43425
C	3.91972	-0.39961	-0.00002
C	4.58800	-0.23775	-1.24095
C	4.58800	-0.23775	1.24092
C	5.88529	0.07646	-1.53700
H	3.96974	-0.38749	-2.15063
C	5.88529	0.07646	1.53697
H	3.96974	-0.38749	2.15060
C	6.97862	0.34126	-0.68032
H	6.13245	0.13632	-2.61834
C	6.97862	0.34126	0.68029
H	6.13246	0.13632	2.61831
H	7.93405	0.57267	-1.19335
H	7.93405	0.57267	1.19332
C	-3.10989	-0.25540	-0.00002
C	-3.40089	-1.15030	-1.17992
C	-3.39660	-1.15167	1.17988
H	-3.29152	-0.80541	-2.20562
C	-3.79504	-2.37311	-0.73585
H	-3.28347	-0.80805	2.20559
C	-3.79239	-2.37398	0.73592
C	-4.19373	-3.60244	-1.57333
H	-3.74988	-4.48018	-1.15205
H	-5.25878	-3.70523	-1.57127
H	-3.84955	-3.47607	-2.57855
C	-4.18802	-3.60415	1.57364
H	-5.22256	-3.82623	1.41459
H	-3.59354	-4.44321	1.27790
H	-4.02284	-3.39772	2.61046

0.01837

Input Data for 29

%Chk=checkpoint.chk

#n AM1 Polar CPHF=RdFreq

(CH3)2-5OP7

O 1

H	4.96123	0.84707	1.58183
H	2.38959	-0.38442	2.37207
H	2.42860	-0.18226	-2.31626
H	4.98588	0.97480	-1.38035
H	6.63088	-1.29902	0.01924
H	4.94603	-2.14399	2.45142
H	2.25857	-3.22782	1.38422
H	2.28323	-3.10004	-1.57912
H	4.98727	-1.93030	-2.50429
B	4.47670	-1.76937	1.43230
B	2.94184	-2.44455	0.83086
B	5.44807	-1.27703	0.01035
B	2.95665	-2.36780	-0.94913
B	4.50080	-1.64445	-1.46464
B	4.44789	-2.75029	-0.06150
B	4.55106	-0.05943	0.94591
B	3.01734	-0.78705	1.46526
B	3.04149	-0.66190	-1.43716
B	4.56586	0.01722	-0.83172
C	3.10685	0.15800	0.05274
H	4.90278	-3.84194	-0.10479
C	0.63688	-0.97944	-0.01686
B	-0.22496	-1.29927	-1.48649
B	-0.33878	-2.40547	-0.08646
B	-0.05927	0.36317	-0.85793
B	-0.24902	-1.42396	1.40528
B	-0.07411	0.28629	0.92498
H	0.35537	-1.62818	-2.45508
B	-1.61840	-0.21603	-1.44688
B	-1.79011	-1.92425	-0.97028
H	0.16579	-3.46736	-0.12805
B	-1.80494	-2.00107	0.81127
H	0.63202	1.14368	-1.40684
B	-1.52322	0.76290	0.04030
H	0.31538	-1.83543	2.35147
B	-1.64239	-0.34033	1.43591
H	0.60741	1.01616	1.55044
H	-2.19327	0.19825	-2.38971
C	-2.45277	-0.66436	-0.02898
H	-2.48319	-2.64441	-1.59638
H	-2.50780	-2.77195	1.36146

H	-2.03236	1.82617	0.08191
H	-2.23313	-0.00833	2.40122
C	2.16779	-1.16048	-0.01192
C	2.35180	1.49921	0.10429
C	2.22116	2.39047	-1.10660
C	1.71992	2.07427	1.16156
H	2.46198	2.52049	-2.19077
C	1.42070	3.55665	-0.58032
C	1.13920	3.35745	0.73455
H	1.62875	1.69142	2.17702
C	-3.98497	-0.50977	-0.03506
C	-4.67986	-0.49864	1.20176
C	-4.65834	-0.38286	-1.27732
C	-6.01048	-0.37846	1.49220
H	-4.05484	-0.60493	2.11293
C	-5.98382	-0.23506	-1.57831
H	-4.01753	-0.40428	-2.18346
C	-7.12230	-0.22558	0.63204
H	-6.27288	-0.40338	2.57132
C	-7.11050	-0.16210	-0.72703
H	-6.22746	-0.15909	-2.65943
H	-8.10482	-0.15083	1.14061
H	-8.08413	-0.03949	-1.24337
C	0.34922	4.27663	1.68462
H	0.92714	5.15185	1.89652
H	-0.57225	4.56126	1.22118
H	0.14389	3.75545	2.59627
C	1.02977	4.74790	-1.47458
H	0.00554	5.00374	-1.30023
H	1.65153	5.58723	-1.24253
H	1.16062	4.48042	-2.50231

0.01837

Input Data for 79

%Chk=checkpoint.chk

#n AM1 Polar CPHF=RdFreq

5-hind-6-7

0 1

C	2.39288	-1.19449	-0.09749
C	0.98072	-1.19714	-0.09701
C	0.25896	0.00254	-0.03408
C	0.98131	1.20239	0.01818
C	2.39349	1.19890	0.01774
C	1.69134	-3.49500	-0.34052
H	1.69708	-4.33187	0.40034
H	1.68701	-3.95223	-1.36208
C	1.69365	3.51288	0.00323
H	1.69110	4.07314	-0.96565
H	1.69892	4.26900	0.82641
C	2.93945	-2.60245	-0.16546
C	3.87374	-2.80362	-1.34571
H	4.81311	-2.21402	-1.19938
H	4.13784	-3.88487	-1.43785
H	3.38645	-2.47118	-2.29294
C	3.65691	-2.97077	1.12362
H	4.02072	-4.02487	1.06809
H	4.53339	-2.29332	1.27936
H	2.96590	-2.87502	1.99510
C	0.43912	-2.60831	-0.15230
C	0.44046	2.61268	0.09769
C	2.94109	2.60635	0.08745
C	-0.50088	2.94713	-1.04612
H	-1.47650	2.41866	-0.92470
H	-0.69862	4.04662	-1.06421
H	-0.04998	2.64817	-2.02245
C	3.87364	2.92199	-1.06889
H	4.13732	4.00720	-1.05558
H	4.81345	2.32150	-0.98193
H	3.38511	2.68323	-2.04332
C	-0.25522	2.86278	1.42684
H	-0.57450	3.93096	1.49361
H	-1.15955	2.21658	1.52704
H	0.43968	2.64237	2.27277
C	-0.50922	-2.83080	-1.31729
H	-0.70212	-3.92389	-1.44482
H	-1.48647	-2.32263	-1.13661
H	-0.06714	-2.43267	-2.26173
C	3.66105	2.84540	1.40531

H	4.53636	2.15428	1.49266
H	4.02683	3.89920	1.45268
H	2.97101	2.66604	2.26427
C	-1.20706	0.00178	-0.02174
C	-1.91610	-0.05653	1.18968
C	-1.93239	0.05885	-1.22482
C	-3.30446	-0.06381	1.19996
H	-1.35793	-0.09406	2.13957
C	-3.32009	0.06446	-1.21747
H	-1.38403	0.09636	-2.18005
H	-3.83446	-0.08833	2.16455
H	-3.86293	0.08819	-2.17486
C	-0.24877	-2.98532	1.15079
H	0.45345	-2.85378	2.00910
H	-1.14801	-2.34678	1.32141
H	-0.57435	-4.05301	1.11359
C	-4.03292	-0.00010	-0.00376
C	-5.48472	-0.00085	0.00571
C	-6.14280	0.79848	-0.95549
C	-6.12930	-0.80096	0.97538
C	-7.48138	0.98882	-1.17712
H	-5.46516	1.37688	-1.62343
C	-7.46465	-0.99219	1.21501
H	-5.44235	-1.37920	1.63389
C	-8.58734	0.43312	-0.49977
H	-7.74538	1.68522	-2.00133
C	-8.57999	-0.43677	0.55299
H	-7.71709	-1.68911	2.04240
H	-9.57969	0.75447	-0.87976
H	-9.56691	-0.75841	0.94657
C	3.12860	0.00141	-0.02757
C	4.57442	-0.00097	0.01082
C	5.45915	0.05652	-1.12296
C	5.39042	-0.06153	1.18888
H	5.13752	0.10919	-2.15887
C	6.77285	0.03163	-0.65006
H	5.01494	-0.11293	2.20686
C	6.73155	-0.04173	0.79110
H	7.67927	0.06137	-1.24659
H	7.60162	-0.07492	1.43931

0.01837

Input Data for 80

%Chk=checkpoint.chk

#n AM1 Polar CPHF=RdFreq

5-6-Hind-7

0 1

C	-1.20123	0.00000	-0.18347
C	-1.20531	0.00000	-1.59445
C	-0.00000	-0.00000	-2.31000
C	1.20531	-0.00000	-1.59445
C	1.20123	-0.00000	-0.18347
C	0.00000	0.00000	0.55016
C	-3.51745	0.00000	-0.88937
H	-4.18085	0.90096	-0.88913
H	-4.18085	-0.90096	-0.88913
C	3.51745	-0.00000	-0.88937
H	4.18085	-0.90096	-0.88913
H	4.18085	0.90096	-0.88913
C	-2.61182	0.00000	0.36272
C	-2.89707	-1.24190	1.19164
H	-2.29040	-1.22839	2.13115
H	-3.97874	-1.26919	1.46862
H	-2.64980	-2.16460	0.61493
C	-2.89707	1.24190	1.19164
H	-3.97874	1.26919	1.46862
H	-2.29040	1.22839	2.13115
H	-2.64980	2.16460	0.61493
C	-2.61350	0.00000	-2.14408
C	2.61350	-0.00000	-2.14408
C	2.61182	-0.00000	0.36272
C	2.90695	-1.24341	-2.96743
H	2.33899	-1.23093	-3.92880
H	3.99655	-1.28829	-3.21087
H	2.62965	-2.16228	-2.39696
C	2.89707	-1.24190	1.19164
H	3.97874	-1.26919	1.46862
H	2.29040	-1.22839	2.13115
H	2.64980	-2.16460	0.61493
C	2.90695	1.24341	-2.96743
H	3.99655	1.28829	-3.21087
H	2.33899	1.23093	-3.92880
H	2.62965	2.16228	-2.39696
C	-2.90695	-1.24341	-2.96743
H	-3.99655	-1.28829	-3.21087
H	-2.33899	-1.23093	-3.92880
H	-2.62965	-2.16228	-2.39696
C	2.89707	1.24190	1.19164

H	2.29040	1.22839	2.13115
H	3.97874	1.26919	1.46862
H	2.64980	2.16460	0.61493
C	0.00000	0.00000	2.01005
C	0.00000	1.20706	2.73255
C	0.00000	-1.20706	2.73255
C	0.00000	1.21073	4.11167
H	0.00000	2.16077	2.18267
C	0.00000	-1.21073	4.11167
H	0.00000	-2.16077	2.18267
C	0.00000	0.00000	4.86318
H	0.00000	2.16537	4.65632
H	0.00000	-2.16537	4.65632
C	-2.90695	1.24341	-2.96743
H	-2.62965	2.16228	-2.39696
H	-2.33899	1.23093	-3.92880
H	-3.99655	1.28829	-3.21087
C	-0.00000	-0.00000	-3.78228
C	-0.00000	-1.25244	-4.41671
C	-0.00000	1.25244	-4.41671
C	-0.00000	-1.55440	-5.76818
H	-0.00000	-2.12489	-3.71992
C	-0.00000	1.55440	-5.76818
H	-0.00000	2.12489	-3.71992
C	-0.00000	-0.69221	-6.86095
H	-0.00000	-2.64033	-6.01579
C	-0.00000	0.69221	-6.86095
H	-0.00000	2.64033	-6.01579
H	-0.00000	-1.18038	-7.86074
H	-0.00000	1.18038	-7.86074
C	0.00000	0.00000	6.26180
C	0.00000	1.15715	7.13020
C	0.00000	0.72057	8.44987
C	0.00000	-0.72057	8.44987
C	0.00000	-1.15715	7.13020
H	0.00000	-2.18890	6.79009
H	0.00000	2.18890	6.79009
H	0.00000	1.34015	9.34134
H	0.00000	-1.34015	9.34134

0.01837

Input Data for 81

%Chk=checkpoint.chk

#n AM1 Polar CPHF=RdFreq

5-6-Hind-6-7

O 1

C	-1.20090	0.00000	1.16519
C	-1.20202	0.00000	-0.24803
C	0.00000	-0.00000	-0.96970
C	1.20202	-0.00000	-0.24803
C	1.20090	-0.00000	1.16519
C	-0.00000	0.00000	1.89137
C	-3.51635	0.00000	0.45956
H	-4.18038	0.90051	0.45992
H	-4.18038	-0.90051	0.45992
C	3.51635	-0.00000	0.45956
H	4.18038	-0.90051	0.45992
H	4.18038	0.90051	0.45992
C	-2.61123	0.00000	1.71146
C	-2.90064	-1.24260	2.53789
H	-2.30795	-1.23109	3.48429
H	-3.98558	-1.27567	2.80182
H	-2.64290	-2.16349	1.96250
C	-2.90064	1.24260	2.53789
H	-3.98558	1.27567	2.80182
H	-2.30795	1.23109	3.48429
H	-2.64290	2.16349	1.96250
C	-2.61249	0.00000	-0.79366
C	2.61249	-0.00000	-0.79366
C	2.61123	-0.00000	1.71146
C	2.90516	-1.24325	-1.61783
H	2.32182	-1.23423	-2.56911
H	3.99214	-1.27998	-1.87318
H	2.64103	-2.16259	-1.04240
C	2.90064	-1.24260	2.53789
H	3.98558	-1.27567	2.80182
H	2.30795	-1.23109	3.48429
H	2.64290	-2.16349	1.96250
C	2.90516	1.24325	-1.61783
H	3.99214	1.27998	-1.87318
H	2.32182	1.23423	-2.56911
H	2.64103	2.16259	-1.04240
C	-2.90516	-1.24325	-1.61783
H	-3.99214	-1.27998	-1.87318
H	-2.32182	-1.23423	-2.56911
H	-2.64103	-2.16259	-1.04240
C	2.90064	1.24260	2.53789

H	2.30795	1.23109	3.48429
H	3.98558	1.27567	2.80182
H	2.64290	2.16349	1.96250
C	0.00000	-0.00000	-2.43667
C	0.00000	1.20145	-3.16107
C	0.00000	-1.20145	-3.16107
C	0.00000	1.20048	-4.54893
H	0.00000	2.15933	-2.61564
C	0.00000	-1.20048	-4.54893
H	0.00000	-2.15933	-2.61564
H	0.00000	2.18595	-5.03649
H	0.00000	-2.18595	-5.03649
C	-0.00000	0.00000	3.35784
C	-0.00000	1.20770	4.07637
C	-0.00000	-1.20770	4.07637
C	-0.00000	1.21118	5.46034
H	-0.00000	2.16124	3.52596
C	-0.00000	-1.21118	5.46034
H	-0.00000	-2.16124	3.52596
C	-0.00000	0.00000	6.20080
H	-0.00000	2.16785	6.00320
H	-0.00000	-2.16785	6.00320
C	-2.90516	1.24325	-1.61783
H	-2.64103	2.16259	-1.04240
H	-2.32182	1.23423	-2.56911
H	-3.99214	1.27998	-1.87318
C	0.00000	-0.00000	-5.29756
C	0.00000	-0.00000	-6.74928
C	0.00000	-1.24086	-7.43684
C	0.00000	1.24086	-7.43684
C	0.00000	-1.53693	-8.77162
H	0.00000	-2.15051	-6.80067
C	0.00000	1.53693	-8.77162
H	0.00000	2.15051	-6.80067
C	0.00000	-0.68029	-9.89660
H	0.00000	-2.61828	-9.02588
C	0.00000	0.68029	-9.89660
H	0.00000	2.61828	-9.02588
H	0.00000	-1.19332	-10.87965
H	0.00000	1.19332	-10.87965
C	-0.00000	0.00000	7.60688
C	-0.00000	1.16342	8.47748
C	-0.00000	0.72919	9.79018
C	-0.00000	-0.72919	9.79018
C	-0.00000	-1.16342	8.47748
H	-0.00000	-2.19359	8.13154
H	-0.00000	2.19359	8.13154
H	-0.00000	1.34114	10.68772

H -0.00000 -1.34114 10.68772

0.01837

Input Data for 82

%Chk=checkpoint.chk

#n AM1 Polar CPHF=RdFreq

5-6-Hind-6-6-7

O 1

C	-2.67036	1.19676	0.08578
C	-1.25704	1.19749	0.08443
C	-0.53349	0.00008	0.00014
C	-1.25699	-1.19736	-0.08420
C	-2.67031	-1.19670	-0.08561
C	-3.39710	0.00001	0.00007
C	-1.96399	3.48739	0.38944
H	-1.96158	3.89849	1.43064
H	-1.96615	4.35595	-0.31389
C	-1.96380	-3.48728	-0.38938
H	-1.96132	-3.89828	-1.43062
H	-1.96595	-4.35589	0.31387
C	-3.21390	2.60553	0.17344
C	-3.89999	3.00791	-1.12312
H	-4.78720	2.35650	-1.31235
H	-4.24478	4.06796	-1.05582
H	-3.19363	2.91373	-1.98253
C	-4.16890	2.79807	1.33853
H	-4.36079	3.88788	1.49231
H	-5.14484	2.29453	1.13488
H	-3.73557	2.37407	2.27546
C	-0.71416	2.60669	0.16697
C	-0.71402	-2.60652	-0.16678
C	-3.21377	-2.60550	-0.17336
C	0.24775	-2.80391	-1.32531
H	1.22829	-2.31401	-1.11379
H	0.42849	-3.89504	-1.48396
H	-0.17472	-2.37066	-2.26313
C	-4.16873	-2.79801	-1.33848
H	-4.36055	-3.88783	-1.49234
H	-5.14471	-2.29455	-1.13482
H	-3.73541	-2.37392	-2.27538
C	-0.03901	-3.00874	1.13569
H	0.30597	-4.06899	1.07230
H	0.84574	-2.35807	1.33561
H	-0.75446	-2.91440	1.98779
C	-0.03909	3.00889	-1.13547
H	0.30581	4.06917	-1.07213
H	0.84573	2.35828	-1.33530
H	-0.75447	2.91443	-1.98762

C	-3.89986	-3.00799	1.12316
H	-4.78711	-2.35663	1.31241
H	-4.24460	-4.06805	1.05578
H	-3.19352	-2.91382	1.98259
C	0.93552	0.00008	0.00014
C	1.64870	-0.07013	1.20574
C	1.64870	0.07025	-1.20547
C	3.04061	-0.07397	1.20591
H	1.09921	-0.11374	2.15909
C	3.04061	0.07405	-1.20564
H	1.09920	0.11385	-2.15881
H	3.58487	-0.12332	2.16114
H	3.58487	0.12337	-2.16087
C	-4.86411	-0.00002	0.00000
C	-5.58195	-0.07462	1.20522
C	-5.58185	0.07455	-1.20528
C	-6.96688	-0.07605	1.20829
H	-5.03170	-0.12445	2.15751
C	-6.96677	0.07590	-1.20847
H	-5.03151	0.12439	-2.15752
C	-7.70552	-0.00008	-0.00013
H	-7.50947	-0.13601	2.16330
H	-7.50928	0.13585	-2.16353
C	0.24753	2.80422	1.32556
H	-0.17499	2.37101	2.26338
H	1.22811	2.31438	1.11414
H	0.42818	3.89537	1.48414
C	-9.11398	-0.00012	-0.00019
C	-9.98383	-0.07487	1.16099
C	-11.29674	-0.04701	0.72796
C	-11.29668	0.04674	-0.72853
C	-9.98373	0.07458	-1.16145
H	-9.63740	0.14081	-2.18938
H	-9.63759	-0.14111	2.18895
H	-12.19446	-0.08633	1.33843
H	-12.19434	0.08606	-1.33908
C	3.75266	0.00003	0.00014
C	5.21142	0.00002	0.00014
C	5.92709	-0.80763	0.89823
C	5.92711	0.80765	-0.89796
C	7.31590	-0.81244	0.89537
H	5.37986	-1.44784	1.60799
C	7.31592	0.81243	-0.89511
H	5.37988	1.44788	-1.60771
C	8.03564	-0.00002	0.00012
H	7.85428	-1.44337	1.61926
H	7.85431	1.44337	-1.61898
C	9.49184	-0.00004	0.00007

C	10.13998	1.23720	-0.20213
C	10.14000	-1.23725	0.20231
C	11.47557	1.53492	-0.24960
H	9.45616	2.10651	-0.32482
C	11.47560	-1.53503	0.24924
H	9.45620	-2.10650	0.32556
C	12.58788	0.67244	-0.11060
H	11.73532	2.60107	-0.41318
C	12.58789	-0.67268	0.10926
H	11.73537	-2.60114	0.41307
H	13.57602	1.17044	-0.19118
H	13.57605	-1.17080	0.18902

0.01837

Input Data for 83

%Chk=checkpoint.chk

#n AM1 Polar CPHF=RdFreq

5-6-6-Hind-6-7

0 1

C	0.29463	-1.19095	0.14990
C	1.70812	-1.19165	0.14850
C	2.43070	0.00003	0.00010
C	1.70810	1.19170	-0.14828
C	0.29461	1.19097	-0.14967
C	-0.43049	0.00000	0.00011
C	1.00160	-3.46104	0.57949
H	0.99953	-4.36845	-0.07298
H	1.00419	-3.81170	1.64263
C	1.00152	3.46109	-0.57922
H	0.99943	4.36847	0.07329
H	1.00408	3.81180	-1.64233
C	-0.24854	-2.59316	0.31352
C	-1.20508	-2.72306	1.48601
H	-2.18315	-2.23714	1.25270
H	-1.39242	-3.80324	1.70137
H	-0.77571	-2.24443	2.39816
C	-0.93163	-3.06638	-0.96055
H	-1.27769	-4.12075	-0.83502
H	-1.81764	-2.42614	-1.18876
H	-0.22300	-3.02103	-1.82208
C	2.25122	-2.59421	0.30691
C	2.25115	2.59428	-0.30667
C	-0.24860	2.59316	-0.31327
C	2.92352	3.06713	0.97325
H	3.80721	2.42801	1.21123
H	3.26963	4.12200	0.85214
H	2.20614	3.02071	1.82773
C	-0.93174	3.06634	0.96079
H	-1.27779	4.12071	0.83530
H	-1.81775	2.42609	1.18895
H	-0.22313	3.02095	1.82234
C	3.21476	2.72849	-1.47267
H	3.39378	3.80947	-1.69157
H	4.19597	2.25353	-1.23243
H	2.79509	2.24290	-2.38581
C	3.21483	-2.72837	1.47290
H	3.39384	-3.80934	1.69185
H	4.19605	-2.25343	1.23262
H	2.79518	-2.24273	2.38603
C	-1.20513	2.72305	-1.48578

H	-2.18317	2.23706	-1.25251
H	-1.39253	3.80324	-1.70109
H	-0.77571	2.24450	-2.39794
C	3.89909	0.00003	0.00004
C	4.61386	-0.13553	-1.20007
C	4.61395	0.13557	1.20010
C	6.00397	-0.14103	-1.20067
H	4.06391	-0.22765	-2.15022
C	6.00407	0.14104	1.20059
H	4.06408	0.22769	2.15030
H	6.54223	-0.23145	-2.15659
H	6.54240	0.23145	2.15648
C	-1.89928	-0.00001	0.00008
C	-2.61246	-0.13929	-1.19885
C	-2.61252	0.13925	1.19898
C	-4.00361	-0.14080	-1.19866
H	-2.06506	-0.23740	-2.14875
C	-4.00367	0.14076	1.19873
H	-2.06517	0.23735	2.14891
H	-4.54753	-0.24091	-2.15031
H	-4.54764	0.24086	2.15035
C	2.92359	-3.06705	-0.97301
H	2.20619	-3.02070	-1.82748
H	3.80723	-2.42789	-1.21102
H	3.26976	-4.12190	-0.85187
C	6.72248	0.00000	-0.00007
C	8.17981	-0.00002	-0.00013
C	8.82700	0.89670	0.87586
C	8.82689	-0.89676	-0.87618
C	10.16303	1.11347	1.08562
H	8.14261	1.53663	1.47634
C	10.16289	-1.11354	-1.08610
H	8.14242	-1.53669	-1.47657
C	11.27473	0.48766	0.47600
H	10.42258	1.89190	1.83238
C	11.27467	-0.48770	-0.47664
H	10.42235	-1.89199	-1.83287
H	12.26320	0.84910	0.82724
H	12.26310	-0.84913	-0.82802
C	-4.72221	-0.00002	0.00002
C	-6.17584	-0.00003	-0.00002
C	-6.89795	-0.79151	-0.91243
C	-6.89799	0.79146	0.91235
C	-8.27987	-0.79661	-0.91313
H	-6.35157	-1.42637	-1.62680
C	-8.27992	0.79657	0.91298
H	-6.35165	1.42632	1.62676
C	-9.02154	-0.00002	-0.00010

H	-8.82338	-1.42907	-1.63054
H	-8.82346	1.42903	1.63036
C	-10.42593	-0.00001	-0.00014
C	-11.29765	0.76583	0.87648
C	-11.29761	-0.76585	-0.87681
H	-10.95103	1.44360	1.65209
C	-12.60944	0.48020	0.54945
C	-12.60941	-0.48021	-0.54985
H	-10.95095	-1.44363	-1.65239
H	-13.50765	0.88229	1.00964
H	-13.50760	-0.88229	-1.01010

0.01837

References

- (1) Pearsall, T.; Fulbert, L. *IEEE Nanotechnology* **2008**, *2*, 6-12.
- (2) Yelleswarapu, C. S.; Kothapalli, S.; Rao, D. V. G. L. N. *Opt. Commun.* **2008**, *281*, 1876-1888.
- (3) Chen, Y. H.; Lin, Y. Y.; Chen, C. H.; Huang, Y. *Optics Letters*. **2005**, *30*, 1045-1047.
- (4) Mukhopadhyay, P.; et. al. *Journal of Materials Chemistry*. **2002**, *12*, 2237-2244.
- (5) Boyd, Robert W. *Nonlinear Optics*, 3rd Ed. Elsevier 2008.
- (6) Allis, D. G.; Spencer, J. T. *Inorg. Chem.* **2001**, *40*, 3373-3380.
- (7) Birnboim, M. H.; Neeves, A. E. US5023139 A. Jun 11, 1991.
- (8) K. H. Jürgen Buschow, Robert W. Cahn, Merton C. Flemings, Bernard Ilshner (print), Edward J. Kramer, Subhash Mahajan, and Patrick Veysseyre (updates). *Encyclopedia of materials and technology*. 2011.
- (9) Kanis, D. R.; Ratner, M. A.; Marks, T. J. *Chem. Rev.* **1994**, *94*, 195.
- (10) (a) Kurtz, H. A.; Dudis, D. S. *Reviews in Computational Chemistry*; Wiley-VCH, 1998. (b) Kurtz, H. A.; Stewart, J. J. P.; Dieter, K. M. *J. Comp. Chem.* **1990**, *11*, 82. (c) Jensen, F. *Introduction to Computational Chemistry*. John Wiley & Son, 1999.
- (11) Grüner, B.; Janoušek, Z.; King, B. T.; Woodford, J. N.; Wang, C. H.; Vřetečka, V.; Michl, J. *J. Am. Chem. Soc.* **1999**, *121*, 3122.
- (12) Abe, J.; Nemoto, N.; Nagase, Y.; Shirai, Y.; Iyoda, T. *Inorg. Chem.* **1998**, *37*, 172.
- (13) Murphy, D. M.; Mingos, D. M. P.; Forward, J. M. *J. Mater. Chem.* **1993**, *3*, 67.
- (14) Murphy, D. M.; Mingos, D. M. P.; Haggitt, J. L.; Powell, H. R.; Westcott, S. A.; Marder, T. B.; Taylor, N. J.; Danis, D. R. *J. Mater. Chem.* **1993**, *3*, 139.

- (15) Marder, S. R.; Beratan, D. N.; Cheng, L. T. *Science*. **1991**, *252*, 103.
- (16) Marder, S. R.; Perry, J. W. *Science*. **1994**, *263*, 1706.
- (17) Milam, D.; Marvin, W. *Journal of Applied Physics*. **1976**, *47*, 2497-2501.
- (18) Ramirez, M. O.; Bausa, L. E.; Jaque, D.; et al. *Journal of Physics: Condensed Matter*. **2003**, *15*, 7780-7801.
- (19) Private communications with Dr. Spencer.
- (20) Takahashi, K.; Takase, K. *Tetrahedron Letters*. **1975**, *4*, 245-248.
- (21) Unpublished Group Data
- (22) Takahashi, K.; Sakae, T.; Takase, K. *Chemistry Letters*. **1978**, 237.
- (23) Takahashi, K.; Takase, K. *Tetrahedron Letters*. **1975**, *4*, 245.
- (24) Takahashi, K.; Ishikawa, F.; Takase, K. *Tetrahedron Letters*. **1976**, *50*, 4655.
- (25) Takahashi, K.; Oikawa, I.; Takase, K. *Chemistry Letters*. **1974**, 1215.
- (26) Grimes, R. N. *Carboranes*; Academic Press: New York and London, 1970.
- (27) YongQing, Q.; Hui, C.; ShiLing, S.; HongLing, F.; ZhongMin, S. *Chinese Science Bulletin*. **2007**, *52*, 2326-2330.
- (28) Li, X.; Sun, S.; Ma, N.; Fan, M.; Qiu, Y.; Fu, Q. *Huaxue Xuebao*. **2011**, *69*(5), 523-528.
- (29) Taylor, J. W. *The Synthesis and characterization of New Metallaborane and Carborane Derivatives on the Way to Novel Nonlinear Optical Materials and Molecular Nanosystems*. Ph.D. Thesis, Syracuse University, 2001.
- (30) Newlon, A. E. *The Synthesis and Structure of Novel Carborane Based and Related Nonlinear Optical Materials*. Ph.D. Thesis, Syracuse University, 2003.

- (31) Niem, T.; Rausch, M. D.; *J. Org. Chem.* **1977**, *42*, 275.
- (32) Liu, Y.; Yang, G.; Sun, S.; Yu, F.; Su, Z. *J. Theoretical and Comp. Chem.* **2012**, *11*, 1121-1133.
- (33) Taylor, J.; Caruso, J.; Newlon, A.; English, U.; Ruhlandt-Senge, K.; Spencer, J.T. *Inorg. Chem.* **2001**, *40*, 3381-3388.
- (34) Li, X.; Wang, C.; Zhang, M.; Zou, H.; Ma, N. Qui, Y. *J. Organometallic Chem.* **2014**, *749*, 327-334.
- (35) Bartoli, G.; Marcantoni, E.; Marcolini, M.; Sambri, L. *Chem. Rev.* **2010**, *110*, 6104–6143.
- (36) Ren, S.; Xie, Z. *Organometallics*. **2008**, *27*, 5167–5168.
- (37) Bruker; Bruker AXS Inc. Madison, Wisconsin, USA, 2012.
- (38) Blessings, R. *Acta Crystallogr., Sect. A.* **1995**, *51*, 33-38.
- (39) Sheldrick, G. *Acta Crystallogr., Sect. A.* **1990**, *46*, 467-473.
- (40) Sheldrick, G. *Acta Crystallogr., Sect. A.* **2008**, *64*, 112-122.
- (41) Spek, A. L. *Journal of Applied Crystallography.* **2003**, *36*, 7-13.
- (42) Spek, A. L. *Acta Crystallogr., Sect. D.* **2009**, *65*, 148-155.
- (43) van der Sluis, P.; Spek, A. L. *Acta Crystallogr., Sect. A.* **1990**, *46*, 194-201.
- (44) Schwartz, K.; White, J. *Organic Syntheses.* **2006**, *83*, 49-54.
- (45) Kreuzer, A. et al. *Organic Letters.* **2013**, *15*, 3420-3423.
- (46) Jolly, W. J. *Synthetic Inorganic Chemistry*; Prentice-Hall, Inc., 1960.
- (47) Tanaka, J.; Suib, S. L. *Experimental Methods in Inorganic Chemistry*; Prentice-Hall, Inc., 1999.

- (48) Brand, C.; Meerts, W. L.; Schmitt, M. *J. Phys. Chem. A*, **2011**, *115*, 9612–9619
- (49) Tezuka, T.; Handa, K.; Mukai, T. *Chemistry Letters*. **1974**, 1341-1346.
- (50) Liu, H. J., Shia, K. S., Shang, X., Zhu, B. Y. *Tetrahedron*. **1999**, *55*, 3803.; Brown, C. A.; Yamaichi, A. *J. Chem. Soc., Chem. Commun.* **1979**, 100.
- (51) Imamoto, T., Takiyama, N., Nakamura, K., Hatajima, T., Kamija, Y. *J. Am. Chem. Soc.* **1989**, *111*, 4392.
- (52) Liu, J. J., Shia, K. S., Shang, X. Zhu, B. Y. *Tetrahedron*. **1999**, *55*, 3803.
- (53) Yang, X., Jiang, W., Knobler, C. B., Hawthorne, F. *J. Am. Chem. Soc.* **1992**, *114*, 9721-9722.
- (54) Spokoyny, A. M., Farha, O. K., Mulfort, K. L., Hupp, J. T., Mirkin, C. A. *Inorganica Chimica Acta*. **2010**, *364*, 266-271.
- (55) Stadlbauer, S., Lönnecke, P., Welzel, P., Hey-Hawkins, E., *Eur. J. Org. Chem.* **2010**, 3129–3139.
- (56) (a) Brunton, G.; Gray, J. A.; Griller, D.; Barclay, L. R. C.; Ingold, K. U. *J. Am. Chem. Soc.* **1978**, *100*, 4197. (b) Myhre, P. C.; Owen, G. S.; James, L. L. *J. Am. Chem. Soc.* **1968**, *90*, 2115.
- (57) Kang, H.; et. al. *J. Am. Chem. Soc.* **2007**, *129*, 3267-3286
- (58) Brown, E. C.; Marks, T. J.; Ratner, M. A. *J. Phys. Chem. B*. **2008**, *112*, 44-50.
- (59) Chang, V. S. C.; Kennedy, J. P. *Polymer Bull.* **1981**, *4*, 513.
- (60) Harrison, A. G.; Honnen, L. R.; Dauben, J. J.; Lossing, F. P. *J. Am. Chem. Soc.* **1960**, *82*, 5593.
- (61) Tezuka, T.; Handa, K. *Chemistry Letter Jpn.* **1974**, 1341-1346.

- (62) Matsuo, T.; Suzuki, K.; Fukawa, T.; Li, B.; Ito, M.; Shoji, Y.; Otani, T.; Li, L.; Kobayashi, M.; Hachiya, M.; Tahara, Y.; Hashizume, D.; Fukunaga, T.; Fukazawa A.; Li, Y.; Tsuji, H.; Tamao, K. *Bull. Chem. Soc. Jpn.* **2011**, *84*, 1178-1191.
- (63) (a) Zheng, S. et al. United States Patent Application Publication. 2003, US 2009/0082401 A1. (b) Huang, H.L.; Lin, C. J.; Chao; T. C.; Lee, H. C.; Cheng, C. H. United States Patent Application Publication. 2011, 20110198571.
- (64) This work.
- (65) Takahashi, K.; Oikawa, I.; Takase, K. *Chemistry Letters*, **1974**, 1215.
- (66) Takahashi, K.; Ishikawa, F.; Takase, K. *Tetrahedron Letters*, **1976**, *50*, 4655.
- (67) Terazzi, E.; Guenee, L.; Morgantini, P.; et. al. *Chem. Eur. J.* **2007**, *13*, 1674-1691
- (68) Corey, E. J.; Cho, H.; Rucker, C. Hua, D. H. *Tetrahedron Letters*. **1981**, *22*, 3455.
- (69) Skov, Louise; Petersen, Michael Aaxman; Broman, Soren Lindbaek; Bond, Andrew D.; Nielsen, Brondsted, M. *Organic & Biomolecular Chemistry*. **2011**, *9*, 6498-6501.
- (70) Davies, Cathryn E. et al. *Inorg Chem.* *4*, 669-683
- (71) Sudhakar, A.;Katz, T. J. *J. Am. Chem. Soc.* **1986**, *108*, 179-181.
- (72) Davis, J. H.; et al. *J. Am. Chem. Soc.* **1989**, *111*, 4784-4790.
- (73) Tatsuya, S.; Hirofuni, N.; Tetsuo, N.; Shigenori, K. *Tetrahedron Letters*. **1990**, *31*, 895-898.
- (74) Picotin, G.; Faye, A.; Miginiac, P. et al. *Bulletin de la Societe Chimique de France*. **1990**, 245-251.
- (75) (a) Schenk, W. K.; Kyburz, R.; Neuenschwander, M. *Helvetica Chimica Acta*. **1975**, *58*, 1101-1119. (b) Dahnke K. R.; Paquette, L. A. *Org. Synth.* **1993**, *71*, 181.
- (76) Bonifacio, M. C.; Robertson, C. R.; Jung, J. Y., King, B. T. *J. Org. Chem.* **2005**, *70*, 8522-8526.

- (77) Lamba, Jaydeep J. S. and Tour, James M. *J. Am. Chem. Soc.* **1994**, *116*, 11723-11736.
- (78) Chen, H. H. et al. China Patent Publication. 2009, CN 101475568.
- (79) Applequist, D. E.; O'Brien, D. F. *J. Am. Chem. Soc.* **1962**, *85*, 743.
- (80) *p-toluenesulfonic acid*; MSDS No. 01968; Acros Organics: Fair Lawn NJ June 24, 1999.
- (81) Lemoigne, M. *Bulletin de la Societe de Chimie Biologique.* **1926**, *8*, 770-782.
- (82) Garbisch, J. *Am. Chem. Soc.* **1964**, *86*, 5561.
- (83) Pavia, D.; Lampman, G.; Kriz, G. *Introduction to Spectroscopy.* Harcourt College Publishers, Orlando Florida 2001.
- (84) Barfield, M.; Chakrabarti, B. *Chem. Rev.* **1969**, *69*, 757.
- (85) Hachiya, M.; Ito, M.; et. al. *Organic Letters.* **2011**, *13*, 102666–102669.
- (86) Otani, T.; Hachiya, M.; Hashizume, D.; Matsuo, T.; Tamao, K. *Chem. Asian J.* **2011**, *6*, 350 – 354.
- (87) Fukazawa, A.; Li, Y.; Yamaguchi, S.; Tsuji, H.; Tamao, K. *J. Am. Chem. Soc.* **2007**, *129*, 14164-14165.
- (88) Matsuo, T.; Kobayashi, M.; Tamao, K. *Dalton Trans.* **2010**, *39*, 9203–9208.
- (89) Darwish, A.; Chong, J. *J. Org. Chem.* **2007**, *72*, 1507-1509.
- (90) Ramharter, J.; Weinstabl, H.; Mulzer, J. *J. Am. Chem. Soc.* **2010**, *132*, 14338–14339.
- (91) Matsumotoa, K.; Kotokua, N.; Shizukaa, T.; Tanakab, R.; Okeya, S. *Inorganica Chimica Acta.* **2001**, *321*, 167-170.
- (92) Ukai, T.; Kawazura, H.; Ishii, Y. *J. Organometallic Chem.* **1974**, *65*, 253-266.

- (93) Comins, D.; Dehghani, A. *Tetrahedron Letters*. **1992**, *33*, 6299-6302.
- (94) Milne, J.; Buchwald, S. *J. Am. Chem. Soc.* **2004**, *126*, 13028-13032.
- (95) Sofia, A.; Karlstrom, E.; Itami, K.; Backvall, J. *J. Org. Chem.* **1999**, *64*, 1745-1749.
- (96) Yuen, A. Lafon, O. Charpentier, T.; Roy, M.; Brunet, F.; Berthault, P.; Sakellariou, D.; Robert, B.; Rinsky, S.; Pilon, F.; Cintrat, J.; Rousseau, B. *J. Am. Chem. Soc.* **2010**, *132*, 1734-1735.
- (97) *J. Org. Chem.* *42*, *2*, 1977
- (98) *Helvetica Chimica Acta*. **2000**, *83*, 1633.
- (99) Zweifel, G. S.; Nantz, M. H. *Modern Organic Synthesis: An Introduction*. W. H. Freeman and Company. New York. 2007.
- (100) Bower, J. F.; Patman, R. L.; Krische, M. J. *Org. Lett.* **2008**, *10*, 1033–1035.
- (101) Bruno, N. C.; Buchwald, S. L. *Org. Lett.* **2013**, *15*, 2876-2879.
- (102) Barder, T. E.; Walker, S. D.; Martinelli, J. R.; Buchwald, S. L. *J. Am. Chem. Soc.* **2005**, *127*, 4687.
- (103) Sharmoukh, W.; Ko, K. C.; Park, S. Y.; Ko, J. H.; Lee, J. M.; Noh, C.; Lee, J.Y.; Son, S. U. *Org. Lett.*, **2008**, *10*, 5358-5365.
- (104) Sharmoukh, W.; Ko, K. C.; Noh, C.; Lee, J. Y.; Son, S. U. *J. Org. Chem.*, **2010**, *75*, 6708-6711.

CASEY SIMONS

4405 Grassland • Harrison, AR 72601

H (870) 204-6536 • C (520) 270-0209

crsimons@syr.edu • www.linkedin.com/chemistcaseysimons/

EDUCATION	Syracuse University <i>PhD Candidate: Organic, Inorganic and Materials Chemistry</i> (March 17, 2015) Advisor: James T. Spencer <i>MPhil Chemistry</i> (Aug 2011) University of Arizona, <i>BS in Chemistry</i> (May 2005)	Syracuse, New York Tucson, Arizona
RESEARCH EXPERIENCE	Syracuse University Department of Chemistry <i>Graduate Student Researcher</i> (December 2009 – August 2014) <ul style="list-style-type: none">• Successfully worked on the synthesis of hindered compounds.• Constructed synthetic hypotheses of total formation of optically active compounds.• Contributed in the construction of new non-covalent bonded materials for solar cells. University of Arizona Department of Chemistry <i>Undergraduate Student Researcher</i> (August 2007 – May 2009) <ul style="list-style-type: none">• Developed methodology for controlled sulfonation of polyarylenes.• Created molecular weight dependant solubility measurements for polyarylenes.• Successfully accomplished assigned tasks and was deemed an effective teaching assistant.	Syracuse, NY Tucson, AZ
INDUSTRY EXPERIENCE	Ventana Medical Systems Inc <i>NexGen Group Intern</i> (May 2008 – August 2009) <ul style="list-style-type: none">• Successfully developed quick staining hematoxylin formulation for reduced staining time. University of Arizona Accelerator Mass Spectrometry Laboratory <i>Process Chemist</i> (December 2005 – May 2007) <ul style="list-style-type: none">• Extracted carbon-13 for isotopic dating from samples through a multi-step process varying based on material received.	Oro Valley, AZ
TEACHING EXPERIENCE	State University of New York Polytechnic Institute <i>Adjunct Professor</i> (January 2014 – May 2014) <ul style="list-style-type: none">• Provided academic support and supervision to engineering students in the chemistry lab. Syracuse University <i>Graduate Teaching Assistant</i> (August 2009 – May 2014) <ul style="list-style-type: none">• Head Teaching Assistant for multiple courses University of Arizona <i>Undergraduate Teaching Assistant</i> (August 2007 – May 2009) <ul style="list-style-type: none">• Successfully taught proper laboratory skills and techniques to new students	Utica, NY Syracuse, NY Tucson, AZ

- SKILLS** Organic and Inorganic Synthesis, Organic Methodology, Material Science, Polymer Synthesis, Air-Sensitive Reactions, Laboratory Management, X-Ray Diffraction Scanning Electron Microscopy, Nuclear Magnetic Resonance, Infrared Spectroscopy UV-Vis Spectroscopy, Thermal Gravimetric Analysis, Differential Scanning Calorimetry Bomb Calorimetry, Gas Chromatography, Mass Spectrometry, Atomic Absorption Spectroscopy, Liquid Chromatography, Column Chromatography
- PRESENTATION** Simons, C. R., Spencer, J. T.; "Functionalization of [5.6.7] quinarene for nonlinear optical tuning" *247th American Chemical Society National Meeting & Exposition*. Dallas, TX, **March 16-20, 2014**.
- SELECTED POSTERS** Simons, C. R., Spencer, J. T.; "Functionalization of [5.6.7] quinarene for nonlinear optical tuning" *31st Annual Graduate Student Symposium*. Buffalo, NY, **May 15-17, 2013**.
- Simons, C. R., Spencer, J. T.; "Functionalization of [5.6.7] quinarene for nonlinear optical tuning" *246th American Chemical Society National Meeting & Exposition*. Indianapolis, IN, **September 8-12, 2013**.
- Simons, C. R., Romero, J., Spencer, J.T.; "Formation of Boron Doped Carbon Nanotubes through Ultrasonic Nebulization" *Boron in the Americas XII Conference*. East Lansing, MI, **June 6-10, 2010**.
- VOLUNTEER EXPERIENCE** **Merit Badge Counselor**, Boy Scouts of America, Syracuse, NY
- Assisted scouts in the attainment of their chemistry badge
- Science Fair Judge**, Various, Tucson, AZ & Central New York
- Judged science fair posters and presentations at various levels
- Chemistry Tutor**, Syracuse University Athletic Department, Syracuse, NY
- Tutored students in general chemistry and organic chemistry